Journal of Naval Sciences and Engineering

Deniz Bilimleri ve Mühendisliği Dergisi

National Defence University
Milli Savunma Üniversitesi

Barbaros Naval Sciences and Engineering Institute
Barbaros Deniz Bilimleri ve Mühendisliği Enstitüsü

Volume/Cilt:17
Number/Sayı:2
November/2021

PRINTED BY/BASKI
Turkish Naval Academy Printing House/Deniz Harp Okulu Basımevi

CORRESPONDENCE AND COMMUNICATION ADDRESS/YAZIŞMA VE HABERLEŞME ADRESİ

Milli Savunma Üniversitesi
Barbaros Deniz Bilimleri ve Mühendisliği Enstitüsü
Deniz Harp Okulu Yerleşkesi
Tuzla/İstanbul/Türkiye

Phone/Telefon : +90 216 395 26 30/2100-2104
Fax/Belgegeçer : +90 216 395 26 58
E-mail/E-posta : *jnse@dho.msu.edu.tr*
Web : https://dergipark.org.tr/tr/pub/jnse

NATIONAL DEFENCE UNIVERSITY
BARBAROS NAVAL SCIENCES AND ENGINEERING INSTITUTE
JOURNAL OF NAVAL SCIENCES AND ENGINEERING

MİLLİ SAVUNMA ÜNİVERSİTESİ
BARBAROS DENİZ BİLİMLERİ VE MÜHENDİSLİĞİ ENSTİTÜSÜ
DENİZ BİLİMLERİ VE MÜHENDİSLİĞİ DERGİSİ

Volume/Cilt: 17 Number/Sayı: 2 November/Kasım 2021 ISSN: 1304-2025

Owner on Behalf of the Barbaros Naval Sciences and Engineering Institute
Barbaros Deniz Bilimleri ve Mühendisliği Enstitüsü Adına Sahibi ve Sorumlusu
Assoc.Prof.Dr. (Doç.Dr.) Ertan YAKICI

Journal of Naval Sciences and Engineering (JNSE) is a peer reviewed, international, inter-disciplinary journal in science and technology, which is published semi-annually in April and November since 2003. It publishes full research articles, review articles, technical notes, short communications, book reviews, letters to the editor and extended versions of conference papers. Topics of interest include the technological and scientific aspects of the following areas: **Computer Science and Engineering**, **Electrical and Electronics Engineering**, **Naval/Mechanical Engineering**, **Naval Architecture and Marine Engineering, Industrial Engineering** and **Basic/Social Sciences**. The journal aims to provide a scientific contribution to the increasing needs of Turkish Armed Forces. The papers in the journal are published in English.

Following the Open Access Model of Publishing, Journal of Naval Sciences and Engineering presents a variety of scientific viewpoints. The authors are responsible for the scientific, contextual and linguistic aspects of the articles published in the journal. The views expressed or implied in this publication, unless otherwise noted, should not be interpreted as official positions of the Institution.

Our journal uses “double-blind review”, which means that both the reviewer and author identities are concealed from the reviewers, and vice versa, throughout the review process. The articles submitted to JNSE to be published are free of article submission, processing and publication charges. The accepted articles are published free-of-charge as online from the journal website and printed.

DATABASES INDEXING OUR JOURNAL / TARANDIĞIMIZ VERİ TABANLARI

Open Academic Journals Index (OAJI) (13.03.2016)
Sobiad Citation Index (31.01.2018)
Scientific Indexing Services (SIS) (28.02.2018)
Arastirmax Scientific Publication Index (13.03.2018)
CiteFactor Academic Scientific Journals (14.05.2018)
Asian Digital Library (03.09.2018)
Idealonline (05.09.2018)
Directory of Open Access Journals (DOAJ) (09.10.2018)
ULAKBİM TR Dizin (14.05.2020)

Deniz Bilimleri ve Mühendisliği Dergisi (DBMD); uluslararası düzeyde, hakemli, multi-disipliner, Nisan ve Kasım aylarında olmak üzere 2003 yılından bu yana yılda iki kez yayımlanan, bilim ve teknoloji dergisidir. Dergide; **Bilgisayar, Makine, Gemi İnşa, Elektrik/Elektronik, Endüstri Mühendisliği** ile **Temel/Sosyal Bilimler** alanlarında bilimsel nitelikli araştırma makaleleri, derlemeler, teknik notlar, kitap incelemeleri, editöre mektuplar ile konferans ve toplantıların genişletilmiş raporlarına yer verilmektedir. Dergi, Türk Silahlı Kuvvetlerinin artan ihtiyaçlarına bilimsel katkı sağlamayı amaçlamaktadır. Dergide yer alan makaleler İngilizce olarak yayımlanmaktadır.

Açık Erişimli Yayın Politikası izleyen Deniz Bilimleri ve Mühendisliği Dergisi, farklı bilimsel bakış açılarını okuyucularına sunmaktadır. Dergide yayınlanan makalelerin bilim, içerik ve dil bakımından sorumluluğu yazarlarına aittir. Dergide doğrudan veya dolaylı olarak ifade edilen görüşler, kurumun resmi görüşleri olarak görülmemelidir.

Dergimiz, makale değerlendirme sürecinde “çift-kör hakemlik” sistemini kullanmaktadır. Buna göre, değerlendirme süreci boyunca hakemler ve yazarlar birbirlerinin bilgilerini görememektedir. DBMD’ne yayımlanmak üzere gönderilen makaleler; makale gönderim, işlem ve yayın ücretinden muaftır. Kabul edilen makaleler, ücretsiz olarak basılı şekilde ve dergi web sayfasından çevrimiçi (online) olarak yayınlanmaktadır.

NATIONAL DEFENCE UNIVERSITY
BARBAROS NAVAL SCIENCES AND ENGINEERING INSTITUTE
JOURNAL OF NAVAL SCIENCES AND ENGINEERING

MİLLİ SAVUNMA ÜNİVERSİTESİ
BARBAROS DENİZ BİLİMLERİ VE MÜHENDİSLİĞİ ENSTİTÜSÜ
DENİZ BİLİMLERİ VE MÜHENDİSLİĞİ DERGİSİ

Volume/Cilt: 17 Number/Sayı: 2 November/Kasım 2021 ISSN: 1304-2025

NATIONAL DEFENCE UNIVERSITY
BARBAROS NAVAL SCIENCES AND ENGINEERING INSTITUTE
JOURNAL OF NAVAL SCIENCES AND ENGINEERING

VOLUME: 17 **NUMBER: 2** **NOVEMBER 2021** **ISSN: 1304-2025**

CONTENTS / İÇİNDEKİLER

MİLLİ SAVUNMA ÜNİVERSİTESİ
BARBAROS DENİZ BİLİMLERİ VE MÜHENDİSLİĞİ ENSTİTÜSÜ
DENİZ BİLİMLERİ VE MÜHENDİSLİĞİ DERGİSİ

CİLT: 17 **SAYI: 2** **KASIM 2021** **ISSN: 1304-2025**

NATIONAL DEFENCE UNIVERSITY
BARBAROS NAVAL SCIENCES AND ENGINEERING INSTITUTE
JOURNAL OF NAVAL SCIENCES AND ENGINEERING

VOLUME: 17 **NUMBER: 2** **NOVEMBER 2021** **ISSN: 1304-2025**

CONTENTS / İÇİNDEKİLER

MİLLİ SAVUNMA ÜNİVERSİTESİ
BARBAROS DENİZ BİLİMLERİ VE MÜHENDİSLİĞİ ENSTİTÜSÜ
DENİZ BİLİMLERİ VE MÜHENDİSLİĞİ DERGİSİ

CİLT: 17 **SAYI: 2** **NOVEMBER 2021** **ISSN: 1304-2025**

Journal of Naval Sciences and Engineering
2021, Vol. 17, No. 2, pp. 217-239
Computer Engineering/Bilgisayar Mühendisliği

RESEARCH ARTICLE

**An ethical committee approval and/or legal/special permission has not been required within the scope of this study.*

ON THE EFFECT OF WORD POSITIONS IN GRAPH-BASED KEYWORD EXTRACTION*

Osman KABASAKAL[1]
Alev MUTLU [2]

[1]*Kocaeli University, Department of Computer Engineering, Kocaeli, Turkey,*
185112060@kocaeli.edu.tr; ORCID: 0000-0003-1187-5147

[2]*Kocaeli University, Department of Computer Engineering, Kocaeli, Turkey,*
alev.mutlu@kocaeli.edu.tr; ORCID: 0000-0003-0547-0653

Received: 28.11.2020 **Accepted: 25.06.2021**

ABSTRACT

In this study, we focus on the effect of word positions in unsupervised, graph-based keyword extraction. To this aim, we discuss the performance of four node-weighting procedures, namely Word Position (WP), Word Position Bidirectional (WPB), Sentence Position (SP), and Sentence Position Bidirectional (SPB). WP assigns higher weights to words that appear at the beginning of a text. WPB assigns higher weights to words that appear either at the beginning or end of a text. SP assigns higher weights to words that appear in the very first sentences of a text. SPB assigns higher weights to words that appear in sentences that are either close to the beginning or end of a text. Experiments conducted on six benchmark datasets show that WP and SP do not statistically differ. However, for datasets whose keywords appear early in the text WP performs better than SP with no statistical difference, while for datasets where keywords are evenly distributed in text SP statistically performs better than WP.

Keywords: *Keyword Extraction, Sentence Position, Word Position.*

Osman KABASAKAL, Alev MUTLU

ÇİZGE TABANLI ANAHTAR KELİME ÇIKARIMINDA KELİME POZİSYONLARININ ETKİSİ

ÖZ

Bu çalışmada gözetimsiz, çizge tabanlı anahtar kelime çıkarma yöntemlerinde kelime pozisyonlarının etkisine odaklanılmaktadır. Bu amaçla, düğümler için; Kelime Pozisyonu (WP), Kelime Pozisyonu Çift Yönlü (WPB), Cümle Pozisyonu (SP) ve Cümle Pozisyonu Çift Yönlü (SPB) isimli ilk ağırlıklandırma yöntemleri üzerinde durulmakta ve bunların performans üzerindeki etkileri tartışılmaktadır. WP, bir metnin başında yer alan kelimelere daha fazla ağırlık vermektedir. WPB, bir metnin başında ya da sonunda bulunan kelimelere daha fazla ağırlık vermektedir. SP, metnin ilk cümlelerinde geçen kelimelere daha fazla ağırlık vermektedir. SPB ise metnin başında ve sonunda yer alan cümlelerdeki kelimelere daha fazla ağırlık vermektedir. Altı veri kümesi üzerinde yapılan deneylerde, WP ve SP ağırlıklandırmalarına istatistiksel bir fark gözelemlenmemiştir. Ancak anahtar kelimelerin metnin başında geçen veri kümelerinde WP daha yüksek başarım göstermekle birlikte SP'den istatistiksel olarak ayrılmamaktadır. Anahtar kelimelerin metin içinde dağıtılmış olan veri kümelerinde SP, WP'den daha başarılı olmakta ve istatistiksel fark göstermektedir.

Anahtar Kelimeler: *Anahtar Kelime Çıkarımı, Cümle Konumu, Kelime Konumu.*

1. INTRODUCTION

Keyword extraction is the process of mining descriptive words from texts. It is a challenging text mining task as keywords provide means for document indexing, search, classification, and clustering. Furthermore, keywords may provide readers with the concept and theme of a text. With the increasing amount of stored online documents, the problem has gathered further importance, and the need for automated keyword extraction techniques has emerged.

Keyword extraction techniques differ by various aspects, such as the type of algorithm they employ, the type of the document they focus on, and the data structure they use to represent documents. Primarily, keyword extraction techniques can be classified as supervised and unsupervised. Supervised keyword extraction is considered as a binary classification task where words of a document are assigned either to the keyword or the non-keyword class. In literature, there are supervised keyword extraction studies that employ support vector machines (Ni, Liu, & Zeng, 2012; Armouty & Tedmori, 2019), neural networks (Azcarraga, Liu, & Setiono, 2012; Tafti et al., 2019), and conditional random fields (Patel & Caragea, 2019; Anju, Ramesh, & Rafeeque, 2018). Unsupervised methods for keyword extraction follow unsupervised learning methods. These include simple statistics methods that focus on word statistics such as *tf-idf* score (Sun, Wang, & Xia, 2017; Yao, Pengzhou, & Chi, 2019) and term relatedness (Campos et al., 2020); NLP-based approaches employ NLP tools such as lexical chains (Ercan & Cicekli, 2007); and graph-based approaches that focus graph algorithms such as node ranking (Florescu & Caragea, 2017). Keyword extraction studies also differ through text representation models. Schemes such as simple graphs (Tixier, Malliaros, & Vazirgiannis, 2016; Florescu & Caragea, 2017; Biswas, Bordoloi, & Shreya, 2018), hypergraphs (Bellaachia & Al-Dhelaan, 2014), and bag-of-words (Hulth, 2003) are extensively used. Furthermore, keyword extraction studies differ by the type of document they focus on. There are keyword extraction techniques developed specifically for microblog posts (Biswas, 2019), scientific documents (Thushara, Krishnapriya, & Nair, 2018), and news articles (Yao et al., 2019).

In this study, we focus on unsupervised graph-based keyword extraction. Such studies represent a text as a graph where nodes represent the text's unique words and edges indicate relations between nodes. Such approaches formulate the keyword extraction problem as a node-ranking problem. An essential issue in this approach is the initialization of node weights. A good initial weight may produce high-quality keywords and speed up the process. Motivated by the discussion on the relationship between the position of a sentence and its informativeness presented in (Lynn, Lee, Choi, & Kim, 2017), in this study, we investigate the performance of three initial weight assignment procedures for nodes, namely Word Position Bidirectional (WPB), Sentence Position (SP), and Sentence Position Bidirectional (SPB) and compare them against initial node assignment procedure of PositionRank (Florescu & Caragea, 2017), namely WP. WP assigns higher initial weights to words that appear at the beginning of a text. In WPB, words appearing at the beginning and at the end of a text are assigned with higher initial weights than those appearing in the middle of a text. In SP, words appearing at the first sentences of a text are assigned with higher initial weights, and in SPB, words appearing in the sentences either close to the beginning or the end of a text is assigned to higher initial weights than words appearing in the middle sentences. Hence, WP and WPB consider word positions in weight assignment while SP and SPB consider sentence positions.

The performance of the initial weight assignment techniques is evaluated using six benchmark datasets, and the results are statistically analyzed. The experimental results regarding all datasets show that SP ranks best in terms of F1-score; however, it does not statistically differ from WP. Regarding the datasets whose author assigned keywords are mostly populated in the very beginning of texts, WP performs better than other weighting procedures but statistically differs only from WPB. Regarding the datasets whose author assigned keywords are evenly spread in the text, SP ranks first and statistically differs from WP. WPB always ranked last.

The organization of the paper is as follows. In Section 2, we provide the general framework of the unsupervised, graph-based keyword extraction procedure, and introduce the PositionRank algorithm in some detail. In

Section 3, we introduce the proposed word weighting heuristics. In Section 4, we introduce the datasets used to evaluate the proposed word weighting heuristics, the experimental setting, and discuss the findings. The last section concludes the paper.

2. BACKGROUND

This section introduces the general framework for unsupervised, graph-based keyword extraction, and later explains the PositionRank algorithm.

2.1. Graph-based Keyword Extraction

Graph-based keyword extraction is an unsupervised procedure (Biswas et al., 2018; Beliga, 2014). The general framework for graph-based keyword extraction consists of text preprocessing, word-graph construction, candidate keyword generation, and keyword extraction steps. Below we describe these steps.

- **Text Preprocessing:** In this step, a text is tokenized, and tokens are annotated with the part of speech tags. These tags are later used to filter words of certain types. This step also includes the removal of stop words and unimportant words.
- **Word-graph Construction:** In this step, a graph called *word-graph* is constructed to represent a text document. In this representation, unique words of a text constitute the nodes, and edges imply certain relations among the words. In word-graphs, nodes are also assigned with initial weights that indicate the importance of the words they represent. TextRank (Mihalcea & Tarau, 2004) considers all words equally important and assigns initial weight 1 to all nodes. PositionRank (Florescu & Caragea, 2017) determines the initial weight of a word according to its positions in the document. Keyword Extraction using Collective Node Weight (KECNW) (Biswas et al., 2018) considers several features of a node such as the distance of the node from the central node, node's selectivity centrality, and the position of the word. Keyword from Weighted Graph (KWG) (Biswas, 2019) aggregates word frequency and degree of the node in the initial weight assignment. In TextRank and

PositionRank, edges connect nodes that represent co-occurring words, i.e. words that appear within a predefined size of windows. In KECNW and KWG edges connect nodes that are immediate neighbors.

- **Candidate Keyword Generation:** Candidate keywords are generated by applying a node-ranking algorithm on the word-graphs. These ranking algorithms are generally derived from the Hyperlink-Induced Topic Search (HITS) algorithm (Kleinberg, 1999) and the PageRank algorithm (Brin & Page, 1998).
- **Keyword Extraction:** *k* nodes with highest ranks are extracted from a word-graph as keywords. However, in word-graphs nodes represent individual words and this procedure generates single-word keywords. To generate key-phrases, i.e. keywords with two or more words, keyword extraction algorithms employ various heuristics. The PositionRank algorithm concatenates one-word keywords that appear in contiguous positions of the original text to generate candidate keyphrases. Scores of the candidate keyphrase is calculated by summing individual words' scores. Then it selects top-*k* ranking candidate keywords / keyphrases as a solution. The TextRank algorithm, on the other hand, firstly selects top-*k* ranking single word-keywords from the word-graph and then merges those that appear in contiguous positions of the original text.

2.2. The PositionRank Algorithm

PositionRank is an unsupervised, graph-based algorithm proposed for keyword extraction from scientific publications. In the data-preprocessing step of PositionRank, all words other than nouns and adjectives are removed. Word-graph of PositionRank is weighted and undirected, where nodes represent unique words of the preprocessed text and edges connect nodes representing words that are at most *d*-distant from each other. Edge weights, w_{ij}, indicate the number of the co-occurrences of two words. Initial node weights are assigned relative to the positions of the words they represent. The first word of a text has initial weight 1/1; word appearing at position *p* has weight 1/*p*. If a word appears in multiple positions their weights are summed. PositionRank follows the PageRank's node ranking procedure. The node weighting procedure is formulated in Equation 1,

where $S(v_i)$ is the weight of node v_i after iteration i. $O(v_j)$ is the summation of the edge weights of the nodes that are adjacent to v_j. w_{ji} is the weight of the edge between v_i and v_j, p_i is the initial weight of node v_i. λ is a dumping factor determining the transition probability from a node to the next node.

$$S(v_i) = (1-\lambda).\widetilde{p_i} + \lambda \sum_{v_j \in Adj(v_i)} \frac{w_{ji}}{O(v_j)} S(v_j) \quad \textbf{(1)}$$

PositionRank is assumed to converge when nodes' weights differ by at most 0.001 between two consecutive iterations or the iteration number reaches 100. Once the node weights converge, PositionRanks sorts nodes based on their ranks. If two or more words are immediate neighbors, they are concatenated to form a keyphrase with a weight equal to the summation of weights of the words in the keyphrase. Top *k*-keywords/key-phrases are selected as the solution.

3. THE INITIAL WEIGHTS PROCEDURES

In (Lynn et al., 2017), sentences forming a text are classified into three groups: topic sentences, supporting sentences, and concluding sentences. The study states that the topic sentences appear at the beginning of a text, concluding sentences appear at the end, and supportive sentences are placed in between. Furthermore, the study cites that topic and concluding sentences are more informative compared to supportive sentences hence are more likely to contain keywords. Motivated by these observations we investigate three procedures for initial weight assignment for words, namely SentenceRank (SP), SentenceRankBidirectional (SPB), and WordPositionBidirectional (WPB). Below we describe these procedures:

- **Sentence Position (SP):** In this approach, we assign weights to sentences based on their positions, i.e. the first sentence gets weight 1 and the second sentence gets weight 2. The weight of a word is calculated according to the weight of the sentence it appears in. A word that appears in a sentence with weight *i*, has initial weight of $1/i$. If a word appears in multiple sentences, individual weights of the word are summed. Equation (1) formulates this initial weight

assignment procedure, where w_i is a word in sentence S_t, t indicating position of the sentence.

$$SP(w_i) = \frac{1}{t}, w_i \in S_t \quad \textbf{(1)}$$

- **Sentence Position Bidirectional (SPB):** In this approach, the first and the last sentences of a text are assigned weight 1; the second sentence and the second to the last sentence are assigned weight 2 and so on. Similar to SP, a word that appears in a sentence with weight i, has initial weight $1/i$. If a word appears in multiple sentences, these individual weights of the word are summed. Both in SP and SPB, words appearing in the same sentence have equal weights. This assignment procedure is formulated in Equation (2), where n is the number of sentences in the text, t is the position of the sentence S_t.

$$SPB(w_i) = \begin{cases} \frac{1}{t}, & w_i \in S_t, \quad t < n/2 \\ \frac{1}{n+1-i}, & w_i \in S_t, \quad t \geq n/2 \end{cases} \quad \textbf{(2)}$$

- **Word Position Bidirectional (WPB):** In this approach, we follow weighting procedure of PositionRank, however, we also favor words that appear close to the end of a text. In WPB, the first and the last words are assigned with initial weight 1/1, the second word and the second to the last word are assigned with initial weight of 1/2 and so on. This procedure is formulated in Equation (3), where i indicates the position of a word, n is the number of words in the text.

$$WPB(w_i) = \begin{cases} \frac{1}{i}, & i < n/2 \\ \frac{1}{n+1-i}, & i \geq n/2 \end{cases} \quad \textbf{(3)}$$

When compared to ranking procedure of PositionRank, SP and SPB assign more gradual initial weights to words. However, WPB is steep in initial weight assignment while also favoring last words of a text.

4. EXPERIMENTS

In this section, we firstly introduce the datasets and metrics used to evaluate the performance of proposed initial weight assignment procedures. Later, we discuss the experimental findings.

4.1. Datasets and Experimental Setting

- **Inspec:** It is a collection of abstracts of 2000 scientific journals written in English and related to computer science and information technology. The dataset is introduced in (Hulth, 2003) and is one of the most cited datasets in keyword extraction studies.
- **Nguyen:** This dataset is introduced in (Nguyen & Kan, 2007) and consists of 211 academic conference papers written in English. Each article has two keyword sets: one provided by the authors of the article and the other provided by annotators. In this study, we use the union of these keywords sets. Although the dataset provides full text of the articles, we consider the abstracts.
- **SemEval2010:** This dataset consists of 284 scientific papers written in English, compiled from the ACM library, and focusing on various domains such as economics, information retrieval, and multi-agent systems. The dataset is introduced in (Kim, Medelyan, Kan, & Baldwin, 2010).
- **SemEval2017:** The SemEval2017 dataset is introduced in (Augenstein, Das, Riedel, Vikraman, & McCallum, 2017) and consists of 500 academic papers written in English related to computer science, material sciences, and physics.
- **WWW:** This dataset is introduced in (Gollapalli & Caragea, 2014) and consists of abstracts of 1330 papers presented in the World Wide Web conference between 2004 and 2014.

- **KDD:** This dataset is introduced in (Gollapalli & Caragea, 2014) and contains abstracts of 755 papers presented in ACM Conference on Knowledge Discovery and Data Mining between 2004 and 2014.

To evaluate the performance of the initial weight assignment procedures, precision, recall, and F-score are used. In the context of keyword extraction, precision refers to the fraction of the number of correctly extracted keywords over the total number of keywords extracted; recall refers to the fraction of the number of correctly extracted keywords over the number of keywords assigned to the document, and F-score is the harmonic mean of precision and recall. Recall, precision, and F-score are defined, respectively, in equations (4), (5), and (6).

$$Recall = \frac{number\ of\ correctly\ matched\ keywords}{number\ of\ assigned\ keywords} \quad \textbf{(4)}$$

$$Precision = \frac{number\ of\ correctly\ matched\ keywords}{number\ of\ extracted\ keywords} \quad \textbf{(5)}$$

$$F - score = 2x\frac{precision\ x\ recall}{precision + recall} \quad \textbf{(6)}$$

Friedman's test and Nemenyi post-hoc test are used to statistically analyze the results. Friedman's test is a non-parametric test to detect differences of variance by ranks across multiple attempts. The null hypothesis for the Friedman test is that there are no differences among the attempts, i.e. groups come from populations with the same median (Pereira, Afonso, & Medeiros, 2015). Although the Friedman test can discover if any of the attempts statistically differ, it cannot detect the differing attempts. Nemenyi post-hoc test is employed to detect the differing attempts. It performs pairwise multiple comparisons of the ranked data. To this aim, the pairwise multiple comparison of mean ranks (PMCMR) package (Pohlert, 2016) of R is used. The tool is also used to create the plots. The visual representation of the Nemenyi test consists of methods that are placed on an axis according to their mean rank and a critical difference (CD) ruler. If the difference in average rank between two attempts, say *i* and *j*, exceeds critical difference,

$R_i - R_j > \Delta_\alpha$, then the performance of algorithm i is better than the performance of algorithm j. Methods that do not statistically differ are connected via straight lines. Methods with higher ranks, in the context of this study, are assumed to perform better compared to methods with lower ranks.

In the experiments, we set the window size, d, to 3, and the dumping factor in PageRank algorithm, λ, to 0.85, which is the common practice (Mihalcea & Tarau, 2004; Florescu & Caragea, 2017; Biswas, Bordoloi, & Shreya, 2018). We evaluated the proposed initial node weighting procedures for 2, 4, 6, 8, 10, and 15 keywords. In the subsequent tables, cells highlighted in yellow indicate the highest scores.

4.2. Results

In Table 1, we report the recall results. As the results show, WP achieved the best results for the WWW and KDD datasets. For the Nguyen dataset, WP achieved the best score for four cases and SP for three cases. For the SemEval2010 dataset, best scores are obtained for SP and SPB. For the SemEval2017, SP achieved the best score for five cases and SPB for three cases. For the Inspec dataset, SP achieved the best score for five cases, WP for one case, and SPB for one case. WPB did not score any best result.

In Table 2, we report the precision results. WP achieved the highest results for the WWW and KDD datasets for all cases, and all but for the Inspec dataset. For SemEval2010, SemEval2017, and Inspec datasets, SP and SPB achieved the best results for the most of the cases. More specifically, for the SemEval2010 dataset, SP achieved the best result for all cases and SPB for three cases. For the SemEval2017 dataset, SP achieved the best result for five cases, and SPB for three. For the Inspec dataset, SP achieved the best results for five cases, WP and SPB for one cases. Similar to recall results, WPB did not score any best result.

Table 1. Recall results.

Dataset	Method	R@2	R@4	R@6	R@8	R@10	R@15
WWW	WP	0.057	0.105	0.138	0.16	0.178	0.206
	SP	0.044	0.09	0.12	0.142	0.16	0.194
	WPB	0.041	0.082	0.112	0.137	0.153	0.186
	SPB	0.045	0.089	0.115	0.138	0.159	0.193
KDD	WP	0.06	0.121	0.161	0.188	0.207	0.234
	SP	0.052	0.108	0.15	0.171	0.184	0.23
	WPB	0.05	0.091	0.131	0.16	0.179	0.211
	SPB	0.05	0.105	0.144	0.163	0.182	0.225
Nguyen	WP	0.041	0.082	0.112	0.145	0.164	0.198
	SP	0.042	0.08	0.112	0.137	0.16	0.201
	WPB	0.028	0.074	0.106	0.13	0.149	0.186
	SPB	0.04	0.079	0.111	0.134	0.158	0.198
SemEval2010	WP	0.018	0.032	0.047	0.06	0.07	0.09
	SP	0.019	0.036	0.049	0.063	0.073	0.095
	WPB	0.017	0.028	0.044	0.058	0.069	0.091
	SPB	0.019	0.035	0.05	0.063	0.073	0.094
SemEval2017	WP	0.049	0.092	0.131	0.168	0.2	0.272
	SP	0.052	0.098	0.141	0.176	0.208	0.279
	WPB	0.049	0.094	0.131	0.169	0.2	0.27
	SPB	0.052	0.096	0.138	0.172	0.21	0.279
Inspec	WP	0.065	0.107	0.144	0.174	0.2	0.248
	SP	0.063	0.109	0.148	0.18	0.208	0.257
	WPB	0.062	0.106	0.143	0.173	0.2	0.247
	SPB	0.062	0.108	0.148	0.178	0.207	0.256

Table 2. Precision results.

Dataset	Method	P@2	P@4	P@6	P@8	P@10	P@15
WWW	WP	0.113	0.108	0.094	0.084	0.075	0.059
	SP	0.087	0.089	0.082	0.074	0.067	0.056
	WPB	0.08	0.083	0.077	0.071	0.065	0.053
	SPB	0.088	0.089	0.078	0.072	0.066	0.056
KDD	WP	0.109	0.111	0.099	0.086	0.076	0.058
	SP	0.1	0.101	0.092	0.08	0.068	0.057
	WPB	0.094	0.082	0.079	0.074	0.066	0.052
	SPB	0.097	0.099	0.088	0.075	0.067	0.056
Nguyen	WP	0.196	0.189	0.174	0.168	0.155	0.126
	SP	0.172	0.175	0.165	0.158	0.15	0.129
	WPB	0.141	0.164	0.155	0.147	0.138	0.118
	SPB	0.165	0.167	0.161	0.15	0.144	0.126
SemEval2010	WP	0.136	0.118	0.117	0.112	0.106	0.091
	SP	0.142	0.135	0.123	0.119	0.11	0.097
	WPB	0.123	0.101	0.108	0.108	0.103	0.092
	SPB	0.14	0.131	0.123	0.118	0.11	0.097
SemEval2017	WP	0.383	0.368	0.348	0.335	0.322	0.296
	SP	0.412	0.392	0.376	0.356	0.338	0.306
	WPB	0.382	0.369	0.349	0.339	0.322	0.296
	SPB	0.403	0.381	0.37	0.348	0.339	0.307
Inspec	WP	0.355	0.302	0.278	0.257	0.242	0.214
	SP	0.352	0.313	0.29	0.27	0.255	0.223
	WPB	0.339	0.302	0.279	0.258	0.244	0.214
	SPB	0.346	0.309	0.288	0.267	0.253	0.222

In Table 3, we report the F1 scores. Similar to the recall and precision results, WP achieved the best results for the WWW, KDD, and Nguyen datasets. For the SemEval2010, SemEval2017, and Inspec datasets SP and SPB achieved the highest scores for all scores but 2.

Table 3. F1 score results.

Dataset	Method	F1@2	F1@4	F1@6	F1@8	F1@10	F1@15
WWW	WP	0.073	0.103	0.108	0.107	0.103	0.09
	SP	0.057	0.086	0.094	0.094	0.092	0.084
	WPB	0.052	0.08	0.088	0.091	0.088	0.081
	SPB	0.058	0.086	0.09	0.092	0.091	0.084
KDD	WP	0.075	0.112	0.119	0.115	0.108	0.091
	SP	0.067	0.101	0.111	0.106	0.097	0.09
	WPB	0.063	0.083	0.095	0.098	0.094	0.082
	SPB	0.064	0.098	0.106	0.1	0.096	0.088
Nguyen	WP	0.066	0.106	0.126	0.143	0.146	0.142
	SP	0.063	0.102	0.122	0.135	0.143	0.145
	WPB	0.045	0.095	0.115	0.126	0.132	0.134
	SPB	0.059	0.098	0.12	0.13	0.138	0.143
SemEval2010	WP	0.032	0.05	0.067	0.077	0.084	0.089
	SP	0.034	0.057	0.07	0.082	0.087	0.094
	WPB	0.03	0.043	0.062	0.075	0.081	0.091
	SPB	0.033	0.055	0.07	0.082	0.086	0.095
SemEval2017	WP	0.085	0.144	0.184	0.216	0.238	0.272
	SP	0.091	0.153	0.198	0.227	0.248	0.281
	WPB	0.085	0.145	0.184	0.217	0.237	0.271
	SPB	0.09	0.149	0.195	0.222	0.249	0.281
Inspec	WP	0.106	0.151	0.18	0.197	0.208	0.22
	SP	0.104	0.155	0.186	0.205	0.218	0.228
	WPB	0.101	0.15	0.18	0.197	0.209	0.219
	SPB	0.102	0.153	0.186	0.203	0.216	0.227

As seen from the results, WP performs better for WWW, KDD, and Nguyen datasets while SP performs better for SemEval2010, SemEval2017, and Inspec. To understand why SP and WP perform better for different datasets, we analyzed the spatial distribution of the author assigned keywords in the documents. As seen in Figure 1, keywords of SemEval2010 and SemEval2017 are evenly distributed within the documents. However, for

KDD and WWW keywords are mostly clustered at the beginning of the documents. As WP assigns higher weights to words that appear early in a document, it performs better than SP for KDD and WWW. On the other hand, SP assigns weights in a more gradual manner, and assigns higher weights to words that appear at the end of a document. The Nguyen and Inspec datasets do not pose such a clear difference with respect to the spatial distribution of the keywords, however decrease in the frequency of the keywords that occur in at the very end are sharper for the Nguyen dataset. This may be the reason SP performs better for Inspec compared to Nguyen.

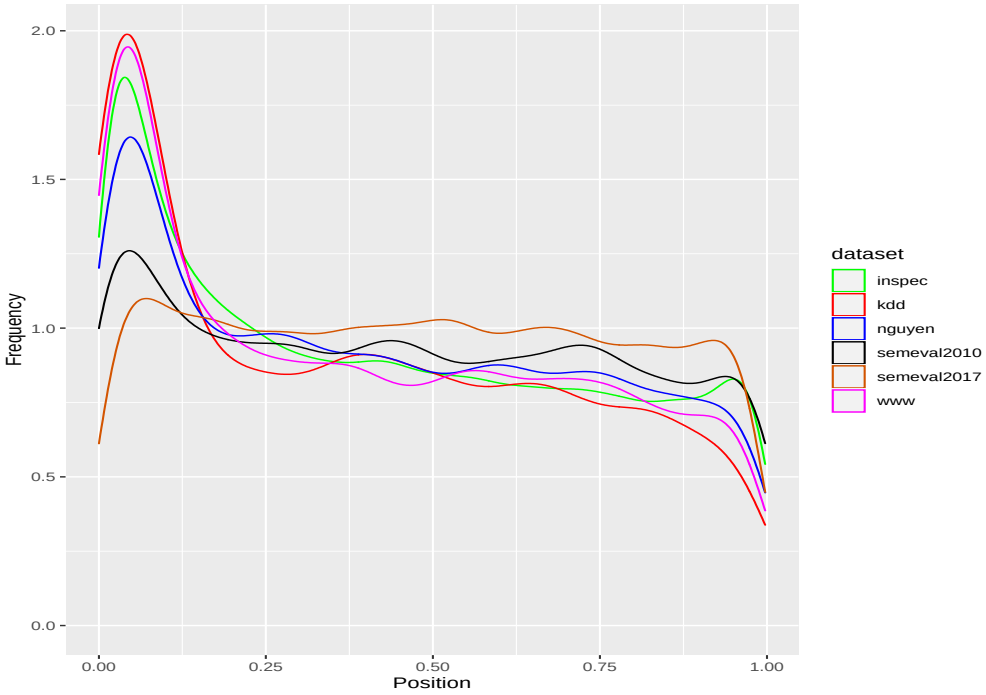

Figure 1. Spatial distribution of the author assigned keywords within documents.

We also statistically analyzed the performance of the weighting procedures. To this aim we conducted the Friedman's test to see if weighting procedures statistically differ, and if so, we conducted the Nemenyi post-hoc test to

detect the differing weighing procedures. In Figure 2, we report the Nemenyi test results. More specifically, in Figure 2.a, we compare all methods considering all datasets. In Figure 2.b, we compare all methods for KDD, WWW, and Nguyen dataset where WP performs better compared to the other methods. In Figure 2.c, we compare all methods for SemEval2010, SemEval2017, and Inspec dataset where SP performs better than the other methods.

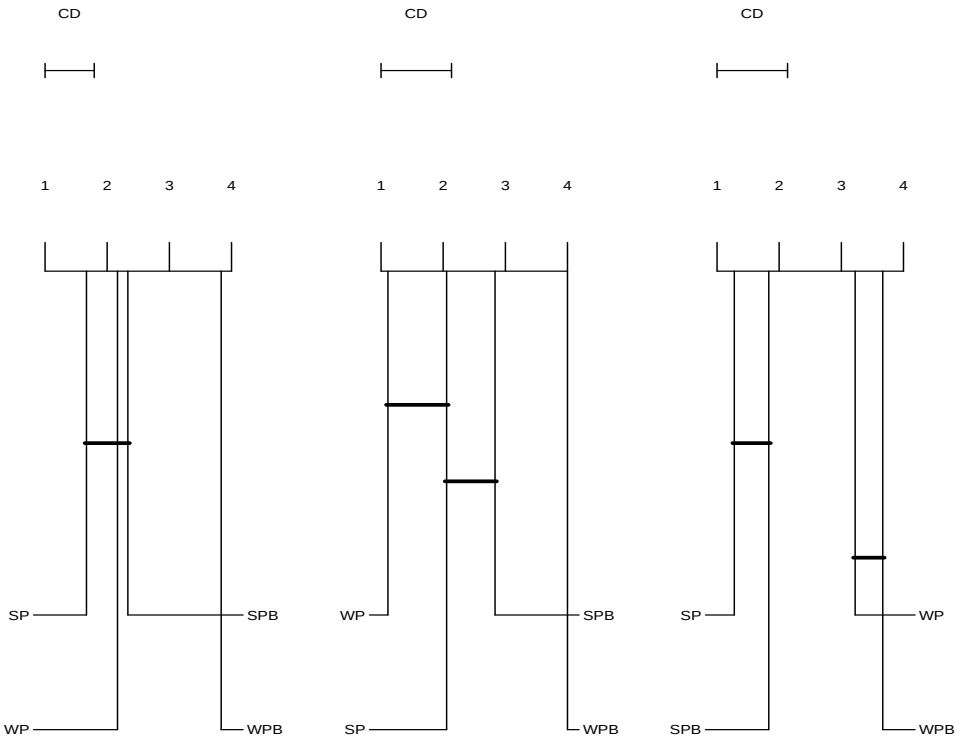

p=2.2e-16 p=2.2e-16 p=4.441e-16

(a) **(b)** **(c)**

Figure 2. Nemenyi pot-hoc test results.

As seen in Figure 2(a), when all datasets are considered, SP, WP, and SPB do not statistically differ, however, SP ranks the top. WPB statistically differs from the other weighting procedures and ranks the least. In case of the WWW, KDD, and Nguyen datasets, WP ranks the top but does not statistically differ from SP. When considered for the SemEval2010, SemEval2017, and Inspec datasets, SP ranks the best, SPB ranks the second best, however, they do not statistically differ. SP and SPB statistically differ from WB, which ranks third.

As the experimental results show, WPB did not perform well for any of the datasets. We believe that this is due to the shortness of the text. Moreover, the last words in scientific publication abstracts report some experimental finding, which are not likely to be keywords.

In Table 4, we compare performance of WP and SP to three statistical keyword extraction systems, namely TF.IDF, KP-Miner, and Rake; and to a supervised keyword extraction system KEA. The results of the reference methods are reported in (Campos et al., 2020). The results report F1 score for 10 keywords, and the best scores are highlighted. As the results indicate, TF.IDF, KP-Miner, and SP score the best results for two datasets. Although supervised approach did not score any top results regarding the six datasets used in this study, (Campos et al., 2020) reports several datasets for which KEA ranks best.

Table 4. Comparison to other systems, F1@10.

	WP	SP	TF.IDF	KP-Miner	RAKE	KEA
WWW	0.103	0.092	0.130	0.037	0.011	0.072
KDD	0.108	0.097	0.115	0.036	0.006	0.063
Nguyen	0.146	0.143	0.225	0.314	0.002	0.221
SemEval2010	0.084	0.087	0.177	0.261	0.003	0.215
SemEval2017	0.238	0.248	0.181	0.071	0.065	0.201
Inspec	0.208	0.218	0.155	0.047	0.052	0.150

5. CONCLUSION

In this study, we evaluated the performance of three initial node weighting procedures for graph based keyword extraction and compared them against PositionRank's initial node weight assignment procedure. The first procedure, namely WPB, considers positions of the words and assigns higher weights to words that are either at the beginning or at the end of a text. The second procedure, namely SP, assigns higher weights to words that appear in the sentences close to the beginning of the text relative to the position of sentence. The last procedure, namely SPB, assigns higher weights to words that appear in the sentences either close to the beginning of the text or end of the text, relative to the position of the sentences. Hence, WPB assigns weights to words that steeply decrease while SP and SPB assign gradually decreasing weights. Experiments show that, WP performs better for documents whose keywords appear close to the beginning of the document, while SP and SPB perform better for documents whose keywords are evenly spread within the text.

ACKNOWLEDGEMENT

This work is partially supported by TUBITAK with grant number 117E566.

REFERENCES

Armouty, B., & Tedmori, S. (2019). "Automated Keyword Extraction using Support Vector Machine from Arabic News Documents". In *2019 IEEE Jordan International Joint Conference on Electrical Engineering and Information Technology (JEEIT)*, IEEE, 342-346. doi:10.1109/JEEIT.2019.8717420.

Anju, R. C., Ramesh, S. H., & Rafeeque, P. C. (2018). "Keyphrase and Relation Extraction from Scientific Publications". In Damodar Reddy Edla, Pawan Lingras, and Venkatanareshbabu K. (Eds), *Advances in Machine Learning and Data Science: Recent Achievements and Research Directives* (pp. 113-120). Vol. 705, Singapore, Springer.

Augenstein, I., Das, M., Riedel, S., Vikraman, L., & McCallum, A. (2017). "Semeval 2017 Task 10: ScienceIE-Extracting Keyphrases and Relations from Scientific Publications". arXiv preprint arXiv:1704.02853. Retrieved from https://arxiv.org/pdf/1704.02853.pdf

Azcarraga, A., Liu, M. D., & Setiono, R. (2012, June). "Keyword extraction using backpropagation neural networks and rule extraction". In *the 2012 International Joint Conference on Neural Networks (IJCNN)*, IEEE, 1-7. doi:10.1109/IJCNN.2012.6252618.

Beliga, S. (2014). "Keyword Extraction: A Review of Methods and Approaches". University of Rijeka, Department of Informatics, Rijeka, 1-9.

Bellaachia, A., & Al-Dhelaan, M. (2014). "HG-Rank: A Hypergraph-based Keyphrase Extraction for Short Documents in Dynamic Genre". In *#MSM, #Microposts2014, 4th Workshop on Making Sense of Micropost*, 42-49.

Biswas, S. K. (2019). "Keyword Extraction from Tweets Using Weighted Graph". In Pradeep Kumar Mallick, Valentina Emilia Balas, Akash Kumar Bhoi, and Ahmed F. Zobaa (Eds.), *Cognitive Informatics and Soft Computing: Proceeding of CISC 2017* (pp. 475-483). Vol 768, Singapore, Springer.

Biswas, S. K., Bordoloi, M., & Shreya, J. (2018). "A graph based keyword extraction model using collective node weight". *Expert Systems with Applications,* Vol. 97, 51-59. doi:10.1016/j.eswa.2017.12.025.

Brin, S., & Page, L. (1998). "The anatomy of a large-scale hypertextual web search engine". *Computer Networks and ISDN Systems.* Vol. 30, Issues 1-7, 107-117.

Campos, R., Mangaravite, V., Pasquali, A., Jorge, A., Nunes, C., & Jatowt, A. (2020). "YAKE! Keyword extraction from single documents using multiple local features". *Information Sciences,* Vol. 509, 257-289. doi:10.1016/j.ins.2019.09.013.

Ercan, G., & Cicekli, I. (2007). "Using lexical chains for keyword extraction". *Information Processing & Management,* 43(6), 1705-1714. doi:10.1016/j.ipm.2007.01.015.

Florescu, C., & Caragea, C. (2017). "Positionrank: An unsupervised approach to keyphrase extraction from scholarly documents". In *Proceedings of the 55th Annual Meeting of the Association for Computational Linguistics*, Vol. 1, 1105-1115.

Gollapalli, S. D., & Caragea, C. (2014). "Extracting keyphrases from research papers using citation networks". In *AAAI'14: Proceedings of the Twenty-Eighth AAAI Conference on Artificial Intelligence*, 28(1), 1629-1635.

Hulth, A. (2003). "Improved automatic keyword extraction given more linguistic knowledge". In *Proceedings of the 2003 Conference on Empirical Methods in Natural Language Processing*, 216-223.

Kim, S. N., Medelyan, O., Kan, M.-Y., & Baldwin, T. (2010). "SemEval-2010 Task 5 : Automatic Keyphrase Extraction from Scientific Articles". In *Proceedings of the 5th International Workshop on Semantic Evaluation*, 21-26.

Kleinberg, J. M. (1999). "Authoritative sources in a hyperlinked environment". *Journal of the ACM (JACM),* 46(5), 604-632.

Lynn, H. M., Lee, E., Choi, C., & Kim, P. (2017). "SwiftRank: An Unsupervised Statistical Approach of Keyword and Salient Sentence Extraction for Individual Documents". *Procedia Computer Science,* Vol. 113 , 472-477.

Mihalcea, R., & Tarau, P. (2004). "Textrank: Bringing order into text". In *Proceedings of the 2004 Conference on Empirical Methods in Natural Language Processing,* 404-411.

Nguyen, T. D., & Kan, M.-Y. (2007). "Keyphrase Extraction in Scientific Publications". In *10th International Conference on Asian Digital Libraries, ICADL 2007,* DBLP, 317-326.

Ni, W., Liu, T., & Zeng, Q. (2012). "Extracting keyphrase set with high diversity and coverage using structural svm", In APWeb'12: Proceedings of the 14th Asia-Pacific international conference on Web Technologies and Applications, 122-133.

Patel, K., & Caragea, C. (2019). "Exploring word embeddings in crf-based keyphrase extraction from research papers". In *K-CAP '19: Proceedings of the 10th International Conference on Knowledge Capture*, 37-44.

Pereira, D. G., Afonso, A., & Medeiros, F. M. (2015). "Overview of Friedman's test and post-hoc analysis". *Communications in Statistics-Simulation and Computation,* 44(10), 2636-2653.

Pohlert, T. (2016). "The Pairwise Multiple Comparison of Mean Ranks Package (PMCMR)". *R package.* Retrieved from https://cran.r-project.org/web/packages/PMCMR/vignettes/PMCMR.pdf

Sun, P., Wang, L., & Xia, Q. (2017). "The Keyword Extraction of Chinese Medical Web Page Based on WF-TF-IDF Algorithm". In *2017 International Conference on Cyber-enabled Distributed Computing and Knowledge Discovery (CYBERC)*, 193-198. Retrieved from https://ieeexplore.ieee.org/stamp/stamp.jsp?tp=&arnumber=8250358&tag=1

Tafti, A. P., Wang, Y., Shen, F., Sagheb, E., Kingsbury, P., & Liu, H. (2019). "Integrating word embedding neural networks with pubmed abstracts to extract keyword proximity of chronic diseases". In *2019 IEEE EMBS International Conference on Biomedical & Health Informatics (BHI)*, 1-4.

Thushara, M. G., Krishnapriya, M. S., & Nair, S. S. (2018). "Domain Classification of Research Papers Using Hybrid Keyphrase Extraction Method". In Pankaj Kumar Sa, Sambit Bakshi, Ioannis K. Hatzilygeroudis, and Manmath Narayan Sahoo (Eds.), *Recent Findings in Intelligent Computing Techniques : Proceedings of the 5th ICACNI* (pp. 387-398). Vol. 708, Singapore, Springer.

Tixier, A., Malliaros, F., & Vazirgiannis, M. (2016). "A Graph Degeneracy-based Approach to Keyword Extraction". In *Proceedings of the 2016 Conference on Empirical Methods in Natural Language Processing*, 1860-1870.

Yao, L., Pengzhou, Z., & Chi, Z. (2019). "Research on News Keyword Extraction Technology Based on TF-IDF and TextRank". In 2019 IEEE/ACIS 18th International Conference on Computer and Information Science (ICIS), 452-455.

Journal of Naval Sciences and Engineering
2021, Vol. 17, No. 2, pp. 241-263
Industrial Engineering/Endüstri Mühendisliği

RESEARCH ARTICLE

**An ethical committee approval and/or legal/special permission has not been required within the scope of this study.*

A LAGRANGEAN RELAXATION-BASED SOLUTION APPROACH FOR MULTICOMMODITY NETWORK DESIGN PROBLEM WITH CAPACITY VIOLATIONS*

Levent ERİŞKİN[1]

[1]*National Defence University, Turkish Naval Academy, Department of Industrial Engineering, Istanbul, Turkey,*
leriskin@dho.edu.tr; ORCID: 0000-0002-9128-2167

Received: 04.05.2021 **Accepted: 25.06.2021**

ABSTRACT

In this study, we formulate and compare two different Lagrangean relaxation-based decompositions for multicommodity network problems with penalized constraints. These problems are different versions of capacitated multicommodity network problems where capacity constraints can be violated for additional penalty costs. These costs are reflected as nonlinear terms in the objective function; hence, these problems turn out to be nonlinear mixed-integer optimization problems. To the best of our knowledge, there is no exact solution algorithm for this type of problem. We propose two kinds of Lagrangean relaxation-based decompositions and solve these problems with the subgradient algorithm. The resulting subproblems are easy to solve and the proposed algorithms can reach reasonable solutions where CPLEX solver cannot even find a solution. In the study, we also conduct a computational analysis where we compare two relaxations over various performance measures. Even though two relaxations present similar performances in terms of computation times and the number of iterations, we observed that Relaxation 1 statistically outperforms Relaxation 2.

Keywords: *Multicommodity Network Design Problem, Lagrangean Relaxation, Subgradient Algorithm, Decomposition.*

A Lagrangean Relaxation-based Solution Approach for Multicommodity Network Design Problem with Capacity Violations

KAPASİTE İHLALLİ ÇOKLU MAL ŞEBEKE DİZAYN PROBLEMİ İÇİN LAGRANGEAN GEVŞETMESİ TABANLI BİR ÇÖZÜM YAKLAŞIMI

ÖZ

Bu çalışmada, cezalandırıcı kısıtlara sahip çoklu mal şebeke problemi için Lagrangean gevşetmesi tabanlı iki farklı ayrıştırma yaklaşımı formüle edilmekte ve karşılaştırılmaktadır. Bu problemler kapasite kısıtlarının ilave bir ceza maliyeti ile ihlal edilebilediği kapasite kısıtlı çoklu mal şebeke problemlerinin farklı versiyonlarıdır. Bu maliyetler amaç fonksiyonuna doğrusal olmayan terimler olarak yansıtılmakta, bu kapsamda bu problemler doğrusal olmayan karışık tam sayılı eniyileme problemlerine dönüşmektedir. Bilgimiz dahilinde, bu tip problemlerin çözümü için herhangi bir kesin çözüm algoritması bulunmamaktadır. Bu problemler için iki farklı Lagrangean gevşetmesi tabanlı ayrıştırma teklif etmekte ve gradyant altı algoritması ile çözmekteyiz. Ortaya çıkan alt-problemler kolaylıkla çözülebilmekte ve önerilen algoritmalar CPLEX çözücünün herhangi bir çözüm bile bulamadığı durumlar için makul sonuçlar elde etmektedir. Çalışmada ayrıca bu iki gevşetmenin farklı performans metrikleri bazında karşılaştırmasının yapıldığı bir hesaplamalı analiz de yapmaktayız. Her ne kadar iki gevşetme de çözüm süresi ve iterasyon adedi açısından benzer performanslar gösterse de Gevşetme 1'nin istatistiksel olarak Gevşetme 2'den daha üstün olduğunu gözlemledik.

Anahtar Kelimeler: *Çoklu Mal Şebeke Dizayn Problemi, Lagrangean Gevşetmesi, Gradyan Altı Algoritması, Ayrıştırma.*

1. INTRODUCTION

Multicommodity network flow (MCNF) problems are used extensively in operations research or management applications such as production scheduling and planning, transportation, and routing where more than one commodity is to be shipped over a network from a designated origin node to a destination node. There are mainly three types of MCNF problems: max MCNF problem, the max-concurrent flow problem, and min-cost MNCF problem (Wang, 2018a). In max MCNF problem sum of all flows of commodities is aimed to be maximized. Max-concurrent flow problem maximizes the percentage of satisfied demands of all commodities. Min-cost MCNF, on the other hand, aims to satisfy all demands for all commodities by finding a feasible assignment of flows to arcs. For this problem type, the major variant is incapacitated MCNF where there are no capacity limits enforced for arcs.

Even though min-cost MCNF models arise in different forms, two of them are mostly seen. These are network routing and network design problems (Wang, 2018a). Network routing problems seek a feasible assignment of flows to arcs for all commodities with a minimum cost without violating the capacity constraints of arcs. Network routing problems are usually seen in telecommunication and warehouse management applications (Yousefi Nejad Attari et al., 2020). In network design problems, we design a network on a given graph by determining which arcs to include in the network and the amount of flow on a given arc by satisfying the demands of all commodities. In capacitated version, the capacities of arcs cannot be violated. Network design problems have numerous applications in transportation, postal services, and telecommunication (Ghaffarinasab et al., 2020).

In this study, we consider a min-cost multicommodity network design problem where arc capacities can be violated for a penalty cost. The penalty cost for excess flow on an arc is reflected in the objective function on quadratic form; hence, the problem turns out to be a nonlinear mixed-integer multicommodity network flow problem. As Bektaş et al. (2010) remark, there is no exact solution method for this type of problem. In this respect, we consider two types of Lagrangean-based decompositions, one of which

was proposed by Bektaş et al. (2010) as flow decomposition. These decompositions yield subproblems that can be solved efficiently compared to the original problem. To find solutions for these decompositions, we employ a subgradient algorithm. With this study, we aim to contribute to the MNCF literature by introducing various solution techniques.

The study is organized as follows: Section 2 provides a literature review for the problem. In section 3 we formulate the problem and present two different decompositions. Additionally, we give details of the algorithm based on subgradient optimization in this section. Section 4 gives details of an empirical study conducted for comparing two decompositions on a test set. Finally, we conclude in Section 5.

2. LITERATURE REVIEW

Being very popular among many scheduling, routing, and transportation applications, MNCF problems are well studied in the literature. In his paper, Wang (2018a) surveys the last three decades and provides a summary for applications and various mathematical formulations for MCNF problems. Focusing mainly on min-cost MCNF problems, he remarks that most of the MCNF problems are formulated as network routing and network design problems. In his follow-up paper, Wang (2018b) surveys MCNF solution methods that are proposed in the literature. He classifies solution methods as; primal and dual-based solution methods, approximation methods, interior-point methods, and convex programming methods.

Among solution approaches, Holmberg and Yuan (2000) propose a branch and bound algorithm for knapsack relaxation of the multicommodity capacitated network design problem. Utilizing a subgradient algorithm having additional features such as special penalty tests and cutting criteria, they show that they obtain optimal solutions in very short computation times with respect to commercial software packages. Regarding the Lagrangean-relaxation approach, Crainic et al. (2001) studied different relaxation techniques for large-scale capacitated MCNF problems. They propose two types of relaxations for the problem: by relaxing the capacity constraints they get a shortest path relaxation and by relaxing the network flow constraints they get knapsack relaxation. They utilize a bundle-based

algorithm and subgradient method for solving them. They remark that both solution approaches perform well provided that the subgradient method is tuned properly. Costa (2005) focuses on applications of Benders decomposition to MCNF network design problems and presents a review of these applications. Katayama et al. (2009) propose a capacity scaling heuristic by utilizing a column generation and row generation technique for solving multicommodity capacitated network design problems. Combining row and column generation techniques, their proposed heuristic generates high-quality results based on computational experiments involving 196 problem instances. Alysson et al. (2009) compare three sets of inequalities that are used for strengthening the multicommodity capacitated network design problem formulation. They show that theoretical results apply to any network design problem for which feasible solutions are obtained by solving subproblems. Karsten et al. (2015) study a multicommodity network flow problem where a time constraint is imposed and apply it to a liner shipping network design case. The problem imposes time limits on the duration of the transit of the commodities through the network. They remark that ignoring time constraints results in significant differences in revenues compared to solving the same problem while these constraints are imposed. Considering that time constraints make the problem more complex, they propose an algorithm to reduce computation times. They show that the proposed technique solves the problem in reasonable times. Moradi et al. (2015) present a column generation algorithm for solving a bi-objective problem. Their approach is based on bi-objective simplex and Dantzig-Wolfe decomposition. They start the methodology by solving a single objective MCNF problem with Dantzig-Wolfe decomposition. Afterward, the algorithm moves from one non-dominated extreme point to another, as in simplex until there is no entering variable left. Gendron and Gouveia (2016) consider the piecewise linear multicommodity network design problem with an additional constraint enforcing that the total flow on each arc must be an integer. These types of problems are common in transportation and logistics because the total flow might be represented with vehicles or containers. They propose a formulation by using discretization which is commonly used in mixed-integer programming. They develop a Lagrangean relaxation solution approach and show that their approach is efficient and effective. Chouman et al. (2018) propose a novel branch-and-cut algorithm for solving

multicommodity capacitated fixed charge network design problem. They incorporate several filtering methods to the algorithm that exploits the structure of the problem. Thus, they inhibit combinations of values of some variables. They show that filtering significantly improves the performance of the branch-and-cut algorithm. Oğuz et al. (2018) consider restricted continuous facility location problems where location of a facility can be anywhere on the planet except for in restricted regions. They model the problem as a MCNF problem and propose Benders decomposition algorithm to find the optimal solution to the model. They conduct computational experiments and show that the proposed method outperforms commercial solvers.

Among newer studies dealing with MNCF problems, Anisi and Fathabadi (2019) consider the survivable multicommodity network design with node capacities and flow restrictions. Being a variant of the multicommodity network design problem, these problems aim to minimize the cost of failure in addition to design cost. The design aims to ensure a feasible flow in case of a simultaneous failure on arcs. They utilize Benders decomposition to solve the problem as well as a new approach that considers particular failure scenarios. Guimaraes et al. (2020) studied a variant of the MNCF problem where multiple transport lines and time windows are considered. They proposed two mixed-integer programming models and two objective functions, in particular, minimization of network operational costs and minimization of travel times. Trivella et al. (2021) studied a generalization of MCNF where transit time restrictions are modeled as soft constraints and delays are penalized. Kazemzadeh et al. (2021) introduced node-based Lagrangian relaxation where the resulting subproblem decomposes by nodes.

There are not many studies that deal with nonlinear integer multicommodity network design problems. Crainic and Rousseau (1986) study a nonlinear mixed-integer multicommodity network flow problem. They present an algorithm combining heuristics and optimization. Belotti et al. (2007) consider a multicommodity network design problem with discrete node costs. Costs are defined as stepwise functions of facilities installed at these nodes. They propose a branch-and-cut algorithm for solving the problem. Bektaş et al. (2010) propose Lagrangean-based decomposition algorithms

for multicommodity network design problems where arc capacities can be violated at the expense of a penalty. This penalty adds nonlinear cost to the min-cost objective function. They propose two decompositions: flow decomposition that is obtained by relaxing capacity constraints, and arc decomposition that is obtained by relaxing flow constraints. They show that with the help of a special algorithm developed to solve subproblems in arc decomposition, arc decomposition performs better in terms of convergence but worse in terms of computation time and the number of iterations. Paraskevopoulos et al. (2016) study a variant of fixed-charge multicommodity network design problem having additional congestion costs. They model the problem as a nonlinear integer programming model, and they propose two solution approaches. The first solution approach is the reformulation of the problem as a mixed-integer second-order cone program. The second uses an evolutionary algorithm combining iterated local search and scatter search. They remark that the first solution approach provides satisfactory results provided that conic representations of nonlinear terms are available. Additionally, they observe that the evolutionary algorithm is not only satisfactory but also achieves good quality solutions in short computational times.

For a recent survey regarding classification, applications, and solution methods of MNCF problems, the interested reader is referred to Salimifard and Bigharaz (2020).

3. PROBLEM FORMULATION AND OPTIMIZATION WITH LAGRANGEAN RELAXATION

We formulate the min-cost multicommodity network flow problem with capacity violations in harmony with the definition of Bektaş et al. (2010). We have a graph of $G = (N, A)$ where N corresponds to set of nodes and A corresponds to set of arcs. Two different sets $N_i^+ = \{j \in N | (i,j) \in A\}$ and $N_i^- = \{j \in N | (j,i) \in A\}$ are defined for each node. We have a set of commodities P. In this respect, we formulate the problem as follow:

Parameters:

B_{ij}: Upper bound on the amount of excess flow on each arc

f_{ij}: Fixed cost of activating a network

w^p: Quantity of commodity p that is to be sent from $o(p)$ to $d(p)$

$d_i^p = w^p$ if $i = o(p)$, $d_i^p = -w^p$ if $i = d(p)$

c_{ij}^p: The unit cost of routing the demand for commodity p over arc (i,j)

u_{ij}: Capacity of arc (i,j)

C_{ij}: Penalty cost for excess flow on arc (i,j)

Decision Variables:

x_{ij}^p: The amount of commodity p flowing on arc (i,j) where $x_{ij}^p \geq 0$

y_{ij}: Design variable for selecting arc (i,j) where $y_{ij} \in \{0,1\}$

e_{ij}: Excess flow on arc (i,j) where $e_{ij} \geq 0$.

The Model:

$$(F) \qquad Minimize \sum_{(i,j)\in A} f_{ij}\, y_{ij} + \sum_{(i,j)\in A} \sum_{p\in P} c_{ij}^p\, x_{ij}^p + \sum_{(i,j)\in A} C_{ij}(e_{ij})^2 \qquad \textbf{(1)}$$

$Subject\ to$

$$\sum_{j\in N_i^+} {x_{ij}}^p - \sum_{j\in N_i^-} {x_{ji}}^p = {d_i}^p \qquad \forall i \in N, p \in P \qquad \textbf{(2)}$$

$$x_{ij}^p \leq w^p y_{ij} \qquad \forall (i,j) \in A, p \in P \qquad \textbf{(3)}$$

$$\sum_{p\in P} {x_{ij}}^p \leq u_{ij} y_{ij} + e_{ij} \qquad \forall (i,j) \in A \qquad \textbf{(4)}$$

$$e_{ij} \leq B_{ij} y_{ij} \qquad \forall (i,j) \in A \qquad \textbf{(5)}$$

$$x_{ij}^{p} \geq 0,\ e_{ij} \geq 0, y_{ij} \in \{0,1\} \qquad \forall (i,j) \in A, p \in P \qquad \textbf{(6)}$$

The penalty term $(e_{ij})^2$ adds nonlinearity to the formulation. This term is quadratic in our formulation, however, the power of this term could be cubic or higher, as well (Bektaş et al., 2010). Constraint (2) is the flow conservation constraint, Constraint (3) ensures that flow of an arc is positive provided that it is selected, Constraint (4) enforces that total flow on an arc should be less than and equal to the sum of the capacity of that arc and excess flow on that arc, Constraint (5) imposes that maximum amount of excess flow on an arc cannot be more than a predefined value and can be positive unless it is selected.

This problem is a nonlinear mixed-integer problem and as Bektaş et al. (2010) remark, there exists no exact solution method proposed in the literature. In this respect, we define two different Lagrangean relaxations for the problem. Lagrangean relaxation aims to get rid of complicating constraints by adding them to the objective function by multiplying them with Lagrengean multipliers so that the resulting problem can be partitioned into small subproblems which can be solved relatively easily. The Lagrangean relaxation approach is classified as price-directive methods since Lagrangean multipliers place prices on the dualized constraints (Ahuja et al., 1993). In this respect, this technique aims to find proper prices so that an optimal solution to the Lagrangean subproblem provides a solution to the main problem.

3.1. Relaxation 1

This relaxation is proposed by Bektaş et al. (2010) and obtained by relaxing capacity constraints (Constraint sets (3) and (4)). By defining Lagrangean variables μ_{ij}^{p} and σ_{ij} for these constraint sets respectively, we formulate the relaxed problem as follows.

$$(LR1) \qquad Min \sum_{(i,j)\in A} [f_{ij} - \sum_{p\in P} \mu_{ij}^p w^p - \sigma_{ij} u_{ij}] y_{ij} + \sum_{(i,j)\in A} \sum_{p\in P} (c_{ij}^p + \mu_{ij}^p + \sigma_{ij})\, x_{ij}^p + \sum_{(i,j)\in A} \left[C_{ij}(e_{ij})^2 - \sigma_{ij} e_{ij}\right] \quad \textbf{(7)}$$

$$Subject\ to \qquad (2), (5), (6) \quad \textbf{(8)}$$

We can decompose $(LR1)$ into two subproblems. The first subproblem is defined over y and e variables. As shown by Bektaş et al. (2010), this problem can be solved by inspection.

$$(SP1) \qquad Min \sum_{(i,j)\in A} [f_{ij} - \sum_{p\in P} \mu_{ij}^p w^p - \sigma_{ij} u_{ij}] y_{ij} + C_{ij}(e_{ij})^2 - \sigma_{ij} e_{ij} \quad \textbf{(9)}$$

$$Subject\ to \qquad (5) \quad \textbf{(10)}$$

We define the second problem over x variables as shown below.

$$(SP2) \qquad Min \sum_{(i,j)\in A} \sum_{p\in P} (c_{ij}^p + \mu_{ij}^p + \sigma_{ij})\, x_{ij}^p \quad \textbf{(11)}$$

$$Subject\ to \qquad (2) \quad \textbf{(12)}$$

This problem can be decomposed into $|P|$ single commodity minimum cost network problems. We know that this problem is well-solved in the sense that an efficient algorithm is known. We can use the shortest path algorithm to solve each of these problems.

3.2. Relaxation 2

The second relaxation dualizes constraint sets (3), (4), and (5). We define nonnegative Lagrangean variables μ_{ij}^p, σ_{ij}, and γ_{ij} for these constraint sets respectively and formulate the relaxed problem as follows.

$$(LR2) \qquad Min \sum_{(i,j)\in A} [f_{ij} - B_{ij}\gamma_{ij} - \sum_{p\in P} \mu_{ij}^{p}\, w^{p} - \sigma_{ij}u_{ij}]y_{ij} + \sum_{(i,j)\in A} \sum_{p\in P} (c_{ij}^{p} + \mu_{ij}^{p} + \sigma_{ij})\, x_{ij}^{p} + \sum_{(i,j)\in A} \left[C_{ij}(e_{ij})^{2} - (\gamma_{ij} - \sigma_{ij})e_{ij}\right] \quad \textbf{(13)}$$

$$Subject\ to \qquad (2) \quad \textbf{(14)}$$

This problem can be decomposed into 3 subproblems. The first problem is defined over x variables.

$$(SP1) \qquad Min \sum_{(i,j)\in A} \sum_{p\in P} (c_{ij}^{p} + \mu_{ij}^{p} + \sigma_{ij})\, x_{ij}^{p} \quad \textbf{(15)}$$

$$Subject\ to \qquad (2) \quad \textbf{(16)}$$

This subproblem decomposes into a set of minimum cost network flow problems for each commodity p. Therefore, we need to solve $|P|$ minimum cost network flow problems.

The second subproblem is defined over y variables and formulated as follows. This problem is an unconstrained binary optimization problem and can be solved by inspection easily.

$$(SP2) \qquad Min \sum_{(i,j)\in A} [f_{ij} - B_{ij}\gamma_{ij} - \sum_{p\in P} \mu_{ij}^{p}\, w^{p} - \sigma_{ij}u_{ij}]y_{ij} \quad \textbf{(17)}$$

The last subproblem is defined over e variables.

$$(SP3) \qquad Min \sum_{(i,j)\in A} \left[C_{ij}(e_{ij})^{2} - (\gamma_{ij} - \sigma_{ij})e_{ij}\right] \quad \textbf{(18)}$$

This problem is a quadratic nonlinear programming problem. Since e_{ij} nonnegative, this is a convex function with a unique minimum. That is, the second derivative is positive and thus the solution to the first derivative gives the unique minimum. Therefore, this problem is easy to solve, too (Bektaş et al., 2010).

3.3. Optimization with Subgradient Algorithm

The subgradient algorithm is an easy and simple technique to solve non-differentiable Lagrangean multiplier problems. For a given set of multipliers, the relaxed problem provides a Lower Bound (LB) for the original problem. To obtain an Upper Bound (UB), problem F is solved while $(\mathbf{y}, \mathbf{q})$ is fixed to $(\mathbf{y}^*, \mathbf{q}^*)$ where these values correspond to the solution to the relaxed problem. In this case, the resulting problem turns out to be a linear programming problem. The subgradient algorithm is shown in Figure 1.

Define:

t: Number of iterations

s^t: Step size at each iteration

SP_1, SP_2, SP_3: Optimal objective values for $SP1, SP2, SP3$, respectively.

W_{LD}: Optimal objective value for the Lagrangean problem.

$\phi^t = \begin{pmatrix} {\mu_{ij}}^p \\ {\sigma_{ij}}^p \end{pmatrix}$: Vector of Lagrangean multipliers for Relaxation 1.

$\phi^t = \begin{pmatrix} {\mu_{ij}}^p \\ {\sigma_{ij}}^p \\ {\gamma_{ij}}^p \end{pmatrix}$: Vector of Lagrangean multipliers for Relaxation 2.

$g^t = \begin{pmatrix} {g_{ijp}}^1 \\ {g_{ij}}^2 \\ {g_{ij}}^3 \end{pmatrix}$: Vector of subgradients for $SP1, SP2, SP3$, respectively.

---

1. Initialize $\phi^t = \phi^0$
2. $LB = -\infty$ and $UB = \infty$
3. $t = 1$
4. While $gap = \frac{UB-LB}{UB} \geq \varepsilon$ do

4.1 Solve Lagrangean dual

4.1.1 Solve $SP1$, get $\bar{y}_{ij}$ and $\bar{e}_{ij}$ (Relaxation 1)

Solve $SP1$, get $\bar{x}_{ij}^{p}$ (Relaxation 2)

4.1.2 Solve $SP2$, get $\bar{x}_{ij}^{p}$ (Relaxation 1)

Solve $SP2$, get $\bar{y}_{ij}$ (Relaxation 2)

4.1.3 Solve $SP3$, get $\bar{e}_{ij}$ (Relaxation 2)

4.2 $W_{LD} = SP_1 + SP_2$ (Relaxation 1)

$W_{LD} = SP_1 + SP_2 + SP_3$ (Relaxation 2)

4.3 If $W_{LD} > LB$ then

$$LB = W_{LD}$$

4.4 Solve $\{F_r = F|\bar{y}_{ij}$ and $\bar{e}_{ij}$ values are fixed$\}$ and get ${F_r}^*, {x_{ij}}^{p^*}$

4.5 $$UB = {F_r}^* - \sum_{(i,j)\in R} f_{ij} \quad \text{where } R = \{(i,j) \in A | {y_{ij}}^* = 1 \ and \ \sum_{p\in P} {x_{ij}}^{p^*} = 0\}$$

4.6 Calculate subgradients

4.6.1 $${g_{ijp}}^1 = \bar{x}_{ij}^{p} - w^p \bar{y}_{ij} \quad \forall (i,j) \in A, p \in P$$

$${g_{ij}}^2 = \sum_{p\in P} x_{ij}^{p} - u_{ij}\bar{y}_{ij} - \bar{e}_{ij} \quad \forall (i,j) \in A$$

$${g_{ij}}^3 = \bar{e}_{ij} - B_{ij}\bar{y}_{ij} \quad \forall (i,j) \in A$$

$$g^t = \begin{pmatrix} {g_{ijp}}^1 \\ {g_{ij}}^2 \end{pmatrix} \text{ (Relaxation 1)}$$

$$g^t = \begin{pmatrix} {g_{ijp}}^1 \\ {g_{ij}}^2 \\ {g_{ij}}^3 \end{pmatrix} \text{ (Relaxation 2)}$$

4.7 Calculate step length

$$s^t = \lambda \frac{UB - W_{LD}}{\|g^t\|^2}$$

4.8 Update Lagrangean multipliers

$$\phi^{t+1} = \phi^t + s^t g^t$$

4.9 $t = t + 1$

5. End while

Figure 1. Subgradient algorithm for the relaxations.

Simplicity of the subgradient algorithm has made it a popular option for solving Lagrangean multiplier problems. At each iteration, the algorithm takes a small step from the current point in the direction opposite to a subgradient. The most important parameter in the algorithm is the step length. One option is to use a constant step length. This option guarantees convergence; however, the convergence is too slow. In this respect, we employ a dynamic step length which provides faster convergence (Wolsey, 1998).

4. COMPUTATIONAL ANALYSIS

We have performed a computational analysis to compare the performances of these two relaxations. For this purpose, we used the first 36 instances defined in Crainic et al. (2001) which are also used by Bektaş et al. (2010). As done by Bektaş et al. (2010), we reduced capacities of arcs in the instances as $u'_{ij} = u_{ij}/2$ and set penalty costs C_{ij} to twice the flow cost of each arc. Subproblems are solved by using IBM ILOG CPLEX 12.5. Additionally, original problem is solved with IBM ILOG CPLEX 12.5 to

evaluate lower bounds achieved. For both relaxations, subgradient algorithm is stopped whenever the gap does not improve for 30 consecutive iterations. The algorithm is coded with Java and run using an Intel Core i7 2.6 GHz. 8 GB RAM computer. Computational results are shown in Table 1.

Table 1. Computational results.

				Relaxation 1				**Relaxation 2**			
Inst.	N	A	P	i	t	g_s	g_0	i	t	g_s	g_0
1.1	10	35	10	128	6.90	0.67	0.67	154	5.10	0.24	0.24
1.2	10	35	10	29	3.14	2.63	0.62	50	3.34	1.80	1.01
1.3	10	35	10	14	1.83	16.61	6.43	22	1.89	9.34	4.99
1.4	10	35	10	18	1.87	29.19	-	18	1.78	28.81	-
1.5	10	35	10	81	3.84	35.86	31.56	94	4.37	33.86	32.22
1.6	10	35	10	95	5.52	27.31	-	92	3.90	27.24	-
2.1	10	35	25	25	3.57	53.78	48.02	22	2.98	19.90	18.48
2.2	10	35	25	102	5.56	71.63	-	102	5.56	32.93	-
2.3	10	35	25	64	6.54	67.94	65.30	62	4.31	41.91	40.53
2.4	10	35	25	33	4.30	72.78	54.32	43	3.125	45.55	45.16
2.5	10	35	25	52	5.38	70.66	52.72	37	3.57	50.01	49.48
2.6	10	35	25	33	4.04	60.20	42.06	117	7.20	40.46	39.94
3.1	10	35	50	25	4.71	70.92	48.45	33	6.45	37.56	35.02
3.2	10	35	50	32	5.29	63.56	31.45	100	10.09	32.98	32.04
3.3	10	35	50	52	8.57	69.43	-	77	6.187	39.29	-
3.4	10	35	50	32	5.59	75.27	52.97	31	3.39	56.93	53.56
3.5	10	35	50	48	5.76	67.75	47.43	85	5.62	45.67	44.53
3.6	10	35	50	52	6.52	50.27	-	149	11.25	36.99	-
4.1	10	60	10	44	4.33	6.99	3.50	67	6.00	11.33	0.66
4.2	10	60	10	27	3.44	19.61	10.17	23	2.10	12.39	0.98
4.3	10	60	10	132	5.92	9.25	14.45	178	6.60	8.49	8.49
4.4	10	60	10	45	4.53	4.87	0.32	46	3.26	8.36	1.07
4.5	10	60	10	150	6.63	8.81	7.45	34	2.73	12.83	0.47
4.6	10	60	10	17	2.56	38.86	12.78	70	3.85	32.25	13.10
5.1	10	60	25	41	5.64	28.01	17.39	37	4.2	20.32	12.61
5.2	10	60	25	115	13.2	20.38	7.73	34	3.73	20.29	3.11
5.3	10	60	25	70	7.41	50.30	10.85	59	5.14	15.54	10.24
5.4	10	60	25	45	4.32	74.49	-	45	4.32	22.79	-
5.5	10	60	25	44	5.69	67.46	-	59	5.73	49.68	-
5.6	10	60	25	54	6.2	60.84	-	48	3.406	58.12	-
6.1	10	60	50	34	7.12	67.38	23.22	88	12.39	27.15	22.87
6.2	10	60	50	62	11.8	63.52	-	44	7.03	35.69	-

-Continuation of the Table 1.

6.3	10	60	50	74	14.02	40.25	-	69	5.68	25.77	-
6.4	10	60	50	34	5.54	81.09	-	84	15.17	36.33	-
6.5	10	60	50	42	7.24	75.78	-	82	13.23	40.62	-
6.6	10	60	50	69	7.76	77.51	-	69	7.77	37.46	-

In Table 1, columns 2-4 correspond to the size of the instance in terms of the number of arcs, nodes, and commodities, respectively. Next two main columns present results for Relaxation 1 and 2. Under these columns, we provide the number of iterations performed for solution (i), computation time (CPU time) of the algorithm in seconds (t), gap value (in %) calculated based on UB and LB difference (g_s) and gap value (in %) calculated based on optimal value achieved by CPLEX solver and LB difference (g_0). The dashed lines under the last columns indicate those instances for which CPLEX cannot obtain optimal values. As clearly seen, CPLEX fails to find an optimal solution for 13 problems (36% of the problem set). As problem size increases, the performance of the CPLEX decreases, as expected. Table 1 indicates that computation times for both relaxations are less than a minute (maximum being 16 seconds) while we observe a slight increase as problems get more complex. To compare performances of these two relaxations visually, we plot performance measures vs. instances as shown in Figures 2-5. The gap g_0 is computed and graphed only for those instances that CPLEX solves optimally.

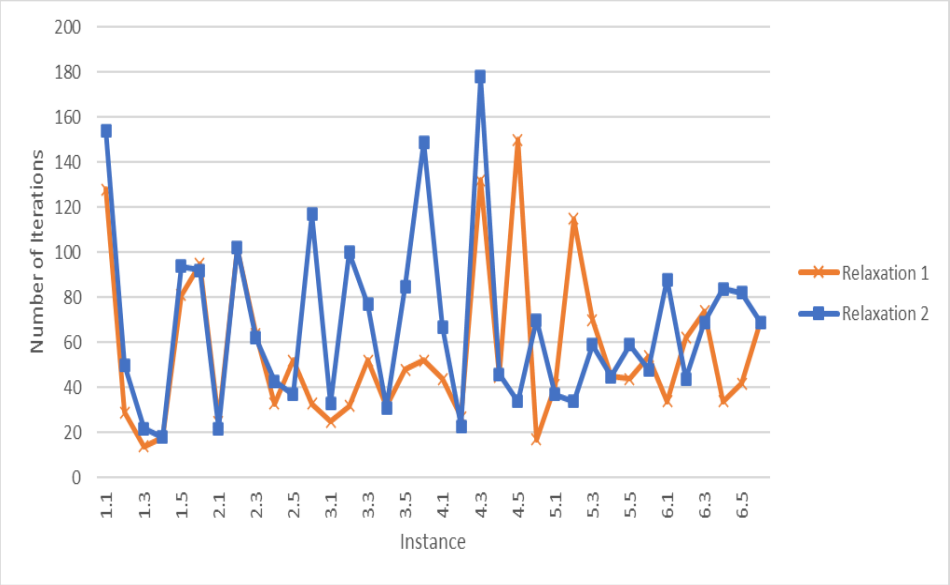

Figure 2. Number of iterations vs. instances.

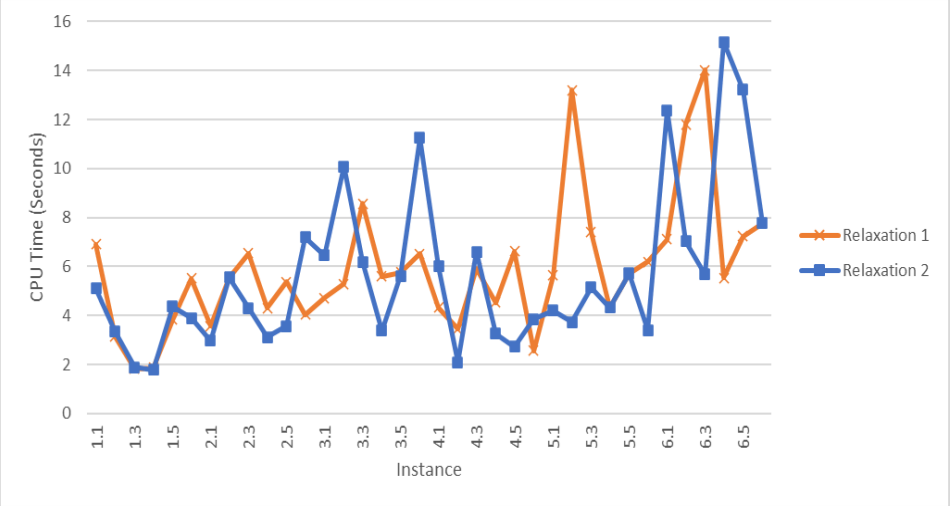

Figure 3. CPU times (in seconds) vs. instances.

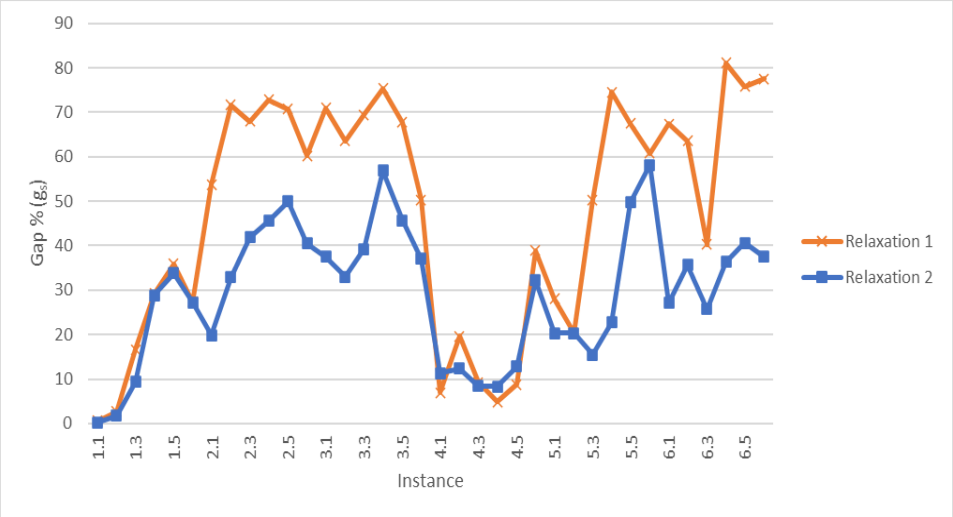

Figure 4. Gaps (g_s) vs. instances.

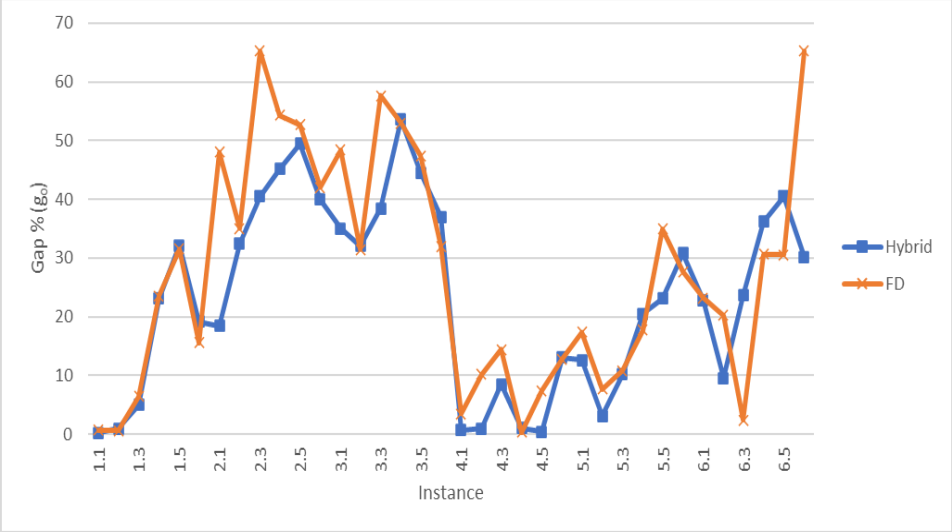

Figure 5. Gaps (g_0) vs. instances.

5. CONCLUSION

In this study, we consider a min-cost multicommodity network design problem where arc capacities can be violated for a penalty cost. When the penalty term is quadratic or has higher power, the problem turns out to be a nonlinear mixed-integer problem that does not have an exact solution method proposed in the literature. To solve this problem efficiently, we consider two different Lagrangean relaxations which decompose the original problem into smaller and easy to solve subproblems. One of these relaxations was proposed by Bektaş et al. (2010). We propose another relaxation and compare this relaxation with the former one. We implemented a computational study over a set of instances and solved these instances with the CPLEX solver and two relaxation approaches. Our computational study has shown that the CPLEX solver cannot obtain a solution for %36 of the test instances while two relaxation-based approaches achieve solutions with reasonable gaps. We also observe from the computational study that, our relaxation (Relaxation 2) outperforms that of Bektaş et al. (2010) (Relaxation 1) in terms of performance measures gap g_0 and gap g_s. Hence, this relaxation can be used for solving aforementioned problems which do not have exact solution methods and cannot be solved by on-the-shelf optimizers efficiently.

We used a subgradient algorithm to optimize the Lagrangean problem. One of the drawbacks of this algorithm is that it requires fine-tuning of parameters to achieve satisfactory results. Particularly, we observed that parameter λ that is used to calculate step length should be tuned carefully and values varying between 0.05 and 0.9 provide good results. Additionally, initial values of Lagrangean multipliers have a dramatic impact on the performance of the algorithm. Hence, as future work, a starting heuristic that will find suitable parameter settings would increase the performance of the algorithm.

As we stated previously, gap g_0 improves better than the gap g_s as problem size increases. This result indicates that we need to have a better procedure to generate UBs for the algorithm. Therefore, this could be another future work for this study.

REFERENCES

Ahuja, R. K., Magnanti, T. L. and Orlin, J. B. (1993). *Network Flows: Theory, Algorithms, and Applications*, New Jersey, Prentice Hall.

Anisi, M., and Fathabadi, H. S. (2019). "Survivable multi-commodity network flow design: case of node capacities and arc failure". *International Journal of Operational Research*, 35(3), 355–365. doi:10.1504/IJOR.2019.10022713.

Bektaş, T., Chouman, M. and Crainic, T. G. (2010). "Lagrangean-based decomposition algorithms for multicommodity network design problems with penalized constraints". *Networks*, 55(3), 171–180.

Belotti, P., Malucelli, F., and Brunetta, L. (2007). "Multicommodity network design with discrete node costs". *Networks*, 49(1), 90–99.

Chouman, M., Crainic, T. G., and Gendron, B. (2018). "The Iimpact of filtering in a branch-and-cut algorithm for multicommodity capacitated fixed charge network design". *EURO Journal on Computational Optimization*, Vol. 6, 143–184.

Costa, A. M. (2005). "A survey on benders decomposition applied to fixed-charge network design problems". *Computers & Operations Research*, 32(6), 1429–1450. doi:10.1016/j.cor.2003.11.012.

Costa, A. M., Cordeau, J.-F. and Gendron, B. (2009). "Benders, metric and cutset inequalities for multicommodity capacitated network design". *Computational Optimization and Applications*, Vol. 42, 371–392. doi:10.1007/s10589-007-9122-0.

Crainic, T. G., and Rousseau, J.-M. (1986). "Multicommodity, multimode freight transportation: A general modeling and algorithmic framework for the service network design problem". *Transportation Research Part B: Methodological*, 20(3), 225–242. doi:10.1016/0191-2615(86)90019-6.

Crainic, T. G, Frangioni, A., and Gendron, B. (2001). "Bundle-based relaxation methods for multicommodity capacitated fixed charge network design". *Discrete Applied Mathematics*, Vol. 112, Issues 1–3, 73–99. doi:10.1016/S0166-218X(00)00310-3.

Gendron, B., and Gouveia, L. (2016). "Reformulations by discretization for piecewise linear integer multicommodity network flow problems". *Transportation Science*, 51(2), 629–649.

Ghaffarinasab, N., Zare Andaryan, A., and Ebadi Torkayesh, A. (2020). "Robust single allocation p-hub median problem under hose and hybrid demand uncertainties: models and algorithms". *International Journal of Management Science and Engineering Management*, 15(3), 184-195.

Guimarães, L. R., de Sousa, J. P., and Prata, B. D. A. (2020). "Variable fixing heuristics for the capacitated multicommodity network flow problem with multiple transport lines, a heterogeneous fleet and time windows". *Transportation Letters*, 1-10.

Holmberg, K., and Yuan, D. (2000). "A Lagrangian heuristic based branch-and-bound approach for the capacitated network design problem". *Operations Research*, 48(3), 461–481.

Karsten, C. V., Pisinger, D., Røpke, S., and Brouer, B. D. (2015). "The time constrained multi-commodity network flow problem and its application to liner shipping network design". *Transportation Research Part E: Logistics and Transportation Review*, Vol. 76, 122–138. doi:10.1016/j.tre.2015.01.005.

Katayama, N., Chen, M., and Kubo, M. (2009). "A capacity scaling heuristic for the multicommodity capacitated network design problem". *Journal of Computational and Applied Mathematics*, 232(1), 90–101. doi:10.1016/j.cam.2008.10.055.

Kazemzadeh, M. R. A., Bektaş, T., Crainic, T. G., Frangioni, A., Gendron, B., and Gorgone, E. (2021). "Node-based Lagrangian relaxations for multicommodity capacitated fixed-charge network design". *Discrete Applied Mathematics*. doi:10.1016/j.dam.2020.12.024.

Moradi, S., Raith, A., and Ehrgott, M. (2015). "A bi-objective column generation algorithm for the multi-commodity minimum cost flow problem". *European Journal of Operational Research*, 244(2), 369–378. doi:10.1016/j.ejor.2015.01.021.

Oğuz, M., Bektaş, T., and Bennell, J. A. (2018). "Multicommodity flows and Benders decomposition for restricted continuous location problems". *European Journal of Operational Research,* 266(3), 851–863. doi:10.1016/j.ejor.2017.11.033.

Paraskevopoulos, D. C., Gürel, S., and Bektaş, T. (2016). "The congested multicommodity network design problem". *Transportation Research Part E: Logistics and Transportation Review,* Vol. 85, 166–187. doi:10.1016/j.tre.2015.10.007.

Salimifard, K., and Bigharaz, S. (2020). "The multicommodity network flow problem: State of the art classification, applications, and solution methods". *Operational Research*, 1-47. doi:10.1007/s12351-020-00564-8.

Trivella, A., Corman, F., Koza, D. F., and Pisinger, D. (2021). "The multi-commodity network flow problem with soft transit time constraints: Application to liner shipping". *Transportation Research Part E: Logistics and Transportation Review*, *150*, 102342.

Yousefi Nejad Attari, M., Ebadi Torkayesh, A., Malmir, B., and Neyshabouri Jami, E. (2020). "Robust possibilistic programming for joint order batching and picker routing problem in warehouse management". *International Journal of Production Research*, 59(2), 1-19.

Wang, I.-L. (2018a). "Multicommodity Network Flows : A Survey , Part I : Applications and Formulations". *International Journal of Operational Research*, 15(4), 145–153. doi:10.6886/IJOR.201812.

Wang, I.-L. (2018b). "Multicommodity Network Flows : A Survey, Part II : Solution Methods". *International Journal of Operational Research,* 15(4), 155–173.

Wolsey, L. A. (1998). *Integer Programming*. New York, John Wiley & Sons.

Journal of Naval Sciences and Engineering
2021, Vol. 17, No. 2, pp. 265-282
Physics/Fizik

RESEARCH ARTICLE

**An ethical committee approval and/or legal/special permission has not been required within the scope of this study.*

THE RESONANCE PRODUCTION OF THE SEXTET SCALAR DIQUARKS AT FUTURE CIRCULAR COLLIDER-BASED PROTON-PROTON, (FCC-PP)*

Özlem SEVİNÇ KAYA[1]

[1]*National Defence University, Department of the Fundamental Sciences, Istanbul, Turkey,*
oskaya@dho.edu.tr; ORCID: 0000-0002-8485-3822

Received: 16.06.2021 **Accepted: 29.07.2021**

ABSTRACT

In this study, the resonance production of the sextet scalar diquarks are studied for the FCC (Future Circular Collider) proton-proton collider with 100 TeV centre-of-mass planned to build at the European Organization for Nuclear Research, CERN. For the scalar diquarks, decay width and cross sections are calculated as a function of the diquark's mass. Also, to separate the diquark's signal from the background, the kinematic cuts are applied on diquarks mass and statistical significance calculations are obtained. As a result, at the FCC-pp, for the scalar diquark's mass, discovery (5σ), observation (3σ) and exclusion (2σ) limit values are given. These mass limit values are compared with mass limit values of the Large Hadron Collider (LHC) with 7 TeV centre-of-mass energy and the High Luminosity-Large Hadron Collider (HL-HLC) with 14 TeV centre-of-mass energy.

Keywords: *CERN, FCC-pp, Diquarks, Modelling, Resonance.*

Özlem SEVİNÇ KAYA

FCC PROTON-PROTON ÇARPIŞTIRICISINDA RENK ALTILI SKALER DİKUARKLARIN REZONANS ÜRETİMİ

ÖZ

Bu çalışmada, Avrupa Nükleer Araştırma Merkezi'nde (CERN) kurulacak olan 100 TeV kütle merkezi enerjisine sahip geleceğin dairesel proton-proton tabanlı çarpıştırıcısında (FCC-pp), renk altılı skaler dikuarkların rezonans üretimi çalışılmıştır. Skaler dikuarklar için, dikuark kütlesine bağlı olarak bozunum genişliği ve tesir kesiti hesaplamaları yapılmıştır. Ayrıca dikuark sinyalini fondan ayırmak için kinematik kesmeleri uygulanıp istatistiksel önem hesaplamaları yapılmıştır. Sonuç olarak, 100 TeV kütle merkezi enerjili geleceğin dairesel proton-proton tabanlı çarpıştırıcısında (FCC-pp), skaler dikuarkların kütlesi için keşif (5σ), gözlem (3σ) ve dışarlama (2σ) limitleri verilmiştir. Bu kütle limit değerleri, 7 TeV kütle merkezi enerjisine sahip Büyük Hadron Çarpıştırıcısı (BHÇ) ve 14 TeV kütle merkezi enerjisine sahip Yüksek Işınlıklı Büyük Hadron Çarpıştırıcısından (YI-HLÇ) elde edilen değerler ile karşılaştırılmıştır.

Anahtar Kelimeler: *CERN, FCC-pp, Dikuarklar, Modelleme, Rezonans.*

1. INTRODUCTION

Standard Model (SM) plays an essential role in explaining fundamental particles and their interactions. Some of the very important discoveries such as top quark (CDF and D0 experiments at FERMILAB in 1995), the tau neutrino (DONUT experiment at FERMILAB in 2000) and Higgs boson (CMS and ATLAS collaborations at CERN in 2012) are predicted by the SM. Although SM works in harmony with experimental high energy physics, there are still unsolved mysteries in universe like neutrino mass, the quark-lepton symmetry, dark matter, dark energy, charge quantization and plenty numbers of elementary particles by SM theory. One of the unanswered questions is "why is there three generations in universe"? To solve this question, particle physics suggest composite models as called "preonic models". According to these models leptons and quarks, which are elementary particles, have composite structure. In these models, preons have been proposed as the new elementary particles. Due to their preonic interactions, a large number of new particles will be revealed such as diquarks, leptoquarks, excited quarks, excited leptons, etc (CERN Council, 2013; Abe et al., 1995; Kodama et al., 2001; Chatrchyan et al., 2012; Aad et al., 2012; D'Souza & Kalman, 1992).

Diquarks are predicted in composite models and superstring inspired E6 models. They are including many new physics. In addition, diquarks have been studied phenomenologically in different colliders. They have integer spin and carry baryon number with |B| = 2/3. They have two form, scalar and vector. Scalar forms have spin 0 while vector forms have spin 1. And also, they have electric charge with |Q|=1/3, 2/3 or 4/3 (Wudka, 1986; Hewwtt & Rizzo, 1989; Atağ, Cakir & Sultansoy, 1998; Cakır & Sahin, 2005; Sahin & Cakir, 2010).

In this study, we investigated three types the scalar diquarks. The scalar diquarks are described as scalar uu diquarks ($DQ_{(uu)}$), scalar ud diquarks ($DQ_{(ud)}$) and scalar dd diquarks ($DQ_{(dd)}$). Resonant production signal subprocesses of diquarks are given the following Eq. 1, 2 and 3;

$$pp \rightarrow DQ_{(uu)} + X \rightarrow u + u + X \qquad \textbf{(1)}$$

$$pp \rightarrow DQ_{(ud)} + X \rightarrow u + d + X \quad \textbf{(2)}$$

$$pp \rightarrow DQ_{(dd)} + X \rightarrow d + d + X \quad \textbf{(3)}$$

where, X denotes proton remnant.

In the high energy physics, proton-proton (pp) colliders reach high energy limits in the last decade and they provide good chance to discover new particles for the new physics study. One of them is the Large Hadron Collider-based on pp collision, (LHC-pp) with 7 TeV center of mass energy, (CM). The LHC started to collect data in 2010 and it stopped in June 2018 for an upgrade process (technical stop). Between these years it has recorded tremendous amount of data with an integrated luminosity of 192.29 fb^{-1}. The LHC is planning to restart at the end of 2021 with a high luminosity which is factor of ten higher than the current one. It is called High Luminosity-LHC (HL-LHC) with 14 TeV. The HL-LHC machine plans to reach integrated luminosity up to 3500 fb^{-1} in ten years. The resonant production of the scalar diquarks mass has been searched in both the LHC and the HL-LHC-based pp. The scalar diquarks mass limit is excluded up to 7.5 TeV in the LHC with 13TeV and up to 10 TeV in the HL-LHC with 14 TeV. It has been planning to build a new generation collider the FCC-pp at the CERN to operate for 25 years. The working plan of the FCC-pp divide into two segmentation, Phase I and Phase II according to its final integrated luminosity. It is expected to reach 2.5 ab^{-1} and 15 ab^{-1} final integrated luminosity after 10 years (Phase I) and 15 years (Phase II) of running period, respectively. End of two Phase sections, it is expected to reach 17.5 ab^{-1} in 25 years (CERN Council, 2013; Sirunyan et al., 2020; Kaya, 2020; Abada et al., 2019).

In this paper, the possibilities of existing of $DQ_{(uu)}$, $DQ_{(ud)}$ and $DQ_{(dd)}$ the scalar diquarks are investigated at Future Circular Collider-based proton-proton, (FCC-pp) with 100 TeV. In the Section 2, The FCC-pp and their parameters are presented and in the Section 3, interaction lagrangian, decay widths and total cross section calculations are shown. In the Section 4, in order to distinguish signal from background kinematic cuts are calculated. Finally, in the Section 5, discovery, observation and exclusion limits of the scalar diquarks mass are given.

2. FCC PROTON-PROTON COLLIDER

The FCC-pp is a hadron collider with 100 TeV CM, planned to build at the CERN between Switzerland and France borders. The circumference of the FCC-pp is 97.75 km and in order to keep proton beam at the circular orbit, it has magnetic field with 16T. It has planned to use injected beam with 3.3 TeV from the LHC machine at the CERN. In Figure 1, geological and schematic view of the FCC-pp machine is shown. On the left side in the Figure 1 give 3D view of the underground structure of the FCC-pp, while an illustration on the right side shows geological position and size of the FCC-pp project planned. The green line circle represents main the FCC-pp tunnel besides, blue line circle represents existing the LHC at the CERN (Abada et al., 2019).

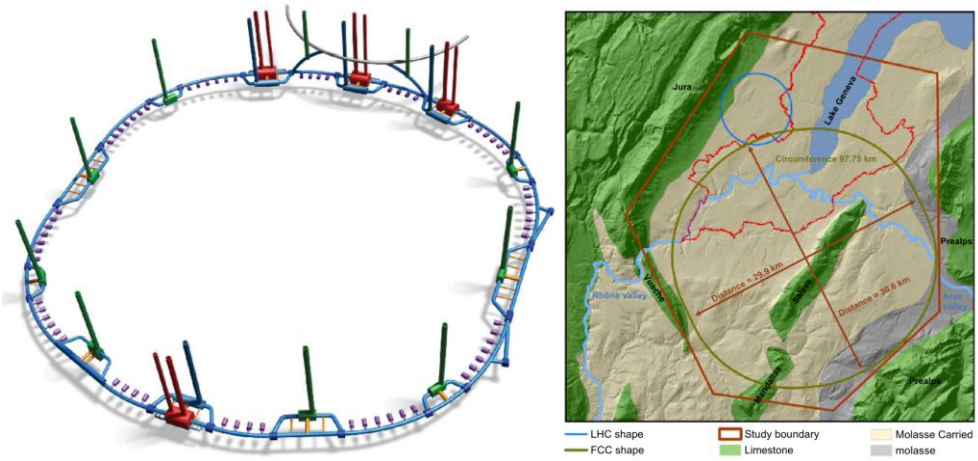

Figure 1. The geological and schematic structures of the FCC-pp machine. Left: 3D view of the underground structure. Right: geological position and size of the FCC-pp (green circle is the FCC-pp, blue circle is the LHC) (Abada et al., 2019).

When the FCC-pp begins to work, the maximum luminosity is planned to be $5x10^{34}$ $cm^{-2}s^{-1}$ as a starter parameter in the first years. In the next years, proposed luminosity will reach up to $3x10^{35}$ $cm^{-2}s^{-1}$ nominal value. At the beginning of the FCC-pp, the integrated luminosity will be provided as 2 fb^{-1} per year while for the nominal parameters is 8 fb^{-1} per year. The FCC-pp

machine will be proved total energy by a factor of 20 more than the LHC. In addition, the level of the synchrotron radiation in arc is by a factor of 200 greater than the LHC. The radiation limit of the magnets of the FCC-pp is 30 MGy. Some of the compared systematic parameters of the FCC-pp, LHC and HL-LHC machine are given in Table 1.

Table 1. Some of the values of the FCC-pp machine compared to the LHC and HL-LHC (Abada et al., 2019).

	LHC	**HL-LHC**	**FCC-pp**	
			Initial	**Nominal**
Basic Parameters				
Maximum E_p (TeV)	7	14	100	
Peak luminosity 10^{34} $cm^{-2}s^{-1}$	1.0	5.0	5.0	<30.0
Average integrated luminosity/day (fb^{-1})	0.47	2.8	2.2	8
Total cross section σ (mbarn)	111/85		153/108	
Beam Parameters				
Number of bunches n	2808		10400	
Bunch spacing (ns)	25	25	25	
Beam current (A)	0.584	1.12	0.5	

3. DECAY WIDTH AND TOTAL CROSS SECTIONS

The decay widths of the diquarks were estimated from invariant effective Lagrangian Eq.4 for each quark pairs uu, ud and dd which scaler diquarks are decayed into. For this study, only the scalar diquarks with baryon number of 2/3 (|B|=2/3) are taken into account.

$$L_{|B|=\frac{2}{3}} = (g_{1L}\bar{q}_L^c i\tau_2 q_L + g_{1R}\bar{q}_R^c d_R)DQ_1^c + \tilde{g}_{1R}\bar{d}_R^c d_R \widetilde{DQ}_1^c + \tilde{g}'_{1R}\bar{u}_R^c u_R \widetilde{DQ}_1^{'c} \quad \textbf{(4)}$$

where, g_{1L} denotes coupling constant used as 0.1 for these calculations. $q_L = (u_L, d_L)$ represents left-handed quark doublet spinor and $q_R =$

(u_R, d_R) represents right-handed quark doublet spinor. DQ_1, $\widetilde{DQ}_1$ and $\widetilde{DQ}_1'$ are the scalar diquarks. Finally, quark conjugated field is given with q^c (Cakir & Sahin, 2005; Sahin & Cakir, 2010).

Figure 2 shows the results of decay width calculations for the scalar diquarks with coupling constant α_s=0.1. As it seen from the Figure 1, calculations of the decay width versus the invariant mass is linear as it expected. The distribution was obtained from 7,5 TeV to 100 TeV invariant mass range for the FCC-pp at 100 TeV. To discriminate signal from the background, decay width cuts are applied on an invariant mass of scalar $DQ_{(uu)}$, $DQ_{(ud)}$ and $DQ_{(dd)}$.

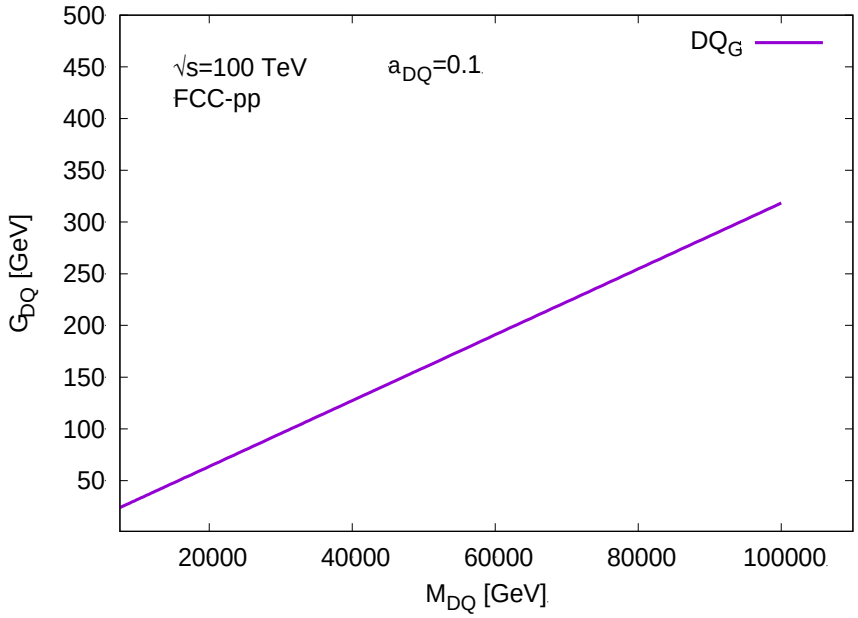

Figure 2. The decay widths calculations for the scalar diquarks.

In this analysis all the calculations are obtained from the Eq. 4, which is implemented to simulation software CALCHEP in the version 3.8.5 via LANHEP programme. The Feynman diagrams of the resonant productions for scalar $DQ_{(uu)}$, $DQ_{(ud)}$ and $DQ_{(dd)}$ with CTEQL1 parton distribution function and coupling constant α_s=0.1 are presented in Figure 3 (Belyaev, Christensen & Pukhov, 2013; Semenov, 2002; Semenov, 2016; Pumplin,

Stump, Huston, Lai, Nadolsky & Tung, 2002; Stump, Huston, Pumplin, Tung, Lai, Kuhlmann & Owens, 2003).

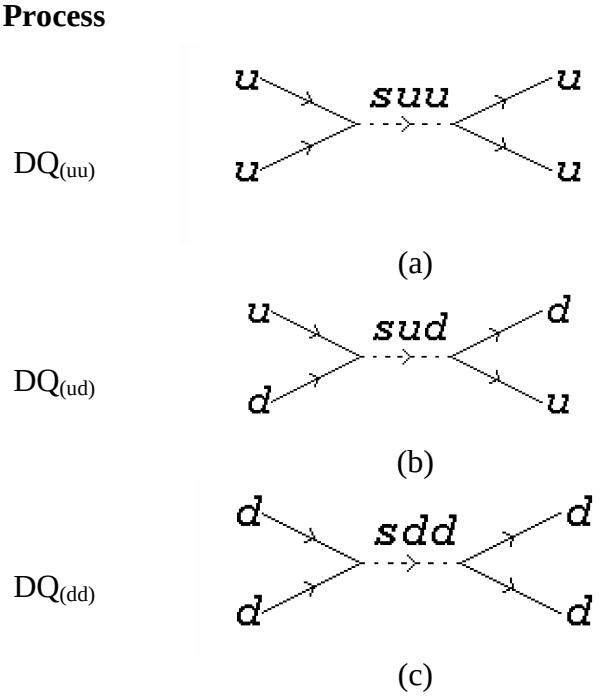

Figure 3. The Feynman diagrams of resonant production of the scalar diquarks for three type process. (a): uu type scalar diquark signal, (b): ud type scalar diquark signal and (c): dd type scalar diquark signal.

Total cross section distributions versus the scalar $DQ_{(uu)}$, $DQ_{(ud)}$ and $DQ_{(dd)}$ mass are given in the Figure 4. According to the SM, protons are composite particles made of two up (u) with charge 2/3 and one down (d) with charge -1/2 valance quarks. In this case, scalar uu diquark made of up quark pairs, scaler ud diquark made of up and down quark pairs and scalar dd diquark made of down quark pairs would have charge with 4/3, 1/3 and -2/3, respectively. As seen in Figure 4, the total cross section distributions of all

three scalar diquarks are aligned. Since proton has two u valance quarks, the $DQ_{(uu)}$ type scalar diquark has the largest cross sections.

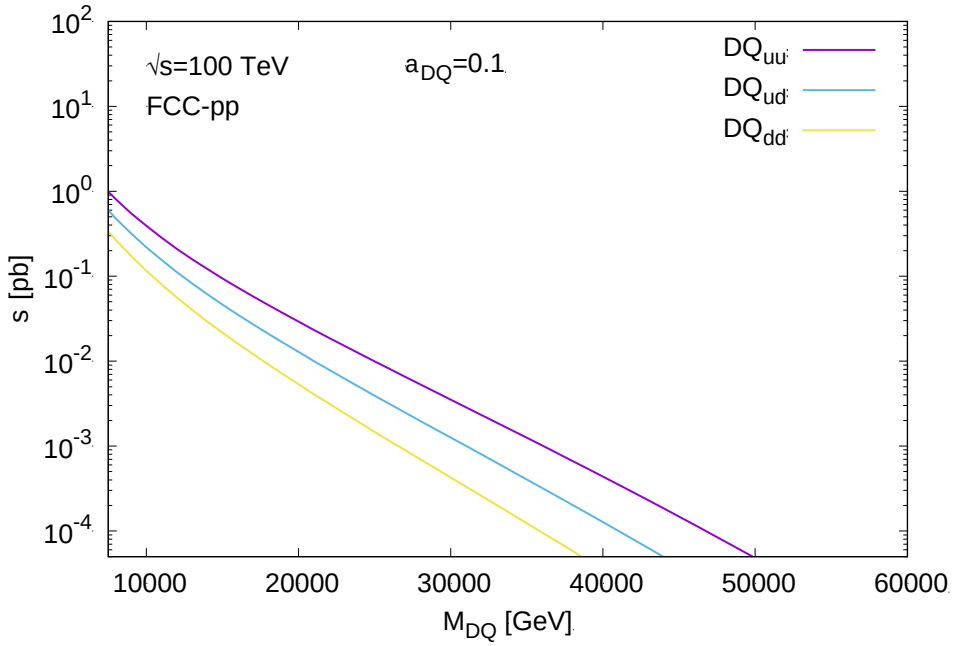

Figure 4. Total cross section distributions versus mass of the scalar diquarks types $DQ_{(uu)}$, $DQ_{(ud)}$ and $DQ_{(dd)}$ with coupling constant $\alpha_{DQ} = 0.1$ at the FCC-pp collisions.

4. SIGNAL AND BACKGROUND ANALYSIS

In order to distinguish signals from background, kinematics cuts are determined from transverse momentum, (p_T) and pseudorapidity, (η) distributions of the final state particles in the FCC-pp at 100TeV. Three type of scalar diquark signals, $DQ_{(uu)}$, $DQ_{(ud)}$ and $DQ_{(dd)}$, are defined in the Section 1. As a background processes, all SM defined quarks and anti-quarks are included except t and anti-t quark, $pp \to j$ and $j + X$ that is generated $(j \to u, \bar{u}, d, \bar{d}, c, \bar{c}, s, \bar{s}, b, \bar{b}\ and\ g)$. CTEQ6L1 Parton Distribution Function is used to generate all signal and background

calculations and calculated by using CALCHEP_385 simulation software programme.

Figure 5 demonstrates p_T distributions of the final state scalar $DQ_{(uu)}$ jets and SM background for the FCC-pp with 100 TeV. The smooth purple line denotes SM background besides, each color denotes resonance peaks at mass values (7.5, 10, 20, 30, 40 and 50 TeV) of the scalar $DQ_{(uu)}$. As seen from distributions, if the p_T > 1000 GeV kinematic cut is applied at $\sqrt{s}$ = 100 TeV, enormous amount of the SM background clear away while final state scalar $DQ_{(uu)}$ jets at each mass does not show significant changes. Also final state scalar $DQ_{(ud)}$ and $DQ_{(dd)}$ jets show same characteristics with $DQ_{(uu)}$. Thus, as an illustration, the scalar $DQ_{(uu)}$ demonstrated for this paper.

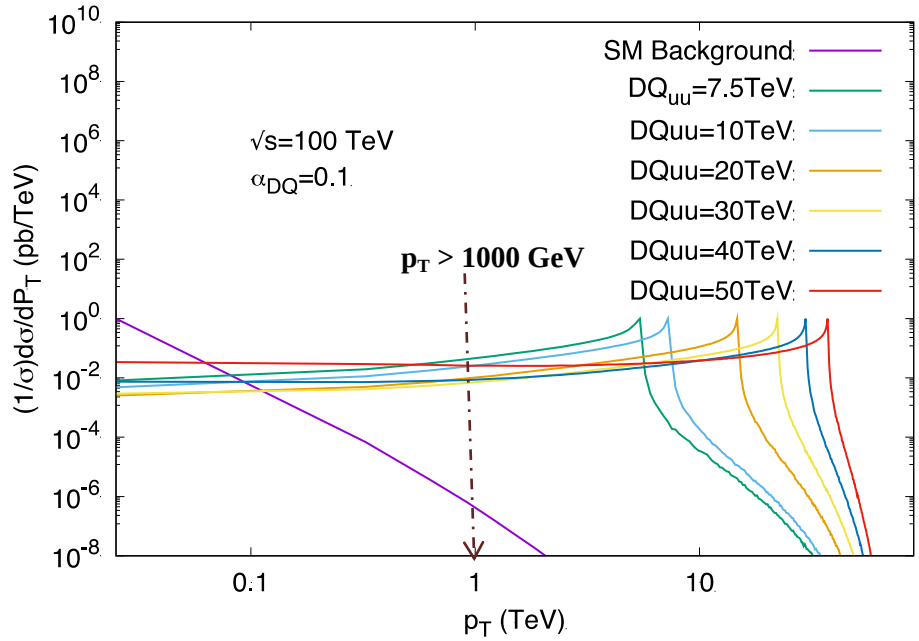

Figure 5. The pT distributions as a function of mass of the scalar diquarks $DQ_{(uu)}$, $DQ_{(ud)}$ and $DQ_{(dd)}$ with coupling constant α_{DQ} = 0.1 at in the FCC-pp collisions at $\sqrt{s}$ = 100 TeV.

Because of the detector's structure, pseudorapidty (η) distributions of the detector placed on the colliders like the CMS detector on the LHC shows symmetric distribution for both left and right side of the detector. In Figure 6, pseudorapidity distributions of final state background and scalar $DQ_{(uu)}$ jets are illustrated for the FCC-pp at $\sqrt{s} = 100$ TeV center of mass energy. η distributions are symmetric for both detector side for SM background and scalar $DQ_{(uu)}$ jets at seven mass values as expected. And also, both SM background and scalar $DQ_{(uu)}$ jets are mostly located at -2.5 < η < 2.5 region. Because of this reason, another kinematic cut -2.5 < η < 2.5 region is selected from distributions for the analysis.

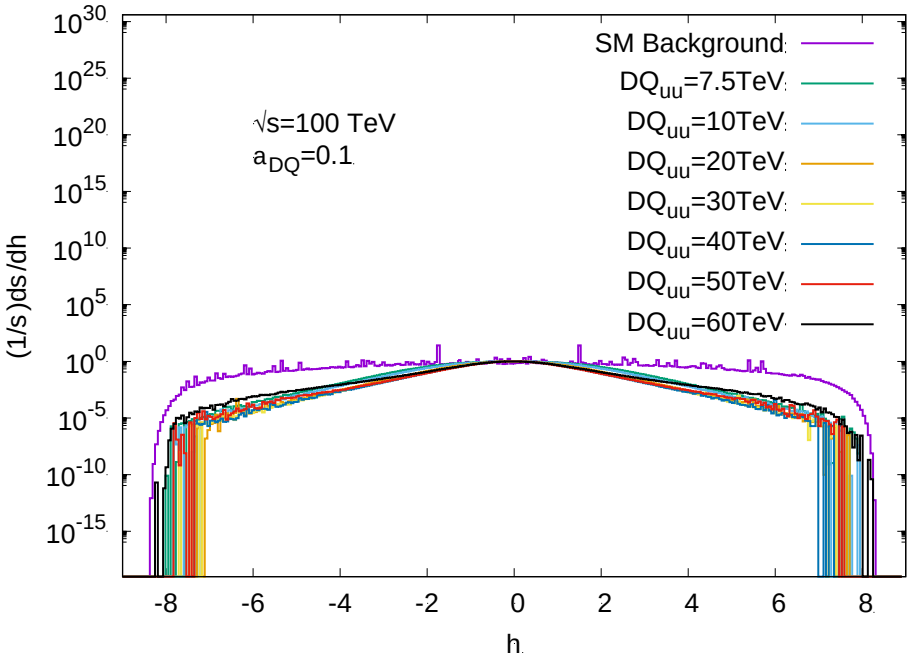

Figure 6. Pseudorapidity distributions of final background and scalar $DQ_{(uu)}$ jets for the FCC-pp with $\sqrt{s} = 100$ TeV center of mass energy.

5. CONCLUSION

In this study, resonance production of the scalar diquarks for the FCC-pp with 100 TeV are studied. As a kinematic cuts which were specified for this work to discriminate background from signal, transverse momentum p_T > 1000 GeV, pseudorapidity -2.5 < η < 2.5 are applied on mass of the final state the scalar diquarks. Furthermore, in order to select particle jets cone angle radius, cut ΔR > 0.4 is applied for the FCC-pp, in addition, invariant mass cut M-2Γ < Mjj < M+2Γ is applied, where M denotes the final state scalar diquark mass and Γ is total decay width given in the Section 3. In this analysis, statistical significance (SS) calculations are performed using the following formula (Eq.5),

$$SS = \frac{\sigma_S}{\sqrt{\sigma_S + \sigma_B}}\sqrt{\mathcal{L}_{int}} \qquad \textbf{(5)}$$

where, σ_S and σ_B represent the signal and background cross sections, respectively. The L_{int} denotes integrated luminosity of the FCC-pp during the phase I (Sahin, Aydin & Gunaydin, 2019).

As a result, after all these calculations, the limit values of the discovery (5σ), observation (3σ) and exclusions (2σ) of the final state resonance the scalar diquarks are presented for the FCC-pp at first round (Phase I) that total integrated luminosity will reach 2.5 ab^{-1} in 10 years.

In Figure 7, distributions of the discovery (5σ), observation (3σ) and exclusions (2σ) mass limits depending on integrated luminosity for the scalar $DQ_{(uu)}$ are shown. The red dots denote discovery of the mass limit values of skalar $DQ_{(uu)}$ changing from 44 TeV up to 53 TeV between 200 and 2500 fb^{-1} integrated luminosity for the FCC-pp at 100 TeV. The observation of the mass limit values depending on increasing integrated luminosity are pointed out with green dots. The observation (3σ) range is from 48 to 57 TeV for scalar $DQ_{(uu)}$ mass. Also, the exclusion limit values of the scalar $DQ_{(uu)}$ for the FCC-pp are figured out with blue dots. At the FCC-pp with 100 TeV center of mass, the exclusion limit values change between 52 and 60 TeV.

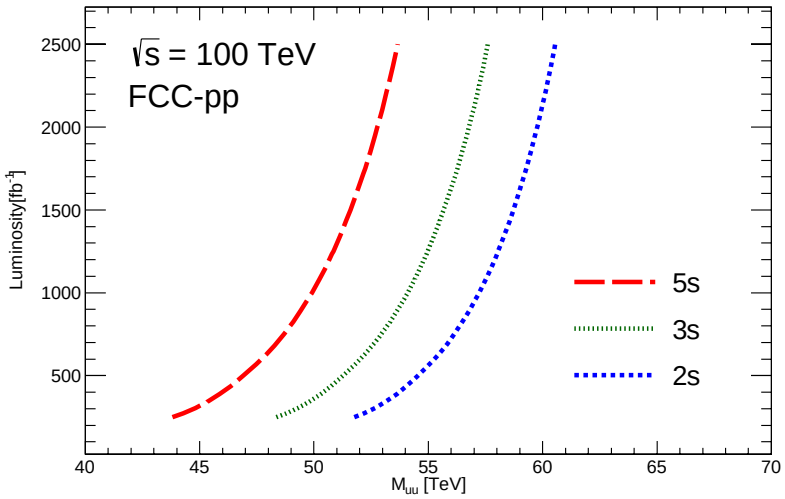

Figure 7. Discovery (5 σ), observation (3 σ) and exclusions (2 σ) mass limits values depending on integrated luminosity for the scalar $DQ_{(uu)}$ in the FCC-pp with $\sqrt{s} = 100$ TeV.

The mass limit values of discovery (5σ), observation (3σ) and exclusion (2σ) depending on integrated luminosity for the scalar $DQ_{(ud)}$ are given in Figure 8. As seen from the Figure 8, discovery (5σ), of the mass limit values of scaler $DQ_{(ud)}$ changes from 35 TeV up to 44 TeV between 200 and 2500 fb^{-1} integrated luminosity for the FCC-pp at 100 TeV. The observation (3σ) range is from 39 to 48 TeV, while exclusion limit values change between 52 and 60 TeV of the scalar $DQ_{(ud)}$ for the FCC-pp with $\sqrt{s} = 100$ TeV.

As seen from Figure 9, discovery (5σ), of the mass limit values of scalar $DQ_{(dd)}$ are illustrated from 31 TeV up to 38 TeV while observation (3σ) limits are from 35 to 42 TeV. And, exclusion limit values change between 34.5 and TeV of the scalar $DQ_{(ud)}$ for the FCC-pp with $\sqrt{s} = 100$ TeV.

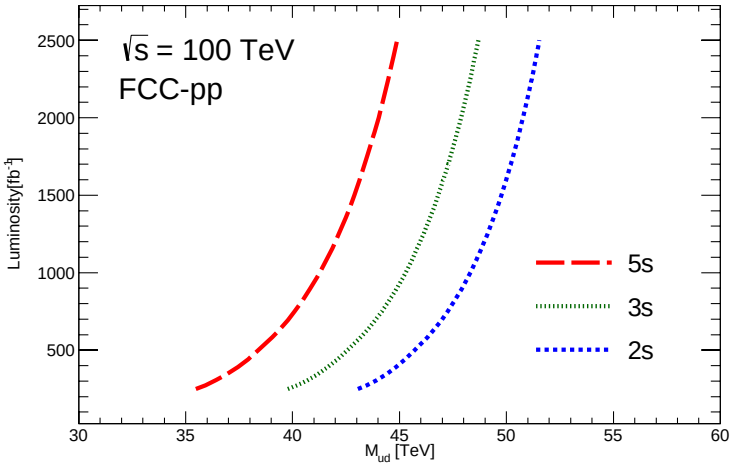

Figure 8. Discovery (5 σ), observation (3 σ) and exclusions (2 σ) mass limit values depending on integrated luminosity for the scalar $DQ_{(ud)}$ in the FCC-pp with $\sqrt{s} = 100$ TeV.

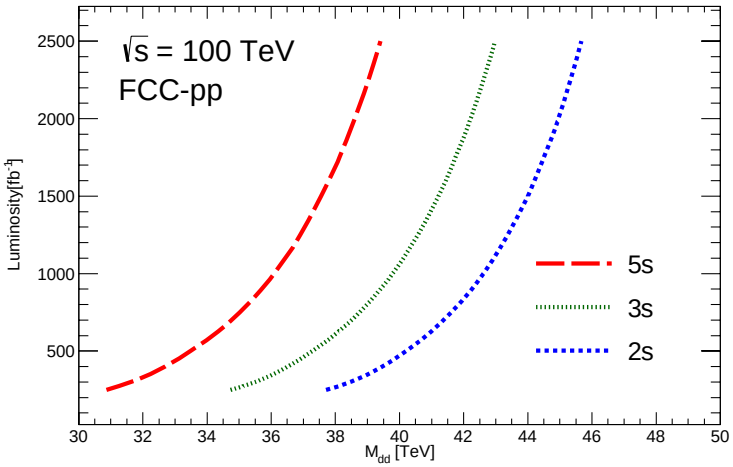

Figure 9. Discovery (5 σ), observation (3 σ) and exclusions (2 σ) mass limit values depending on integrated luminosity for the scalar $DQ_{(dd)}$ in the FCC-pp with $\sqrt{s} = 100$ TeV.

ACKNOWLEDGEMENT

The author thanks Dr. Mehmet SAHIN who has made this article possible with his guidance, technical support and insightful feedback.

The author also thanks Dr. Yusuf GUNAYDIN for his technical support and guidance on this article.

REFERENCES

Aad, G., Abajyan, T., Abbott, B., Abdallah, J., Khalek, S. A., Abdelalim, A. A., … Zwalinski, L. (ATLAS Collaboration). (2012). "Observation of a new particle in the search for the Standard Model Higgs boson with the ATLAS detector at the LHC". *Physics Letters B.* Vol. 716, Issue 1, 1-29. doi:10.1016/j.physletb.2012.08.020.

Abada, A., Abbrescia M., AbdusSalam, S. S., Abdyukhanov I., Fernandez, J.-A., Abramov A., … Zurita, J. (FCC-hh Collaboration) (2019). "FCC-hh: The Hadron Collider". *Eur.Phys.J.ST* 228 (2019) 4, 755-1107. doi:10.1140/epjst/e2019-900087-0.

Abe, F., Akimoto, H., Akopian, A., Albrow, M. G., Amendolia, S. R., Amidei, D., … Zucchelli, S. (CDF Collaboration). (1995). "Observation of Top Quark Production in pp Collisions with the Collider Detector at Fermilab". *Physical Review Letters.* Vol. 74, No. 14, 2626-2631.

Atağ, S., Cakir O., and Sultansoy, S. (1998). "Resonant production of diquarks at the CERN LHC". *Physical Review D*. Vol. 59, Issue 1, 015008. doi:10.1103/PhysRevD.59.015008.

Belyaev, A., Christensen D. N., and Pukhov, A. (2013). "CalcHEP 3.4 for collider physics within and beyond the Standard Model". *Computer Physics Communications*. Vol. 184, Issue 1729. arXiv:1207.6082 [hep-ph]. doi:10.1016/j.cpc.2013.01.014.

Cakır, O., and Sahin, M. (2005). "Resonant production of diquarks at high energy pp , ep and $e^+ e^-$ colliders". *Physical Review D.* Vol. 72, Issue 11.

CERN Council (May 30, 2013). "The European Strategy for Particle Physics". European Strategy Session of Council. CERN-Council-S/106.

Chatrchyan, S., Khachatryan, V., Sirunyan, A. M., Tumasyan, A., Adam, W., Aguilo, E., … Wenman, D. (CMS Collaboration). (2012). "Observation of a new boson at a mass of 125 GeV with the CMS experiment at the LHC". *Physics Letters B.* Vol. 716, Issue 1, 30-61. doi:10.1016/j.physletb.2012.08.021.

D'Souza, I. A., and Kalman, C. S. (1992). "Preons: Models of Leptons, Quarks and Gauge Bosons as Composite Objects". *World Scientific*. doi:10.1142/1700.

Hewett, J. L., and Rizzo, T. G. (1989). "Low-Energy Phenomenology of Superstring Inspired E(6) Models". *Physics Reports.* Vol. 183, Issues 5-6, 193-381. doi:10.1016/0370-1573(89)90071-9.

Kaya, O., (2020); "Resonance Production of Sextet Scalar Diquarks at The High Luminosity Large Hadron Collider (HL-LHC)". In 4^{th} *International Marmara Sciences Congress* (Spring 2020) Abstract Book (pp. 11-23). Kocaeli/Turkey.

Kodama, K., Ushida, N., Andreopoulos, C., Saoulidou, N., Tzanakos, G., Yager, P., … Schneps, J. (DONUT Collaboration). (2001). "Observation of tau neutrino interactions". *Physics Letters B.* Vol. 504, Issue 3, 218-224. doi:10.1016/S0370-2693(01)00307-0.

Pumplin, J., Stump, D. R., Huston, J., Lai, H.-L., Nadolsky, P., and Tung, W.-K. (2002). "New generation of parton distributions with uncertainties from global QCD analysis". *Journal of High Energy Physics.* JHEP 07 (2002) 012. doi:10.1088/1126-6708/2002/07/012.

Sahin, M., and Cakır O. (2010). "Search for Scalar Diquarks at the LHeC Based Gamma-Proton Collider". *Balk.Phys.Lett.* Vol. 18. arXiv:0911.0496 [hep-ph], Balk.Phys. Lett. 18 (2010) 024.

Sahin, M., Aydin, G., and Günaydin, Y. O. (2019). "Excited Quarks Production at FCC and SppC pp Colliders". *International Journal of Modern Physics A.* Vol. 34, No. 29. arXiv:1906.09983 [hep-ph], Int.J.Mod.Phys.A 34 (2019).

Semenov, A. (2016). "LanHEP - A package for automatic generation of Feynman rules from the Lagrangian. Updated version 3.2". *Computational Phys.* Vol. 201, Issue 167. arXiv:1412.5016 [physics.comp-ph].

Semenov, A. V. (2002). "LanHEP - A package for automatic generation of Feynman rules in field theory. Version 2.0". arXiv:hep-ph/0208011 [hep-ph].

Sirunyan, A. M., Tumasyan, A., Adam, W., Ambrogi, F., Bergauer, T., Dragicevic M., … Trembath-reichert, S. (CMS Collaboration). (2020). "Search for high mass dijet resonances with a new background prediction method in proton-proton collisions at sqrt (13 TeV)*". Journal of High Energy Physics*, JHEP 05 (2020) 033. doi:10.1007/JHEP05(2020)033.

Stump, D., Huston, J., Pumplin, J., Tung, W.-K., Lai, H.-L., Kuhlmann, S., and Owens, J. F. (2003). "Inclusive Jet Production, Parton Distributions, and the Search for New Physics". *Journal of High Energy Physics*. JHEP 0310 (2003) 046. doi:0.1088/1126-6708/2003/10/046.

Wudka, J. (1986). "Composite Leptoquarks". *Physics Letters B.* Vol. 167, Issue 3, 337-332. doi:10.1016/0370-2693(86)90356-4.

Journal of Naval Sciences and Engineering
2021, Vol. 17, No. 2, pp. 283-308
Industrial Engineering/Endüstri Mühendisliği

REVIEW ARTICLE

**An ethical committee approval and/or legal/special permission has not been required within the scope of this study.*

GREEN SUPPLY CHAIN MANAGEMENT AND SAMPLE APPLICATIONS*

Beste DESTİCİOĞLU[1]

[1]*National Defence University, Alparslan Defence Sciences Institute, Department of Operations Research, Ankara, Turkey,*
bdesticioglu@kho.edu.tr; ORCID: 0000-0001-8321-4554

Received: 13.05.2021 **Accepted: 17.06.2021**

ABSTRACT

It has become inevitable to develop new distribution strategies with the depletion of natural resources, global warming, increased environmental pollution due to the increasing competition conditions in recent years. In addition, the concepts of green supply chain and green logistics come into effect the literature with the awareness of both non-governmental organizations and national and international administrations about this danger. Green supply chain includes all activities, carried out in the design process of the product, the selection of the machinery, raw materials and semi-finished products used in the manufacture of the product to the retailer and/or the end customer, and the recycling of the product from the customer after the economic life and function is completed, and recycling. In this study, firstly, the emergence of green supply chain management and green logistics concepts are discussed within the literature review, taking into account the current developments. Later, green supply chain management and new concepts that emerged with this approach were discussed. In the continuation of the study, examplary green supply chain studies in Turkey were mentioned and suggestions were made to guide companies that will implement this approach.

Keywords: *Green Supply Chain, Green Logistics, Sustainability, Recycling.*

YEŞİL TEDARİK ZİNCİRİ YÖNETİMİ VE ÖRNEK UYGULAMALAR

ÖZ

Son yıllarda artan rekabet şartlarıyla beraber doğal kaynakların tükenmesi, küresel ısınma, çevre kirliliğinin artmasıyla beraber yeni dağıtım stratejilerinin geliştirilmesi kaçınılmaz olmuştur. Ayrıca gerek sivil toplum kuruluşlarının gerekse ulusal ve uluslararası yönetimlerin tehlikenin farkına varmasıyla birlikte yeşil tedarik zinciri ve yeşil lojistik kavramları literatüre girmeye başlamıştır. Yeşil tedarik zinciri, ürünün tasarım sürecinden, üretiminde kullanılan makine, hammadde ve yarı mamulün seçimi, üretilen ürünün perakendeciye ve/veya son müşteriye ulaştırılması ile ürünün ekonomik ömrü ve işlevi tamamlandıktan sonra müşteriden toplanarak, geri dönüştürülmesiyle yeniden üretime kazandırılması faaliyetlerinin tümü olarak tanımlanabilir. Bu çalışmada da öncelikle yeşil tedarik zinciri yönetimi ile yeşil lojistik kavramlarının ortaya çıkışı, günümüzdeki gelişmeler de dikkate alınarak literatür taraması içerisinde ele alınmıştır. Sonrasında yeşil tedarik zinciri yönetimi ile bu yaklaşımla ortaya çıkan yeni kavramlar incelenmiştir. Çalışmanın devamında ise Türkiye'deki örnek yeşil tedarik zinciri çalışmalarından bahsedilmiş ve bu yaklaşımı uygulayacak firmalara yol göstermesi amacıyla önerilerde bulunulmuştur.

Anahtar Kelimeler: *Yeşil Tedarik Zinciri, Yeşil Lojistik, Sürdürülebilirlik, Geri Dönüşüm.*

1. INTRODUCTION

In the globalizing world, companies need to develop new strategies to compete with each other, to increase their sales figures in the market or to find a place in different markets. Today, logistics management practices, which ensure the rapid supply of customers' demands, are among the most important strategies that companies apply to achieve this goal. Although the term logistics used to describe only distribution activities in the past, today the term of logistics defines the process that includes all activities from the process of the product to the delivery to the customer, as well as the transportation. Logistics can be defined as ensuring and controlling the allocation and control of the resources required for the realization of production, distribution and supply activities. As can be seen, logistics does not only include distribution activities, it includes all activities from the production stage of the product to the delivery to the customer. Logistics management, on the other hand, is to ensure the management and control of the activities that need to be done from the production stage to the delivery of the products and services to the customer. Another term that comes up with logistics management is Supply Chain Management (SCM). SCM covers all processes from collecting raw materials, semi-finished products and resources together in the manufacturing of a product or service to the manufacturing and supplying at the minimum cost, and to the delivery of the products to the customer (Timur et al., 2013).

Increased production activities have caused negative effects such as unconscious use of natural resources, climate change, global warming, air pollution, cutting down trees and depletion of natural resources. These negative developments started to attract the attention of environmentalists and they argued that new regulations should be introduced to prevent this situation. With the increasing awareness of people about the environment, a new term of sustainability has begun to enter the literature. Sustainability is to make development sustainable by ensuring that the daily needs of humanity are met without jeopardizing the situation of meeting the needs of future generations. With the implementation of the sustainability approach, people's sensitivity to the environment has started to increase, and with these developments, green logistics and green supply chain management (GSCM) approaches have emerged. Researchers state that green approaches

provide savings in the use of companies' resources and are beneficial in disposal of their wastes and increase in production efficiency (Porter and van der Linde, 1995).

2. DEVELOPMENT OF GREEN SUPPLY CHAIN MANAGEMENT APPROACH

The depletion of natural resources and the increase in environmental pollution started to attract the attention of environmentalists and the concept of sustainability entered the literature with the thought of taking precautions against these negativities. The concept of sustainability was first included in the "Our Common Future" report of the World Commission of Environment and Development published by the United Nations in 1987. Accordingly, sustainable development is the ability of the environment to make development sustainable by ensuring that the daily needs of humanity are met without jeopardizing the situation of meeting the needs of future generations (WCED, 1987). With the use of the concept of sustainability, GSCM and green logistics approaches have become a subject that attracts the attention of researchers.

Wilkerson states that GSCM which provides success from tactical decisions to strategic decisions also provides an opportunity for the effective use of recycling and activates the use of resources in his study. In addition, it was argued in the study that both the supply chain can be effective and environmental awareness is provided with GSCM (Wilkerson, 2005). Sarkis defines GSCM as the processes that include all of green production, green purchasing, green distribution and reverse logistics activities (Sarkis, 1998). Blanchard (2017) points out that GSCM is an approach aimed at reducing the carbon footprint while implementing SCM activities.

GSCM is an approach that aims to increase the profit and market share of the company by reducing the damage to the environment while performing the production / distribution activities of the companies. In GSCM, companies should prefer environmentally friendly materials in raw materials and semi-products used in the production process, and aim to minimize the environmental damage by carrying out the transportation of the materials used inside or outside the facility within a plan. In addition, it is important

to use recyclable materials in the packaging of products. With the proper packaging of the product, it is aimed to reduce the material used in packaging to a minimum (Zhu, Sarkis and Lai, 2007). Büyüközkan and Vardaroğlu (2008) discussed in detail the green approaches in the literature and the activities for GSCM in their study.

When the studies about GSCM are examined, it is noteworthy that researchers generally focus on GSCM applications and the effects of these applications on business performance. Kopicki et al. (1993) argued that proactive, reactive and value-creating approaches should be applied to achieve environmental management. In their study, Zhu, Sarkis, and Geng (2005) examined how businesses in China apply the GSCM approach and the effects of these practices on business performance. In another study, the researchers evaluated the operational performance of companies in the chemical, electrical / electronics, automotive and energy sectors in China after applying the GSCM activities. In another study conducted in the same year, the researchers examined how companies in the automotive industry in China implement GSCM activities and how the performance of the company is affected by these practices (Zhu, Sarkis and Lai, 2007a; 2007b). Another study examining the effects of GSCM applications on performance was conducted by Green, Zelbst, Meacham, and Bhadauria (2012). Researchers stated in this study that GSCM practices increase the economic environmental performance of companies.

Yang, Hu, Haider and Marlow (2013) examined the GSCM practices of companies engaged in transportation in Taiwan and tried to analyze the environmental and green transportation performance of these practices. In the research, they found that these practices positively affect the performance of companies. Mahmood, Rahman, Deros et al. (2013) tried to analyze the effects of GSCM applications on production performance. In the study, the practices of 242 businesses in Malaysia were examined, but it could not be proven that there was a strong correlation that these practices had a positive effect on business performance.

While GSCM approaches are applied, deciding on the companies from which raw materials or products will be supplied becomes an important

issue. For this reason, they prefer the company that gives the least harm to the environment, not the one that offers the lowest price when choosing a supplier (Ozyoruk, 2018). The green supplier selection approach includes monitoring the environmental awareness of suppliers and working only with suppliers that aim to cause little damage to the environment (Arimura et al., 2011). In determining the green supplier, criteria such as using recycled or recyclable materials of the company, reducing the consumption of harmful substances to the environment, and using environmentally friendly transportation methods can be used. In GSCM, the selection of the supplier has become an issue that has attracted the attention of researchers in recent years. Ozyoruk (2018) examined in detail the studies on green supplier selection in her study.

In the study, Lipmann gave information about the work to be done to establish an effective GSCM and examined how to communicate with suppliers (Lipmann, 1999). Wycherley (1999) discussed what stages should be considered in GSCM and the difficulties encountered as a result of implementation. Geffen and Rothenberg (2000) determined that the success of GSCM can only be achieved by the success of their suppliers.

It is noteworthy that researchers have focused on more specific applications on GSCM. There are studies in the literature that aim to increase the efficiency of the supply chain and reduce carbon emissions by applying sustainable development and various green activities (Zhen et al., 2019; Mardani et al., 2020). There are also studies in the literature that suggest a mathematical model for the green supply chain (Bai and Sarkis, 2018; Sarkis et al., 2019). In the research conducted, it has been determined that many studies in GSCM in recent years have been carried out on green product design, the effects of this approach on foreign policy and the supply chain focusing on the environment (Louly et al., 2008; Rao et al., 2015; 2020; Beemsterboer et al., 2017; Moktadir et al., 2019; Zhang and Yousaf, 2020).

Tunc (2020) mentioned green practices in Turkey by using qualitative research methods in his study. The researcher examined 18 companies that are in the ISO 500 list in Turkey and attach importance to green practices

and 4 companies with foreign capital and serving in Turkey. In the study, analyzes were made by conducting a questionnaire with employees to evaluate the green practices in companies (Tunç, 2020).

3. GREEN SUPPLY CHAIN MANAGEMENT

GSCM covers the management of all supply chain activities, including the process of returning the product from the supplier to the manufacturer, from the manufacturer to the customer, and from the customer to the manufacturer, starting from the purchasing stage, throughout the life cycle (Zhua et al., 2008). GSCM includes all of the following stages:

- Making the products included in an environmentally friendly process throughout their life cycle;
- Minimizing the amount of harmful waste that the product gives to the environment from the raw material to the depletion stage;
- Implementation of production activities with environmental and quality certificates (Ozyoruk, 2018).

Green logistics also includes activities for the use of renewable resources in production, distribution, taking measures to protect natural resources, reducing air pollution and carbon emissions, and minimizing the amount of waste. Green logistics is the realization of all processes within the logistics of the product or service in an environmentally friendly manner. Green logistics aims to minimize the negative effects on the environment (Temur et al., 2015). GSCM consists of a combination of green purchasing, green production, green distribution, reverse logistics and green packaging activities. These concepts need to be defined in order to understand GSCM approaches.

Green Purchasing: Green purchasing covers activities in the process of purchasing recycled materials, recyclable or reusable products (Zhua et al., 2008). Thus, it is tried to reduce the damage to the environment for purchased materials.

Green Production: It is the realization of activities without harming the environment at all stages of the manufacturing of a product. Green production also includes the process of remanufacturing from recycled products. In green production, it is aimed to use recyclable products, reduce the consumption of natural resources, and satisfy the needs of the customer without harming the environment and people (Büyüközkan and Vardaroğlu, 2008). Green production includes zero waste or reduction of waste, green product design and recycling.

Green Distribution: Green distribution includes the activities of determining the locations to which the products will be transported, realizing both forward and backward transports with just-in-time production, determining the characteristics (capacity, type, etc.) of the vehicles on which the transportation will be carried out, and realizing the distribution operations in a way that aims to reduce carbon emissions. The type of vehicle used, fuel type, capacity, round trip transportation frequency, the distance between customer positions affect the performance of green distribution (Sarkis, 2003).

Green Packaging: The materials used in the packaging of the products can also affect the effectiveness of GSCM. In order for packaging operations to be carried out in an environmentally friendly manner, it is necessary to use environmentally friendly materials or recycled materials and to consider the size of the packages. In addition, the fact that the packages used are designed to be recyclable also provides benefits on the performance of the company (Büyüközkan and Vardaroğlu, 2008). When the packaging strategy is created in this way, it ensures that less material is used and the space is used more efficiently by placing the products in the warehouse in a more orderly manner. In addition, with a good packaging, the products can be placed on the trucks more properly and the product capacity of the truck / transport vehicle can be increased. Thus, by reducing the number of trips for distribution, less fuel consumption is achieved and carbon emissions are reduced (Sarkis, 2003).

Reverse Logistics: Reverse logistics is all the activities applied for the reuse of materials or products. Normally, logistics includes processes from the

manufacturing of the product to its delivery to the customer. In reverse logistics, products are sent from the customer to the distributor or directly to the manufacturer. For example, if the product is defective, the customer sends it back to the factory. The factory, on the other hand, must carry out the collection activity of the defective product, detect the defect by breaking the product, repair it, and if it cannot be repaired, it must be separated into parts and recycle some or all of it. The defective product can travel backward from the customer to the factory. These activities are included in reverse logistics activities.

The reverse logistics flow is seen in Figure 1. In forward logistics, the flow is from the factory to the customer, while in reverse logistics, the flow is from the customer to the factory, as seen in Figure 1.

Figure 1. The flows of reverse logistics.

Reverse Logistics activities can be classified as follow:

1. Recycling
2. Reproduction
3. Reuse
4. Disposal

Recycling: Reverse logistics can generally be considered as processes making the product included in recycling. Recycling involves the collection of reusable wastes such as metal, plastic, glass, paper-cardboard, and reuse by chemical and/or physical processes (Özhesen, 2009). It is noteworthy that in recent years, recycled material is used in product packaging. Additionally, about 98% of the materials used in the electronics and household appliances industry are also recyclable. In our country, companies working in this sector collect products that have expired from customers with various campaigns to recycle. Thus, with the recycling of the products, both energy savings are achieved, and the negative effects on the environment are minimized by reusing these products as raw materials, and it is prevented that these products are collected without being thrown into the environment as waste and causing environmental pollution.

Reproduction: The reproduction process begins with the redelivery of the products that have completed their functions to the factory for recycling. These products are separated into their parts and it is determined whether the parts meet the expected properties for reuse or not. As a result of these processes, it is decided that some parts shall become waste, while others can be reused. These used parts and some new parts are combined by reassembly to recover the original product or create a new product. Remanufactured products generally have the same or similar performance characteristics and quality standards as new parts. Sending of aircraft which are used in the Turkish Armed Forces, to relevant companies due to technology change or renewal, and subsequently being examined by engineers, implementation of necessary modernization and reuse of aircraft can be given as an example of reproduction activities.

Reuse: It is the repeated use of the products throughout their economic life without any processing other than collecting and cleaning the products from the customers. Reuse occurs in many sectors and provides companies with a great advantage in terms of cost.

Disposal: In the disposal activities, it is checked whether the product contains harmful substances. Disposal is all of the activities carried out for the destruction of hazardous wastes generated during the manufacturing of the product itself, using appropriate technology, without harming the environment (Sarkis, 1998).

4. SAMPLE APPLICATIONS

It is noteworthy that the studies in the literature, researchers generally examine the green supply chain activities implemented by logistics companies. For this reason, in this study, in order to create a perspective for other sectors, GSCM activities implemented by companies in different sectors are examined. In this study, the studies of Arçelik brand, which produces electronics and household appliances, a grocery chain operating in the retail sector, the studies of Tofaş, an automobile brand, and the GSCM activities implemented by Sütaş, which produces perishable products in the retail sector, are discussed. The data used in this section are obtained from the sustainability reports published by the relevant companies once a year or every two years.

Migros is one of the leading companies that have been effectively implementing GSCM activities in our country for years. The company tries to reduce its negative effects on the environment both in production applications and in chain markets. In this context, it tries to reduce carbon gas emission and water consumption, reduces the use of paper and attaches importance to the use of recycled materials, and also adopts the zero waste principle in production and sends the wastes generated during production to licensed recycling facilities for recycling. In order to reduce paper and plastic consumption, the company uses recyclable materials in the packaging of its own products and carries out the transportation of fruits and vegetables with reusable plastic crates. In addition, it collects waste oil and waste batteries from its customers through both the “Sanal Market”

application and the boxes in its stores and sends them to licensed facilities. The company also works to increase efficiency in logistics and distribution areas in order to save energy and reduce carbon emissions. It tries to determine the optimum routes for the vehicles used in distribution by calculating the distances between the distribution centers and the stores and accordingly determines the location of the future distribution centers (Migros Sustainability Report, 2019).

Another company that attaches importance to GSCM applications in our country is Arçelik. The company attaches importance to renewable energy investments to combat global warming, reduces CO_2 emissions with the production of energy-efficient household appliances, and tries to reduce carbon emissions by preferring rail and sea transportation instead of road transport in logistics. In the packaging of products, it attaches importance to the use of recyclable / recycled materials and tries to minimize the negative impact on the environment by minimizing volume and weight of the packaging materials of the products. In addition, by applying the zero waste principle, the company reduces the waste generated as a result of production and provides recycling by separating the waste according to their classes. The company tries to reduce the damage to the environment, especially by using recyclable materials. Arçelik conducts various campaigns to collect end-of-life electrical and electronic items from its customers. With the Waste Electrical and Electronic Equipment facilities established in Bolu and Eskişehir, it separates the products it collects into materials such as metal, iron, plastic, aluminum and recycles them. In addition, it tries to reduce the negative effects on the environment by sending the wastes outside these categories to licensed recycling facilities (Arçelik Sustainability Report, 2020).

It is noteworthy that, in Tofaş, which is in the automotive sector, importance is given to GSCM activities. The company works to reduce global warming and carbon emission. For this purpose, it tries to reduce the amount of emission occurring in production stages, to increase the emission and global warming awareness of its suppliers in SCM and to ensure energy efficiency by using alternative fuel in vehicles. In addition to these studies, the company tries to reduce the amount of volatile organic compounds

occurring in dyeing operations and implements projects that will reduce the amount of CO_2 generated. In addition, the company aims to achieve minimum water consumption by ensuring the proper management of water and wastewater processes (Tofaş Sustainability Report, 2020).

Sütaş, which is involved in the production of perishable products, also has important studies on GSCM. Sütaş tries to reduce the distance covered and carbon emission by creating appropriate routes for the transportation of milk from suppliers located in different locations. In addition, it aims to reduce carbon emission and fuel consumption by ensuring that vehicles transporting products from factories to product distribution points also transport products to factories with a reverse flow. The company turns towards efforts to reduce greenhouse gases generated due to its production activities, to generate renewable energy from waste and to increase energy efficiency. In order to achieve this, the company has established an energy production facility where animal wastes are used as fuel. In addition, Sütaş makes product packaging by using recyclable materials in order to realize the zero waste strategy, and collects and recycles product packaging materials in cooperation with licensed companies (Sütaş, 2020).

In this section, the activities of four different companies in different sectors within the scope of GSCM and green logistics were discussed. Figure 2 has been created in order to determine which activities the companies mostly concentrate on, by taking into account the practices made by the companies.

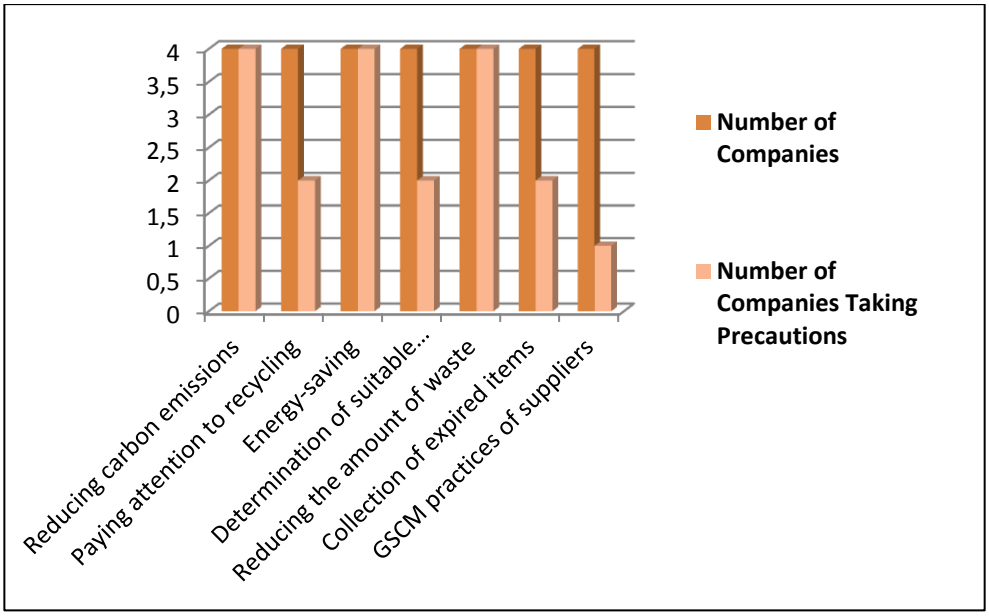

Figure 2. Comparison of the activities implemented by firms within the scope of the green supply chain.

When Figure 2 is examined, it is noteworthy that all companies implement activities to reduce carbon emission, energy saving and reduce waste amount within the scope of GSCM. Half of the companies attach importance to the use of recycled or recyclable materials in their packaging or products. In addition, 2 out of 4 companies are trying to reduce carbon emission and fuel consumption by trying to create appropriate routes while delivering their products to their customers or collecting their products from their suppliers. In addition to these, companies ensure that half of the end-of-life products are collected for recycling. Only one of the four companies works with suppliers who attach importance to GSCM activities and tries to implement green practices together with their suppliers.

In recent years, both legal regulations and customers' preference of companies that implement green policies have led many companies to turn to green policies. In the coming years, it is thought that companies will turn

to green activities in more areas, taking into account the green policies implemented in other countries.

5. SUGGESTIONS

It is noteworthy that in studies on GSCM, researchers generally examine companies in the logistics sector. Therefore, in this study, the activities implemented by leading companies in different sectors in our country to realize GSCM are discussed. In the study, the sustainability reports published by the companies were examined and their GSCM practices were discussed. In this section, based on the GSCM activities implemented in our country, GSCM activities that can be applied by companies in different sectors are mentioned with the aim of guiding these companies.

Green activities that companies in different sectors can implement during the transition to GSCM can be listed as follows:

- Companies should improve their operations and produce without damaging the environment.
- They should carry out studies to ensure reducing energy and water use.
- They should establish the facilities that will ensure the recycling of water.
- They should focus on the use of renewable energy sources.
- Studies should be made to reduce greenhouse gas emissions.
- They should use recyclable materials in production stage.
- They should ensure that recycled / recyclable materials are used in the packaging of the products.
- They should minimize the material used in the packaging of the products.
- They should ensure that the products are packaged properly.
- It should be ensured that the packaged products are properly loaded on the vehicles.
- Vehicles used in logistics activities should be operated at full capacity.

- It should be ensured that the amount of waste is kept to a minimum by working with the zero waste principle during production.
- Wastes generated during production should be separated and sent to appropriate recycling facilities.
- In the transportation of products, sea or rail should be preferred instead of road.
- Necessary efforts should be made to collect recyclable materials from customers or employees.
- If the company has customers/branches or stores in different locations, it should be ensured that appropriate routes are created for distribution to these locations.
- Fuel consumption and carbon emission should be reduced with an additional effort by transporting materials or recycled products to the factory with the vehicles used in distribution activities.
- They should establish recycling facilities within its own structure or deliver the products and wastes which they collect to licensed recycling facilities.

6. CONCLUSION

With the development of technology, the increase of competition and the unconscious use of resources in production activities for years; they caused the depletion of natural resources, the occurrence of global warming with the increase of carbon emissions and the deterioration of the environmental order. Countries and non-governmental organizations that have become aware of this situation have started to draw attention to the implementation of new environmentally sensitive approaches. Nowadays, businesses have started to apply GSCM approaches in their production and distribution activities with the effect of legal obligations, pressures of non-governmental organizations and the assumption that environmentally sensitive companies are preferred by customers. In this context, companies try to carry out environmentally friendly production/distribution activities such as performing recycling operations, using recycled/recyclable products, reducing carbon emissions, and decreasing energy consumption.

In this study, firstly, it was stated how the concepts of GSCM and green logistics emerged, and a literature review on these issues was included. In the scope of the study, brief information was given about the green approaches that emerged with GSCM. When the studies conducted in recent years are examined, it is noteworthy that the researchers examined the activities of GSCM in more detail. In recent studies, it is seen that researchers focus on topics such as supplier selection, reduction of carbon emission, and determination of appropriate routes to reduce energy consumption, reverse logistics and collecting recyclable products in GSCM.

In the following parts of the study, information was given about the concepts that entered the literature with GSCM. When the previous studies are examined, it has been determined that the researchers generally studied the green practices in the logistics sector. Therefore, in this study, the practices of companies in different sectors were examined in order to have information about green practices in different sectors. Within the scope of this study, the green activities of a market chain serving in the retail sector in our country, a company that produces electrical and electronic equipment, a brand that conducts automotive production and a company that manufactures perishable dairy products was examined. This information has been obtained from the sustainability reports published by the companies every year or every two years via their internet addresses. Green practices of these companies have been examined in detail in order to set an example for companies in different sectors. Subsequently, the joint activities implemented by these four companies within the scope of GSCM and other unique activities were determined. When the studies carried out by four companies within the scope of GSCM are examined, it is seen that all of them are conducting studies for energy saving, reducing carbon emission and reducing the amount of waste. In the last part of the study, suggestions were made in order to guide the companies that will turn to GSCM activities based on the activities implemented by the companies.

Green supply chain and green logistics are among the issues that have attracted attention both in the world and in our country in recent years. In this study, companies that attach importance to GSCM approaches in our country and take part in different sectors were examined. In this context, it

is seen that companies turn to renewable energy sources, implement practices to reduce carbon emissions, try to use environmentally friendly recyclable materials and attach importance to recycling activities. In particular, companies producing electronics and household appliances collect electronic products from their customers with reverse logistics from the facilities they have established, and recycle the products at a rate of 98%. For example, Arçelik conducts campaigns to collect end-of-life products with a reverse logistics approach by gathering old products from customers who will buy new products for a certain fee. With the Waste Electrical and Electronic Equipment facilities established in Bolu and Eskişehir, it separates the products it collects into materials such as metal, iron, plastic, aluminum and recycles them. In addition, it tries to reduce the negative effects on the environment by sending the wastes outside these categories to licensed recycling facilities. In the last few years, with the "Zero Waste" project of the Ministry of Environment and Urbanization, companies and individuals have raised awareness about recycling with environmentally sensitive approaches. This project has been implemented in places such as many universities and shopping centers, especially public institutions and organizations. Although GSCM approaches have been among the remarkable issues in our country in recent years, they are still not widely applied. In the coming years, green supply chain and green logistics activities will gain more importance with the increase of legal obligations and awareness of companies and people. It is thought that the suggestions made in this study will guide companies in different sectors.

ACKNOWLEDGEMENT

This study is the developed version of the declaration which has been entitled as "Çevreci Bir Lojistik Yaklaşımı: Yeşil Lojistik ve Türkiye'den Örnek Uygulamalar" and presented at the "4th National Logistics and Transportation Congress".

REFERENCES

ARÇELİK (2019). "Sürdürülebilirlik Raporu". Retrieved from https://www.arcelikglobal.com/media/5546/arcelik_master_online_1606.pdf

Beemsterboer, B., Land, M., and Teunter, R. (2017). "Flexible lot sizing in hybrid make-toorder make-to-stock production planning". *Eurepean Journal of Operations Research*, 260(3), 1014-1023. doi: 10.1016/j.ejor.2017.01.015.

Blanchard, D. (2017). *Tedarik Zinciri Yönetimi En İyi Uygulamalar* (Second Ed. M. Tanyaş & M. Düzgün, Transl.) Ankara: Nobel.

Bowen, F. E., Cousins, P. D. Lamming, R. C., and Faruk, A. C. (2001). "The Role of Supply Management Capabilities in Green Supply". *Production and Operations Management.* 10(2), 174-189. doi:10.1111/j.1937-5956.2001.tb00077.x.

Büyüközkan, G., and Çapan, A. (2008). "Improving Supply Chain Management Practices: A Case Study". *Proceeding of the 5th International Logistics and Supply Chain Congress*, 595-605, 8-9 Kasım, İstanbul.

Büyüközkan, G., and Vardaloğlu, Z. (2008). "Yeşil Tedarik Zinciri Yönetimi". *Lojistik Dergisi*, Vol. 8. 66-73.

Geffen, C. A., and Rothenberg. S. (2000). "Suppliers and Environmental Innovation: The Automotive Paint Process". *International Journal of Operations & Production Management.* 20(2), 166-186. doi:10.1108/01443570010304242.

Green Fr., K. W., Zelbst, P. F., Meacham, F., and Bhadauria, V. S. (2012). "Green Supply Chain Management Practices: Impact on Performance". *Supply Chain Management: An International Journal*. 17(3), 290–305. doi:10.1108/13598541211227126

Kopicki, R., Berg, M. J., Legg, L., and Poist, R. F. (1995). "Reuse and Recycling-Reverse Logistics Opportunities". *Transportation Journal*, 34(3), 64.

Lippman, S. (1999). "Supply Chain Environmental Management: Elements for Success". *Environmental Management.* 6(2), 175-182. doi:10.1016/S1066-7938(00)80027-5.

Lippman, S. (2001). "Supply Chain Environmental Management". *Environmental Quality Management*. Vol. Winter, 11-14. doi:10.1016/S1066-7938(00)80027-5.

Louly, M. A., Dolgui, A., and Hnaien, F., (2008). "Supply planning for single-level assembly system with stochastic component delivery times and service-level constraint". *International Journal of Production Econonomy*, 115(1), 236-247. doi:10.1016/j.ijpe.2008.06.005.

Mahmood, W., Hasrulnizzam, W., Ab Rahman, M. N., Deros, B., Jusoff, K., Saptari, A., and Bakar, A. (2013). "Manufacturing performance in green supply chain management". *World Applied Sciences Journal*. Vol. 21 (Special Issue of Engineering and Technology), 76-84. doi:10.5829/idosi.wasj.2013.21.1010.

Mardani, A., Kannan, D., Hooker, R. E., Ozkul, S., Alrasheedi, M., and Tirkolaee, E. B. (2020). "Evaluation of green and sustainable supply chain management using structural equation modelling: a systematic review of the state of the art literature and recommendations for future research". *Journal of Cleaner Production,* Vol. 249, 119-138. doi:10.1016/j.jclepro.2019.119383.

MİGROS (2019). "Sürdürülebilirlik Raporu". Retrieved from https://www.migroskurumsal.com/surdurulebilirlikfiles/pdf/Migros-Surdurulebilirlik-Raporu-2019.pdf

Moktadir, M. A., Ali, S. M., Jabbour, C.J.C., Paul, A., Ahmed, S., Sultana, R., and Rahman, T. (2019). "Key factors for energy-efficient supply chains: implications for energy policy in emerging economies". *Energy*, 189(15), 1-15. doi:10.1016/j.energy.2019.116129.

Ozyoruk, B. (2018). "A Literature Survey on Green Supplier Selection". *The Eurasia Proceedings of Science Technology Engineering and Mathematics*, Vol. 2, 407-411.

Porter, M. E., and van der Linde, C. (1995). "Green and Competitive: Ending the Stalemate". *Harvard Business Review*, 73(5) (September-October).

Rao, C. J., Goh, M., Zhao, Y., and Zheng, J. J. (2015). "Location selection of city logistics centers under sustainability". *Transportation Research D-Transportation Environ*ment, Vol. 36, 29-44. doi:10.1016/j.trd.2015.02.008.

Rao, C.J., Lin, H., and Liu, M. (2020). "Design of comprehensive evaluation index system for P2P credit risk of "three rural" borrowers". *Soft Computing*, 24(15), 11493-11509. doi:10.1007/s00500-019-04613-z.

Sarkis, J. (1998). "Evaluating environmentally conscious business practices". *European Journal of Operational Research*, 107(1), 159-174. doi:10.1016/S0377-2217(97)00160-4.

Sarkis, J. (2003). "A Strategic Framework for Green Supply Chain Management". *Journal of Cleaner Production*, Vol.11, 397-409. doi:10.1016/S0959-6526(02)00062-8

Sarkis, J., Hervani, A. A., and Helms, M. M. (2005), "Performance Measurement for Green Supply Chain Management". *Benchmarking: An International Journal*, 12(4), 330-353. doi:10.1108/14635770510609015.

Simpson, D., and Power, D. (2005). "Use The Supply Relationships to Develop Lean and Green Suppliers". *Supply Chain Management: An International Journal*, 10(1), 60-68. doi:10.1108/13598540510578388.

SÜTAŞ (2020). "Sürdürülebilirlik". Retrieved from https://www.sutassurdurulebilirlik.com//yazilar/tag/ %C3% A7evre

Temur G. T., Ayvaz, B., and Bolat, B. (2015). *Tersine Lojistik Yönetimi*, Nobel, Ankara.

Timur, M. N., Başkol, M., Çekerol, G. S., and Suvacı, B. (2013). *Tedarik Zinciri Yönetimi*, T.C. Anadolu Üniversitesi Yayını, No: 2889, Açıköğretim Fakültesi Yayını, No: 1846.

TOFAŞ (2019). "Sürdürülebilirlik Raporu 2019" Retrieved from https://www.tofas.com.tr/Surdurulebilirlik/SurdurulebilirlikRaporlari/Documents/2019_surdurulebilirlik_tr.pdf

Tunç, T. (2020). "Yeşil Stratejiler ve Uygulama Alanlarına Yönelik Nitel Bir Araştırma: Türkiye Örneği". *Üçüncü Sektör Sosyal Ekonomi Dergisi*, 55(4), 2288-2322. doi:10.15659/3.sektor-sosyal-ekonomi.20.10.1439.

Van Hoek, R. I. (1999). "From Reversed Logistics to Green Supply Chains". *Supply Chain Management*, 4(3), 129-134. doi:10.1108/13598549910279576.

Wilkerson, T. (2005, April 05). "Best Practices in Implementing Green Supply Chains". [PowerPoint Slides]. North America Supply Chain World Conference and Exposition. Retrieved from UN Environment Programme (UNEP). Retrieved from https://postconflict.unep.ch/humanitarianaction/documents/02_08-04_05-25.pdf

World Commission on Environment and Development (WCED). (1987). *Our Common Future*. Oxford: Oxford University.

Wycherley, I. (1999). "Greening Supply Chains: The Case of the Body Shop International". *Business Strategy and the Environment*. 8(2), 120-127.

Yang, C. S., Lu, C. S., Haider, J. J., and Marlow, P. P. (2013). "The Effect of Green Supply Chain Management on Green Performance and Firm Competitiveness in the Context of Container Shipping in Taiwan". *Transportation Research Part E*, Vol. 55, 55–73. doi:10.1016/j.tre.2013.03.005.

Zhang, X., and Yousaf, H.M.A.U. (2020). "Green supply chain coordination considering government intervention, green investment, and customer green preferences in the petroleum industry". *Journal of Cleaner Production*, 246(10), 1-7. doi:10.1016/j.jclepro.2019.118984.

Zhen, L., Huang, L., and Wang, W. (2019). "Green and sustainable closed-loop supply chain network design under uncertainty". *Journal of Cleaner Production*, Vol. 227, 1195-1209. doi:10.1016/j.jclepro.2019.04.098.

Zhu, Q., and Sarkis, J. (2004). "Relationships between Operational Practices and Performance Among Early Adopters of Green Supply Chain Management Practices in Chinese Manufacturing Enterprises". *Journal of Operations Management*, Vol. 22, 265-289. doi:10.1016/j.jom.2004.01.005.

Zhu, Q., Sarkis, J., and Geng, Y. (2005). "Green Supply Chain Management in China: Pressures, Practices and Performance". *International Journal of Operations & Production Management*. 25(5), 449-468. doi:10.1108/01443570510593148.

Zhu, Q., Sarkis, J., and Lai, K. (2007a). "Initiatives and Outcomes of Green Supply Chain Management Implementation by Chinese Manufacturers". *Journal of Environmental Management*, Vol. 85, 179-189. doi:10.1016/j.jenvman.2006.09.003.

Zhu, Q., Sarkis, J., and Lai, K. (2007b). "Green Supply Chain Management: Pressures, Practices and Performance within the Chinese Automobile Industry". *Journal of Cleaner Production*. Vol. 15. 1041-1052. doi:10.1016/j.jclepro.2006.05.021.

Zhu, Q., Sarkis, J., and Lai, K. (2008). "Confirmation of A Measurement Model For Green Supply Chain Management Practices Implementation". *International Journal of Production Economics*, Vol. 111, 261–273. doi:10.1016/j.ijpe.2006.11.029.

Zhu, Q., Sarkis, J., and Lai, K. (2008). "Green Supply Chain Management Implications for Cloosing the Loop". *Transportation Research Part E*, Vol. 44, 1-18. doi:10.1016/j.tre.2006.06.003.

Zsidisin, G. A. and Siferd, S. P. (2001). "Environmental Purchasing: A Framework for Theory Development". *European Journal of Purchasing & Supply Management.* 7(1), 61-73. doi:10.1016/S0969-7012(00)00007-1.

Journal of Naval Sciences and Engineering
2021, Vol. 17, No. 2, pp. 309-341
Naval Architecture and Marine Engineering/Gemi İnşaatı ve Gemi Makineleri Mühendisliği

RESEARCH ARTICLE

**An ethical committee approval and/or legal/special permission has not been required within the scope of this study.*

ASSESSMENT OF PURE LOSS OF STABILITY FOR A TURKISH NAVY TANKER*

Muhammet Ali YILMAZER[1]
Burak YILDIZ[2]

[1]*Yıldız Technical University, Department of Naval Architecture and Marine Engineering, Istanbul, Turkey,*
f0819004@std.yildiz.edu.tr; ORCID: 0000-0001-6554-6838

[2]*Yıldız Technical University, Department of Marine Engineering Operations, Istanbul, Turkey,*
buraky@yildiz.edu.tr; ORCID: 0000-0002-0559-8772

Received: 18.05.2021 **Accepted: 17.08.2021**

ABSTRACT

The second generation intact stability criteria (SGISC) have been developed by the International Maritime Organization's (IMO) Sub-committee on Ship Design and Construction (SDC). The SGISC involve improving the current intact stability criteria by including dynamic movements of ships in waves. The criteria are structured around five failure modes, pure loss of stability being one of these. This paper presents sample calculations regarding the assessment of pure loss of stability for a Turkish navy tanker. The calculations involve two steps that this study explains: Level 1 and Level 2. In addition, Option A and Option B are used as solution methods for both levels. Minimum metacentric heights (GM_{min}) are calculated at the lowest draft (Option A) and at different wave crest locations alongside the ship (Option B) for Level 1. Values for the angle of vanishing stability, angle of loll, angle of stable equilibrium and maximum righting lever have been calculated from the GZ curves for Level 2. As a result, the subject ship was found not to be vulnerable to pure loss of stability. Level 1 results for both options are inconsistent due to Level 2 results being consistent.

Keywords: *Second Generation Intact Stability Criteria, Pure Loss of Stability, Level 1, Level 2, Navy Tanker.*

BİR TÜRK DONANMA TANKERİ İÇİN TOPLAM STABİLİTE KAYBININ DEĞERLENDİRİLMESİ

ÖZET

İkinci nesil hasarsız stabilite kriterleri, Uluslararası Denizcilik Örgütü'ne (IMO) bağlı olan Gemi Tasarımı ve İnşası Alt Komitesi (SDC) tarafından geliştirilmiştir. İkinci nesil hasarsız stabilite kriterleri, geminin dalgaların etkisi ile yaptığı dinamik hareketlerini inceleyerek mevcut hasarsız stabilite kriterlerinin iyileştirilmesi hakkındadır. İkinci nesil hasarsız stabilite kriterleri, beş zafiyet modu üzerinde yapılandırılmıştır. Dalga tepesinde toplam stabilite kaybı, beş zafiyet modundan biridir. Bu makalede, Türk donanmasına ait bir tanker için dalga tepesinde toplam stabilite kaybı zafiyet durumunun değerlendirmesi hakkında örnek hesaplamalar sunulmaktadır. Hesaplamalar Seviye 1 ve Seviye 2 olmak üzere iki aşamada incelenmiştir. Ayrıca Opsiyon A ve Opsiyon B çözüm yöntemleri kullanılmıştır. Seviye 1 hesaplamaları için minimum metasentır yükseklikleri (GM_{min}), en düşük draft drumunda (Opsiyon A) ve gemi boyunca 11 farklı dalga tepesi konumu arasından (Opsiyon B) hesaplanmıştır. Devrilme açısı, bayılma açısı, dengeye gelme açısı ve maksimum doğrultucu kol değerleri, Level 2 için GZ eğrilerinden hesaplanmıştır. Hesaplamalar sonucunda, seçilen geminin dalga tepesinde toplam stabilite kaybı açısından güvenli olduğu tespit edilmiştir. Her iki opsiyon için yapılan Seviye 1 hesaplama sonuçları tutarsızlık gösterirken, Seviye 2 sonuçları tutarlılık göstermiştir.

Keywords: *İkinci Nesil Hasarsız Stabilite Kriterleri, Dalga Tepesinde Toplam Stabilite Kaybı, Seviye 1, Seviye 2, Askeri Tanker.*

1. INTRODUCTION

Despite complying with the International Code on Intact Stability 2008 (IS Code 2008), many ships (e.g., APL China, Chicago Express, JRS Canis) have been involved in stability-related accidents (Petacco, 2019). These accidents show the insufficiency of the current intact stability criteria. As a result, IMO has started work on the Second Generation Intact Stability Criteria (SGISC) to identify the new intact stability criteria regarding the dynamic stability of ships in waves.

SGISC have been under development through IMO's sub-committee on Ship Design and Construction (SDC) since 2005. SGISC are intended to improve the current intact stability rules by adding safety in waves. SGISC are gathered under the following five stability failure modes: pure loss of stability, parametric roll, dead ship condition, surf-riding/broaching and excessive acceleration (IMO-SDC, 2019).

SGISC have many different aspects apart from the current stability rules that make up 2008 IS Code. 2008 IS Code involves the following basic parameters: righting lever arm (GZ) and initial metacentric height (GM) as calculated for a ship in calm water. These parameters are strictly related to the vertical position of the ship's centre of gravity (KG). Meanwhile, SGISC generally focus on wave-based dynamic forces using a probabilistic approach. SGISC have three assessment levels in each failure mode. Level 1 concerns the GM_{min} calculation based on a simplified physical and deterministic approach. Level 2 is based on a probabilistic approach that requires calculations on hydrostatics in waves (GZ). Level 3 uses a direct assessment method and consists of experiments or numerical simulations of the ship's behaviour in waves.

In the last 15 years, SGISC development has been one of the most important topics for SDC. At the beginning of 2020, SDC 7^{th} session finalized SGISC after a long and demanding process. SGISC are expected to come into force as recommendations; nevertheless, IMO endorses their application for assessing their consistency and validity (Petacco and Gualeni, 2020). Therefore many studies have been carried out for different ship types by the

committee members during the development of the new criteria. Some of these studies have focused on pure loss of stability. For example, Chorab carried out sample calculations for pure loss of stability on a fishing vessel. Pure loss of stability mainly affects ships with small hulls, which is why a fishing vessel was chosen (Chorab, 2014). Grinnaert et al. studied both pure loss of stability and parametric roll phenomena. Level 1 and Level 2 assessment steps were applied for three naval ships of different sizes (helicopter carrier, destroyer, offshore patrol vessel) (Grinnaert, 2016). Chouliaras presented information about SGISC failure modes apart from the dead ship condition and applied them to a post-Panamax container ship (Chouliaras, 2015). Panagiotellis applied SCISC to a series of RoRo Passenger (RoPax) and RoRo Cargo Ships (Panagiotellis, 2018). Grinnaert carried out SGISC calculations for a variety of civilian and naval ships (Grinnaert, 2017).

This study concerns sample calculations regarding the failure mode of pure loss of stability. The following chapters present theoretical calculation procedures and the physical background of proposed criteria for pure loss of stability. A Turkish navy tanker is used as the sample ship. Both Level 1 and Level 2 calculations have been carried using the option A and option B solution methods. All calculation steps are presented in detail and the results have been presented for the subject ship.

2. SECOND GENERATION INTACT STABILITY CRITERIA

2.1. Pure Loss of Stability

Pure loss of stability is the reduction of stability due to wave passage when a ship is sailing in longitudinal waves. As can be seen in Figures 1 and 2, the waterline area undergoes a significant change in waves, which also leads to a change in the righting lever arm (GZ) curve. If the waterline area decreases, the area under the righting lever arm (GZ) curve decreases. As a result, the stability of the ship decreases and the failure mode of pure loss of stability may occur.

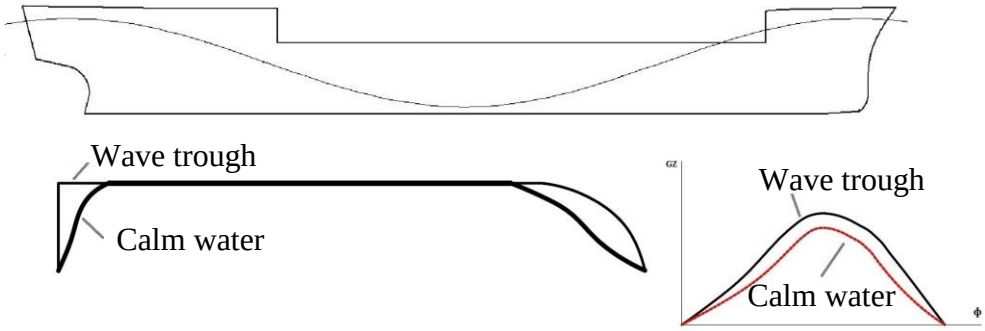

Figure 1. Changes in waterplane and GZ curve when a wave trough is amidships.

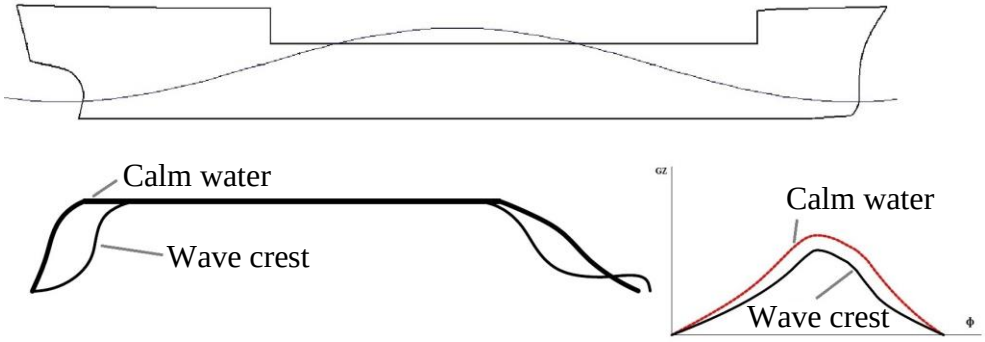

Figure 2. Changes in waterplane and GZ curve when a wave crest is amidships.

The vulnerability assessment method for pure loss of stability applies to ships over 24 meters in length with a Froude number greater than 0.24.
The Froude number is calculated as follows:

$$F_N = \frac{V_S}{\sqrt{gL}} \qquad \textbf{(1)}$$

where:

F_N -Froude number [–],
L -ship's length [m],
g -acceleration due to gravity [m/s^2],
V_s -service speed [m/s].

In addition, the following requirement must be met in order to apply the method:

$$\frac{V_D - V}{A_W (D - d)} \geq 1{,}0 \qquad \textbf{(2)}$$

where:
V_D -volume of displacement at draft equal to depth, D [m^3],
V -volume of displacement for the loading condition under consideration [m^3],
d -mean draft corresponding to the loading condition under consideration [m],
A_W -waterplane area [m^2],
D -molded depth at side to the weather deck [m].

2.1.1. Level 1 Assessment (Option A)

The Level 1 assessment using Option A requires calculating the GM_{min} value associate with the lowest draft as a longitudinal wave passes the ship. The ship is considered not to be vulnerable to pure loss of stability if GM_{min}>0.05 m.
The wave length (λ) is equal to the ship length (L) where the wave height (H_W) is calculated as:

$$H_W = 0.0334 \cdot \lambda \qquad \textbf{(3)}$$

If both 1 and 2 conditions are satisfied, the following Equation can be used to calculate GM_{min}:

$$GM_{\min} = KB + \frac{I_L}{V} - KG \qquad \textbf{(4)}$$

where:

V -displacement volume [m^3],
KB -vertical height of center of buoyancy [m],
KG - vertical height of center of gravity [m],
I_L - moment of inertia for the waterplane corresponding to d_L [m^4].

The method for Option A assumes the moment of inertia of the waterplane area in the waves to be equal to that of the parallel waterplane area in calm water at the lowest draught shown in Figure 3 (denoted by d_L).

The lowest draught d_L for the moment of inertia of the waterplane (I_L) corresponding to the loading case is computed as:

$$d_L = d - \delta d_L \quad \textbf{(5)}$$

$$\delta d_L = \min\left(d - 0.25 d_{full}, 0.5 H_W\right) \quad \textbf{(6)}$$

where:
d_{full} -draft corresponding to the full loading condition [m],
d_L -draft for calculating the transverse moment of inertia of the waterplane [m],
δd_L -draft difference to be deducted due to ship's loading condition; the smallest value from Equation 6 [m],
H_W -wave height in Equation 3.

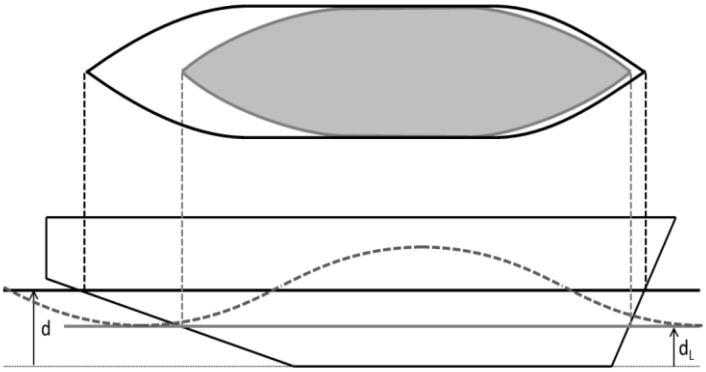

Figure 3. Parallel waterplane at the lowest draft (d_L) (Grinnaert, 2017).

2.1.2. Level 1 Assessment (Option B)

The method for option B consists of computing the minimum metacentric height for different wave crest locations. GM_{min} calculations are carried out for 11 points along the wave crest: with the wave crest located amidships and intervals of 0.1L, 0.2L, 0.3L, 0.4L, 0.5L forward and aft of amidships, and the lowest value among these is chosen.

Wave length (λ) is equal to ship length (L), and wave height (H_W) is calculated as shown in Equation 3. The ship is considered to not be vulnerable to pure loss of stability in Option B when $GM_{min} > 0.05$ m. If Level 1 is satisfied, the Level 2 assessment is unnecessary.

2.1.3. Level 2 Assessment (Option A)

Level 2 consists of a probabilistic approach associated with a wave scattering table that includes 16 different waves. Table 1 is used for the Level 2 Option A assessment of pure loss of stability.

The Level 2 assessment is done using the actual GZ curves (Figure 4). A ship is considered not to be vulnerable to the failure mode of pure loss of stability when the greatest value of parameters CR_1, CR_2, CR_3 does not exceed 0.06 m. This is presented as follows.

$$CR_{\max} < 0.06 \quad \textbf{(7)}$$

$$CR_{\max} = \max\begin{cases} CR_1 \\ CR_2 \\ CR_3 \end{cases} \quad \textbf{(8)}$$

CR_1, CR_2, CR_3 are a weighted average of specific stability parameters for a ship considered to be statically positioned in defined waves as in Table 1.

$$CR_1 = \sum_{i=1}^{N} W_i C1_i \quad \textbf{(9)}$$

$$CR_2 = \sum_{i=1}^{N} W_i C2_i \quad \textbf{(10)}$$

$$CR_3 = \sum_{i=1}^{N} W_i C3_i \tag{11}$$

where:

W_i -weight factor obtained from Table 1 for Option A,
i -number of each wave described in Table 1,
N -total wave number in Table 1.

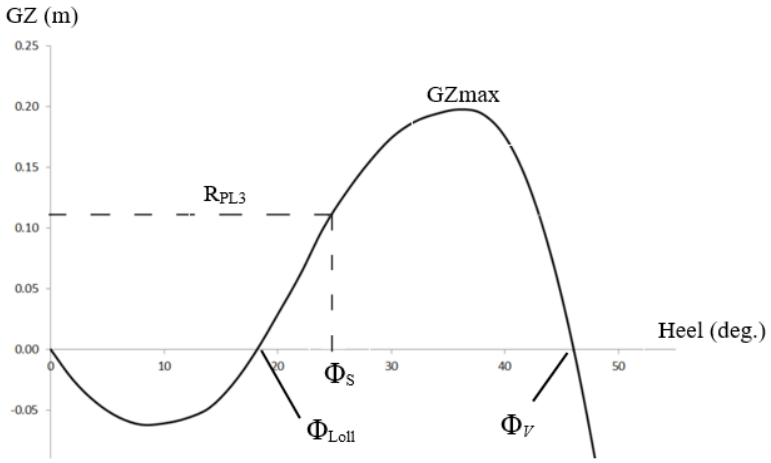

Figure 4. GZ curve with an angle of stability (Φ_S), equilibrium under heeling lever R_{PL3}, angle of vanishing stability (Φ_V) and angle of Loll (Φ_{Loll}).

The first short-term criterion of $C1_i$ concerns the minimum angle of vanishing stability ($\Phi_{V,min}$) and is determined as the minimum of the computed values for each wave height (H_W) in Table 1 with the wave crest located amidships and intervals of 0.1L, 0.2L, 0.3L, 0.4L, 0.5L forward and aft of amidships.

$$C1_i = \begin{cases} 1 & \Phi_{V\min i} < 30 \\ 0 & otherwise \end{cases} \tag{12}$$

The second short-term criterion of $C2_i$ concerns the angle of loll (Φ_{Loll}) caused by a negative value for the initial metacentric height and is determined as the minimum of the computed values for each wave height

(H_W) in Table 1 with the wave crest located amidships and intervals of 0.1L, 0.2L, 0.3L, 0.4L, 0.5L forward and aft of amidships.

$$C2_i = \begin{cases} 1 & \Phi_{loll,\min i} > K_{PL2} \\ 0 & otherwise \end{cases} \quad \textbf{(13)}$$

where:

K_{PL2} -15 degrees for passenger ships,
-25 degrees for all other ships

The third short-term criterion for $C3_i$ refers to the ship's maximum righting lever ($GZmax_)$ and determined as the minimum of the computed values for each wave height (H_W) in Table 1 with the wave crest located amidships and intervals of 0.1L, 0.2L, 0.3L, 0.4L, 0.5L forward and aft of amidships.

$$C3_i = \begin{cases} 1 & GZ\max_{\min i}(m) < R_{PL3} \\ 0 & otherwise \end{cases} \quad \textbf{(14)}$$

$$R_{PL3} = 8\left(\frac{H_i}{\lambda_i}\right)dFn^2 \text{ [m]} \quad \textbf{(15)}$$

where:

H -significant wave height,
λ -wave length,
d -draft corresponding to the loading condition,
F_n -Froude number corresponding to ship's service speed.

The ship is considered to not be vulnerable when the largest value among CR_1, CR_2 and CR_3 does not exceed 0.06.

Table 1. Wave parameters used in Level 2 Option A Assessment.

Regular wave number	**Weighting factor**	**Wave length**	**Wave height**	**Wave steepness**	**Reversed wave steepness parameter**
	Wi	*λi* [m]	*Hi* [m]	*Swi* [–]	1/*Swi* [–]
1	1,30E-05	22,574	0,700	0,0310	32,2
2	1,65E-03	37,316	0,990	0,0265	37,7
3	2,09E-02	55,743	1,715	0,0308	32,5
4	9,28E-02	77,857	2,589	0,0333	30,1
5	1,99E-01	103,655	3,464	0,0334	29,9
6	2,49E-01	133,139	4,410	0,0331	30,2
7	2,09E-01	166,309	5,393	0,0324	30,8
8	1,29E-01	203,164	6,351	0,0313	32,0
9	6,25E-02	243,705	7,250	0,0297	33,6
10	2,48E-02	287,931	8,080	0,0281	35,6
11	8,37E-03	355,843	8,841	0,0263	38,0
12	2,47E-03	387,440	9,539	0,0246	40,6
13	6,58E-04	422,723	10,194	0,0230	43,4
14	1,58E-04	501,691	10,739	0,0214	46,7
15	3,40E-05	564,345	11,241	0,0199	50,2
16	7,00E-06	630,684	11,900	0,0189	53,0

2.1.4. Level 2 Assessment (Option B)

Level 2 Option B also consists of a probabilistic approach associated with a wave scattering table. According to the SDC, the North Atlantic wave scatter diagram (Table 2) from IACS Recommendation No. 34 can be used for Level 2 Option B (IMO-SDC, 2019). This table lists 16 wave periods and 17 wave heights, with 197 waves having a non-zero number of occurrence. Because many waves need to be calculated, Grim proposed a new method based on the concept of effective wave height (Grim, 1961). The method consists of computing the effective height of the 3% highest waves corresponding to an equivalent wave whose length is equal to the ship's length. The effective wave heights are generated using Equations 16-23 from Table 2. For the subject ship, the calculated effective wave heights are presented in Table 3.

$$Hr_i = \begin{cases} 5.97 \cdot \sigma_{Heff} & if \quad 4.0 \cdot \sigma_{Heff} \le 0.1 \cdot L \\ 0.1 \cdot L & 4.0 \cdot \sigma_{Heff} > 0.1 \cdot L \end{cases} \tag{16}$$

$$\sigma^2_{Heff} = \sum_{i=1}^{N_{eff}} \left(RAO_{Heff}(\omega_i) \right)^2 S_W(\omega_i) \Delta\omega \tag{17}$$

$$RAO_{Heff}(\omega) = \begin{cases} \left\{ \dfrac{k_w(\omega) \cdot L \sin\left(0.5 k_w(\omega) \cdot L\right)}{\pi^2 - \left(0.5 k_w(\omega) \cdot L\right)^2} \right\} & if \quad \omega \neq \omega_L \\ 1.0 & if \quad \omega = \omega_L \end{cases} \tag{18}$$

$$k_W(\omega) = \frac{\omega^2}{g} \tag{19}$$

$$\omega_i = (i+1)\Delta\omega; \quad i = 1,2,..N_{eff} \tag{20}$$

$$\Delta\omega = \frac{3\omega_L}{N_{eff}} \text{ ; and} \tag{21}$$

$$\omega_L = \sqrt{\frac{2g\pi}{L}} \tag{22}$$

$$S_W(\omega) = \frac{H_S^2}{4\pi} \cdot \left(\frac{2\pi}{T_Z} \right)^4 \omega^{-5} \exp\left(-\frac{1}{\pi} \left(\frac{2\pi}{T_Z} \right)^4 \omega^{-4} \right) \tag{23}$$

where:

Hr_i	-effective wave height;
RAO_{eff}	-response amplitude operators;
H_S	-significant wave height in Table 2;
T_Z	-zero-crossing period in Table 2;
S_W	-wave steepness
N_{eff}	-total wave number (197 in Table 2);
i	-from 1 to 197 (total wave in Table 2).
w_i	-wave frequency

Table 2. Wave scatter diagram for the North Atlantic (from IACS, 2001).

HS	3,50	4,50	5,50	6,50	7,50	8,50	9,50	10,50	11,50	12,50	13,50	14,50	15,50	16,50	17,50	18,50
0,50	1,30	133,70	865,60	1186,00	634,20	186,30	36,90	5,60	0,70	0,10	0,00	0,00	0,00	0,00	0,00	0,00
1,50	0,00	29,30	986,00	4976,00	7738,00	5569,70	2375,70	703,50	160,70	30,50	5,10	0,80	0,10	0,00	0,00	0,00
2,50	0,00	2,20	197,50	2158,80	6230,00	7449,50	4860,40	2066,00	644,50	160,20	33,70	6,30	1,10	0,20	0,00	0,00
3,50	0,00	0,20	34,90	695,50	3226,50	5675,00	5099,10	2838,00	1114,10	337,70	84,30	18,20	3,50	0,60	0,10	0,00
4,50	0,00	0,00	6,00	196,10	1354,30	3288,50	3857,50	2685,50	1275,20	455,10	130,90	31,90	6,90	1,30	0,20	0,00
5,50	0,00	0,00	1,00	51,00	498,40	1602,90	2372,70	2008,30	1126,00	463,60	150,90	41,00	9,70	2,10	0,40	0,10
6,50	0,00	0,00	0,20	12,60	167,00	690,30	1257,90	1268,60	825,90	386,80	140,80	42,20	10,90	2,50	0,50	0,10
7,50	0,00	0,00	0,00	3,00	52,10	270,10	594,40	703,20	524,90	276,70	111,70	36,70	10,20	2,50	0,60	0,10
8,50	0,00	0,00	0,00	0,70	15,40	97,90	255,90	350,60	296,90	174,60	77,60	27,70	8,40	2,20	0,50	0,10
9,50	0,00	0,00	0,00	0,20	4,30	33,20	101,90	159,90	152,20	99,20	48,30	18,70	6,10	1,70	0,40	0,10
10,50	0,00	0,00	0,00	0,00	1,20	10,70	37,90	67,50	71,70	51,50	27,30	11,40	4,00	1,20	0,30	0,10
11,50	0,00	0,00	0,00	0,00	0,30	3,30	13,30	26,60	31,40	24,70	14,20	6,40	2,40	0,70	0,20	0,10
12,50	0,00	0,00	0,00	0,00	0,10	1,00	4,40	9,90	12,80	11,00	6,80	3,30	1,30	0,40	0,10	0,00
13,50	0,00	0,00	0,00	0,00	0,00	0,30	1,40	3,50	5,00	4,60	3,10	1,60	0,70	0,20	0,10	0,00
14,50	0,00	0,00	0,00	0,00	0,00	0,10	0,40	1,20	1,80	1,80	1,30	0,70	0,30	0,10	0,00	0,00
15,50	0,00	0,00	0,00	0,00	0,00	0,00	0,10	0,40	0,60	0,70	0,50	0,30	0,10	0,10	0,00	0,00
16,50	0,00	0,00	0,00	0,00	0,00	0,00	0,00	0,10	0,20	0,20	0,20	0,10	0,10	0,00	0,00	0,00

Table 3. Effective wave heights generated from wave scatter diagram (in Table 2).

HS	3,50	4,50	5,50	6,50	7,50	8,50	9,50	10,50	11,50	12,50	13,50	14,50	15,50	16,50	17,50	18,50
0,50	0,414	0,539	0,514	0,444	0,371	0,309	0,258	0,217	0,185	0,159	0,000	0,000	0,000	0,000	0,000	0,000
1,50	0,000	1,616	1,542	1,331	1,113	0,926	0,773	0,652	0,554	0,476	0,412	0,360	0,317	0,000	0,000	0,000
2,50	0,000	2,693	2,570	2,218	1,855	1,543	1,289	1,086	0,923	0,793	0,687	0,600	0,528	0,468	0,000	0,000
3,50	0,000	3,770	3,598	3,105	2,597	2,160	1,805	1,520	1,293	1,110	0,961	0,840	0,739	0,655	0,585	0,000
4,50	0,000	0,000	4,626	3,992	3,339	2,777	2,320	1,955	1,662	1,427	1,236	1,080	0,951	0,843	0,752	0,000
5,50	0,000	0,000	5,654	4,879	4,081	3,394	2,836	2,389	2,032	1,744	1,511	1,320	1,162	1,030	0,919	0,824
6,50	0,000	0,000	6,682	5,766	4,823	4,012	3,352	2,823	2,401	2,061	1,786	1,560	1,373	1,217	1,086	0,974
7,50	0,000	0,000	0,000	6,653	5,565	4,629	3,867	3,258	2,770	2,378	2,060	1,800	1,584	1,404	1,253	1,124
8,50	0,000	0,000	0,000	7,541	6,307	5,246	4,383	3,692	3,140	2,696	2,335	2,040	1,795	1,592	1,420	1,274
9,50	0,000	0,000	0,000	8,428	7,049	5,863	4,898	4,127	3,509	3,013	2,610	2,280	2,007	1,779	1,587	1,424
10,50	0,000	0,000	0,000	0,000	7,791	6,480	5,414	4,561	3,879	3,330	2,884	2,520	2,218	1,966	1,754	1,574
11,50	0,000	0,000	0,000	0,000	**8,533**	7,097	5,930	4,995	4,248	3,647	3,159	2,760	2,429	2,153	1,921	1,724
12,50	0,000	0,000	0,000	0,000	5,770	7,715	6,445	5,430	4,617	3,964	3,434	3,000	2,640	2,340	2,088	0,000
13,50	0,000	0,000	0,000	0,000	0,000	8,332	6,961	5,864	4,987	4,281	3,709	3,239	2,852	2,528	2,255	0,000
14,50	0,000	0,000	0,000	0,000	0,000	5,770	7,477	6,298	5,356	4,598	3,983	3,479	3,063	2,715	0,000	0,000
15,50	0,000	0,000	0,000	0,000	0,000	0,000	7,992	6,733	5,726	4,915	4,258	3,719	3,274	2,902	0,000	0,000
16,50	0,000	0,000	0,000	0,000	0,000	0,000	0,000	7,167	6,095	5,232	4,533	3,959	3,485	0,000	0,000	0,000

The maximum effective height is obtained from Table 3, with 11 effective wave heights being generated from zero to the maximum effective wave height whose wave length is equal to the ship's length. The minimum angle of vanishing stability ($\Phi_{V,min}$) and maximum angle of stable equilibrium ($\Phi_{S,max}$) are calculated for these 11 waves for the wave crest centered at the longitudinal center of gravity and each $\lambda/10$ increment forward and aft thereof. Next, the values for $\Phi_{V,min}$ and $\Phi_{S,max}$, which are required to

calculate coefficients $C1_i$ and $C2_i$ associated to all waves in the scatter diagram, are calculated by interpolating the values of the previously calculated 11 effective wave heights. After obtaining all these values, the Level 2 assessment of the vulnerability to pure loss of stability is done as follows:

$$CR_{\max} < 0{,}06 \tag{24}$$

$$CR_{\max} = \max\begin{cases} CR_1 \\ CR_2 \end{cases} \tag{25}$$

According to this method, the CR parameters are calculated as follows:

$$CR_1 = \sum_{i=1}^{N} W_i C1_i \tag{26}$$

$$CR_2 = \sum_{i=1}^{N} W_i C2_i \tag{27}$$

where:

W_i -weight factor or wave occurrence value

$C1_i$ concerns the minimum angle of vanishing stability ($\Phi_{V\min}$) and is calculated as:

$$C1_i = \begin{cases} 1 & \Phi_{V\min i} < 30 \\ 0 & otherwise \end{cases} \tag{28}$$

$C2_i$ concerns the maximum angle of stable equilibrium ($\Phi_{S,\max}$) and is calculated as:

$$C2_i = \begin{cases} 1 & \Phi_{S,\max i} > 25 \\ 0 & otherwise \end{cases} \tag{29}$$

For each wave, the heeling lever R_{PL3} is defined as follows:

$$R_{PL3} = 8\left(\frac{H_i}{\lambda_i}\right) dFn^2 \text{ [m]} \quad \textbf{(30)}$$

where:

H -significant wave height,
λ -wave length,
d -draft corresponding to the loading condition,
F_n -Froude number corresponding to ship's service speed.

The ship is considered to not be vulnerable when the largest value among CR_1 and CR_2 does not exceed 0.06.

2.1.5. Level 3 Direct Assessment Method

When a ship qualifies for a Level 3 assessment, (after obtaining a negative vulnerability evaluation at both Levels 1 and 2), it is subject to a direct stability assessment (DSA).

DSA is an additional model test that may involve numerical calculations using a mathematical model that broadly describes pure loss of stability. Performing model experiments in DSA is a very expensive task. Therefore, the demand for direct stability assessment using computer simulations is expected to increase.

3. SAMPLE CALCULATIONS FOR THE PURE LOSS OF STABILITY

Vulnerability assessments for pure loss of stability have been performed in two stages (i.e., Levels 1 and 2). Calculations have been made using two different solution methods (i.e., Options A and B).

This study uses a Turkish navy tanker as the sample ship. The main dimensions are presented in Table 4, and the plan views are presented in Figure 5. Half load condition with free surface effect has been assumed as

the loading condition. The hydrostatic parameters and GZ curves have been calculated using the program Maxsurf Stability (Bentley, 2020).

Table 4. Main dimensions of Turkish Navy Tanker.

L (L_{BP})	57.7	m
B	9.40	m
D	4.25	m
d (%50 load)	2.817	m
L_{CG}	29.407	m
V_{CG}	3.778	m
KB	1.496	m
V_S	12	knot

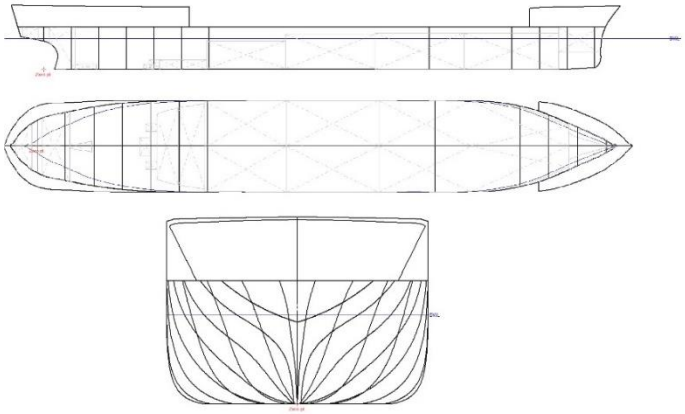

Figure 5. Hull plan views of the Turkish Navy Tanker.

3.1. Example Calculations

3.1.1. Level 1 Criterion Assessment (Option A)

Conditions 1 and 2 are satisfied for the subject ship as follows:

$$F_N = \frac{V_S}{\sqrt{gL}} = \frac{12x0.5144}{\sqrt{9.81x57.7}} = 0.259 \quad \textbf{(31)}$$

$$0.259 > 0.24$$

The Froude number is greater than 0.24, so the requirement is satisfied. The second check is as follows:

$$\frac{V_D - V}{A_W (D-d)} \geq 1.0$$

$$\frac{1849.094 - 1086.588}{442.762x(4.450-2.817)} = 1.054 \quad \textbf{(32)}$$

The expression described in Equation 2 is satisfied.

According to the method, the wave length is equal to ship length as in Eq. 33. The wave height is calculated using Equation 3 as shown in Eq. 34.

$$\lambda = \mathrm{L} = 57.7 \text{ m} \quad \textbf{(33)}$$

$$H_W = 0.0334 \cdot \lambda = 1.927 \text{ m} \quad \textbf{(34)}$$

In the next step, the lowest draught d_L and I_L are calculated using Equations 5 and 6 as follows.

$$\delta d_L = \min\left(d - 0.25 d_{full}, 0.5 H_W\right)$$

$$\delta d_L = \min(1.867, 0.963) \quad \textbf{(35)}$$

$$\delta d_L = 0.963$$

$$d_L = d - \delta d_L$$

$$d_L = 2.817 - 0.963 \quad \textbf{(36)}$$

$$d_L = 1.854 \text{ m}$$

Next, using d_L, the value for I_L is calculated as:

$$I_L = 2530.999 \text{ m}^4 \quad \textbf{(37)}$$

Using Equation 4, the minimum initial metacentric height GM_{min} is calculated as follows:

$$GM_{\min} = KB + \frac{I_L}{V} - KG \quad \textbf{(38)}$$

$$GM_{\min} = 1.49 + \frac{2530.99}{1086.85} - 3.778 \;=\; 0.0467 \text{ m}$$

As a result, the ship is vulnerable to pure loss of stability for Level 1 Option A, because $GM_{min} < 0.05$ m. The Level 2 assessment must be applied to the ship for the next vulnerability check.

3.1.2. Level 1 Criterion Assessment (Option B)

Firstly, both Conditions 1 and 2 must be satisfied as was done in Option A. The wave length (λ) is equal to the ship length (L), and the wave height (H_W) is calculated as follows.

$$\lambda = L = 57.7 \text{ m} \quad \textbf{(39)}$$

$$H_W = 0.0334 \cdot \lambda = 1.927 \text{ m} \quad \textbf{(40)}$$

Using Equation 4, the GM_{min} is calculated as the smallest value among the 11 calculations with the wave crest located amidships and at 0.1L, 0.2L, 0.3L, 0.4L and 0.5L intervals forward, and at 0.1L, 0.2L, 0.3L, 0.4L and 0.5L intervals aft. The calculated GM_{min} values are shown in Table 5.

Table 5. GM_{min} values corresponding to different wave crest locations.

Wave crest location from AP	**GM_{min}**
0L	0.558
0.1L	0.548
0.2L	0.441
0.3L	0.307
0.4L	0.228
0.5L	0.206
0.6L	0.205
0.7L	0.242
0.8L	0.340
0.9L	0.468
1L	0.558
GM_{min}	**0.205**

The ship is considered to not be vulnerable in the Level 1 Option B assessment because $GM_{min} > 0.05$ m. Therefore, no Level 2 assessment is

necessary for further investigation. As can be seen in Table 5, the critical wave crest location is near amidship.

3.1.3. Level 2 Criterion Assessment (Option A)

Level 2 assessment of the vulnerability to pure loss of stability is done by using the 16 different waves shown in Table 1.

The results from the angle of vanishing (Φ_V) stability are listed in Table 6, and the CR_1 assessment is performed with respect to Equations 12 and 9. All the minimum Φ_V values have been calculated to be greater than 30 degrees, which means no critical situation is found for the sample ship. Therefore, CR_1 has been calculated to be equal to zero, as shown in Table 6.

Table 6. Level 2 assessment results for the CR_1 criterion.

Wave number	**Angle of vanishing stability (deg)**	**C1 criterion control**	**Weighting factor**	**CR_1 criterion control**
1	54,54	0	1,30E-05	0
2	55,45	0	1,65E-03	0
3	31,81	0	2,09E-02	0
4	38,18	0	9,28E-02	0
5	32,72	0	1,99E-01	0
6	37,27	0	2,49E-01	0
7	49,09	0	2,09E-01	0
8	48,18	0	1,29E-01	0
9	49,09	0	6,25E-02	0
10	50	0	2,48E-02	0
11	50,9	0	8,37E-03	0
12	52,72	0	2,47E-03	0
13	52,72	0	6,58E-04	0
14	53,63	0	1,58E-04	0
15	52,72	0	3,40E-05	0
16	52,72	0	7,00E-06	0
Value of criterion CR_1				**$\Sigma CR_1=0$**

The results for the minimum angle of loll (Φ_{Loll}) are listed in Table 7, and the CR_2 assessment has been performed with respect to Equations 13 and 10. No situation is found where an angle of loll had occurred.

Table 7. Level 2 assessment results for the CR_2 criterion.

Wave #	**Φ_{Loll} (deg)**	**C2 control**	**Weighting factor**	**CR_2 control**
1	0	0	1,30E-05	0
2	0	0	1,65E-03	0
3	0	0	2,09E-02	0
4	0	0	9,28E-02	0
5	0	0	1,99E-01	0
6	0	0	2,49E-01	0
7	0	0	2,09E-01	0
8	0	0	1,29E-01	0
9	0	0	6,25E-02	0
10	0	0	2,48E-02	0
11	0	0	8,37E-03	0
12	0	0	2,47E-03	0
13	0	0	6,58E-04	0
14	0	0	1,58E-04	0
15	0	0	3,40E-05	0
16	0	0	7,00E-06	0
Value of Criterion CR_2				**$\Sigma CR_2=0$**

Results for the minimum GZmax and R_{PL3} are listed in Table 8; the CR_3 assessment has been performed with respect to Equations 11, 14 and 15. All minimum GZ_{max} values have been calculated to be greater than R_{PL3} as shown in Table 8.

Table 8. Level 2 assessment results for the CR_3 criterion.

Wave #	GZmax (m)	R_{PL3} (m)	Weighting factor	CR_3 control
1	0,435	0,047	1,30E-05	0
2	0,213	0,040	1,65E-03	0
3	0,066	0,047	2,09E-02	0
4	0,076	0,050	9,28E-02	0
5	0,078	0,051	1,99E-01	0
6	0,093	0,050	2,49E-01	0
7	0,126	0,049	2,09E-01	0
8	0,128	0,047	1,29E-01	0
9	0,134	0,045	6,25E-02	0
10	0,142	0,043	2,48E-02	0
11	0,145	0,038	8,37E-03	0
12	0,162	0,037	2,47E-03	0
13	0,162	0,037	6,58E-04	0
14	0,181	0,032	1,58E-04	0
15	0,171	0,030	3,40E-05	0
16	0,170	0,029	7,00E-06	0
Value of criterion CR_3				**$\Sigma CR_3=0$**

The ship has been concluded to not be vulnerable in the Level 2 Option A assessment as CR_{max} has been calculated to be smaller than 0.06 as follows:

$$CR_{\max} = \max\begin{cases} CR_1 = 0 \\ CR_2 = 0 \\ CR_3 = 0 \end{cases} \quad \textbf{(41)}$$

$$CR_{\max} < 0.06 \quad \textbf{(42)}$$

3.1.4. Level 2 Criterion Assessment (Option B)

The Level 2 Option B assessment was applied to the subject ship. The lengths of all waves (λ) used in the calculations are considered equal to the length of the ship (L=57.7 m).

The maximum effective wave height values in Table 3 have been used to generate 11 effective wave heights. The maximum effective wave height was obtained for T_Z=9.5 s and H_s=15.5 m at λ_{max}=8.533 m.

This value was used to generate 11 effective waves whose heights range from 0 to 8.533 m at intervals of 0.853 m. A heeling lever (R_{PL3}) was calculated for each wave, based on the Froude number, draft, and wave steepness; the results are presented in Table 9.

Table 9. Wave charecteristics and R_{PL3} values.

Wave length (m)	**Wave height (m)**	**R_{PL3}**
57.7	0.000	0.000
57.7	0.853	0.022
57.7	1.707	0.045
57.7	2.560	0.067
57.7	3.413	0.089
57.7	4.267	0.112
57.7	5.120	0.134
57.7	5.973	0.156
57.7	6.826	0.179
57.7	7.680	0.201
57.7	8.533	0.224

The GZ values for each wave (Table 9) have been calculated from 0 to 35 degrees at 5 degree intervals. For each wave height and wave length, the angle of vanishing (Φ_V) stability and stable equilibrium (Φ_S) corresponding to the R_{PL3} values have been calculated from the GZ curves. The results are shown in Table 10.

Table 10. Results from the Angle of Vanishing (Φ_V) Stability and Stable Equilibrium (Φ_S) corresponding to $R_{PL3.}$

Wave #	**H_{eff} (m)**	**R_{PL3} (m)**	**$\Phi_{V.min}$ (deg)**	**$\Phi_{S.max}$ (deg)**
Calm	0.000	0.000	35	0
1	0.853	0.022	35	1.8
2	1.707	0.045	35	4.09
3	2.560	0.067	35	6.36
4	3.413	0.089	35	8.18
5	4.267	0.112	35	35
6	5.120	0.134	28.18	35
7	5.973	0.156	16.81	35
8	6.826	0.179	0	35
9	7.680	0.201	0	35
10	8.533	0.224	0	35

The angle of vanishing (Φ_V) and stable equilibrium (Φ_S) values corresponding to the wave heights in Table 11 were derived from Table 10 using linear interpolations. The calculated results are presented in the Appendix in Table 11.

As a result of the calculations, CR_{max} has been calculated as 0.02873 which is smaller than the criterion value 0.06. This means the ship is not vulnerable to pure loss of stability according to the Level 2 Option B assessment.

4. CONCLUSION

This study has examined the case of a Turkish Navy tanker for pure loss of stability, one of the second-generation intact stability (SGISC) failure modes. Level 1 and Level 2 assessments were carried out in detail. The subject ship was found to be vulnerable to pure loss of stability for Level 1 Option A, but not for Level 1 Option B. The subject ship was found to not be vulnerable to pure loss of stability for both Options A and B of the Level 2 assessment.

In conclusion, we offer the following remarks and comments:

a) The Level 1 vulnerability check result showed inconsistency between Options A and B. This reduces the reliability of the method.
b) Applying the Level 1 Option A assessment was found to be easier than Option B, which does not require any software like Maxsurf. However, the reliability of this method is weak as no vulnerability was shown.
c) Applying the Level 2 Option B assessment was found to be easier than the Level 2 Option A assessment because Grim's theorem was used to generate 11 effective wave heights while the values for the other waves were obtained by interpolating data.
d) The stability of the ship differs in the case of different loading weights. Therefore, the vulnerability analysis will also differ for different loading cases. Instead of calculating all load cases, the worst loading condition can be used with the minimum GM.
e) IMO's Second Generation Intact Stability Criteria require the use of computer programs to obtain hydrostatic data on waves.
f) North Atlantic Wave Scatter Data were used for the IMO Second Generation Intact Stability Criteria's Level 2 assessments. A different wave scatter diagram should be used when the ship sails in a restricted area.
g) A new type of ship has been added to the literature with IMO's endorsement of applying the new criteria for assessing consistency and validity.

REFERENCES

Bentley (2020). *Maxsurf Training Manual – Stability*. Bentley Systems Pty. Ltd.

Chorab, P. (2014). "Sample calculations using a draft method for assessment of the vulnerability to pure loss of stability of a fishing vessel". *Scientific Journals of Maritime University of Szczecin*. 40 (112), 39-46.

Chouliaras, S. (2015). "Evaluation Of IMO's Second Generation Intact Stability Criteria" (Bachelor Dissertation). National Technical University of Athens, Greece.

Grim, O. (1961). "Beitrag zu dem Problem der Sicherheit des Schiffes im Seegang". Schiff und Hafen 6, 490-497.

Grinnaert, F. (2017). "Analysis and implementation of second generation criteria in a stability computer code" (Doctoral Dissertation). Université de Bretagne occidentale, Brest, France.

Grinnaert, F., Gualeni, P., Billard, J.-Y., Laurens, J.-M., and Petacco, N. (2016). "Application of 2nd Generation Intact Stability Criteria on Naval Ships". Proceedings of the 15th International Ship Stability Workshop, 13-15 June 2016. Stockholm, Sweden. Retrieved from https://shipstab.org/files/Proceedings/ISSW/ISSW_2016_Stockholm/Papers/8_2_Grinnaert_et_al_ISSW2016.pdf

IMO - SDC 7-INF.2 (2019). *Finalization of Second Generation Intact Stability Criteria, Information collected by the Correspondence Group on Intact Stability (part A)*. London, UK.

Panagiotellis, S. C. (2018). "Evaluation of IMO's 'Second Generation' Intact Stability Criteria Investigation For The Possible Impact On Ro-Ro Ship Design And Operation" (Bachelor Thesis). National Technical University of Athens, Greece.

Petacco, N. (2019). "Second Generation Intact Stability Criteria: Analysis, Implementation and Applications to Significant Ship Typologies" (Doctoral Dissertation). University of Genoa, Italy.

Petacco, N., and Gualeni, P. (2020). "IMO Second Generation Intact Stability Criteria: General Overview and Focus on Operational Measures". *Journal of Marine Science and Engineering*, 8(7):494. doi:10.3390/jmse8070494.

APPENDIX

Table 11. CR_1 and CR_2 results for the Level 2 Option B Assessment.

Tz (s)	Hs (m)	Heff (m)	Φ_v (deg)	Contribution to CR_1	Φ_S (deg)	Contribution to CR_2
3,50	0,50	0,41	35,00	0	0,87	0
4,50	0,50	0,54	35,00	0	1,14	0
4,50	1,50	1,62	35,00	0	3,85	0
4,50	2,50	2,69	35,00	0	6,64	0
4,50	3,50	3,77	35,00	0	19,40	0
5,50	0,50	0,51	35,00	0	1,08	0
5,50	1,50	1,54	35,00	0	3,65	0
5,50	2,50	2,57	35,00	0	6,38	0
5,50	3,50	3,60	35,00	0	13,98	0
5,50	4,50	4,63	32,13	0	35,00	6,00E-05
5,50	5,50	5,65	21,06	2,11E-04	35,00	1,00E-05
5,50	6,50	6,68	2,85	2,85E-05	35,00	2,00E-06
6,50	0,50	0,44	35,00	0	0,94	0
6,50	1,50	1,33	35,00	0	3,08	0
6,50	2,50	2,22	35,00	0	5,45	0
6,50	3,50	3,10	35,00	0	7,52	0
6,50	4,50	3,99	35,00	0	26,37	1,96E-03
6,50	5,50	4,88	30,10	0	35,00	5,10E-04
6,50	6,50	5,77	19,57	1,96E-04	35,00	1,26E-04
6,50	7,50	6,65	3,41	3,41E-05	35,00	3,00E-05
6,50	8,50	7,54	0,00	0,00E+00	35,00	7,00E-06
6,50	9,50	8,43	0,00	0,00E+00	35,00	2,00E-06
7,50	0,50	0,37	35,00	0	0,78	0
7,50	1,50	1,11	35,00	0	2,50	0
7,50	2,50	1,86	35,00	0	4,48	0
7,50	3,50	2,60	35,00	0	6,44	0
7,50	4,50	3,34	35,00	0	8,02	0
7,50	5,50	4,08	35,00	0	29,17	4,98E-03
7,50	6,50	4,82	30,55	0	35,00	1,67E-03
7,50	7,50	5,57	22,25	2,22E-04	35,00	5,21E-04
7,50	8,50	6,31	10,23	1,02E-04	35,00	1,54E-04
7,50	9,50	7,05	0,00	0,00E+00	35,00	4,30E-05
7,50	10,50	7,79	0,00	0,00E+00	35,00	1,20E-05

-Continuation of the Table 11.

7,50	11,50	8,53	0,00	0,00E+00	35,00	3,00E-06
7,50	12,50	5,77	35,00	0	35,00	1,00E-06
8,50	0,50	0,31	35,00	0	0,65	0
8,50	1,50	0,93	35,00	0	1,99	0
8,50	2,50	1,54	35,00	0	3,65	0
8,50	3,50	2,16	35,00	0	5,30	0
8,50	4,50	2,78	35,00	0	6,82	0
8,50	5,50	3,39	35,00	0	8,14	0
8,50	6,50	4,01	35,00	0	26,99	6,90E-03
8,50	7,50	4,63	32,10	0	35,00	2,70E-03
8,50	8,50	5,25	26,50	2,65E-04	35,00	9,79E-04
8,50	9,50	5,86	18,28	1,83E-04	35,00	3,32E-04
8,50	10,50	6,48	6,82	6,82E-05	35,00	1,07E-04
8,50	11,50	7,10	0,00	0,00E+00	35,00	3,30E-05
8,50	12,50	7,71	0,00	0,00E+00	35,00	1,00E-05
8,50	13,50	8,33	0,00	0,00E+00	35,00	3,00E-06
8,50	14,50	5,77	35,00	0	35,00	1,00E-06
9,50	0,50	0,26	35,00	0	0,54	0
9,50	1,50	0,77	35,00	0	1,63	0
9,50	2,50	1,29	35,00	0	2,97	0
9,50	3,50	1,80	35,00	0	4,35	0
9,50	4,50	2,32	35,00	0	5,72	0
9,50	5,50	2,84	35,00	0	6,95	0
9,50	6,50	3,35	35,00	0	8,05	0
9,50	7,50	3,87	35,00	0	22,45	0
9,50	8,50	4,38	34,07	0	35,00	2,56E-03
9,50	9,50	4,90	29,95	2,99E-04	35,00	1,02E-03
9,50	10,50	5,41	24,26	2,43E-04	35,00	3,79E-04
9,50	11,50	5,93	17,39	1,74E-04	35,00	1,33E-04
9,50	12,50	6,45	7,51	7,51E-05	35,00	4,40E-05
9,50	13,50	6,96	0,00	0,00E+00	35,00	1,40E-05
9,50	14,50	7,48	0,00	0,00E+00	35,00	4,00E-06
9,50	15,50	7,99	0,00	0,00E+00	35,00	1,00E-06
10,50	0,50	0,22	35,00	0	0,46	0
10,50	1,50	0,65	35,00	0	1,37	0
10,50	2,50	1,09	35,00	0	2,42	0
10,50	3,50	1,52	35,00	0	3,59	0
10,50	4,50	1,95	35,00	0	4,75	0
10,50	5,50	2,39	35,00	0	5,91	0

-Continuation of the Table 11.

10,50	6,50	2,82	35,00	0	6,92	0
10,50	7,50	3,26	35,00	0	7,85	0
10,50	8,50	3,69	35,00	0	16,95	0
10,50	9,50	4,13	35,00	0	30,60	1,60E-03
10,50	10,50	4,56	32,65	0	35,00	6,75E-04
10,50	11,50	5,00	29,18	2,92E-04	35,00	2,66E-04
10,50	12,50	5,43	24,05	2,41E-04	35,00	9,90E-05
10,50	13,50	5,86	18,26	1,83E-04	35,00	3,50E-05
10,50	14,50	6,30	10,40	1,04E-04	35,00	1,20E-05
10,50	15,50	6,73	1,85	1,85E-05	35,00	4,00E-06
10,50	16,50	7,17	0,00	0,00E+00	35,00	1,00E-06
11,50	0,50	0,18	35,00	0	0,39	0
11,50	1,50	0,55	35,00	0	1,17	0
11,50	2,50	0,92	35,00	0	1,99	0
11,50	3,50	1,29	35,00	0	2,98	0
11,50	4,50	1,66	35,00	0	3,97	0
11,50	5,50	2,03	35,00	0	4,95	0
11,50	6,50	2,40	35,00	0	5,94	0
11,50	7,50	2,77	35,00	0	6,81	0
11,50	8,50	3,14	35,00	0	7,60	0
11,50	9,50	3,51	35,00	0	11,20	0
11,50	10,50	3,88	35,00	0	22,81	0
11,50	11,50	4,25	35,00	0	34,42	3,14E-04
11,50	12,50	4,62	32,20	0	35,00	1,28E-04
11,50	13,50	4,99	29,24	2,92E-04	35,00	5,00E-05
11,50	14,50	5,36	25,03	2,50E-04	35,00	1,80E-05
11,50	15,50	5,73	20,11	2,01E-04	35,00	6,00E-06
11,50	16,50	6,09	14,41	1,44E-04	35,00	2,00E-06
12,50	0,50	0,16	35,00	0	0,33	0
12,50	1,50	0,48	35,00	0	1,00	0
12,50	2,50	0,79	35,00	0	1,67	0
12,50	3,50	1,11	35,00	0	2,49	0
12,50	4,50	1,43	35,00	0	3,34	0
12,50	5,50	1,74	35,00	0	4,19	0
12,50	6,50	2,06	35,00	0	5,03	0
12,50	7,50	2,38	35,00	0	5,88	0
12,50	8,50	2,70	35,00	0	6,65	0
12,50	9,50	3,01	35,00	0	7,33	0
12,50	10,50	3,33	35,00	0	8,00	0

-Continuation of the Table 11.

12,50	11,50	3,65	35,00	0	15,52	0
12,50	12,50	3,96	35,00	0	25,49	1,10E-04
12,50	13,50	4,281	34,88	0	35,00	4,60E-05
12,50	14,50	4,60	32,35	0	35,00	1,80E-05
12,50	15,50	4,92	29,81	2,98E-04	35,00	7,00E-06
12,50	16,50	5,23	26,68	2,67E-04	35,00	2,00E-06
13,50	1,50	0,41	35,00	0	0,87	0
13,50	2,50	0,69	35,00	0	1,45	0
13,50	3,50	0,96	35,00	0	2,09	0
13,50	4,50	1,24	35,00	0	2,83	0
13,50	5,50	1,51	35,00	0	3,56	0
13,50	6,50	1,79	35,00	0	4,30	0
13,50	7,50	2,06	35,00	0	5,03	0
13,50	8,50	2,34	35,00	0	5,76	0
13,50	9,50	2,61	35,00	0	6,47	0
13,50	10,50	2,88	35,00	0	7,05	0
13,50	11,50	3,16	35,00	0	7,64	0
13,50	12,50	3,43	35,00	0	8,83	0
13,50	13,50	3,71	35,00	0	17,46	0
13,50	14,50	3,98	35,00	0	26,10	1,30E-05
13,50	15,50	4,26	35,00	0	34,73	5,00E-06
13,50	16,50	4,53	32,87	0	35,00	2,00E-06
14,50	1,50	0,36	35,00	0	0,76	0
14,50	2,50	0,60	35,00	0	1,27	0
14,50	3,50	0,84	35,00	0	1,77	0
14,50	4,50	1,08	35,00	0	2,41	0
14,50	5,50	1,32	35,00	0	3,05	0
14,50	6,50	1,56	35,00	0	3,70	0
14,50	7,50	1,80	35,00	0	4,34	0
14,50	8,50	2,04	35,00	0	4,98	0
14,50	9,50	2,28	35,00	0	5,61	0
14,50	10,50	2,52	35,00	0	6,25	0
14,50	11,50	2,76	35,00	0	6,79	0
14,50	12,50	3,00	35,00	0	7,30	0
14,50	13,50	3,24	35,00	0	7,81	0
14,50	14,50	3,48	35,00	0	10,26	0
14,50	15,50	3,72	35,00	0	17,80	0
14,50	16,50	3,96	35,00	0	25,35	1,00E-06
15,50	1,50	0,32	35,00	0	0,67	0

-Continuation of the Table 11.

15,50	2,50	0,53	35,00	0	1,11	0
15,50	3,50	0,74	35,00	0	1,56	0
15,50	4,50	0,95	35,00	0	2,06	0
15,50	5,50	1,16	35,00	0	2,63	0
15,50	6,50	1,37	35,00	0	3,19	0
15,50	7,50	1,58	35,00	0	3,76	0
15,50	8,50	1,80	35,00	0	4,33	0
15,50	9,50	2,01	35,00	0	4,89	0
15,50	10,50	2,22	35,00	0	5,45	0
15,50	11,50	2,43	35,00	0	6,01	0
15,50	12,50	2,64	35,00	0	6,53	0
15,50	13,50	2,85	35,00	0	6,98	0
15,50	14,50	3,06	35,00	0	7,43	0
15,50	15,50	3,27	35,00	0	7,88	0
15,50	16,50	3,49	35,00	0	10,44	0
16,50	2,50	0,47	35,00	0	0,99	0
16,50	3,50	0,66	35,00	0	1,38	0
16,50	4,50	0,84	35,00	0	1,78	0
16,50	5,50	1,03	35,00	0	2,27	0
16,50	6,50	1,22	35,00	0	2,78	0
16,50	7,50	1,40	35,00	0	3,28	0
16,50	8,50	1,59	35,00	0	3,78	0
16,50	9,50	1,78	35,00	0	4,28	0
16,50	10,50	1,97	35,00	0	4,78	0
16,50	11,50	2,15	35,00	0	5,28	0
16,50	12,50	2,34	35,00	0	5,78	0
16,50	13,50	2,53	35,00	0	6,27	0
16,50	14,50	2,71	35,00	0	6,69	0
16,50	15,50	2,90	35,00	0	7,09	0
17,50	3,50	0,58	35,00	0	1,23	0
17,50	4,50	0,75	35,00	0	1,59	0
17,50	5,50	0,92	35,00	0	1,98	0
17,50	6,50	1,09	35,00	0	2,42	0
17,50	7,50	1,25	35,00	0	2,87	0
17,50	8,50	1,42	35,00	0	3,32	0
17,50	9,50	1,59	35,00	0	3,77	0
17,50	10,50	1,75	35,00	0	4,22	0
17,50	11,50	1,92	35,00	0	4,66	0
17,50	12,50	2,09	35,00	0	5,10	0

-Continuation of the Table 11.

17,50	13,50	2,25	35,00	0	5,55	0
18,50	5,50	0,82	35,00	0	1,74	0
18,50	6,50	0,97	35,00	0	2,12	0
18,50	7,50	1,12	35,00	0	2,53	0
18,50	8,50	1,27	35,00	0	2,93	0
18,50	9,50	1,42	35,00	0	3,33	0
18,50	10,50	1,57	35,00	0	3,73	0
18,50	11,50	1,72	35,00	0	4,14	0
			ΣCR_1 =	**0,00439**	**ΣCR_2 =**	**0,02873**

Journal of Naval Sciences and Engineering
2021, Vol. 17, No. 2, pp. 343-375
Mechanical Engineering/Makine Mühendisliği

RESEARCH ARTICLE

**An ethical committee approval and/or legal/special permission has not been required within the scope of this study.*

REFERENCE ENERGY SYSTEM ANALYSIS OF A WARSHIP*

Gökhan UYANIK[1]
Egemen SULUKAN[2]

[1]*National Defence University, Barbaros Naval Sciences and Engineering Institute, Department of Marine Mechanical Engineering, Istanbul, Turkey, gokhanreyhangokhan@gmail.com; ORCID: 0000-0001-8613-4074*

[2]*National Defence University, Turkish Naval Academy, Department of Mechanical Engineering, Istanbul, Turkey, esulukan@dho.edu.tr; ORCID: 0000-0003-1138-2465*

Received: 18.04.2021 **Accepted: 18.08.2021**

ABSTRACT

Considering the growing maritime sector in today's conditions, it is of great importance to use the energy used in ship systems in the most efficient and cost-effective manner. The greenhouse gas emissions caused by this energy network emerge as a big problem that needs to be solved. The International Maritime Organization (IMO) has been working since 1958 to control the ship's CO2 emission problem. In this study, a warship was examined as an example in the first stage and the current situation was revealed with Reference Energy System Analysis, taking into account the existing technologies. As a second step, the study in question has handled various scenarios with the Long-range Energy Alternatives Planning System (LEAP) software, which transforms the energy sector into a mathematical model, and within the framework of the results, analysis work has been completed for the improvement of a warship in the field of energy. The results have shown us that improvements can be achieved in the field of energy on a warship, and greenhouse gas emissions can be reduced as a result of these improvements.

Keywords: *Ship Energy System Analysis, Ship Energy System Modeling, Reference Energy System, Warship.*

BİR SAVAŞ GEMİSİNİN REFERANS ENERJİ SİSTEM ANALİZİ

ÖZ

Günümüz koşullarında büyüyen denizcilik sektörü göz önüne alındığında gemi sistemlerinde kullanılan enerjinin en verimli, en az maliyetle kullanılması büyük önem arz etmektedir. Bu enerji ağının ortaya çıkardığı sera gaz emisyonları çözülmesi gereken büyük bir sorun olarak karşımıza çıkmaktadır. Uluslararası Denizcilik Örgütü (IMO) Gemi CO_2 emisyon sorununu kontrol etmek maksadı ile 1958 yılından günümüze kadar çalışmalarını sürdürmektedir. Bu çalışmada birinci aşamada bir savaş gemisi örnek olarak incelenmiş ve mevcut teknolojiler göz önünde bulundurularak Referans Enerji Sistem Analizi ile mevcut durum ortaya koyulmuştur. İkinci aşama olarak bahse konu çalışma, enerji sektörünü matematiksel bir modele dönüştüren Long-range Energy Alternatives Planning System (LEAP) yazılımı ile çeşitli senaryolar ele alınmış ve ortaya çıkan sonuçlar çerçevesinde bir harp gemisinin enerji alanında iyileştirilmesi için analiz çalışması tamamlanmıştır. Ortaya çıkartılan sonuçlar bize bir harp gemisinde de enerji alanında iyileştirme sağlanabileğini ve bu iyileştirmeler sonucunda sera gaz emisyonlarının azaltılabileceğini göstermiştir.

Anahtar Kelimeler: *Gemi Enerji Sistemi Analizi, Gemi Enerji Sistemi Modelleme, Referans Enerji Sistemi, Savaş Gemisi.*

1. INTRODUCTION

Energy has been the cornerstone of life for the human being to survive until this time. Historically, in the journey of energy to the present, the decrease in the world energy resources has made it necessary for human beings to find new methods of energy. The world's energy resources are divided into two groups as renewable (solar, wind, geothermal energy, biomass energy, etc.) and non-renewable energy sources, fossil fuels (coal, oil, natural gas, etc.) and currently continue to meet the global energy needs.

Considering that 80% of energy is obtained from fossil fuels, the excess energy need caused by rapid population growth with the industrial revolution will further reduce fuels such as coal, oil and natural gas as a resource and will make it mandatory for people to use renewable energy. The supply-demand balance that occurs due to the decreasing resources and the increasing population will create an inverse proportional increase in prices, and cost increases will bring more burden to the economies of the country to meet the energy demand.

Although fossil fuels generate high-calorie energy, the environmental damage caused by emission gases is substantial. These effects cause irreversible damage to nature and living things day by day with global warming. All fossil fuels (coal, petroleum, natural gas, etc.) generate energy as a result of combustion and generate greenhouse gases (GHG). The resulting carbon dioxide (CO_2), methane (CH_4), nitrous oxide (N_2O) and ozone (O_3) greenhouse gases increase the temperature in the atmosphere and cause global warming and thus climate change with the greenhouse gas effect. In order to reduce environmental impacts, fossil fuels and the systems they use should be examined in every field and measures should be taken to reduce these impacts.

Although the use of fossil fuels in the maritime sector seems more efficient as in many other sectors, it is one of the sectors that should be emphasized in terms of environmental and economic effects. Transition to a cost-effective, efficient and environmentally friendly structure in the field of maritime, from the smallest ship to the largest ship, necessitates the

establishment of a common control mechanism that will take into account all kinds of situations.

2. LITERATURE REVIEW

It is a fact that the demand for the maritime sector is increasing day by day in our world where approximately 71% is covered with water and this demand will increase even more. This is the scope and analysis of marine vehicles, which are important building blocks of the sector, in terms of energy and effects, has come to the fore compared to the past and many studies have been carried out on this subject.

In the "Ship Systems Energy Analysis" study, the average seasonal temperature values of a gas turbine ship in various conditions (port, anchor, maneuver, and cruise) and the energy use depending on the ship speed were modeled and analyzed. In the energy analysis, the main propulsion system using fuel, electrical systems and the ship's air conditioning system (HVAC), which draws the highest load on the electrical load, were examined and the annual average energy modeling was performed with Matlab / Simulink software. As a result of the study, it was concluded that the conditions under which the systems and devices in the ship will be used will save fuel and it has been revealed that the CO_2 emission will decrease as a result of the fuel saving (Öztürk, 2017).

In the "Reference Energy System Analysis of a Chemical Tanker Ship" study, an energy diagram was created with the reference energy system approach of all systems in the ship. In the study, the energy data resulting from the use of systems and devices within a specified scenario were modeled with LAEP (Long - range Energy Alternatives Planning System) software. As a result of the data obtained in the modeling, it was concluded that in which area energy improvements can be made in the Chemical Tanker Ship system and greenhouse gas emissions can be reduced, accordingly (Sarı, 2019).

"Exergy and Thermodynamic Analysis in Gas Turbine Ships", specifically General Electric LM 2500 gas turbine was examined technologically in the main propulsion system and calculations were made according to the turbine

operating cycles. Total exergy and exergy loss and thermodynamic analysis of the calculations were made. As a result of the analysis, it has been concluded that the use of the General Electric LM 2500 gas turbine used in the ship main propulsion system at high speed will provide more benefits in terms of efficiency (Çubuğuzun, 2006).

In the "Energy and Exergy Analysis of a Passenger Ship" study, the efficiency of the main propulsion system, electrical power, heating and cooling (HVAC) systems in which the majority of the energy demand is met on a cruise ship in the Baltic Sea, was analyzed and energy models were created. In the study, four operational modes were determined: high speed (15 Nm), low speed (between 4-15 Nm), maneuvering speed (between 2-4 Nm) and port state (drift).

In the "Experimental and Theoretical Investigation of Exhaust Emissions from a Ferry" study, the greenhouse gas measurements emitted from a ferry were calculated by experimental methods and the results were compared with international studies in line with the criteria determined by IMO (Durmaz, 2015).

3. METHODOLOGY

3.1. Reference Energy System Concept

MARKAL (Market Allocation) is a model structure that means market allocation. The main purpose of the model is to evaluate the comprehensive and integrated energy technologies. With various technologies that produce or consume with energy carriers, it starts from the extraction, conversion or process in each relevant sector and continues until the end use. These energy technologies create a RES (Reference Energy System) with a single energy input and output in the energy system.

RES is a diagram that models the energy system structure. It defines the flow of energy from sources to end use. It shows all energy flows from primary energy source, large and small scale energy cycles, different distribution forms and end use of energy in different sectors. RES often

contains useful information about energy demand and even energy services; it enables to see how energy conversion technologies affect fuel-technology connections in an energy system. This network is defined with parameters and numerical inputs and the energy balance for the year, which is generally defined, is called a "base scenario". This study actually forms the basis of an on-board sustainable energy action plan mentioned above (Sulukan, 2010).

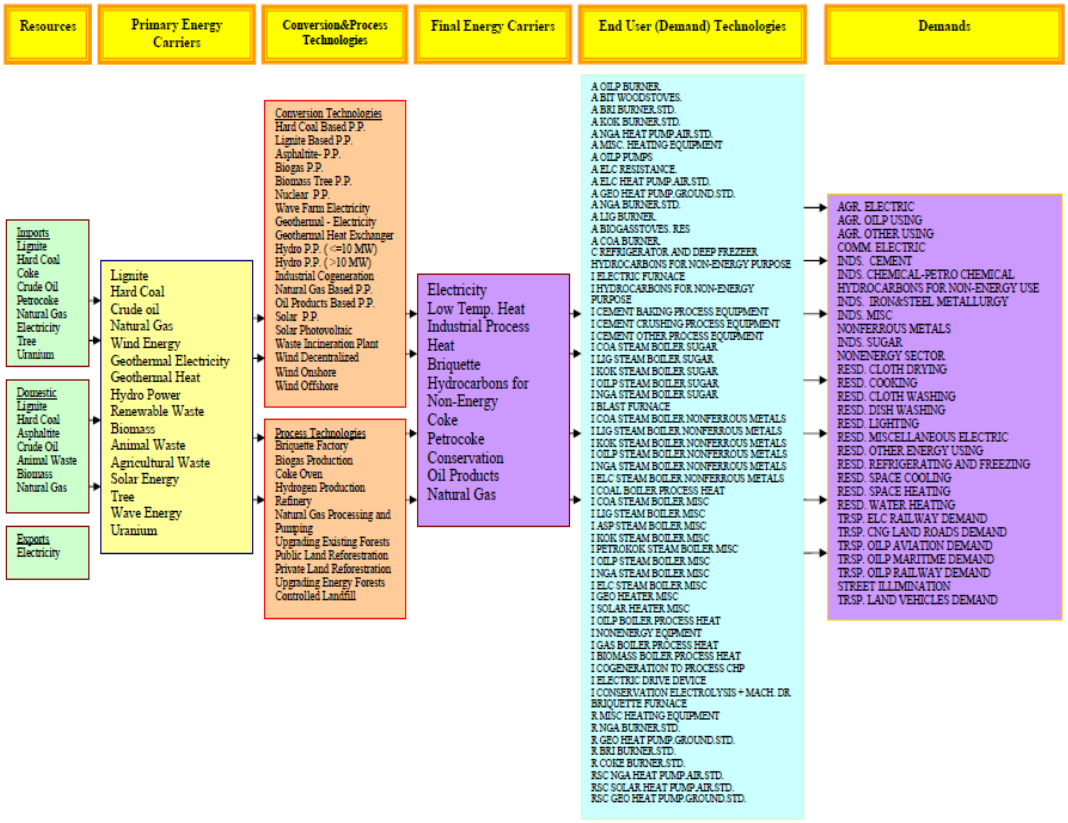

Figure 1. General outline of the RES concept (Sulukan, 2010).

Figure 1 expresses a simplified representation of a typical MARKAL RES, which is generally accepted in each model structure and shows the basic components. Primary Energy Carriers, which are created with existing

resources, are transformed into electricity or heat (final energy carriers) together with Conversion Technologies and Process Technologies, and other energy processing and demand technologies (end user technologies) and the demands for energy services and products (demands). Each can be on the scale of a country, a region, a city, a district or a ship defined as a model (Sulukan, 2010).

3.2. Energy Modeling Tools Overview

Modeling tools, also known as decision support tools, are software that help many integrated systems come together to create a simulation. Although each of the softwares differs in interface and function, its main purpose is to give us some results in order to perform the system analysis with the simulation created. Each result that emerges will help to improve a problem, if any, on the system.

In order to create the simulation, each of the softwares needs parameters and data related to the system to be created. Simulations (building, ship, city, country, etc.) can be done in micro and macro scales. Today, as in many fields, modeling tools are available in the field of energy.
Various modeling tools have been developed to date in order to make accurate analysis in the field of ship energy. The modeling tool (LEAP) chosen for this study is introduced below.

3.2.1. Energy Modeling Tool LEAP Overview

The LEAP modeling tool is windows-based software used below for energy policy analysis and climate change at the Stockholm Environment Institute. Currently, 190 countries and hundreds of countries are developing resource planning, greenhouse gas emission restrictions and low emission, emission strategies in cities, regions, regions or many different regions globally.

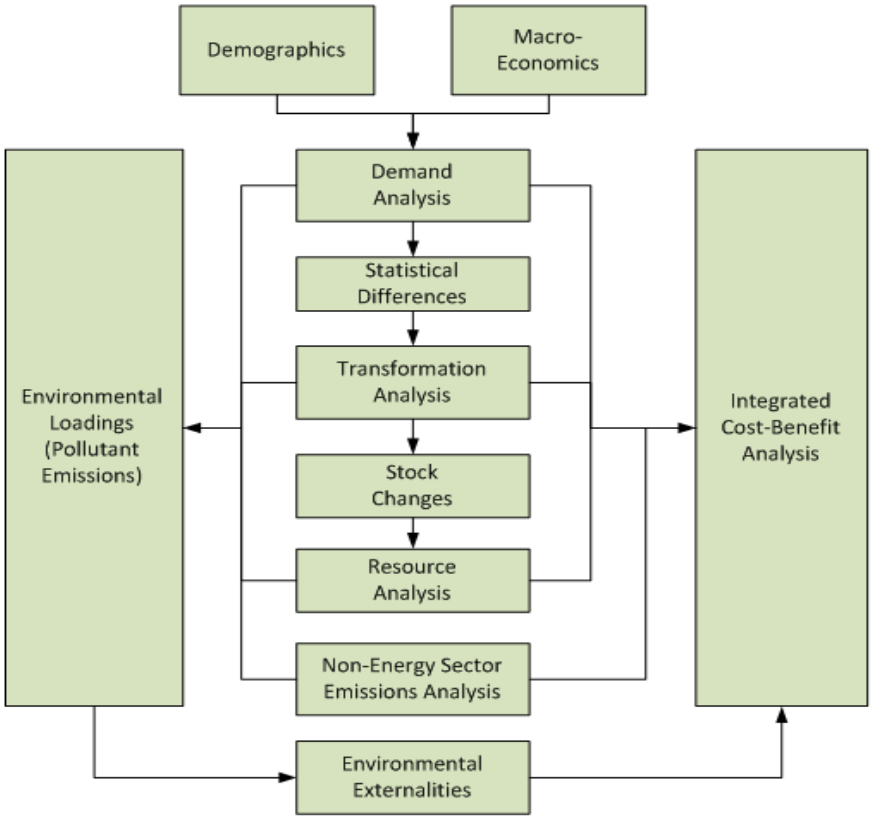

Figure 2. LEAP calculation structure (Low Emissions Analysis Platform, 2021).

LEAP puts all demands in front of us with an integrated structure, thanks to the calculation structure shown in Figure 2, along with the demographic and macroeconomic data, as well as all the demands, technology and expenditures, environmental pollutant emissions. In addition, thanks to its flexible interface, it provides many conveniences for the users who want to work in various fields and levels.

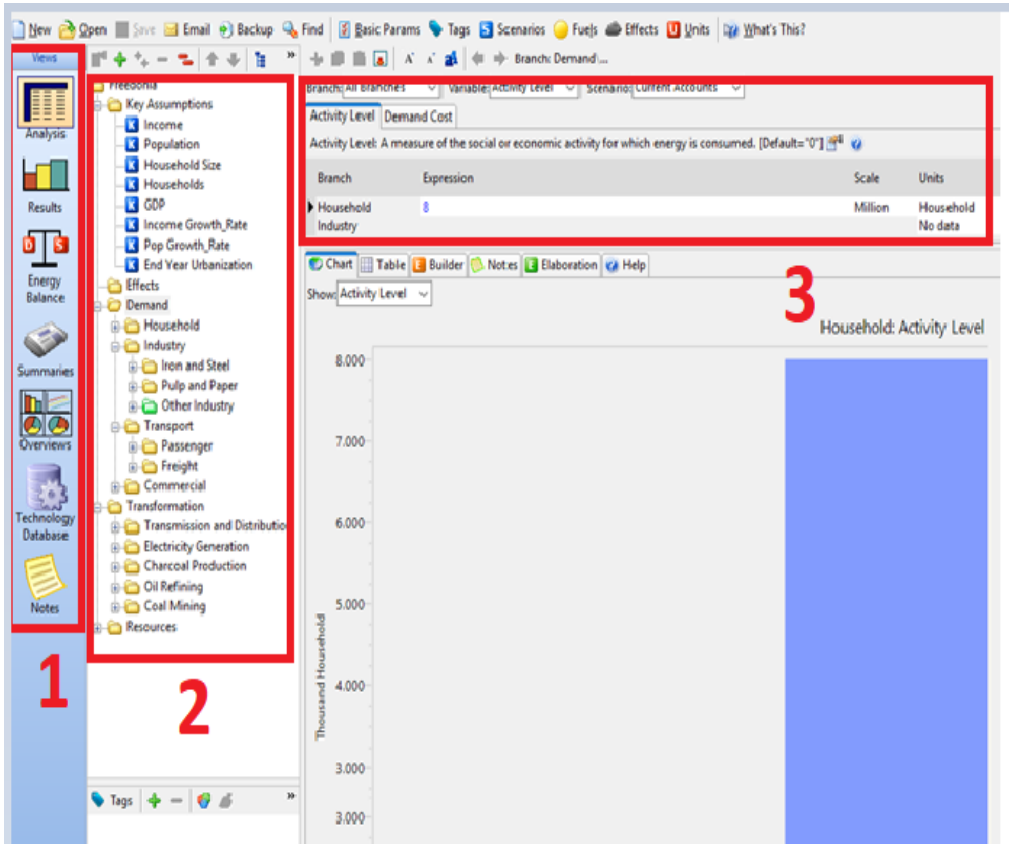

Figure 3. LEAP program interface.

Users can easily name and enter all components of the energy system they will model into the technology tree shown in box 2 in Figure 3, and create sub-categories. Thanks to this structure, the connection and relationship between all components of energy systems can be introduced to the program.

Figure 3 shows the interface encountered when the LEAP application is opened for the first time. Here, the demands of the system, the technologies that meet these demands and the energy carriers and the technologies that

transform these carriers into the necessary final energy carriers are defined and the relationship is established in the above-mentioned technology tree. In section 3, the required data of the technologies are defined as well as the desired unit and scale. Then, in the light of the data and parameters entered in the Result section, calculations are made and results are drawn. In the Energy Balance tab, the distribution of the energy entering the system, spent in the system or given out from the system can be seen. In addition, thanks to the Technology Database available in the program, information about the technologies to be introduced to the system and the relevant parameters of these technologies can be obtained.

Another feature of the program is that it allows forward-looking medium or long-term models in different scales. After choosing a specific year to create the base scenario, the user can model the system up to 2050 annually or five years. Alternative scenarios to be created thanks to the defined ready functions can be easily compared with the base scenario.

In the LEAP Modeling tool, system-based energy consumption of many sectors can be seen. At the same time, with the program, emission analyzes of local and regional air pollutants can be made and as a result of the analysis, it provides benefits by giving an idea to the users about the prevention of local air pollution (Low Emissions Analysis Platform, 2020).

4. APPLICATION OF THE RES SYSTEM CONCEPT TO A WARSHIP

In this study, an AX Class warship, one of the floating elements of the Turkish Naval Forces, was selected and all systems of this ship were examined and energy analysis was made. In analyzes made, 10 knots ship speed was accepted as constant. The main characteristics of the ship are shown in Table 1.

Figure 4. AX class warship overview.

Table 1. Warship main characteristics (Turkish Naval Forces, 2021).

AX Class Warship Main Characteristics	
Length – Width - Draft	98,2 x 11,8 x 4,4 MT
Displacement Tonnage	Full Load 2940 t
Main Drive	6 Maybach Diesel/14400/2 Propellers
Speed	20,5 KTS

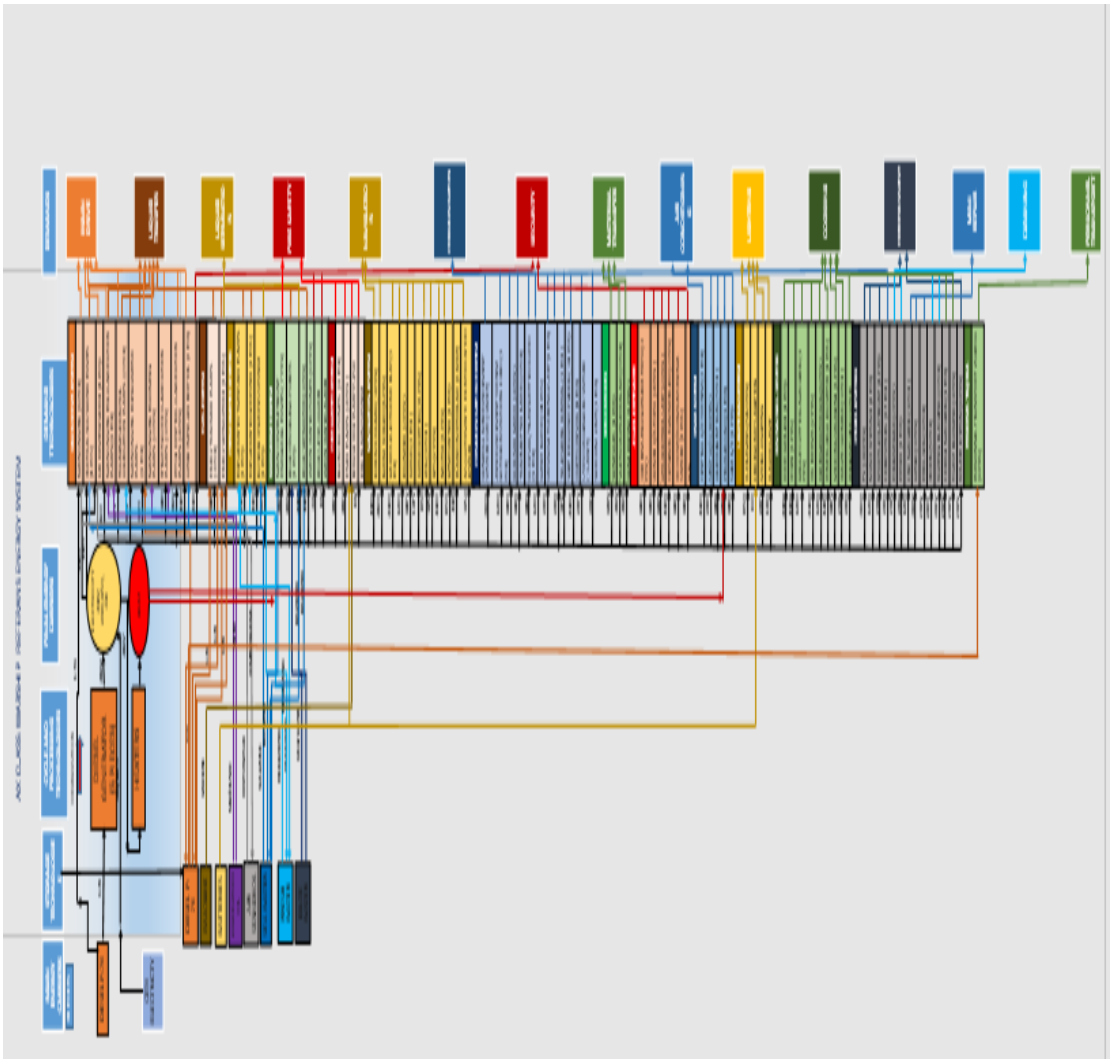

Figure 5. A Warship RES general overview.

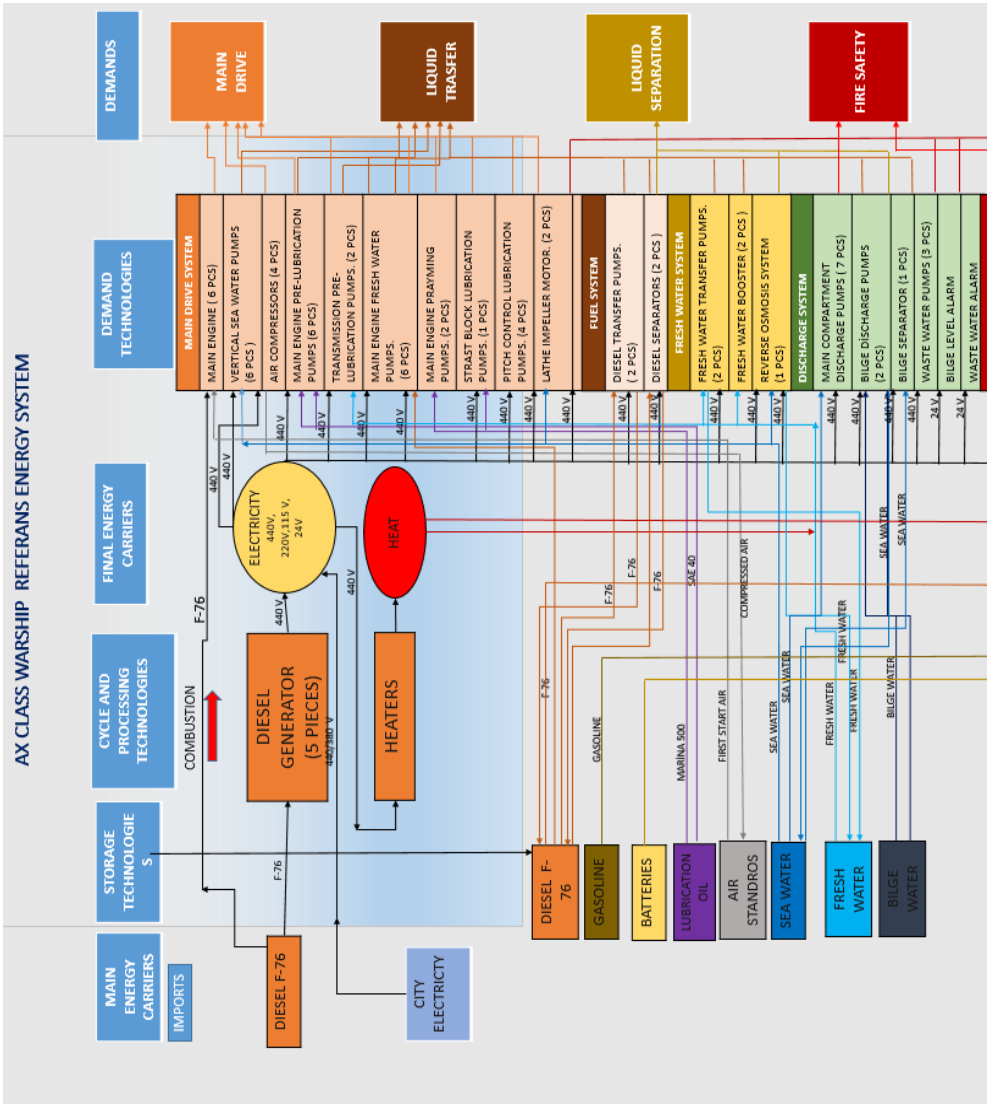

Figure 6. A Warship RES enlarged overview.

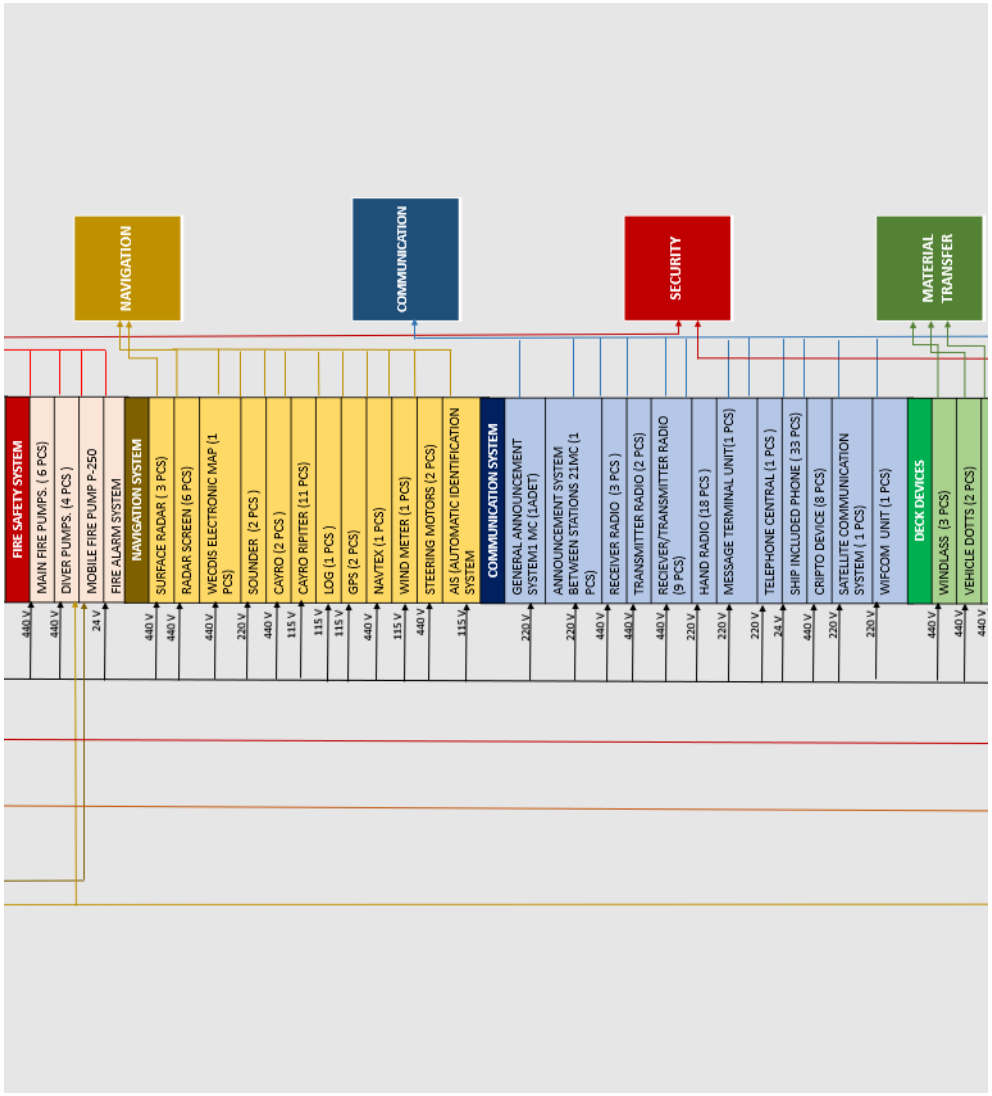

Figure 7. A Warship RES enlarged overview (continued).

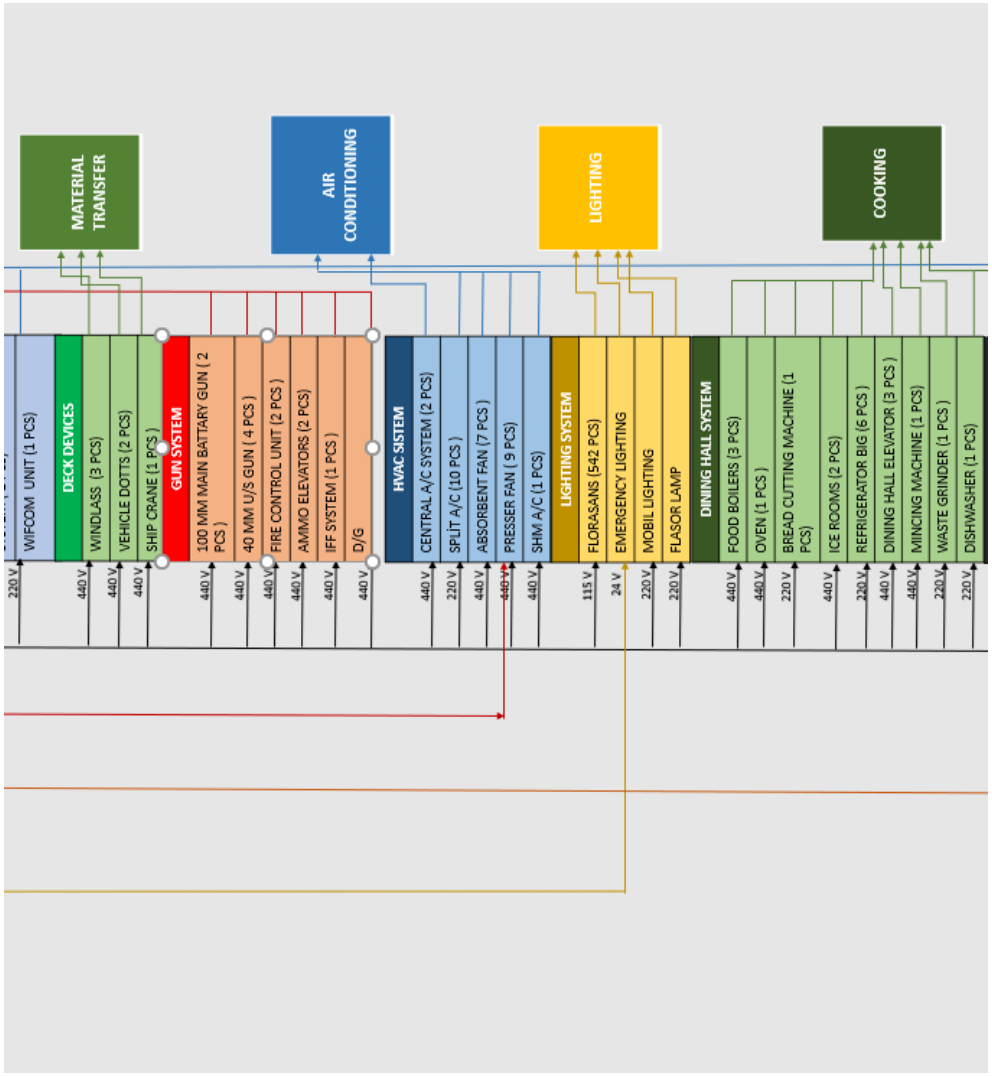

Figure 8. A Warship RES enlarged overview (continued).

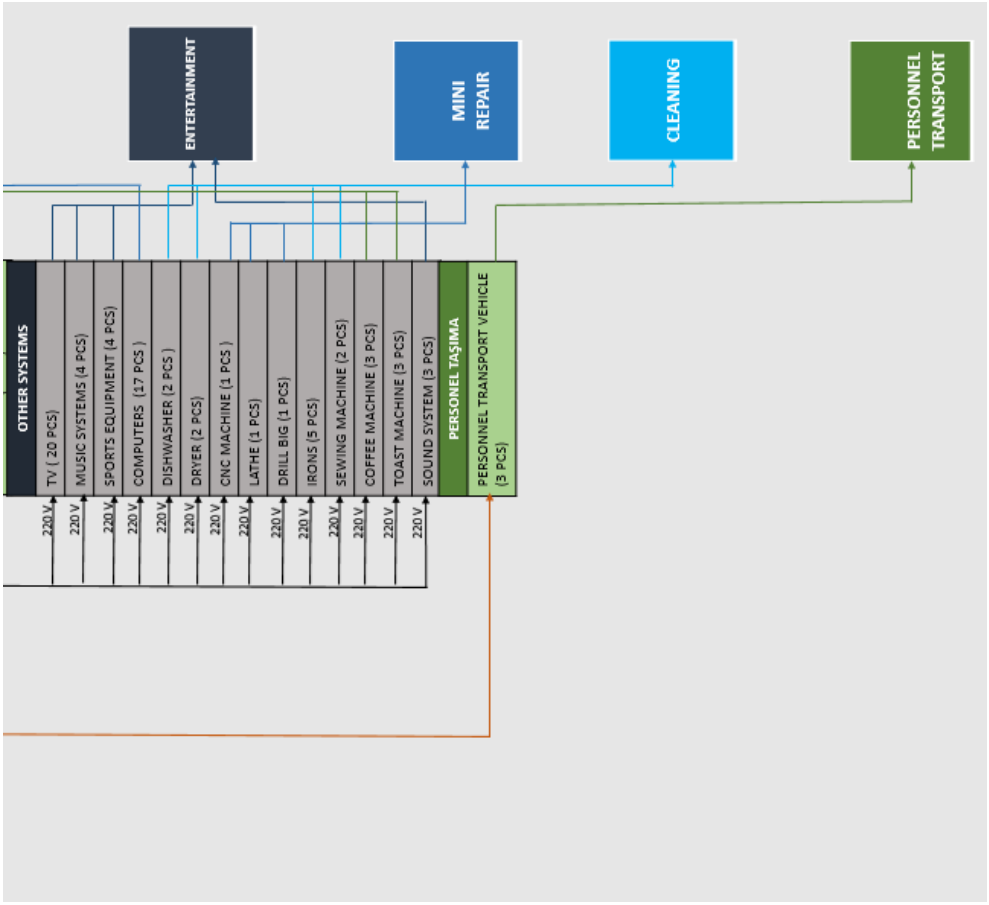

Figure 9. A Warship RES enlarged overview (continued).

4.1. Ship Energy System Resources (Main Energy Carriers)

Described as RES in the MARKAL model refers to the different types and forms of energy produced and consumed at different levels in the energy system. Energy carriers (Energy System Resources) include fossil fuels such as hard coal, lignite, crude oil and petroleum products, electricity and renewable energy (e.g. wind, biomass, solar, geothermal and hydro).
Energy carriers provide connections between various technologies in the MARKAL model by transferring them from one or more technologies to others. The Main Energy Carriers (Import) in the first column of the RES created are Diesel (F-76) and Coastal Electricity (in the case of the port-state).

4.2. Storage Technologies

In order to understand the RES better, the storage technologies in the second column of the RES are specified in Figure 6 and all the elements currently stored in the system are shown. Diesel F-76, Gasoline, Batteries, Lube Oil, Air Stands, Sea Water, Fresh Water and Bilge Water are stored in the system. The stored items are used in Conversion and Process Technologies, Final Energy Carriers, Demand Technologies and Demands. In order to ensure the stability of the ship, the storage is generally carried out under the waterline in the existing storage areas such as cisterns and tanks.

4.3. Conversion and Process Technologies

Some of the main energy carriers have been converted into final energy carriers through conversion or process technologies. Conversion technologies are used to convert primary energy carriers into final energy carriers as electricity or heat. Process technologies, on the other hand, are technologies that change the shape, property or location of energy (Sulukan et al., 2017). 5 diesel generators in the third column of the RES formed in Figure 6 were transformed into electricity, which is the final energy carrier, and the generated electricity into low-voltage electricity and heat with cycle and process technologies such as heater, transformer, and transferred to demand technologies in order to meet all demands on the system.

4.4. Final Energy Carriers

The energy needed by end-use technologies and transformed into primary energy carriers by conversion and process technologies is called final energy carriers. Electricity and heat shown in the fourth column of RES in Figure 6; has emerged as the Ultimate Energy Carrier transformed by conversion and process technologies. Ship electricity is produced in 440 Volt by means of Diesel Generators and distributed to Ship Demand Technologies as 220V, 115V, 24V through Transformers.

4.5. End Use (Demand) Technologies

Demand technologies are devices used to directly meet end-use service requests, including vehicles, pumps and electrical devices (Sulukan, 2017). Technologies are characterized using parameters that define technology costs, fuel consumption and efficiency and availability.
The demand technologies shown in the fifth column are grouped on a system basis and the operating voltages and storage technologies, if any, are specified for each technology.

4.6. Demands

Energy service demands define the quantities required for specific end-use energies services to be distributed to relevant subsectors in an energy system. The demands required by the ship system are defined in the last column. Demands determined on WPP are mixed through demand technologies. In RES analysis, one or more demand technologies can meet one or more demands.

5. MODELING A WARSHIP WITH LEAP AND ANALYSIS RESULTS

5.1. Creating a Reference Scenario

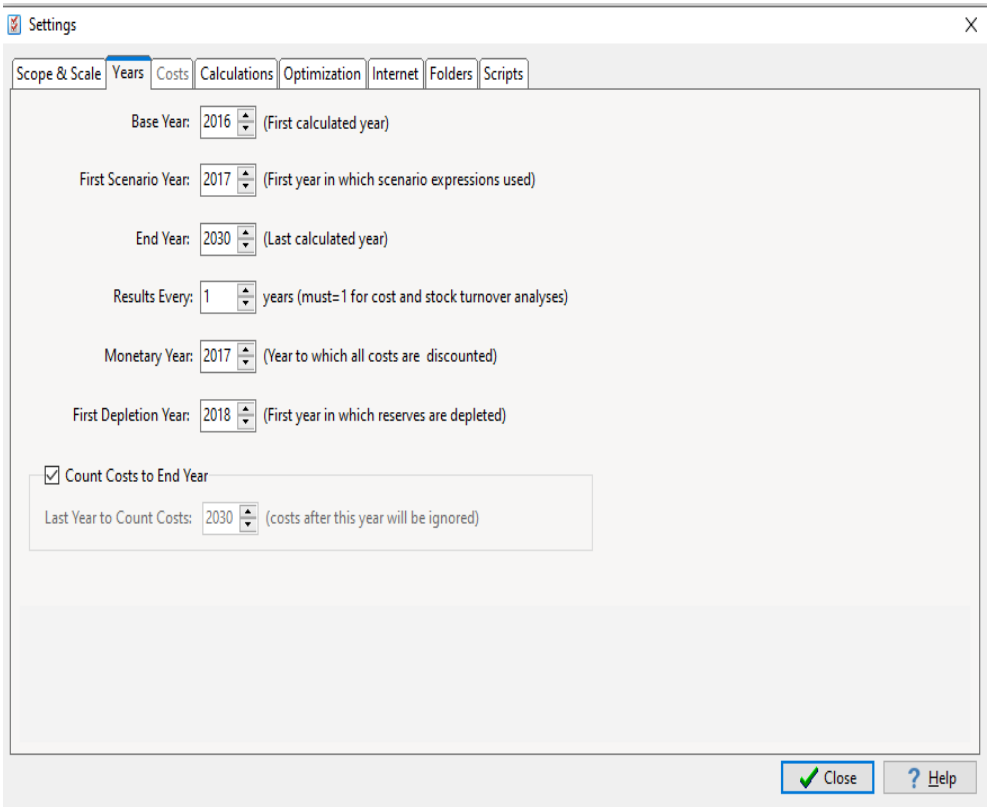

Figure 10. LEAP scenario screen.

The reference energy system analysis made in the previous stage was taken as the basis for the LEAP modeling of AX Class warship. Before starting the modeling, it is aimed to establish the annual energy balance of the warship in question in the modeling. In the study to achieve the target, the cruise and port states of the ship for 2016 were determined from official

records, and the systems used by the ship during the port and cruise were calculated separately. The parameters and technical data used in the energy model are taken from the technical documents, journal records and system registration cards of each technology available in the ship system.

5.2. Creating LEAP Modelling Data

AX SINIFI SAVAŞ GEMİSİ MODELLEME İÇİN GEREKLİ PARAMETRELER VE SİSTEMLERİN TEKNİK BİLGİLERİ							
SİSTEM ADI	MEVCUT SISTEM	ÇALIŞMA VOLTAJI (V)	ÇEKTİĞİ AKIM (A)	1 SAATLİK HARCAMA VE ÇEKİLEN YÜK (kWh)	BAZ ALINAN YIL İÇİNDE KULLANIM SÜRESİ SAAT	TOPLAM KULLANILAN MİKTAR (kW)	TOPLAM KULLANILAN MİKTAR GİGA JOULE
ANA MAKİNE	6	600 KG	0	0	580	348000 KG	42.4
D.DZ.TUL.	6	440	480	292	580	169360	0.1
HAVA KOMPRESOR	4	440	200	121	115	13915	0.1
ANA MK ON Y.Y.TUL	6	440	120	73	30	2190	0.1
SANZUMAN ON Y.Y.TUL.	2	440	100	60	5	300	0.1
ANA MK.TATLI SUTUL.	6	440	96	58	580	33640	0.1
ANA MK MOT.PRIMING TUL.	6	440	120	73	70	5110	0.1
STRAST BLOK Y.Y.TUL.	1	440	10	6.	90	540	0.1
PITCH KONTROLY.Y.TUL.	4	440	128	76	580	44080	0.1
TORNA ÇARK MOT.	2	440	40	24	12	288	0.1
STERN TUP DZ.TUL.	2	440	40	24	580	13920	0.1
MOT.TRANS.TUL.	2	440	20	12	175	2100	0.05
TATLI SU TRANS.TUL.	2	440	20	12	390	4680	0.05
TATLI SU HİDRAFOR TUL.	2	440	32	19	2250	42750	0.1
SINTINE TAHLİYE TUL.	2	440	20	12	1180	14160	0.05
PIS SU TUL	3	440	96	58	120	6960	.0.5
MOTORIN PRUFAYER	2	440	100	60	115	6900	0
TERS OZMOZ	1	440	20	12	0	0	0
SINTINE SEPERATOR	1	440	10	6.	0	0	0
ANA BOLME TAH.TUL.	7	440	140	85	5	425	0.1
ANA YANGIN TUL	6	440	480	292	310	90520	0.2
DALGIC TUL	4	440	128	78	3	234	0
SEYYAR YANGIN TUL.	2	1 KG	0	0	13	13 KG	0
ANA YANGIN ALARMI	1	24	10	0,3	8766	2630	0
SU USTU SEY. RAD.	3	440	30	18	610	10980	39,528
RADAR MONITOR	6	220	6	1,8	610	1098	3,9528
WECDIS ELN. HARITA	1	440	6	3	610	1830	6,588
ELN ISKANDIL	2	220	6	1,8	610	1830	6,588
CAYRO RİPİTER	11	115	24	3,8	610	1098	3,9528
CAYRO	2	440	20	12	750	9000	32,4
PARAKETE	1	115	6	0,9	610	549	1,9794

Figure 11. Warship LEAP parameters for the year of 2016.

Each demand technology determined in the warship energy system analysis created in the first stage has been transferred to excel format. In Figure 10,

the number of each demand technology, the current (A), the operating voltage (V) and the corresponding operating (kWh) values are calculated. The calculated values are shown as the energy (GJ) used by each demand technology during the total working period, taking into account the cruise and port times in the specified year.

5.3. Introducing Technology and Demands to LEAP

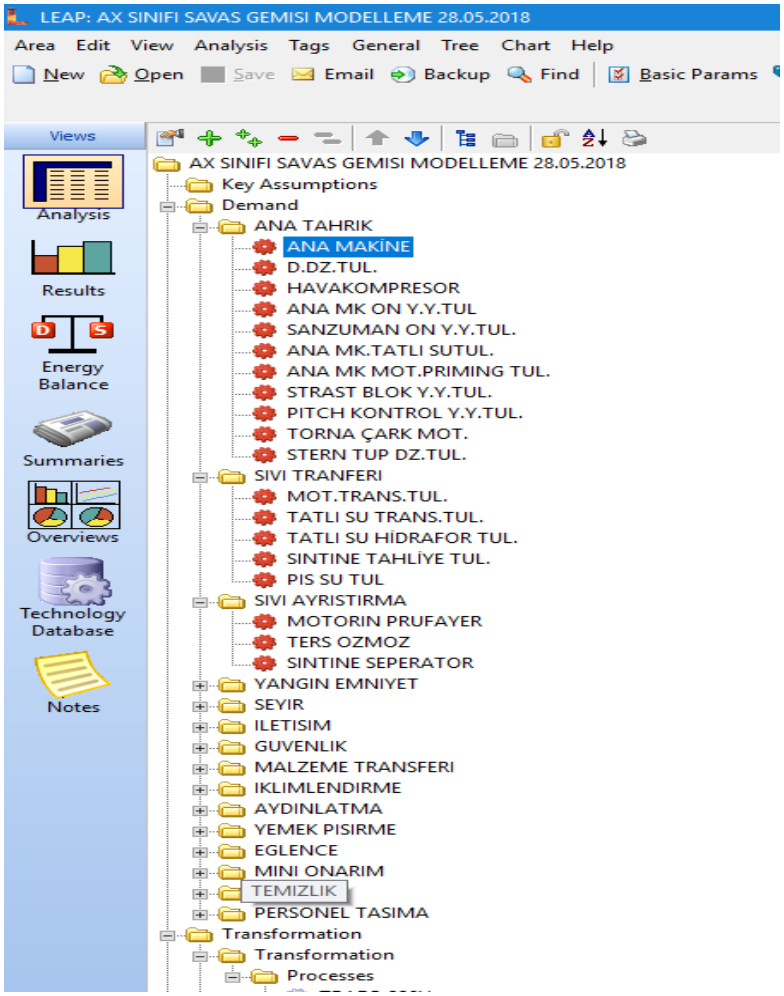

Figure 12. LEAP modelling technology and demands.

A total of fifteen different energy demands are shown in Figure 11 and a total of 93 demand technologies that meet these demands are defined in the Demands section of LEAP as a demand technology that meets each demand.

5.4. LEAP Demand Technology Data Entry

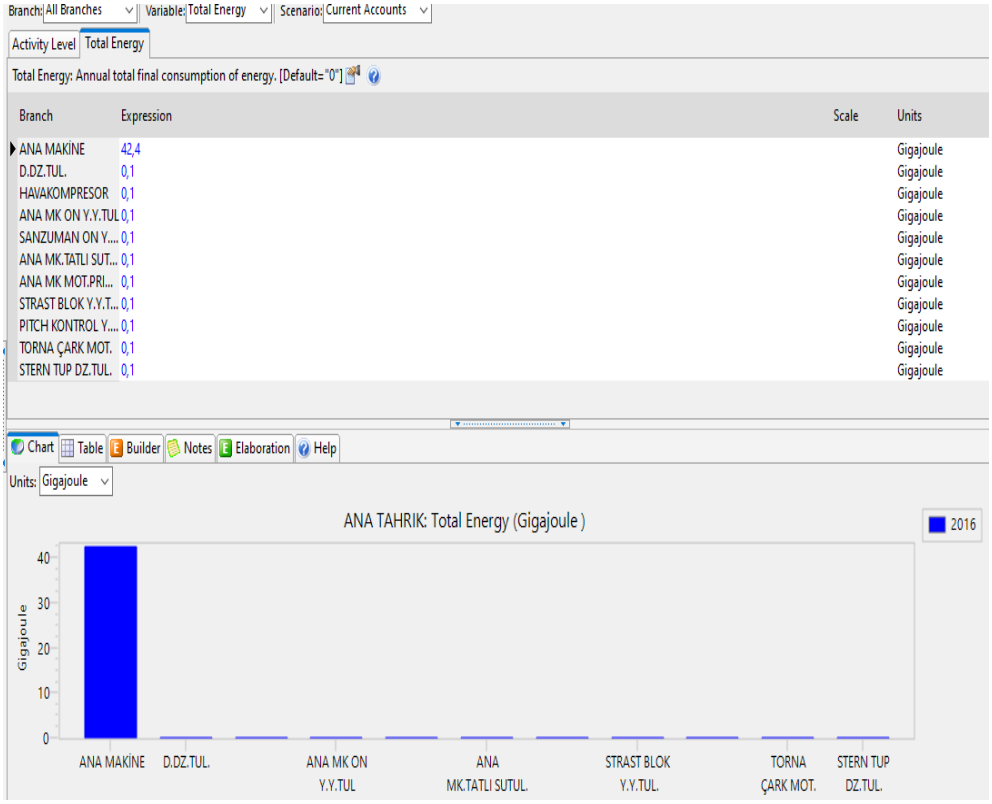

Figure 13. LEAP modelling demand technology data entry.

In Figure 12, the total energy consumption of each demand technology calculated in the following excel table is entered in the Demand technologies section of the LEAP interface as annual expenditure gigajoule (GJ).

5.5. Introduction of Conversion and Process Technologies to LEAP

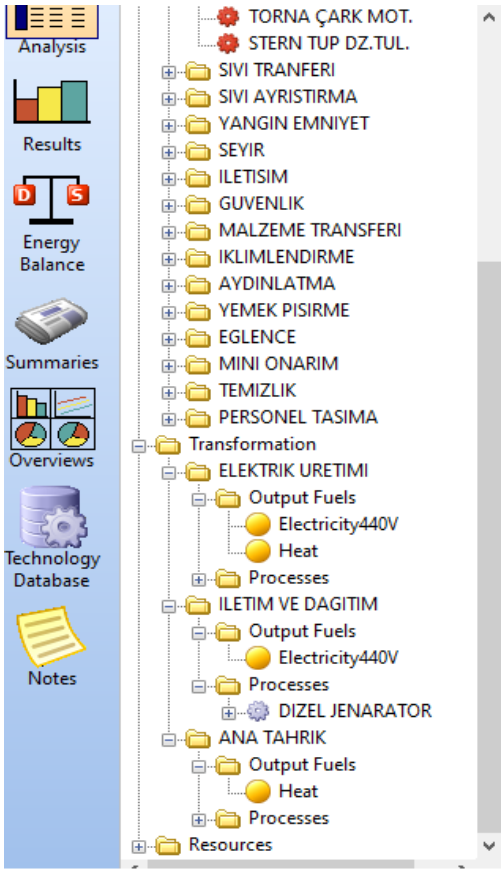

Figure 14. LEAP modelling conversion and process technologies.

In this section under the Transformation section of the LEAP interface, cycle and process technologies are defined. As seen in Figure 13, this section defined in the energy tree under 3 main headings consists of Transformers, Heater and Diesel Generator definitions sequentially. Identification sequences are also important for establishing the energy balance. In the Transformers section, 2 types of transformers used on the

ship are defined and the losses in these transformers during distribution are specified. Fan hits that provide warm air for the warming of the ship in winter are defined under the heading Heater. Finally, Diesel Generators that provide electricity to all systems except the main engines on the ship are defined under the title of Diesel Generator.

5.6. Introducing the Main and Final Energy Carriers to LEAP

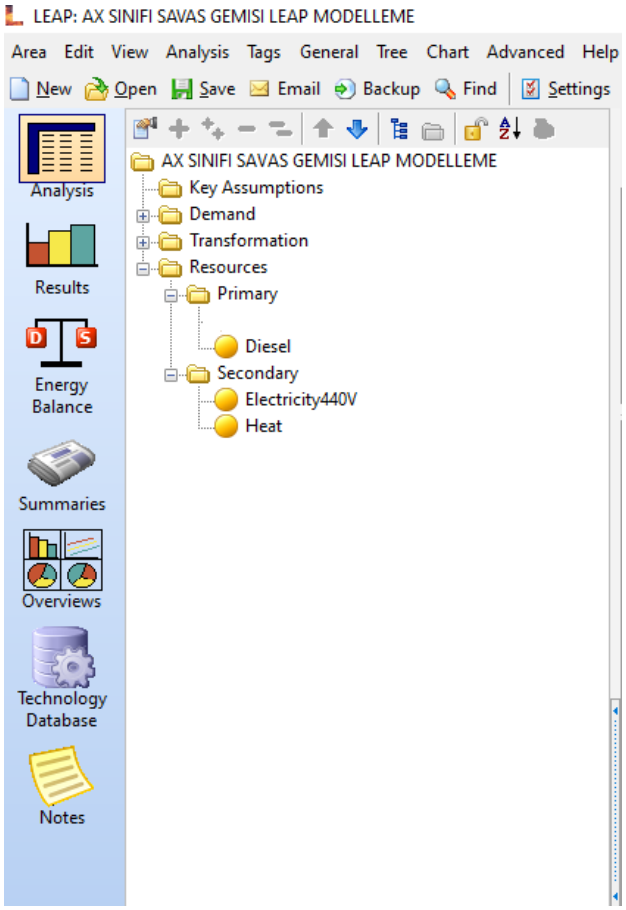

Figure 15. LEAP modelling the main and final energy carriers.

As indicated in Figure 14, the main energy carriers used in the ship's energy system are Diesel under the Primary title under Resources, and the final energy carriers created by Conversion and Process technologies as Electricity 440V and Heat under the title of Secondary.

5.7. One – Year Energy Balance and Analysis

Table 2. LEAP modelling the main and final energy carriers.

Energy Balance for Area "AX SINIFI SAVAS GEMISI LEAP MODELLEME"				
Scenario: Current Accounts, Year: 2016, Units: Gigajoule				
	Electricity440V	Diesel	Heat	Total
Imports	76,3	37,2	52,7	166,2
Exports	-	-	-	-
Total Primary Supply	76,3	37,2	52,7	166,2
İLETİM VE DAGITIM	-47,4	-19,7	-	-67,1
ELEKTRIK URETIMI	-	-	-	-
Total Transformation	-47,4	-19,7	-	-67,1
ANA TAHRIK	1,0	11,2	31,2	43,4
ELEKTRIK URETIMI	19,7	6,3	21,5	47,5
SIVI TRANFERI	0,3	-	-	0,3
SIVI AYRISTIRMA	0,0	-	-	0,0
YANGIN EMNIYET	0,3	-	-	0,3
SEYIR	0,1	-	-	0,1
ILETISIM	0,1	-	-	0,1
GUVENLIK	0,1	-	-	0,1
MALZEME TRANSFERI	0,1	-	-	0,1
IKLIMLENDIRME	4,1	-	-	4,1
AYDINLATMA	2,5	-	-	2,5
YEMEK PISIRME	0,3	-	-	0,3
EGLENCE	0,0	-	-	0,0
MINI ONARIM	0,0	-	-	0,0
TEMIZLIK	0,0	-	-	0,0
PERSONEL TASIMA	0,2	-	-	0,2
Total Demand	28,9	17,5	52,7	99,1
Unmet Requirements	-	-	-	-

After all the data entered and all the definitions, the annual energy requirement of an AX Class warship set forth by LEAP is calculated in Gigajoule and shown in Table 2. The energy need required is seen on the basis of demand and the amount of energy consumed by the system appears as the total demand.

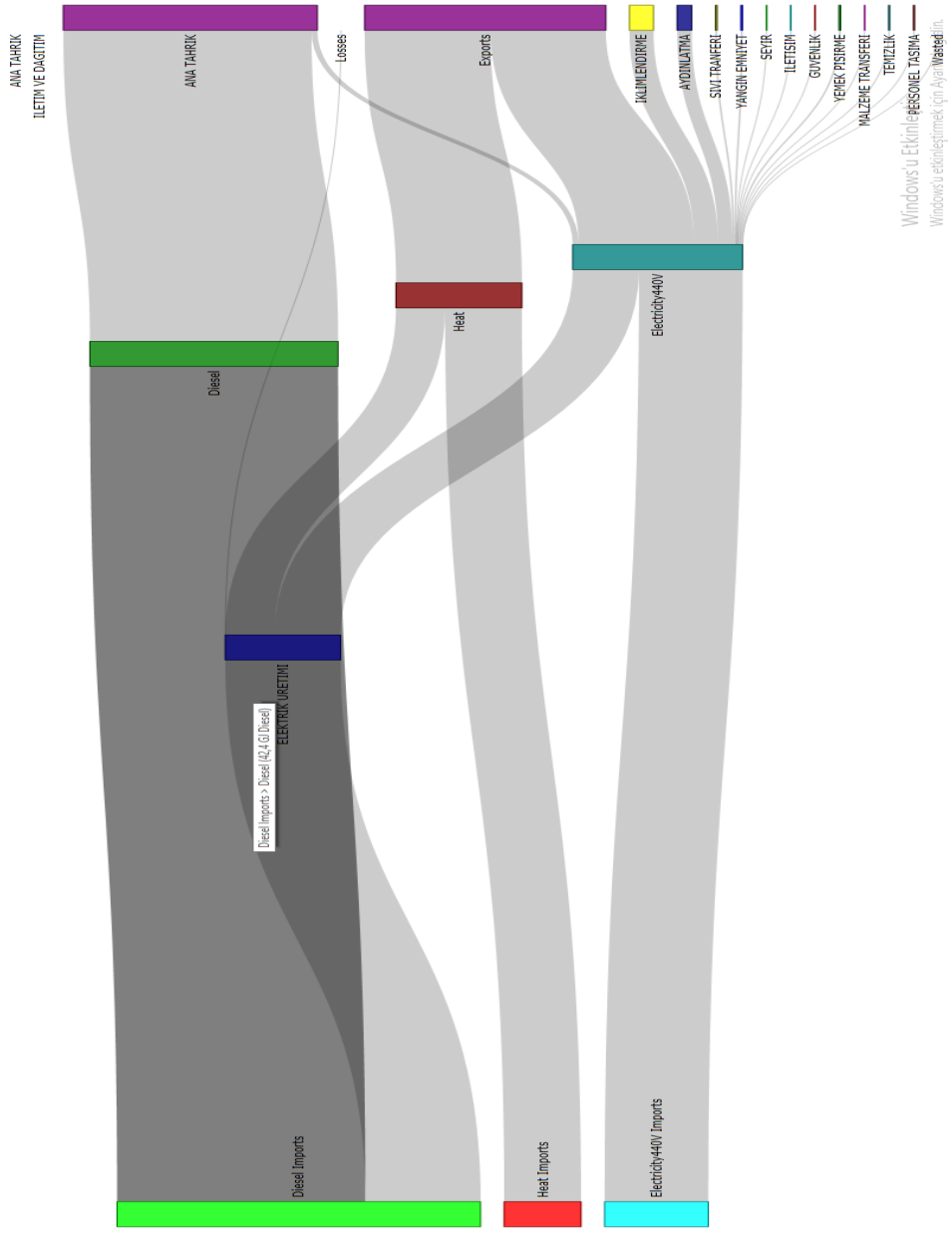

Figure 16. LEAP modelling one-year Energy Sankey Diagram.

In the Sankey Diagram expressed in Figure 15, the energy transformations and energy flows of all technologies, from primary energy carriers to demands, can be seen visually.

6. CONCLUSION

In this study, which is a continuation of the ship reference energy system analysis, taking into account the MARKAL model RES concept, the Reference Energy System analysis of an AX Class warship was integrated into the LEAP modeling program. In the integration, all elements of the system were introduced to the program together with their parameters and the amount of energy required by the system annually was determined.

In this study, it is seen that the total annual energy production of the warship shown in Figure 15 is 166.2 Gigajoules and the part of this demand, which is 99.1 Gigajoules, is the energy produced from the ship fossil fuel used in the Main Engine and Diesel Generators. This constitutes 59.6% of the total energy demand of ships. The remaining 67.1 Gigajoules of ship energy demand represents the energy losses in the cycle, heat, transmission and distribution of the ship energy system.

While the main propulsion requirement of the ship should be 43.4 Gigajoules, 12.2 Gigajoules of energy can be obtained due to heat and transmission losses. This has shown that the existing main engines on the ship operate at an efficiency of 28% and there is a need for technology improvement in the efficiency of the main engines in the main propulsion system.

Ship electricity constitutes all the demand of the ship energy cycle, excluding the main engine and diesel generators. This energy requirement is provided by 5 diesel generators on board. While the electricity requirement of the ship should be 76.3 Gigajoules, 47.4 Gigajoules of the requested energy is seen as loss due to heat and transmission losses. The remaining 28.9 Gigajoule electricity generation meets all the demands within the ship life cycle.

Table 3. IMO Greenhouse Gas Emission Data

(Turkish Chamber of Shipping, 2020).

Type of fuel	Reference	Emission factor ($t\text{-}CO_2/t\text{-}fuel$)
1 Diesel/Gas oil	ISO 8217 Grades DMX through DMB	3.206
2 Light fuel oil (LFO)	ISO 8217 Grades RMA through RMD	3.151
3 Heavy fuel oil (HFO)	ISO 8217 Grades RME through RMK	3.114
4 Liquefied petroleum gas (LPG)	Propane	3.000
	Butane	3.030
5 Liquefied natural gas (LNG)		2.750
6 Methanol		1.375
7 Ethanol		1.913

In Table 3, CO2 emissions corresponding to 1 ton of fuel burned are expressed in tons. According to IMO data, 3,206 tons of CO2 emission occurs as a result of burning 1 ton of diesel fuel. This showed that a total of 693 tons of diesel fuel (F-76) burned in the ship system (Main engine, Diesel Generator) produced 1406,688 tons of CO2 emissions into the atmosphere and was released into the atmosphere.

The first strategy determined by IMO's Marine Environment Protection Committee (MEPC) for reducing greenhouse gas emissions from ships is to determine the needs for increasing energy efficiency for each ship, to reduce CO2 emissions by at least 40% by 2030, to increase this rate to 70% until 2050 and to continue these studies.

The results of the analysis in the study conducted in line with this strategy showed that the slightest efficiency improvement to be made in ship main

engines and diesel generators will reduce the annual fuel consumption as well as decrease the CO2 emission.

REFERENCES

Ayan, M., & Baykal, T. (2010*)*. "Uluslararası Denizcilik Örgütü ve Çevre: Türkiye'nin Örgüt içindeki Durumu". *Mustafa Kemal University Journal of Social Sciences Institute*, 13, 275-297.

Baldi, F. (2013). "Improving ship energy efficiency through a systems perspective" (Master Thesis, Chalmers University of Technology, Department of Shipping and Marine Technology, Gothenburg, Sweden).

Baldi, F. (2016). "Modeling, analysis and optimization of ship energy systems" (Doctoral Thesis, Chalmers University of Technology, Department of Shipping and Marine Technology, Gothenburg, Sweden).

Çubuğuuzun, T. (2006). "Gaz Türbinli Gemilerde Ekserji ve Termodinamik Analiz" (Master Thesis, Yıldız Technical Üniversity, Institute of Science, İstanbul).

Durmaz, M. (2015). "Experimental and Experimental Emissions of Exhaust Emissions from a Ferry Theoretical Review" (Master Thesis, Istanbul Technical University, Institute of Science, Istanbul).

Energy PLAN (2019). Retrieved from http://energy.plan.aau.dk

IMO, T. I. (2014). "Greenhouse Gas Study 2014, Executive Summary and Final Report". *International Maritime Organization (IMO)*, London, 280.

IMO (2018, April 9-13). "Marine Environment Protection Committee (MEPC), 72nd Session". In Meeting Summaries, Media Centre. *International Maritime Organization (IMO)*. Retrieved from https://www.imo.org/en/MediaCentre/MeetingSummaries/Pages/MEPC-72nd-session.aspx

Interactive Energy Modeling (2019). Retrieved from http://www.energianalyse.dk/index.php/software

International Atomic Energy Agency (2019). Retrieved from www.iaea.org

Johnson, H., Johansson, M., Anderson, K., & Södahl, B. (2013). "Will the ship energy efficiency management plan reduce CO2 emissions? A comparison with ISO 50001 and the ISM code". *Maritime Policy & Management*, 40(2): 177-190.

Latin American Energy Organization (2020). Retrieved from http://www.olade.org/producto/super/descripcion/?lang=en

LEAP Calculation Structure (2021). Retrieved from https://leap.sei.org/default.asp?action=introduction

Long Range Energy Alternatives Planning System (LEAP) (2019). Retrieved from https://www.leap.sei.org/Default.asp

Öztürk, Ö. (2017). "Ship Systems Energy Analysis" (Master Thesis, Gebze Technical University, Institute of Science, Gebze).

Pachauri, R. K., Allen, M. R., Barros, V. R., Broome, J., Cramer, W., Christ, R., & Dubash, N. K. (2014). "Climate change 2014" (Synthesis Report). *Contribution of Working Groups I, II and III to the fifth assessment report of the Intergovernmental Panel on Climate Change*, (p. 151). IPCC.

Sarı, A. (2019). "Reference Energy System Analysis of a Chemical Tanker Ship" (Master Thesis, National Defense University, Barbaros Institute of Marine Sciences Engineering, Istanbul).

Shabbir, R., & Ahmad, S. S. (2010). "Monitoring urban transport air pollution and energy demand in Rawalpindi and Islamabad using leap model". *Energy*, 35 (5): 2323-2332.

Sulukan, E. (2010). "Establishing energy efficient utilization and cost-effective energy technologies selection strategies for Turkey using MARKAL family of models" (Doctoral Thesis, Marmara University, Institute of Science, Istanbul).

Sulukan, E., Özkan, D. & Sarı, A. (2018). "Reference Energy System Analysis of a Generic Ship". *Journal of Clean Energy Technologies*, 6 (5): 371-376.

Sulukan, E., Sağlam, M., & Uyar, T. S. (2017). "A native energy decision model for Turkey". In T. S. Uyar (Ed.), *Towards 100% Renewable Energy. Techniques, Costs and Regional Case-Studies* (pp. 167-177). Cham: Springer.

Talay, A. A., Deniz, C., & Durmuşoğlu, Y. (2014). "Analysis of effects of methods applied to increase the efficiency on ships for reducing co2 emissions". *Journal of ETA Maritime Science*, 1(2): 61-74.

Uyar, T. S. (2017). *Enerjide Dönüşüm: Enerjinin Etkin Kullanımı ve Topluluk Enerjisiyle %100 Yenilenebilir Enerjiye Geçiş*. Istanbul: EUROSOLAR Turkey.

Warship Main Characteristics (2021). "Okul Gemileri-Ana Karakteristikleri".
Retrieved from https://www.dzkk.tsk.tr/Destek/icerik/okul-gemileri

Journal of Naval Sciences and Engineering
2021, Vol. 17, No. 2, pp. 377-393
Naval Architecture and Marine Engineering/Gemi İnşaatı ve Gemi Makineleri Mühendisliği

RESEARCH ARTICLE

**An ethical committee approval and/or legal/special permission has not been required within the scope of this study.*

INVESTIGATION OF BOAT MOTION ON OCCUPANT IN PATROL BOATS*

Mehmet Burak KOÇAK[1]
Barış BARLAS[2]

[1] *Istanbul Technical University, Department of Naval Architecture and Marine Engineering, Istanbul, Turkey, kocakmeh@itu.edu.tr; ORCID: 0000-0002-6650-5760*

[2]*Istanbul Technical University, Department of Naval Architecture and Marine Engineering, Istanbul, Turkey, barlas@itu.edu.tr; ORCID: 0000-0002-5846-2369*

Received: 13.06.2021 **Accepted: 19.08.2021**

ABSTRACT

Occupants in high-speed patrol boats are subject to impact forces due to various boat motions. These impact forces should be precisely calculated and accounted for when designing seats for occupants. Hull design and cruising speed are the most critical parameters that cause shock and impact on the boat during the journey. In addition, seat design and material also have a major effect on the impact level sensed by the occupant. In this study, Altair software (Hypermesh and Radioss) is used to build a sample Computer Aided Engineering (CAE) seat and occupant model for patrol boats. The occupant CAE model (50th percentile, Hybrid III) used in our study is already available in the software library and has been verified based on physical testing. During investigation, accelerations coming from reference studies are applied on the model and CAE results are investigated to understand occupant kinematics better. Different accelerations, seat foam thicknesses, and seat foam materials are tested numerically in CAE models. Based on the CAE results, strong relation between boat accelerations and impact level on occupant body regions are compared and verified. Acceleration levels and dummy kinematics was investigated with updates in seat foam design and materials. This study has been conducted in order to avoid injuries for patrol boat occupants and to shed a light on the importance of seat design.

Keywords: *Patrol Boats, Occupant Movement, Impact Forces, Interior Design.*

DEVRİYE BOTLARI KOLTUK TASARIMINDA TEKNE HAREKETİNİN İNCELENMESİ

ÖZ

Yolcular, yüksek süratli devriye botlarında, teknenin hareketi sırasında oluşan ani darbe kuvvetlerine maruz kalabilirler. Oluşan bu darbe kuvvetleri yolcu üzerinde detaylı olarak değerlendirilmesi gereken yüklemeler oluşturabilmektedir. Tekne tasarımı ve teknenin seyir hızı, seyir sırasında teknede şok ve darbeye neden olan en kritik parametrelerdir. Bunların yanında, koltuk tasarımı ve malzemesi de yolcunun maruz kaldığı darbe seviyesi üzerinde önemli bir etkiye sahiptir. Bu çalışmada, Altair yazılımları (Hypermesh ve Radioss) ile devriye botları için koltuk ve yolcu içeren örnek bir Bilgisayar Destekli Mühendislik (CAE) modeli oluşturulmuştur. Oluşturulan modelde yazılım kütüphanesinde bulunan ve ölçüm kabiliyeti ve doğruluğu fiziksel testlere göre korelasyonu yapılmış Hybrid III serisi %50'lik manken kullanılmıştır. Analizler doğrulanmış olan bir manken ile yapıldığı için farklı tasarım parametreleri arasında karşılaştırma yapmak için yeterli seviyede güvenilir sonuçlar vermektedir. İnceleme sırasında, literatür çalışmalarında da kullanılan devriye botlarında oluşabilecek ivme profili modele uygulanmış; analiz sonuçlarında oluşan yolcu kinematiği ve maruz kalınan ivmeler detaylı olarak incelenmiştir. Yapılan CAE analizleri ile farklı ivme profilleri, sünger kalınlıkları ve sünger malzemelerinin yolcu üzerindeki etkileri incelenebilmiştir. CAE sonuçlarına göre tekne çarpma kuvveti ile yolcunun vücudu üzerinde farklı bölgelerde oluşan ivme seviyesi arasında güçlü ilişkinin olduğu gözlemlenmiştir. Ayrıca, koltuk sünger tasarımı ve sünger malzemesindeki değişikliklerin yolcuyu etkileyen kritik iç tasarım unsurları olduğu gözlemlenmiştir.

Anahtar Kelimeler: *Devriye Botu, Yolcu Hareketi, Darbe Kuvvetleri, Tekne İç Dizaynı.*

1. INTRODUCTION

A patrol boat is a moderately small marine vessel generally designed for coastal defense, border protection, search duty, and rescue operations. There have been many designs for patrol boats operated by the navy, coast guard, marine police, coastal safety and customs protection. Most modern patrol boat speeds are generally in the range of 25–45 knots. Their small size and relatively low cost make them one of the most desirable type of high speed crafts in the world (Figure 1).

Figure 1. Fast patrol attack boat (Ekber Onuk).

Occupants in high-speed patrol boats are subjected to impact forces due to boat motion which should be investigated in detail. If the impact force applied on occupant is higher than a threshold value, injuries can be observed. To avoid injuries for patrol boat occupants seat design has the utmost importance. Normally, a boat is exposed to acceleration in six directions: heave, surge, sway, yaw, roll and pitch. The most critical motion which has the highest acceleration on occupant is slamming motion. Several investigations are available in the literature which focuses on boat strength,

motion, and acceleration. Golwitzer and Peterson (1995) worked on the development of an injury/performance prediction method for high-speed planning boats. Data recorded from various sea tests are presented and applicability of computer simulation or model testing is investigated in their report. Townsend et al. (2012) published a paper which focuses on flexible hull design to isolate the occupants from external disturbance. They investigated the effect of the hull stiffness on motion. Compared to a regular hull design, both suspended and elastomer hull designs transferred smaller acceleration levels to the occupants. Ullman (2014) worked on the slamming standards and creating awareness to injuries caused by the impact. His paper specifically mentioned that hull design is not enough to endure extreme slamming motion. Crew and passengers should also be considered to eliminate possible injuries. Besides hull design, seats with suspension, posture, standing up, driving and handling are other parameters which effect the acceleration subjected to the occupants. Riley et al. (2015) published laboratory requirements for marine shock isolation seats. They presented a test criterion for shock isolation seats used in 7 to 30-meter planning craft. In their setup, steel plates or Anthropomorphic Test Devices (ATD) can be used as a payload to represent the occupant as seen in Figure 2.

ATD are developed to represent a human for several test scenarios: aircraft development, vehicle crash, etc. While these test dummies are developed, their sizes are defined based on the weight and height distribution in population. Specifications are defined for three different dummy types: 5^{th}, 50^{th} and 95^{th}. 5^{th} and 95^{th} dummies represent to 5% percent of the population which are in the upper and lower limit (BOSTONtec, 2021). The size of the 50^{th} dummy is based on the average size of the population. Sample view of the distribution is given in Figure 3. Demir and Barlas (2017), analyzed the impact forces on a boat in a towing tank. They used a planning boat model in their study to examine acceleration and shock. Even though the study was completed using a model scale, the results are applicable to full scale using the method given by the authors in the paper. Avcı et al. (2016) experimentally investigated the shocks and hydrodynamic accelerations of high speed inflatable boats at sea. An inflatable boat of 4.7 m was instrumented and a series of tests were conducted regarding vibration. There are also several standards available which consider acceleration or vibration

in boat environment. European Union Directive 2002/44/EC, ISO2631-1 and ISO2631-5 focus on vibration in boat exposed on occupant and IMO HSC 2000 focuses on the acceleration on boat. Based on IMO HSC 2000, passenger seats should not detach during severe impacts. (Ullman, 2014).

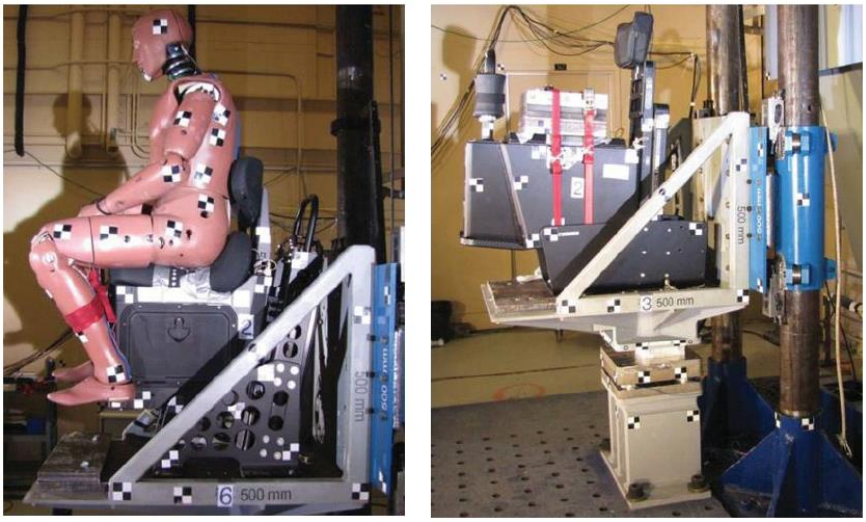

Figure 2. Test setup defined by Riley et al. (2015).

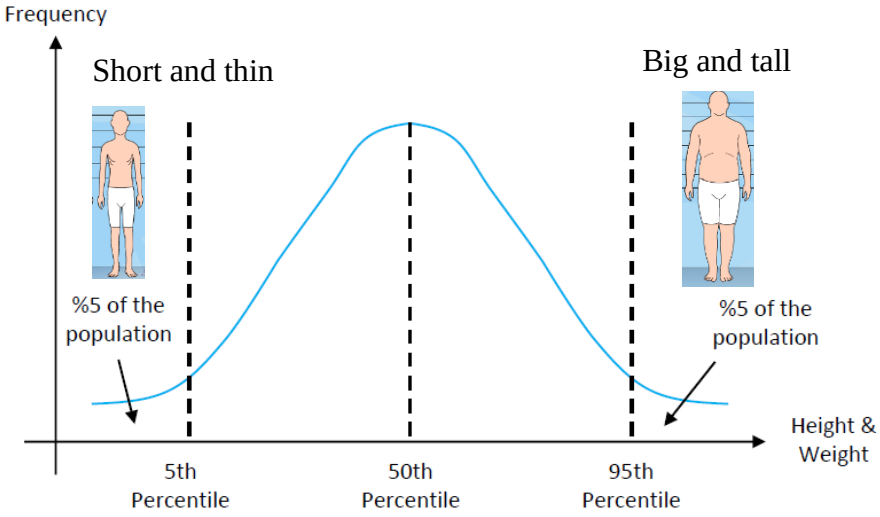

Figure 3. Height and weight distribution of population.

2. METHODOLOGY

In this study, accelerations on the different body regions due to motion of the high-speed marine boat are investigated with computer aided engineering (CAE) tools. Altair software (Hypercrash and Radioss) is used to make detailed investigation with simplified CAE models.

2.1. CAE Modelling

CAE models include seat structure and the 50th percentile Hybrid III occupant model. The CAE setup is given in Figure 4. Model details like nod and element quantity and details of the analysis like CPU and time step are given in Table 1. One dimensional elements used in this study are beams and springs, two dimensional elements are shells and triangular elements, three dimensional elements are bricks and tetrahedral elements, etc. An Intel Xeon 96-core processor is used for all the computations.

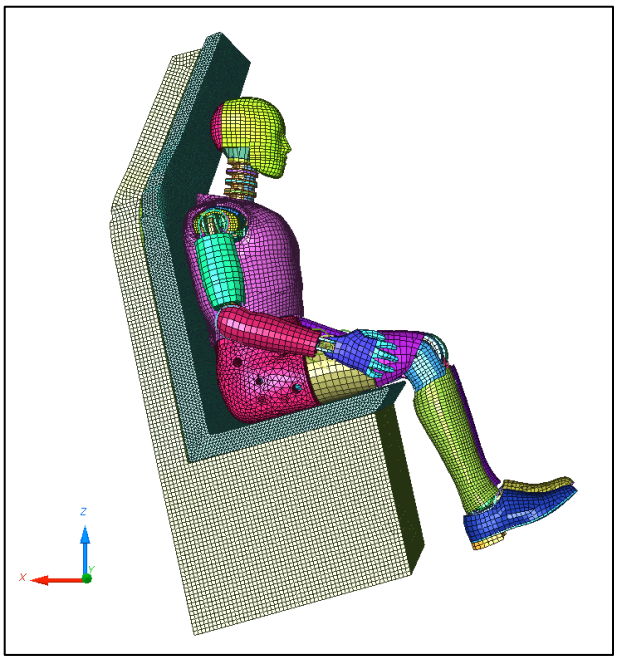

Figure 4. The CAE setup.

Table 1. Model and analysis details.

Model Details		**Analysis Details**	
Node	165129	Solver	Radioss 12.0.226
1D elements	558	CPU	96
2D elements	688823	Runtime (ms)	350
3D elements	329913	Time step (ms)	0.004
Model size (MB)	40	Number of cycles	851789
		Elapsed time (hour)	2.53

The seat model used in the analysis is created using a Computer Aided Design (CAD) environment first. The CAD model is meshed, and material properties are applied from the library. For seat structure, composite material PP-LGF30 is chosen. PP-LGF30 is formed using a polypropylene polymer matrix and reinforced with long glass fibers. Fiber content in the material is 30%. Mechanical properties of the seat structure material are given in Table 2. Polyurethane foam which has 60g/l density is used as cushioning on the seat. CAE investigations on cushion density and shape are completed. 50^{th} percentile Hybrid 3 occupant model available in the CAE library is used.

Table 2. Mechanical properties of seat structure (PlastiComp, 2021).

	SI Metric	**Test Method**
Specific Gravity	1.12	ASTMD-792
Tensile Strength	107 MPa	ASTMD-638
Tensile Modulus	6207 MPa	ASTMD-638
Tensile Elongation	2-3%	ASTMD-638
Flexural Strength	157 MPa	ASTMD-790
Flexural Modulus	5517 MPa	ASTMD-790
Notched Izod Impact	214 J/m	ASTMD-256
Un-notched Izod Impact	828 J/m	ASTMD-4812
DTUL @ 264 psi (1820kPa)	149^{o}C	ASTMD-648

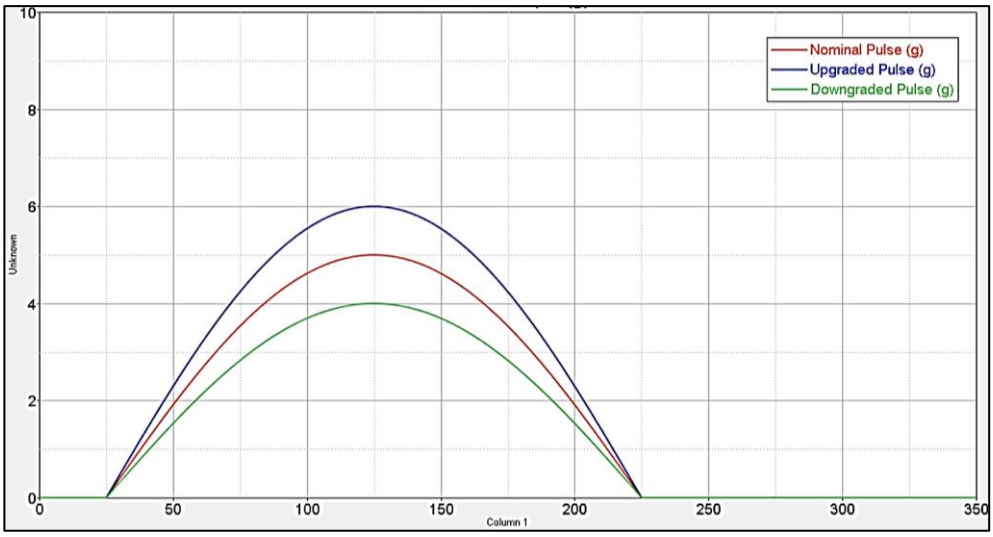

Figure 5. Acceleration profiles used in CAE.

Occupant CAE models in the library are verified using physical tests, so the kinematics and the outputs from the sensors are trustworthy. Acceleration due to patrol boat motion is applied in the CAE model to investigate occupant kinematics and acceleration. Sinus curve is used for imposed acceleration curve characteristics. Ullman (2014) shared accelerations which are measured on platform and seat separately. The paper prepared by Ullman is used as a reference to define maximum acceleration levels in CAE investigation. 5 g is defined as the maximum acceleration level for the reference model. 200ms is used as the duration of the acceleration curve. During CAE investigations, the maximum acceleration level is changed in order to understand the effect of the acceleration on occupant response. Acceleration curves which are used in this investigation is given in Figure 5. In CAE studies, the seat motion is restricted in the X and Y directions. So, the defined acceleration is imposed only on the Z direction. The occupant who is positioned on the seat can freely move as there is no boundary applied on the occupant model. Gravity is also applied on whole model to make the CAE environment more representative.

3. RESULTS

The CAE investigation covers three main areas based on the reference condition. Occupant kinematics and acceleration on the occupant is measured from the head, chest and pelvis area for each condition. The first investigation area is the acceleration levels due to boat motion. Reference acceleration is scaled up and down by %20 to represent different boat motion characteristics. Difference in the occupant kinematics and acceleration in different body regions are given in Figures 6 and 7. As can be seen in Figures 4 and 5, there is a correlation between boat acceleration and occupant response. Increased boat kinematics cause occupant movement and acceleration levels to also increase. Likewise, head and chest acceleration measured on the occupant is higher compared to pelvis and imposed patrol boat acceleration for each case. Movement of the occupant led these phenomena during motion. Pelvis movement can be reduced by the seat better compared to the upper body. Thus, acceleration levels are lower in pelvis area. Rotation observed in the upper body leads to an increase in the final acceleration level on the chest and head. Foam design is the other investigation area of this study. Foam thickness is increased by 50mm and results are compared with the reference model. Design difference between the new and the reference model is given in Figure 8. Difference in the occupant kinematics and acceleration on different body regions are compared in Figures 9 and 10.

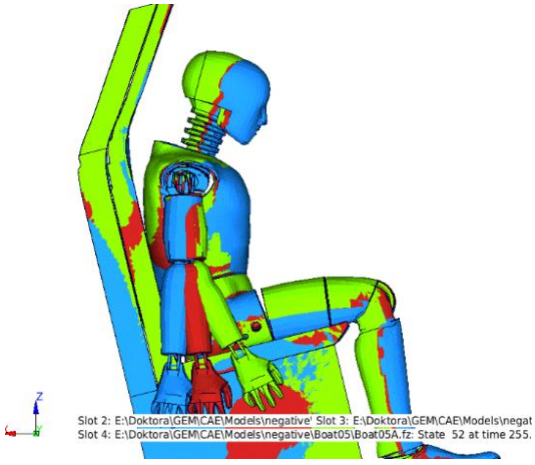

Figure 6. Occupant kinematics in different boat motions.

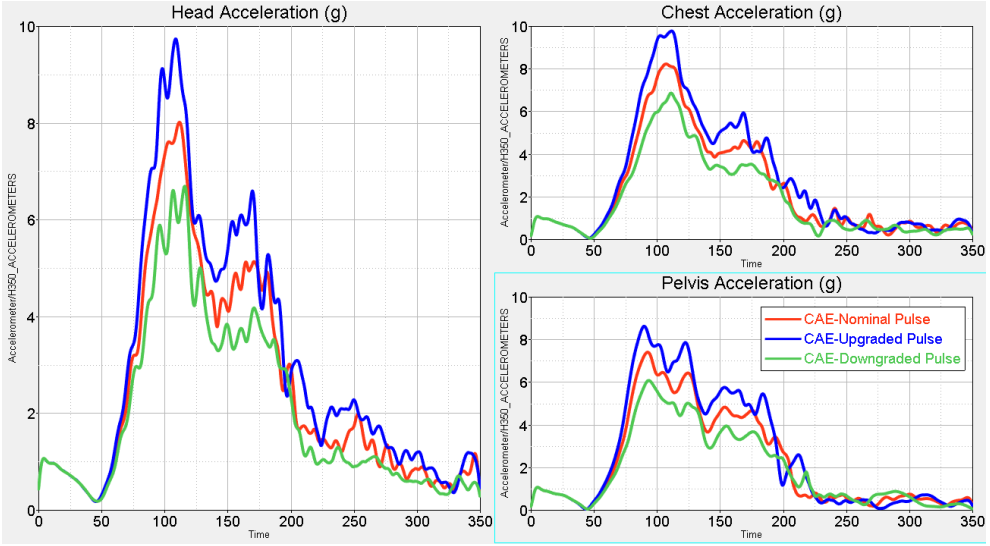

Figure 7. Accelerations in different patrol boat motions.

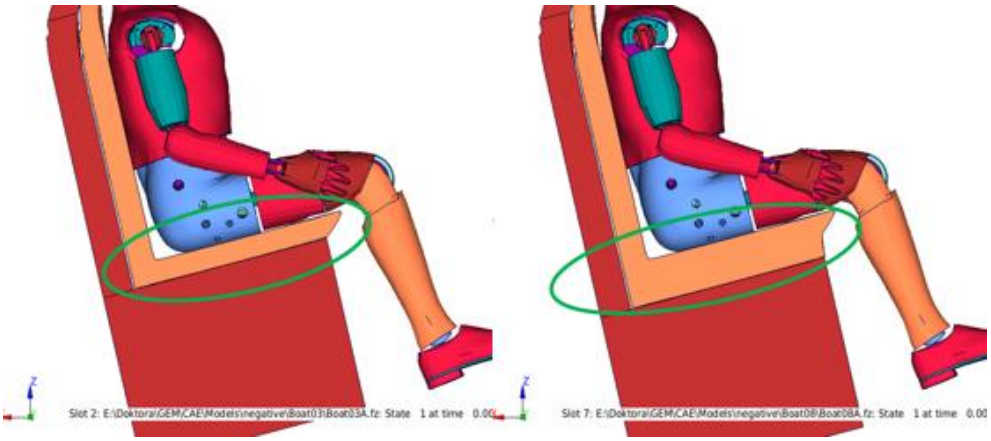

Figure 8. Two different foam designs studied in this study.

When foam thickness is increased, acceleration on the body regions can be reduced until ~100ms. During initial boat loading, less acceleration is observed in each region. Occupant kinematics also show similar phenomena. Effect of the imposed acceleration can be absorbed by thicker foam until the threshold timing. In the animations, the seat can move further

with less effect on the occupant, so acceleration is less in the new design. On the other hand, occupant movement increases after the threshold and the occupant rotates more. Foam material is the last investigation topic of this study. Two additional foam material property is used in the CAE analysis to understand the effect of the foam material on kinematics and acceleration.

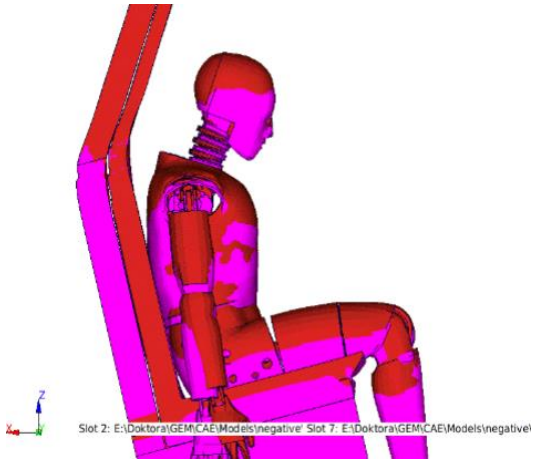

Figure 9. Occupant kinematics in different foam design.

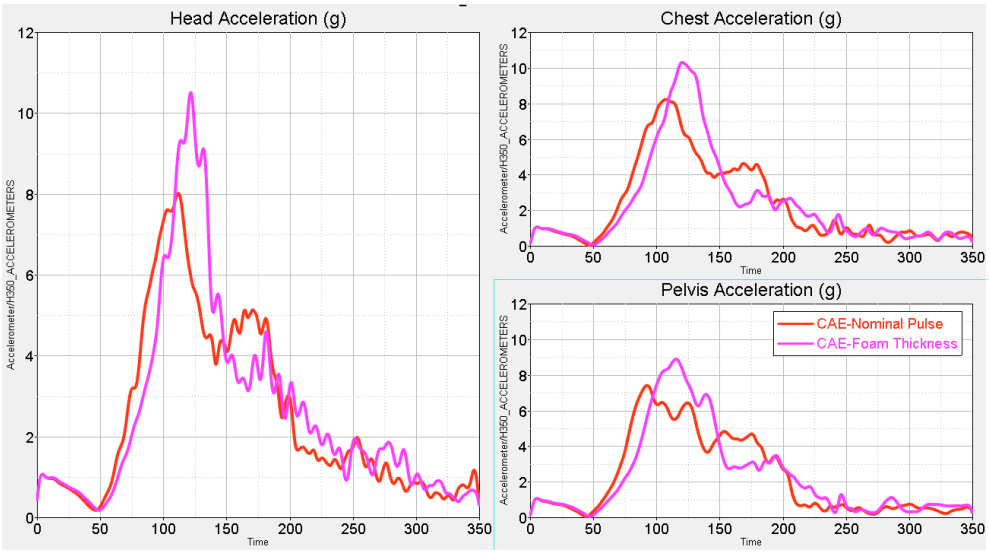

Figure 10. Accelerations in different foam design.

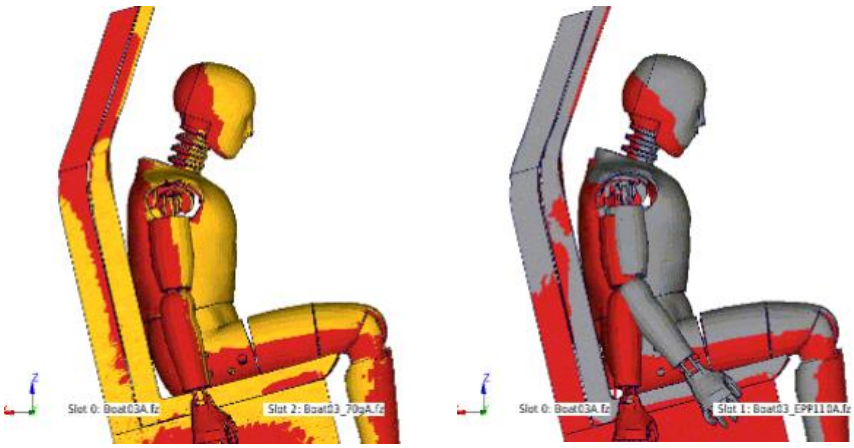

Figure 11. Occupant kinematics in different foam materials.

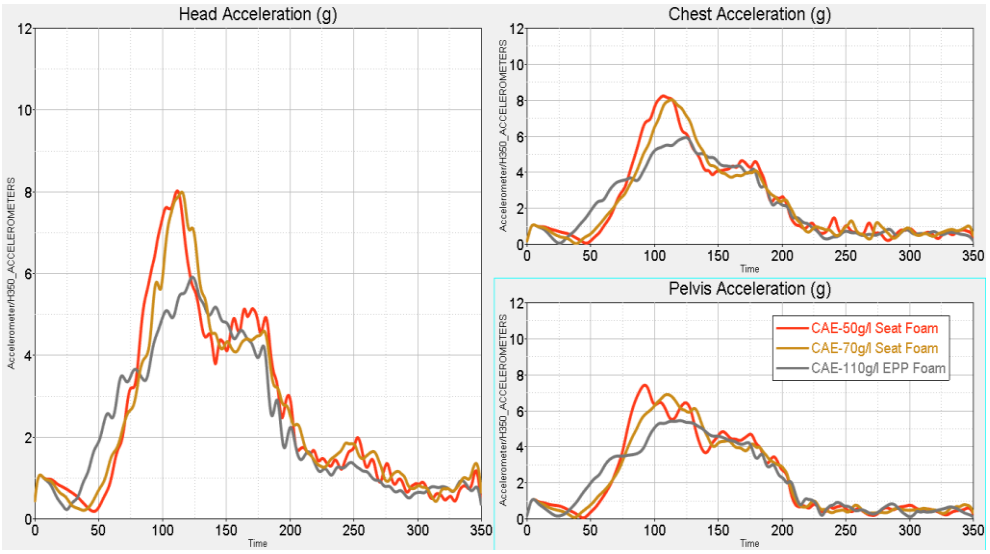

Figure 12. Accelerations in different foam materials.

For the first material iteration, density of the available foam material (60g/l) was increased to 70g/l. Expanded Polypropylene (EPP) foam which has a density of 110g/l was used for the second CAE iteration. EPP foam is stiffer compared to PU foam, which is used in other CAE models. Occupant

kinematics and acceleration comparisons are given in Figures 11 and 12. As can be seen, the difference in kinematics and acceleration (red and yellow) are limited to the density difference in same material. On the other hand, major change in kinematics and acceleration is observed after the foam material is replaced to EPP. As 110g/l EPP is stiffer compared to PU foam, acceleration from boat motion is transferred to the occupant earlier. Therefore, the occupant is exposed to higher acceleration in the first ~75ms. On the other hand, peak acceleration level observed in this model is less compared to the model with PU foam material.

4. CONCLUSION

In this study, impact of the acceleration during patrol boat motion on occupant is investigated. As technology develops, more powerful engines and lighter composite structures cause the patrol boat speeds to increase, therefore increasing the hydrodynamic loads and impacts of the patrol boats. Boats running at high speeds in the rough seas experience six degrees of freedom (heave, surge, sway, yaw, roll and pitch) which is highly complex and dangerous. Furthermore, apparent waves make the acceleration and shock problem on patrol boats very complicated. The patrol boat operating at high speeds is exposed to severe repeated shocks. Therefore, if the impact force applied on the occupant is higher than the threshold, injuries can be observed. Hull design is not enough to endure extreme slamming motion. Crew and passenger seats with suspension and posture aid become important and it should be considered to eliminate possible injuries.

CAE analysis is used to understand the effects on occupant kinematics and acceleration which is measured from different body regions. Correlated CAE models are used in this investigation. Material data used in the CAE analysis comes from physical test results. Thus, system CAE results are reliable to make back-to-back comparison between different cases. Based on the CAE results, correlation is observed between boat motion and occupant movements. Higher acceleration on the boat causes higher occupant movement and acceleration. With changes in seat foam design and material, occupant motion and acceleration can also be changed. This shows that besides boat motion, interior design also has an important effect on kinematics and acceleration acting on the occupant.

In future investigations, full system correlation on the CAE model (contact parameters, friction coefficients etc.) can be planned to understand the correlation level of the system and make more detailed design of experiment studies for interior components, especially seat design. To make full system correlation, the system can be tested in a sled environment and acceleration on different occupant body regions can be compared. Besides correlation of the system, boundaries of the study can be extended for future studies. This study is completed with one directional load case (Z) for one occupant (50^{th} percentile) size. Boat motions in other directions can be implemented into full system evaluation. Also, smaller and bigger occupant sizes (5^{th} and 95^{th} percentile) can be used in further studies to investigate effect of interior design changes for all occupant sizes. Moreover, a vibration dose value (VDV) analysis can be investigated by using the patrol boat in-situ shock and acceleration values. This analysis would yield us the dosage an occupant will be receiving.

REFERENCES

Avcı, A. G., Barlas, B., Merdivenci, M. S. (2016). "An Experimental Investigation of Shock and Accelerations On Inflatable Boats". 1st International Congress on Ship and Marine Technology, Istanbul, Turkey: https://www.gmo.org.tr/upl/misc/yayinlar/gmo-shipmar-bildiri-kitabi.pdf

BOSTONtec (2021). "Designing an Industrial Workbench for Adjustability". Retrieved from: https://www.bostontec.com/designing-an-industrial-workbench-for-adjustability/ (11.06.2021)

Demir, M. F., and Barlas, B. (2017). "An Analysis of Impacts on Model Planning Boats". *GİDB*. No. 9, 43-56.

Gollwitzer, R. M., and Peterson, R. S. (1995). "Repeated Water Entry Shocks on High-Speed Planing Boats". Report by Dahlgren Division Naval Surface Warfare Center. CSS/TR-96/27.

IMO (2008). *International Code of Safety for High-Speed Craft* (2000 HSC Code, 2008 Edition). International Maritime Organization (IMO).

ISO (1997). "Mechanical vibration and shock — Evaluation of human exposure to whole-body vibration — Part 1: General requirements". *International Organization for Standardization (ISO).* ISO 2631-1.

ISO (2003). "Mechanical vibration and shock — Evaluation of human exposure to whole-body vibration — Part 5: Method for evaluation of vibration containing multiple shocks". *International Organization for Standardization (ISO).* ISO 2631-5.

Onuk, E. (2021). "Multi Role Tactical Platform, MRTP34". Retrieved from Ekber Onuk's private archive (22.06.2021).

PlastiComp (2021). "Product Data Sheet of Complēt® LGF30-PP". Retrieved from PlastiComp https://www.plasticomp.com/wp-content/uploads/PlastiComp-Complet-LGF30-PP.pdf

Riley, M. R., Haupt, K. D., Ganey, H. C. N., and Coats, T. W. (2015). "Laboratory Test Requirements for Marine Shock Isolation Seats". Technical Report by Naval Surface Warfare Center, Carderock Division, Naval Architecture and Engineering Department. NSWCCD-80-TR-2015/010 Rev A.

Townsend, N. C., Coe, T. E., Wilson, P. A., and Shenoi, R.A. (2012). "High Speed Marine Craft Motion Mitigation Using Flexible Hull Design". *Ocean Engineering*, Vol. 42, 126-134.doi:10.1016/j.oceaneng.2012.01.007.

Ullman, J. (2014). "Slamming Standards" *Professional Boat Builder*. No. 149, June/July. 48-53. Retrieved from Ullman Dynamics https://ullmandynamics.com/wp-content/uploads/2014/10/ProBoat-Slamming-Standards.pdf

Journal of Naval Sciences and Engineering
2021, Vol. 17, No. 2, pp. 395-411
Naval Architecture and Marine Engineering/Gemi İnşaatı ve Gemi Makineleri Mühendisliği

RESEARCH ARTICLE

** An ethical committee approval and/or legal/special permission has not been required within the scope of this study.*

CHARACTERIZATION OF WELDING ZONE OF SHIPBUILDING STEEL UNDERWATER WELDED AT DIFFERENT DEPTHS*

Dursun Murat SEKBAN[1]
Abdulhabib NACAR[2]

[1]*Karadeniz Technical University, Department of Marine Engineering Operations, Trabzon, Turkey,*
msekban@ktu.edu.tr; ORCID: 0000-0002-7493-1081

[2]*Karadeniz Technical University, Department of Naval Architecture and Marine Engineering, Trabzon, Turkey,*
abdulhabibnacar@gmail.com; ORCID: 0000-0002-9820-0021

Received: 09.08.2021 **Accepted: 18.10.2021**

ABSTRACT

Although welding operations are mostly carried out in atmospheric conditions in shipbuilding, underwater welding is also used intensively in order to speed up the repair processes in the underwater parts of the ships. It is known that due to the nature of the underwater welding, there are significant differences in the weld area compared to the weld made under atmospheric conditions. The most important factor that creates this difference is that the cooling rates achieved after welding contain significant differences compared to welding performed under atmospheric conditions. On the other hand, it is known that the depth of the underwater welding has a significant effect on this cooling rate. In the literature, it is seen that studies on underwater welding are extremely limited. On the other hand, no study has been found that has examined the effect of depth on the microstructure and mechanical properties during underwater welding of steels used in shipbuilding. In this context, in this study, a steel used extensively in shipbuilding was joint with atmospheric conditions welding and underwater welding (two varying depths), and the microstructure and mechanical properties of the welded area were examined comparatively.

Keywords: *Shipbuilding, Welding, Underwater Welding, Mechanical Properties.*

Characterization of Welding Zone of Shipbuilding Steel Underwater Welded at Different Depths

FARKLI DERİNLİKLERDE SUALTI KAYNAĞI UYGULANAN GEMİ İNŞA ÇELİĞİNİN KAYNAK BÖLGESİNİN KARAKTERİZASYONU

ÖZ

Gemi inşaatında kaynak işlemleri yoğunlukla atmosferik şartlarda yapılsa da, gemilerin su altında kalan kısımlarındaki tamir işlemlerini hızlandırmak adına sualtı kaynağı da yoğunlukla kullanılmaktadır. Su altı kaynağının doğası gereği kaynak bölgesinde atmosferik şartlarda yapılan kaynağa göre önemli farklar içerdiği bilinmektedir. Bu farkı oluşturan en önemli etken kaynak sonrasında erişilen soğuma hızlarının atmosferik şartlarda yapılan kaynağa göre önemli farklar içermesidir. Öte yandan bu soğuma hızına su altı kaynağının yapıldığı derinliğin de önemli oranda etki ettiği bilinmektedir. Literatürde sualtı kaynağı ile ilgili çalışmaların son derece sınırlı olduğu görülmektedir. Öte yandan gemi inşaatında kullanılan çeliklerin sualtı kaynağı sırasında derinliğin içyapı ve mekanik özellikler üzerindeki etkisini ayrıntılı olarak incelemiş bir çalışmaya rastlanmamıştır. Bu bağlamda bu çalışmada gemi inşaatında yoğun olarak kullanılan bir çeliğe atmosferik şartlarda ve değişen iki derinlikte sualtı kaynağı yapılarak kaynak bölgesinin içyapı ve mekanik özellikleri (sertlik, mukavamet, eğme ve darbe dayanımı) karşılaştırmalı olarak incelenmiştir.

Anahtar Kelimeler: *Gemi İnşaatı, Kaynak, Su Altı Kaynağı, Mekanik Özellikler.*

1. INTRODUCTION

Ships are built by joining plates and profiles of varying thickness and dimensions to each other with varying welding methods. During the ship's construction process, welds are made under atmospheric conditions. The welds made during the initial construction process vary according to variables such as the thickness of the plates used or the ship area to be welded. When the welding methods used in the shipbuilding process are examined, it is observed that gas metal arc welding; submerged arc welding and electrode arc welding are the 3 most used welding methods. On the other hand, after the first construction process, welding processes are also needed intensively in repair processes.

Welding operations during repair can be done under atmospheric conditions, as well as underwater welding processes are used intensively in order to speed up the process in underwater repair operations of the ship. When the history of underwater welding is examined, it is seen that this welding method gained great importance during the 1.World War. The underwater welding, which started to be used to repair the underwater damage of warships, continues to be used intensively in the construction of oil platforms, the welding of underwater pipelines and the repair of the underwater parts of the ships with the advancement of technology. It is known that the weld area of the weld made underwater differs greatly from the weld made under atmospheric conditions. As it is known, phase changes can occur in steels after welding and the cooling rate affects these changes significantly (Bhadeshia & Svensson, 1993; Boumerzoug, Derfouf & Baudin, 2010; David, Babu & Vitek, 2003; Eroğlu, Aksoy & Orhan, 1999; Gharibshahiyan, Raouf, Parvin & Rahimian, 2011; Gould, Khurana & Li, 2006; Grong & Matlock, 1986; Lars-Erik, 2017; Magnabosco, Ferro, Bonollo & Arnberg, 2006; Zhang, Jing, Xu, Han & Zhao, 2016). These changes in the microstructure also significantly affect the mechanical properties of the weld area (Boumerzoug et al., 2010; Gharibshahiyan et al., 2011; Liu et al., 2020). Again in this context, it is known that the depth at which the underwater welding is made makes a difference on the characteristics of the weld area by affecting the burning carbon rate (İmdat, Kaya & Kahraman, 2018). When the studies in the literature are examined,

it is seen that the studies examining the microstructural and mechanical properties of the weld area after the underwater welding are extremely limited. (Houldcroft, 1990; Kanjilal, Pal & Majumdar, 2006, 2007; Lee, Chandel & Seow, 2000; McPherson, Chi & Baker, 2003; Murugan & Gunaraj, 2005; Pandey, Bharti & Gupta, 1994). On the other hand, after the application of this welding method to the steels used in shipbuilding, it is seen from the literature that a detailed microstructure and mechanical property analysis was not carried out. In this context, in this study, a steel used extensively in shipbuilding was welded at atmospheric condition and underwater with two different depths. After the welds, the microstructural examinations of the structure formed in the weld area under changing conditions were made. After the microstructure examinations, the hardness, strength, bending strength and impact toughness properties of the weld zone were examined comparatively in all conditions.

2. EXPERIMENTAL PROCESS

Within the scope of the study, low-medium strength shipbuilding steel with the dimensions of 200 mm x 40 mm x 8 mm, which is used extensively in shipbuilding, was used. The chemical composition of the steel used is shown in Table 1.

Table 1. Chemical composition of the steel used in the study (% wt.).

C	Mn	P	S	Si	Cu	Cr	V	Mo	Fe
0,17	0,66	0,017	0,01	0,19	0,05	0,1	0,04	0,12	Balance

Before welding, the welding groove was opened to the plates in all conditions and welding processes were carried out by same welder so that there is no difference between the welds due to the welder. Welding processes under atmospheric conditions and underwater were carried out using rutile electrodes. Electrodes with a diameter of 4 mm were used and the electrodes were covered with paraffin material to provide insulation. All of the underwater welds were carried out in the marine environment. On the

day of the underwater weldings done, the sea water temperature was 29 ^{o}C and the sea salinity rate was 28%. In order to examine the effect of different depths in the weld area, welding processes were carried out separately at 1 meter and 5 meter depths.

Optical microscope examinations were made on the samples extracted from the weld area using wire erosion in order to carry out the microstructure examinations of the weld area after welding. Before the optical microscopy examinations, the samples were sanded, polished, and immersed in 3% Nital solution for 10 seconds, respectively.

After welding, the mechanical properties of the samples were investigated using hardness, tensile, 3-point bending and impact tests. Hardness tests were carried out using the Vickers hardness measurement method in struers brand duramin 3 model hardness device. During the experiments, the compression load of the penetrating tip was 500 g and the waiting time under load was 10 s. Tensile tests were carried out with at least 3 replicates at room temperature and the average strength and elongation values are given in the tables. The tests were performed using an Instron-3382 electro-mechanical testing frame with a video type extensometer at a quasi-static strain rate of $5.4x10^{-4}$ s^{-1}. The impact tests were similarly carried out at room temperature and in 3 repetitions, and the average values were determined. Impact experiments were carried out on a Charpy notch impact machine with a 50 J capacity Instron Ceast. Three-point bending tests were performed on an Instron 3220 universal testing machine at room temperature with a gauge speed of 1 mm/min. The amount of force-deflection applied to the sample during the experiment was continuously recorded with the help of a computer, and the bending force and maximum force deflection values were determined.

3. RESULTS AND DISCUSSIONS

3.1. Microstructure

The microstructures of the base, the sample welded under atmospheric conditions and the samples welded underwater at different depths are given in Figure 1. As can be seen from Figure 1a, the microstructure of the pre-

weld steel consists of coarse-grained ferrite and pearlite structures. It is also clearly seen from this image that there is some orientation in the direction of the rolling mill as expected in the perlite structure of the steel supplied as a hot rolled product. It is observed that the grains are slightly finer than base after welding in atmospheric conditions (Figure 1b). This situation is thought to be caused by the transformations during the cooling of the rising temperature during welding. Also, it is clearly seen that the microstructures after welding in water are oriented in the direction of cooling according to the base material with the effect of rapid cooling (Figure 1 (c-d)).

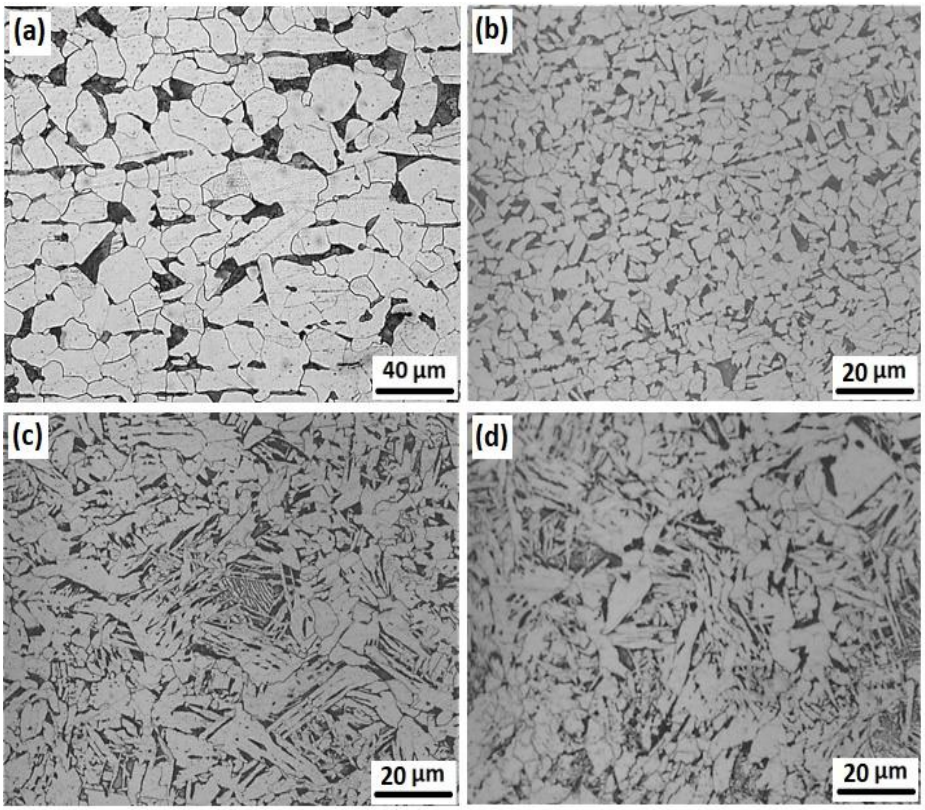

Figure 1. Microstructure of the base, the sample welded under atmospheric conditions and the samples welded in water.

3.2. Mechanical Properties

The hardness values obtained from the weld zone of the base, the sample welded under atmospheric conditions and the samples welded underwater at different depths are given in Table 2. As can be seen from the table, the hardness values increased as a result of the relatively thinned grain size after welding under atmospheric conditions. When we look at the underwater welds, it has been determined that the hardness values reach the highest levels due to both the increase in grain refinement and the effect of possible hard and brittle phases formed during underwater welding. On the other hand, it has been determined that the hardness decreases as the depth at which the weld is made underwater increases. The reason for this situation is that as the depth of the weld increases, the amount of carbon burned during welding increases (İmdat, Kaya & Kahraman, 2018). This situation, which caused a decrease in the amount of carbon in the structure, caused this decrease in hardness values.

Table 2. The hardness values obtained from the weld zone of the base, the sample welded under atmospheric conditions and the samples welded underwater at different depths.

Condition	Hardness (Hv)
Base	135±4
Welding in Atmospheric Conditions	175±6
1 Meter Deep Underwater Welding	220±7
5 Meter Deep Underwater Welding	205±5

The strength and elongation values obtained from the weld zone of the base, the sample welded under atmospheric conditions and the samples welded underwater at different depths are shown in Figure 2 and Table 3. As can be seen, after the grain size decreased as a result of welding performed under atmospheric conditions, the strength values increased while the elongation values decreased. The reason for this situation is the decrease in grain size after welding. As it is known, the decrease in grain size causes an increase in the strength of steels (Hajian et al., 2015). Increasing grain boundary ratio after grain refinement increases the strength values by preventing the

movement of dislocations during plastic deformation. The increase in strength values after welding in atmospheric conditions can be explained in this way. On the other hand, increasing grain boundary amount per unit area after decreasing grain size caused a decrease in the elongation values by preventing the movement of dislocations, and the elongation values decreased after welding performed under atmospheric conditions (Hajian et al., 2015). It has been determined that there is a decrease in the strength and elongation values as a result of the amount of burning carbon in the welds made in water. As expected as a result of decreasing carbon amount after increasing weld depth, it can be seen that there is a higher amount of decrease in strength values.

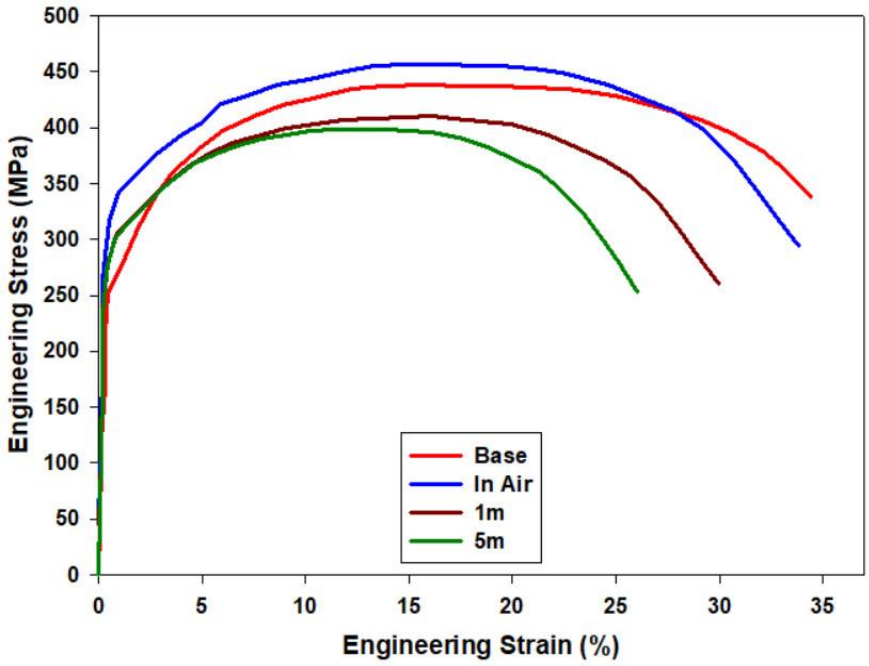

Figure 2. Strength and elongation curves obtained from the weld zone of the base, the sample welded under atmospheric conditions and the samples welded underwater at different depths.

Table 3. Strength and elongation values obtained from the weld zone of the base, the sample welded under atmospheric conditions and the samples welded underwater at different depths.

Condition	Tensile Strength (MPa)	Elongation (%)
Base	441±7	37
Welding in Atmospheric Conditions	457±9	35
1 Meter Deep Underwater Welding	411±8	31
5 Meter Deep Underwater Welding	397±10	26

Bending forces and deflection values at maximum force obtained from the weld zone of the base, the sample welded under atmospheric conditions and the samples welded underwater at different depths are given in Table 4. It is seen that the increased strength values after welding in atmospheric conditions are also reflected in the bending force. Similarly, it was determined that the deflection values at maximum force decreased as a result of decreasing elongation values. When we look at the welds made underwater, it has been determined that the decreasing strength values as a result of the decreasing carbon ratio cause a decrease in the bending force. Deflection values at maximum force also decreased as a result of welding in water.

Table 4. Bending forces and deflection values at maximum force obtained from the weld zone of the base, the sample welded under atmospheric conditions and the samples welded underwater at different depths.

Condition	Bending Force (N)	Deflection (mm)
Base	390±6	6,52±0,2
Welding in Atmospheric Conditions	441±8	6,04±0,3
1 Meter Deep Underwater Welding	404±11	5,91±0,2
5 Meter Deep Underwater Welding	375±14	5,83±0,1

The impact toughness values obtained from the weld zone of the base, the sample welded under atmospheric conditions and the samples welded underwater at different depths are given in Table 5. As can be seen from the table, it can be seen that the impact toughness value increased compared to the main structure as a result of welding performed under atmospheric conditions. Although there is a slight decrease in elongation values after welding in atmospheric conditions, it is thought that the relatively high increase in strength values causes an increase in impact toughness. On the other hand, since both strength and elongation values decreased after welds in water, the impact strength values decreased as expected compared to the main structure. It was determined that the lowest impact strength values were obtained under this condition, since both the strength and elongation values decreased with the increase in the depth of welding.

Table 5. Impact toughness values obtained from the weld zone of the base, the sample welded under atmospheric conditions and the samples welded underwater at different depths.

Condition	Impact Toughness (Joule)
Base	8,3±0,6
Welding in Atmospheric Conditions	8,7±0,7
1 Meter Deep Underwater Welding	7,4±0,4
5 Meter Deep Underwater Welding	6,2±0,5

4. CONCLUSION

Within the scope of the study, low-medium carbon shipbuilding steel, which is used extensively in shipbuilding, was welded under atmospheric conditions and underwater at two different depths, and the microstructural and mechanical properties obtained in the welding region were examined comparatively. The general results obtained in the study are summarized below:

A) It has been determined that after welding in atmospheric conditions, the grains become slightly thinner compared to the main structure, and after welding in water, they are oriented in the direction of cooling.

B) It was determined that the hardness values of the weld zone reached the maximum level after welding in water. On the other hand, as the depth of the weld increases, the hardness values decrease as a result of the increase in the amount of burning carbon.

C) As a result of grain size decrease after welding in atmospheric conditions, it was determined that the strength values increased compared to the main structure. After welding in water, it was determined that the strength and elongation values decreased compared to the main structure.

D) It was determined that the bending force increased as a result of increasing strength values after welding in atmospheric conditions. After welding in water, it was determined that both the bending force and the deflection values at the maximum bending force decreased.

E) While the impact toughness value of the main structure increased after welding in atmospheric conditions, it was determined that the impact toughness values decreased as a result of both decreasing strength and elongation values after welding in water.

ACKNOWLEDGEMENT

The authors would like to thank to Professor Gencaga Purcek (Mechanical Engineering Department, Karadeniz Technical University) for sharing his laboratory facilities.

REFERENCES

Bhadeshia, H.K.D.H. & Svensson, L. E. (1993). "Modelling the evolution of microstructure in steel weld metal". *Mathematical Modelling of Weld Phenomena, 1*, 109-182.

Boumerzoug, Z., Derfouf, C. & Baudin, T. (2010). "Effect of Welding on Microstructure and Mechanical Properties of an Industrial Low Carbon Steel". *Engineering, 2*(7), 502-506. doi:10.4236/eng.2010.27066.

David, S. A, Babu, S. S. & Vitek, J. M. (2003). "Welding: Solidification and Microstructure". *Jom, 55*(6), 14-20. doi:10.1007/s11837-003-0134-7.

Eroğlu, M., Aksoy, M. & Orhan, N. (1999). "Effect of coarse initial grain size on microstructure and mechanical properties of weld metal and HAZ of a low carbon steel". *Materials Science & Engineering: A, 269*(1-2), 59-66. doi:10.1016/S0921-5093(99)00137-9.

Gharibshahiyan, E., Raouf, A. H., Parvin, N. & Rahimian, M. (2011). "The effect of microstructure on hardness and toughness of low carbon welded steel using inert gas welding". *Materials & Design, 32*(4), 2042-2048. doi: /10.1016/j.matdes.2010.11.056.

Gould, J. E., Khurana, S. P. & Li, T. (2006). "Predictions of microstructures when welding automotive advanced high-strength steels". *Welding Journal, 85*(5), 111-116.

Grong, O. & Matlock, D. K. (1986). "Microstructural development in mild and low-alloy steel weld metals". *International Metals Reviews, 31*(1), 27-48. doi:10.1179/imtr.1986.31.1.27.

Hajian, M., Abdollah-zadeh, A., Rezaei-Nejad, S. S., Assadi, H., Hadavi, S. M.M., Chung, K. & Shokouhimehr, M. (2015). "Microstructure and mechanical properties of friction stir processed AISI 316L stainless steel". *Materials & Design, 67* (Supplement C), 82-94. doi:10.1016/j.matdes.2014.10.082.

Houldcroft, P. T. (1990). *Submerged-arc welding*. Woodhead Publishing.

İmdat, K., Kaya, Y. & Kahraman, N. (2018). "Grade A Gemi Sacının Örtülü Elektrod Ark Kaynak Yöntemi ile Sualtı ve Atmosferik Şartlarda Birleştirilebilirliğinin Araştırılması". *Politeknik Dergisi, 21*(3), 543-552.

Kanjilal, P., Pal, T.K., & Majumdar, S.K. (2006). "Combined effect of flux and welding parameters on chemical composition and mechanical properties of submerged arc weld metal". *Journal of Materials Processing Technology, 171*(2), 223-231.

Kanjilal, P., Pal, T.K., & Majumdar, S.K. (2007). "Prediction of element transfer in submerged arc welding". *Magnesium, 10*, 40.

Lars-Erik, S. (2017). *Control of microstructures and properties in steel arc welds*: CRC press.

Lee, C.S., Chandel, R.S., & Seow, H.P. (2000). "Effect of welding parameters on the size of heat affected zone of submerged arc welding". *Materials and Manufacturing Processes, 15*(5), 649-666.

Liu, F., Tan, C., Gong, X., Wu, L., Chen, B., Song, X., & Feng, J. (2020). "A comparative study on microstructure and mechanical properties of HG785D steel joint produced by hybrid laser-MAG welding and laser welding". *Optics & Laser Technology, 128*, 106247.

Magnabosco, I., Ferro, P., Bonollo, F., & Arnberg, L. (2006). "An investigation of fusion zone microstructures in electron beam welding of copper–stainless steel". *Materials Science and Engineering: A, 424*(1-2), 163-173.

McPherson, N.A., Chi, K., & Baker, T.N. (2003). "Submerged arc welding of stainless steel and the challenge from the laser welding process". *Journal of Materials Processing Technology, 134*(2), 174-179.

Murugan, N., & Gunaraj, V. (2005). "Prediction and control of weld bead geometry and shape relationships in submerged arc welding of pipes". *Journal of Materials Processing Technology, 168*(3), 478-487.

Pandey, N.D, Bharti, A., & Gupta, S.R. (1994). "Effect of submerged arc welding parameters and fluxes on element transfer behaviour and weld-metal chemistry". *Journal of Materials Processing Technology, 40*(1-2), 195-211.

Zhang, Z., Jing, H., Xu, L., Han, Y., & Zhao, L. (2016). "Investigation on microstructure evolution and properties of duplex stainless steel joint multi-pass welded by using different methods". *Materials & Design, 109*, 670-685.

Journal of Naval Sciences and Engineering
2021, Vol. 17, No. 2, pp. 413-428
Electric-Electronic Engineering/Elektrik-Elektronik Mühendisliği

RESEARCH ARTICLE

**An ethical committee approval and/or legal/special permission has not been required within the scope of this study.*

AN ANALYTICAL SOLUTION FOR THE ELECTROMAGNETIC OSCILLATIONS CAUSED BY A RECTANGULAR PULSE IN A CAVITY WITH LOSSY WALLS*

Fatih ERDEN[1]
Ayşe YAVUZ ERKAN[2]
Ahmet Arda ÇOŞAN[3]
Serkan AKSOY[4]

[1]*National Defence University, Turkish Naval Academy, Department of Electrical-Electronics Engineering, Istanbul, Turkey,*
ferden@dho.edu.tr; ORCID: 0000-0003-0885-9031

[2]*National Defence University, Turkish Naval Academy, Department of Electrical-Electronics Engineering, Istanbul, Turkey*
ayerkan@dho.edu.tr; ORCID: 0000-0002-6957-9394

[3]*National Defence University, Turkish Naval Academy, Department of Electrical-Electronics Engineering, Istanbul, Turkey*
acosan@dho.edu.tr; ORCID: 0000-0001-6054-725X

[4] *Gebze Technical University, Department of Electronics Engineering, Kocaeli, Turkey*
saksoy@gtu.edu.tr; ORCID: 0000-0001-9709-2279

Received: 17.09.2021 **Accepted: 03.11.2021**

ABSTRACT

The purpose of this study is analytical studying Initial-Boundary-Value Problem for the novel format of Maxwell's equations in SI units. A modified version of the Evolutionary Approach to Electromagnetics (EAE) used herein. The problem is considered for the causal electromagnetic oscillations excited by a given external rectangular pulse signal, $\mathcal{J}(\mathbf{r},t)$*, in a hollow cavity with lossy metallic walls. The cavity volume* V *is finite and closed by a singly connected surface* S *with none of its inner angles exceeds* π*. Physically, cavity walls are lossy (completely or partially). Graphical results are exhibited demonstrating that the electromagnetic oscillations inside the cavity with metallic surface satisfy the causality principle.*

Keywords: *Maxwell's Equations, Time-domain Electrodynamics, Cavity, Evolutionary Equations, Matrix Exponentials.*

An Analytical Solution for the Electromagnetic Oscillations Caused by a Rectangular Pulse in a Cavity with Lossy Walls

KAYIPLI YÜZEYLERE SAHİP BİR KAVİTEDEKİ DİKDÖRTGEN DARBE KAYNAKLI ELEKTROMANYETİK OSİLASYONLAR İÇİN BİR ANALİTİK ÇÖZÜM

ÖZ

Bu çalışmanın amacı, SI birim sisteminde yeniden yazılmış Maxwell denklemlerine ilişkin başlangıç-sınır-değer problemine analitik bir çözüm sunmaktır. Çalışmada Elektromanyetik Teoriye Evrimsel Yaklaşım'ın modifiye edilmiş bir versiyonu kullanılmıştır. Problem, kayıplı metalik yüzeylere sahip boş bir kaviteye verilen dikdörtgen $\mathcal{J}(\mathbf{r}, t)$ darbe sinyalleri, tarafından uyarılan nedensel elektromanyetik osilasyonlar için düşünülmüştür. Kavite hacmi, V, sonludur ve S yüzeyinin iç açılarından hiçbirinin π'den büyük olmadığı pürüzsüz bir S yüzeyiyle kapatılmıştır. Fiziksel olarak yüzey (tamamen ya da kısmen) kayıplıdır. Kayıplı yüzeylere sahip kavite içerisindeki elektromanyetik osilasyonların nedensellik prensibini sağladığını gösteren grafiksel sonuçlar sergilenmiştir.

Anahtar Kelimeler: *Maxwell Denklemleri, Zaman Uzayı Elektrodinamiği, Kavite, Evrimsel Denklemler, Matris Eksponansiyeller.*

1. INTRODUCTION

The goal of the present study is twofold. The first one is to derive an analytical solution for the fields in a hollow cavity with lossy metallic surfaces by making use of the matrix exponential method. The foundations of the approach used in this study, Evolutionary Approach to Electromagnetics (EAE), was proposed at the beginning of 1990s for exact explicit solution of the fields in cavities and waveguides (Tretyakov, 1993). A *new* SI *format* of Maxwell's equations (MEs) presented and acknowledged recently (Tretyakov, 2017; Tretyakov, 2018) where the new electric and magnetic fields have their common physical dimension. The convenience of the *new format*, where the fields have their common dimension, to upgrade the Evolutionary Approach for solving some practical problems was exhibited in the previous studies (Erden, Tretyakov, & Çoşan, 2018; Erden & Tretyakov, 2017; Tretyakov, 2018; Tretyakov, Butrym, & Erden, 2021).

The second goal is to present graphically the evolution of the electromagnetic fields, which can be stimulated in such cavities by a rectangular pulse function. Every rectangular pulse function has a beginning and end, as the digital signals and Walsh functions. This fact requires the involvement of the causality principle at the formulation of our problem (Erden, 2017; Tretyakov, 1993). Since the Walsh functions consist of trains of rectangular pulses, this study can be extended to investigate the evolution of the electromagnetic fields in a cavity excited by digital signals which have been used broadly in telecommunication technology for the last few decades (Aksoy & Tretyakov, 2003; Aksoy & Tretyakov, 2004).

The article is structured as follows. In Sec. II, the formulation is given where the *new format* of MEs and boundary conditions are presented for the problem. In Sec. III, the modal basis, and the modal field expansions available for the time-domain study are presented. In Sec. IV, an ordinary differential equation system for the time-dependent field amplitudes, i.e., the evolutionary equations are derived. In Sec. V and VI, the evolutionary equations are solved by making use of the method of matrix exponential. An analytical method based on Lagrange interpolation is applied therein (Erden & Tretyakov, 2008). In Sec. VII and VIII, we examine our conclusions.

2. FORMULATION OF THE PROBLEM

The central point in rearranging the Maxwell's equations to a new format in SI units (Tretyakov et al., 2021; Tretyakov & Erden, 2021) is based on the *novel definition* of the free-space constants as

$$\varepsilon_0^V = \sqrt{\frac{1N}{\varepsilon_0}} \left\lfloor V = \frac{Nm}{As} \right\rfloor, \quad \mu_0^A = \sqrt{\frac{1N}{\mu_0}} \lfloor A \rfloor \tag{1}$$

where N is a force of one *newton*. Derivations of ε_0^V and μ_0^A are given in Appendix A of the recent paper (Tretyakov & Erden, 2021). One can verify that ε_0^V has the dimension of *volt*, $\lfloor V \rfloor$, with its numerical value of 3.361×10^5, and μ_0^A has the dimension of *ampere*, $\lfloor A \rfloor$, with its numerical value of 8.921×10^2. ε_0^V and μ_0^A can be used as the *scaling coefficients* for the standard electric, $\mathcal{E}$, and magnetic, $\mathcal{H}$, fields to divide the physical dimensions of $\lfloor V/m \rfloor$ and $\lfloor A/m \rfloor$ as

$$\left.\begin{aligned} \underbrace{\boldsymbol{\mathcal{E}}(\mathbf{r},t)}_{\lfloor V/m \rfloor} &= \underbrace{\varepsilon_0^V}_{\lfloor V \rfloor} \underbrace{\mathbb{E}(\mathbf{r},t)}_{\lfloor 1/m \rfloor} = \underbrace{3.361\times10^5}_{\lfloor V \rfloor} \times \underbrace{\mathbb{E}(\mathbf{r},t)}_{\lfloor 1/m \rfloor} \\ \underbrace{\boldsymbol{\mathcal{H}}(\mathbf{r},t)}_{\lfloor A/m \rfloor} &= \underbrace{\mu_0^A}_{\lfloor A \rfloor} \underbrace{\mathbb{H}(\mathbf{r},t)}_{\lfloor 1/m \rfloor} = \underbrace{8.921\times10^2}_{\lfloor A \rfloor} \times \underbrace{\mathbb{H}(\mathbf{r},t)}_{\lfloor 1/m \rfloor} \\ \underbrace{\boldsymbol{\mathcal{J}}(\mathbf{r},t)}_{\lfloor A/m^2 \rfloor} &= \underbrace{\mu_0^A}_{\lfloor A \rfloor} \underbrace{\mathbb{J}(\mathbf{r},t)}_{\lfloor 1/m \rfloor} = \underbrace{8.921\times10^2}_{\lfloor A \rfloor} \times \underbrace{\mathbb{J}(\mathbf{r},t)}_{\lfloor 1/m \rfloor}. \end{aligned}\right\} \tag{2}$$

The SI dimensions of volt $\lfloor V \rfloor$ and of ampere $\lfloor A \rfloor$ are assigned to the factors ε_0^V and μ_0^A, in our new definition. Meanwhile, novel field vectors, $\mathbb{E}$ and $\mathbb{H}$, have the inverse meter $\lfloor 1/m \rfloor$ physical dimension. So, the *new* SI *format* of the Maxwell's equations is

$$\nabla \times \mathbb{H}(\mathbf{r},t) = \mathbb{J}(\mathbf{r},t) + \frac{1}{c}\frac{\partial}{\partial t}\mathbb{E}(\mathbf{r},t)$$
$$\nabla \times \mathbb{E}(\mathbf{r},t) = -\frac{1}{c}\frac{\partial}{\partial t}\mathbb{H}(\mathbf{r},t) \quad (3)$$

where $\mathbb{J}$ is a current density supplying a given signal to the cavity. Consider the case of S composed of the parts as

$$S = S_1 + S_2. \quad (4)$$

In what follows, notation $\mathbf{n}$ and $\mathbf{l}$ are used for the unit vectors outward normal and tangential to the surface S, respectively. The part S_1 is supposed as a lossy surface, over which Leontovich boundary condition (see (Toptygin, 2015)) holds as

$$\mathbf{n} \times \mathbb{E}(\mathbf{r},t) = \alpha\, \mathbf{l} \cdot \mathbb{H}(\mathbf{r},t), \quad \mathbf{r} \in S_1 \quad (5)$$

where $\alpha = \varsigma\rho$ is a small parameter, and ς is the *impedance* of the lossy metallic surface. The constant $\rho = \mu_0^A / \varepsilon_0^V = \sqrt{\varepsilon_0 / \mu_0}$ is numerically very small, i.e., 2.654×10^{-3}. The ρ appears in α when Maxwell's equations are in the new format. But ρ is *absent* (and $\alpha \equiv \varsigma$ becomes large) if Maxwell's equations are standard. The Leontovich *approximate* boundary condition (5), relates the *tangential* components of the electric field, $\mathbf{n} \times \mathbb{E}(\mathbf{r},t)$, to magnetic field, $\mathbf{l} \cdot \mathbb{H}(\mathbf{r},t)$, over the surface of well-conducting bodies. The Leontovich impedance boundary condition is *accurate* for most metals while the impedance ς is *large*, but finite.

The part S_2 is perfect electric conducting where the boundary conditions are

$$\mathbf{n} \times \mathbb{E}(\mathbf{r},t) = 0, \quad \mathbf{n} \cdot \mathbb{H}(\mathbf{r},t) = 0, \quad \mathbf{r} \in S_2. \quad (6)$$

The initial conditions for the fields are

$$\mathbb{E}(\mathbf{r},t)\big|_{t=0} = 0, \quad \mathbb{H}(\mathbf{r},t)\big|_{t=0} = 0, \quad \mathbf{r} \in V. \quad (7)$$

3. MODAL BASIS AND FIELD DECOMPOSITONS

The space of solutions is chosen as Hilbert space L_2 where the inner product of the vectors are defined as

$$\langle \mathbf{A}, \mathbf{B} \rangle = \frac{1}{V} \int_V \mathbf{A} \cdot \mathbf{B}^* dV. \tag{8}$$

The modal basis has been derived *without* postulating fields as time-harmonic in L_2 and presented herein in the form of the boundary-eigenvalue problems as

$$\left.\begin{aligned} \nabla \times \mathbf{H}_n &= -ik_n \mathbf{E}_n, \quad \nabla \cdot \mathbf{H}_n = 0, \quad \mathbf{n} \cdot \mathbf{H}_n\big|_S = 0 \\ \nabla \times \mathbf{E}_n &= ik_n \mathbf{H}_n, \quad \nabla \cdot \mathbf{E}_n = 0, \quad \mathbf{n} \times \mathbf{E}_n\big|_S = 0 \end{aligned}\right\} \tag{9}$$

where the eigenvalues, k_n, $(n = 1, 2, ...)$ have $\lfloor 1/m \rfloor$ physical dimension. The elements of basis satisfy the orthonormal conditions as

$$\left.\begin{aligned} \langle \mathbf{E}_{n'}, \mathbf{E}_n \rangle &= \frac{1}{V} \int_V \mathbf{E}_{n'} \cdot \mathbf{E}_n^* dV = \delta_{n'n} \\ \langle \mathbf{H}_{n'}, \mathbf{H}_n \rangle &= \frac{1}{V} \int_V \mathbf{H}_{n'} \cdot \mathbf{H}_n^* dV = \delta_{n'n} \end{aligned}\right\} \tag{10}$$

where $\delta_{n'n}$ is Kronecker delta. The modal field decompositions for $\mathbb{E}$ and $\mathbb{H}$ fields are presentable as

$$\mathbb{E}(\mathbf{r}, t) = \sum_{n'=1}^{\infty} e_{n'}(t) \mathbf{E}_{n'}(\mathbf{r}), \quad \mathbb{H}(\mathbf{r}, t) = \sum_{n'=1}^{\infty} h_{n'}(t) \mathbf{H}_{n'}(\mathbf{r}) \tag{11}$$

where the modal basis vectors $\mathbf{E}_{n'}$ and $\mathbf{H}_{n'}$ have the same physical dimension of inverse meter as the new fields $\mathbb{E}$ and $\mathbb{H}$, and the time-dependent modal amplitudes are dimension-free.

The current density, $\mathbb{J}$, in equation (3) is responsible for excitation of forced oscillations in the cavity. $\mathbb{J}$ is decomposable as $\mathbb{J} = j(t)\mathbf{I}(\mathbf{r})$ where

$j(t)$ is a given signal. The vector $\mathbf{I}$ is specified by configuration and position within V of an item supplying $j(t)$ to the cavity. Anyway, $\mathbf{I}$ is presentable as

$$\mathbf{I}(\mathbf{r}) = \sum_{n'=1}^{\infty} g_{n'} k_{n'} \mathbf{E}_{n'}(\mathbf{r}) \tag{12}$$

where $g_{n'}$ are constant dimension-free coefficients.

4. EVOLUTIONARY EQUATIONS

Projecting Maxwell's equations (3) onto the modal basis results in

$$\begin{cases} \dfrac{d}{d\tau} e_n(\tau) + i h_n(\tau) = -j(\tau) g_n \\ \dfrac{d}{d\tau} h_n(\tau) + 2\beta h_n(\tau) + i e_n(\tau) = -\alpha I_n'(\tau) \\ e_n(\tau)\big|_{\tau=0} = 0, \quad h_n(\tau)\big|_{\tau=0} = 0 \end{cases} \tag{13}$$

where $n = 1, 2, \ldots$. To make formulas compact and observable in what follows, introduce a set of notations:

$$\left.\begin{aligned} \tau = k_n c t, \quad \beta_n = \alpha \gamma_n, \ \gamma_n = \frac{1}{S}\int_{S_1} \mathbf{H}_n \mathbf{H}_n^* dS \\ I_n'(\tau) = \sum_{n' \neq n}^{\infty} h_{n'}'(\tau)\left(k_{n'} / k_n\right)\gamma_{n'n} \\ \gamma_{n'n} = \frac{1}{S}\int_{S_1} \mathbf{H}_{n'} \mathbf{H}_n^* dS. \end{aligned}\right\} \tag{14}$$

5. METHOD OF SUCCESSIVE SUBSTITUTION

To apply the method of successive substitution to problem (13), the modal amplitudes should be presented as consisting of two parts. Each part is sought for. Thus,

$$e_n(\tau) = e_n'(\tau) + e_n''(\tau), \quad h_n(\tau) = h_n'(\tau) + h_n''(\tau). \tag{15}$$

The problem for e_n' and h_n' is selected from (13) as

$$\begin{cases} \dfrac{d}{d\tau} e_n'(\tau) + i h_n'(\tau) = -j(\tau) g_n \\ \dfrac{d}{d\tau} h_n'(\tau) + 2\beta h_n'(\tau) + i e_n'(\tau) = 0 \\ e_n'(\tau)\big|_{\tau=0} = 0, \quad h_n'(\tau)\big|_{\tau=0} = 0. \end{cases} \tag{16}$$

The remainder of original problem (13) yields

$$\begin{cases} \dfrac{d}{d\tau} e_n''(\tau) + i h_n''(\tau) = 0 \\ \dfrac{d}{d\tau} h_n''(\tau) + 2\beta h_n''(\tau) + i e_n''(\tau) = -\alpha I_n'(\tau) \end{cases} \tag{17}$$

Cauchy problem (16) is solved analytically in the next Section. A quick look at problem (17) suggests that the parts e_n'' and h_n'' are of order of the small parameter α.

6. ANALYTICAL SOLUTION FOR FIELD EXPANSION

Introducing matrix Q_n and two vectors, Y_n' and F_n, as

$$\begin{aligned} Q_n &= \begin{pmatrix} 0 & i \\ i & 2\beta_n \end{pmatrix} \\ Y_n'(\tau) &= \begin{pmatrix} e_n' \\ h_n' \end{pmatrix}, \quad F_n(\tau) = -\begin{pmatrix} j(\tau) g_n \\ 0 \end{pmatrix} \end{aligned} \tag{18}$$

rearranges problem (16) into simple “vector” equation as

$$\frac{d}{d\tau} Y_n'(\tau) + Q_n Y_n'(\tau) = F_n(\tau). \tag{19}$$

The method of matrix exponential (Tretyakov et al., 2021) yields solution as

$$Y_n'(\tau) = e^{-\tau Q_n} \int_0^\tau e^{\tau' Q_n} F_n(\tau')\, d\tau' \tag{20}$$

where Lagrange interpolation of $e^{-\tau Q_n}$, see (Tretyakov et al., 2021), results in

$$e^{-\tau Q_n} = e^{-\tau \beta_n} \begin{pmatrix} \dfrac{\cos(\tau\eta_n - \theta_n)}{\cos(\theta_n)} & i\dfrac{\sin(\tau\eta_n)}{\cos(\theta_n)} \\ i\dfrac{\sin(\tau\eta_n)}{\cos(\theta_n)} & \dfrac{\cos(\tau\eta_n + \theta_n)}{\cos(\theta_n)} \end{pmatrix} \tag{21}$$

$$\beta_n = \alpha\gamma_n, \quad \lambda_n = \sqrt{1-\beta_n^2}, \quad \theta_n = \cos^{-1}\lambda_n.$$

Notice that the matrix $e^{-\tau Q_n}$ turns into the *identity matrix* for time $\tau = 0$. Mathematicians call the matrices with this property as the *evolutionary matrices*. At the integrand in (20), the inverse matrix $(e^{-\tau Q_n})^{-1}$ stands. That one is defined as $e^{-\tau Q_n}$ with replacement τ by $-\tau'$ what yields

$$e^{\tau' Q_n} = e^{\tau' \beta_n} \begin{pmatrix} \dfrac{\cos(\tau'\eta_n + \theta_n)}{\cos(\theta_n)} & -i\dfrac{\sin(\tau'\eta_n)}{\cos(\theta_n)} \\ -i\dfrac{\sin(\tau'\eta_n)}{\cos(\theta_n)} & \dfrac{\cos(\tau'\eta_n - \theta_n)}{\cos(\theta_n)} \end{pmatrix}. \tag{22}$$

Calculation of the integrals in (20) results in

$$e^{-\tau\beta_n} \int_0^\tau e^{\tau' Q_n} F_n(\tau') = g_n \begin{pmatrix} -A_n \\ iB_n \end{pmatrix} \tag{23}$$

where $e^{-\tau\beta_n}$ is transferred from $e^{-\tau Q_n}$ (see (21)), and

$$\begin{aligned} A_n &= \int_0^\tau e^{-(\tau-\tau')\beta_n} j(\tau') \frac{\cos(\tau'\eta_n + Q_n)}{\cos(Q_n)} d\tau' \\ B_n &= \int_0^\tau e^{-(\tau-\tau')\beta_n} j(\tau') \frac{\sin(\tau'\eta_n)}{\cos(Q_n)} d\tau'. \end{aligned} \tag{24}$$

Multiplying the matrix $e^{-\tau Q_n}$ (from (21) without $e^{-\tau\beta_n}$) and vector (23) results in a vector as

$$\begin{pmatrix} e'_n \\ h'_n \end{pmatrix} = -g_n \begin{pmatrix} \left[A_n \dfrac{\cos(\tau\eta_n - \theta_n)}{\cos(\theta_n)} + B_n \dfrac{\sin(\tau\eta_n)}{\cos(\theta_n)} \right] \\ i\left[A_n \dfrac{\sin(\tau\eta_n)}{\cos(\theta_n)} + B_n \dfrac{\cos(\tau\eta_n + \theta_n)}{\cos(\theta_n)} \right] \end{pmatrix}. \tag{25}$$

Finally, observation of modal field expansions (11) and vector (25) results in the *analytical* solution as

$$\begin{aligned} \mathbb{E}(\mathbf{r},\tau) &= \sum\nolimits_{n'=1}^{\infty} e'_{n'}(\tau)\tilde{\mathbf{E}}_{n'}(\mathbf{r}) \\ \mathbb{H}(\mathbf{r},\tau) &= \sum\nolimits_{n'=1}^{\infty} h'_{n'}(\tau)\tilde{\mathbf{H}}_{n'}(\mathbf{r}) \end{aligned} \tag{26}$$

where $\tilde{\mathbf{E}}_{n'}(\mathbf{r})$, $\tilde{\mathbf{H}}_{n'}(\mathbf{r})$ are the *real-valued* elements of the basis. Modal field $\mathbf{E}_n$ can be obtained as a *real-valued* vector. Denote that as $\tilde{\mathbf{E}}_n(\mathbf{r})$. The modal field $\tilde{\mathbf{H}}_n$ is specified via $\tilde{\mathbf{E}}_n(\mathbf{r})$ by formula $\nabla\times\tilde{\mathbf{E}}_n = ik_n\mathbf{H}_n$ what yields $\mathbf{H}_n = (-i)\nabla\times\tilde{\mathbf{E}}_n / k_n = (-i)\tilde{\mathbf{H}}_n$ where $\tilde{\mathbf{H}}_n$ is real-valued, also. This $(-i)$ cancels later that i, which is present in h'_n in (25). $e'_{n'}$ and $h'_{n'}$ are the *real-valued* amplitudes as

$$\begin{aligned} e'_n(\tau) &= -g_n\left[A_n \frac{\cos(\tau\eta_n - \theta_n)}{\cos(\theta_n)} + B_n \frac{\sin(\tau\eta_n)}{\cos(\theta_n)} \right] \\ h'_n(\tau) &= -g_n\left[A_n \frac{\sin(\tau\eta_n)}{\cos(\theta_n)} + B_n \frac{\cos(\tau\eta_n + \theta_n)}{\cos(\theta_n)} \right]. \end{aligned} \tag{27}$$

The graphical results for the modal amplitudes of the electromagnetic oscillations, $e'_n(\tau)$ and $h'_n(\tau)$, caused by a rectangular pulse, $j(\tau')$, in a cavity with lossless surfaces, $\beta_n = 0$, and lossy surfaces, $\beta_n = 0.2$, are exhibited below in Figure 1 and Figure 2, respectively. The dimensionless time, τ; is specified as $\tau = tck_n$ where c is the light speed.

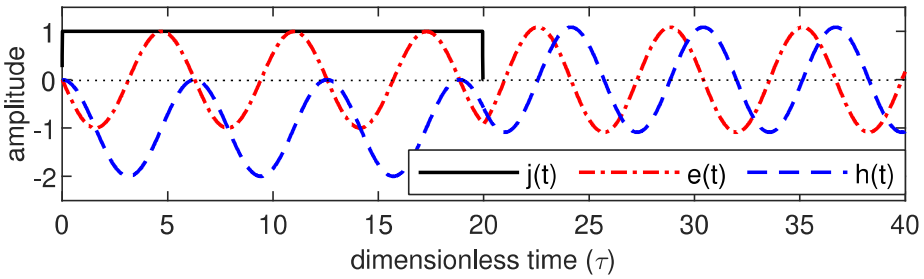

Figure 1. Modal amplitudes for the lossless case: $\beta_n = 0, \quad t \geq 0$.

In Figure 1, electric and magnetic fields' modal amplitudes, $e_n'(\tau)$ and $h_n'(\tau)$, excited by a rectangular pulse, $j_n(\tau)$, can be seen evolving sinusoidally. It can also be seen $\pi/2$ phase shift between electric field and magnetic fields.

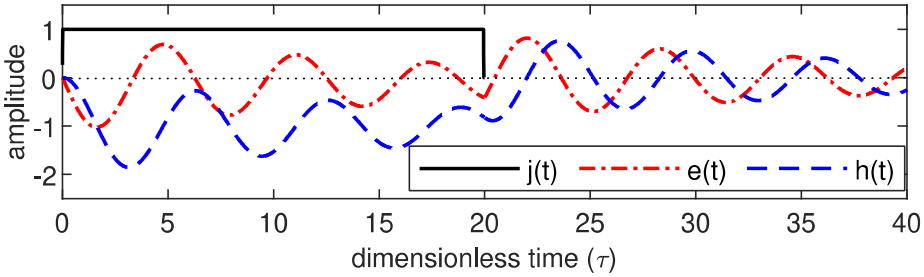

Figure 2. Modal amplitudes for the lossy case: $\beta_n = 0.2, \quad t \geq 0$.

In Figure 2, decaying in time sinusoidal oscillations can be seen due to lossy walls of the cavity. When studying digital signals, duration of this rectangular pulses will be very short.

7. CONCLUSION

The solution given in (26)-(27) satisfies the initial conditions at $\tau = 0$ automatically. The solution is *casual*. Physically, this solution exhibits how the amplitudes of the modes are *evolving* from their initial value (at $\tau = 0$) to the state of observation τ.

The solution is analytical and "pliable" with respect to variations of the given signal, $j(t)$, which participates in the formulas for A_n and B_n in (24).

There are three important cases in choice of the format of the cavity surface S: see (4). 1) If $S_1 = 0$, all the cavity surface S is perfectly electric conducting where boundary conditions (6) hold. 2) If $S_2 = 0$, all the cavity surface S is lossy, over which Leontovich boundary condition (5) holds. The third case, when $S_1 \neq 0$ and $S_2 \neq 0$, but $S_1 + S_2 = S$, is considered herein.

8. DISCUSSION

In the novel simple SI format of Maxwell's equations, and also in the novel format of Leontovich boundary condition, the new electric, $\mathbb{E}(\mathbf{r},t)$, and magnetic, $\mathbb{H}(\mathbf{r},t)$, field vectors; have *a common physical dimension*, as opposed to the standard electric, $\mathcal{E}(\mathbf{r},t)$, and magnetic field, $\mathcal{H}(\mathbf{r},t)$, which have the distinct ones. *Just this property of the new fields* permits one to denote the mechanical equivalents (mass and mechanical momentum) of the energetic field characteristics of the local fields in free space, cavities, and in waveguides. This result may be useful for study of the unsolved as yet problems (Erden et al., 2018) in *radio frequency resonant cavity thruster*, i.e., EmDrive.

ACKNOWLEDGMENT

This work is being sponsored by the TUBITAK under Grant 120E390. The authors are thankful to Prof. O. A. Tretyakov for his recommendations on the project.

REFERENCES

Aksoy, S., & Tretyakov, O. A. (2003). "Evolution equations for analytical study of digital signals in waveguides". *Journal of Electromagnetic Waves and Applications*, *17*(12), 1665–1682. doi:10.1163/156939303322760209

Aksoy, S., & Tretyakov, O. A. (2004). "The evolution equations in study of the cavity oscillations excited by a digital signal". *IEEE Transactions on Antennas and Propagation*, *52*(1), 263–270. doi:10.1109/TAP.2003.822399

Erden, F. (2017). "Evolutionary approach to solve a novel time-domain cavity problem". *IEEE Transactions on Antennas and Propagation*, *65*(11). doi:10.1109/TAP.2017.2752240

Erden, F., & Tretyakov, O. A. (2008). "Excitation by a transient signal of the real-valued electromagnetic fields in a cavity". *Physical Review E - Statistical, Nonlinear, and Soft Matter Physics*, *77*(5), 1–10. doi:10.1103/PhysRevE.77.056605

Erden, F., & Tretyakov, O. A. (2017). "Mechanical properties of the waveguide modal fields in the time domain". *Progress In Electromagnetics Research Symposium (PIERS) 2017*. doi: 10.13140/RG.2.2.20636.18569

Erden, F., & Tretyakov, O. A. (2018). "Electromagnetic inertia of the waveguide modes". *2nd URSI Atlantic Radio Science Meeting (AT-RASC 2018)*, *2*(1). doi:10.13140/RG.2.2.30508.31367

Erden, F., Tretyakov, O. A., & Çoşan, A. A. (2018). "Inertial properties of the TE waveguide fields". *Progress In Electromagnetics Research M*, *68*. doi:10.2528/PIERM18020609

Toptygin, I. N. (2015). *Electromagnetic Phenomena in Matter: Statistical and Quantum Approaches*. doi:10.1002/9783527693474

Tretyakov, O. A. (1993). Essentials of nonstationary and nonlinear electromagnetic field theory. In M. Hashimoto, M. Idemen, & O. A.

Tretyakov, *Analytical and Numerical Methods in Electromagnetic Wave Theory*. Science House Co. Ltd.

Tretyakov, O. A. (2017). "Factorizing Physical Dimensions of the Quantities Ingressed in Maxwell ' s Equations in SI Units Factorizing Physical Dimensions of the Quantities Ingressed in Maxwell ' s Equations in SI Units". *Progress In Electromagnetics Research Symposium (PIERS) 2017*. doi:10.13140/RG.2.2.30148.73604

Tretyakov, O. A. (2018). "Innovating SI Units in Maxwell's Equations. Evolutionary Approach to Electrodynamics as an Alternative to the Time-Harmonic Field Concept". *2018 2nd URSI Atlantic Radio Science Meeting, AT-RASC 2018*. doi:10.23919/URSI-AT-RASC.2018.8471496

Tretyakov, O. A., Butrym, O., & Erden, F. (2021). Innovative tools for SI units in solving various problems of electrodynamics. In K. Kobayashi, & P. D. Smith, *Advances in Mathematical Methods for Electromagnetics* (pp. 673–707). Institution of Engineering and Technology. doi:10.1049/sbew528e_ch27

Tretyakov, O. A., & Erden, F. (2021). "A Novel Simple Format of Maxwell's Equations in SI Units". *IEEE Access*, *9*. doi:10.1109/access.2021.3089673

JOURNAL OF NAVAL SCIENCES AND ENGINEERING (JNSE)
PUBLISHING RULES

Submission of Papers: Manuscripts which are submitted to the journal should not be published elsewhere or sent to be published. Authors are (preferably) requested to submit an electronic copy of their original works to the given "System Address" or one hard copy to the address and a soft-copy to the "E-mail Address" which have been given below. It is necessary for the authors to submit their manuscripts together with the "Copyright Release Form". "Copyright Release Form" can be downloaded from the "Copyright Page" of JNSE's Web Page. Authors are requested to obtain the relevant documents for their studies that require "Ethics Committee Approval and/or Legal/Special Permission" and submit these approval documents to the system together with their study.

System Address:
https://dergipark.org.tr/tr/pub/jnse

Address:
Doç.Dr. Ertan YAKICI
Milli Savunma Üniversitesi
Barbaros Deniz Bilimleri ve Mühendisliği Enstitüsü
Deniz Harp Okulu Yerleşkesi
34942 Tuzla/İstanbul/Türkiye

E-mail: *jnse@dho.edu.tr*

Types of Contributions: The journal publishes original papers, review articles, technical notes, book reviews, letters to the editor, extended reports of conferences and meetings.

Manuscript Evaluation Process: The Peer Review Step:

- The content and layout format of manuscript are examined and the originality of study is checked by iThenticate Software Programme.
- The language and correlation of the English abstract with Turkish abstract are checked.
- Manuscript which has a similarity index above 40% is rejected. The author is informed about the manuscript which has a similarity index between 20% and 40% (must not contain more than 4% from a single source), which is not appropriate for the writing rules of JNSE or needs correction in English and Turkish abstracts and the author is requested to revise the manuscript within "two weeks". Otherwise, the article is considered as a retracted manuscript.

Our journal uses **double-blind** review, which means that both the reviewer and author identities are concealed from the reviewers, and vice versa, throughout the review process. So, the uploaded manuscript does not contain the name, address and affiliation of author(s). The manuscript evaluation steps are as follows:

- Editor is assigned by the Editor-in-Chief.
- The relevant reviewers are assigned by the Editors.
- As a result of the reviewer's evaluation, the manuscript may be rejected, accepted or a correction for the manuscript may be requested.
- If the negative feedback is given by major number of the reviewers the process is terminated and the article is rejected.
- If major/minor revisions are required for the manuscript, the author has to do this revision according to the reviewers' comments in "three weeks".
- If the revision is accepted by the reviewers, the article is accepted.

The Workflow Diagram for the evaluation process can be accessed from the web page of the journal.

The articles submitted to JNSE to be published are free of article submission, processing and publication charges.

The accepted articles are published **free-of-charge** as online from the journal website and printed.

DENİZ BİLİMLERİ VE MÜHENDİSLİĞİ DERGİSİ (DBMD)
YAYIN KURALLARI

Yazıların Gönderilmesi: Dergiye gönderilen makaleler başka bir yerde yayımlanmamış ya da yayımlanmak üzere gönderilmemiş olmalıdır. Yayımlanması istenilen yazılar (tercihen) aşağıda verilen "Sistem Adresi"nden yüklenmeli veya aşağıdaki adrese bir kopya kâğıda basılı olarak ve aynı zamanda "E-mail Adresi"ne dijital olarak gönderilmelidir. Dergimize makale gönderen yazarların makaleleriyle birlikte "Yayın Hakkı Devir Formu"nu da göndermeleri gerekmektedir. "Yayın Hakkı Devir Formu"na DBMD Web Sayfasındaki "Telif Hakkı" sayfasından erişilebilmektedir. Yazarların "Etik Kurul İzni ve/veya Yasal/Özel İzin" gerektiren çalışmaları için ilgili izin belgelerini temin etmesi ve bu izin belgelerini çalışmalarıyla birlikte sisteme yüklemeleri gerekmektedir.

Sistem Adresi:
https://dergipark.org.tr/tr/pub/jnse

Adres:
Doç.Dr. Ertan YAKICI
Barbaros Deniz Bilimleri ve Mühendisliği Enstitüsü
Deniz Harp Okulu Yerleşkesi
34942 Tuzla/ İstanbul/Türkiye

E-mail: *jnse@dho.edu.tr*

Yazı Türleri: Dergide; orijinal yazılar, derlemeler, teknik notlar, kitap incelemeleri, editöre mektuplar ile konferans ve toplantıların genişletilmiş raporları yayımlanır.

Yazıların Değerlendirilme Süreci: Makalenin Ön Kontrol Süreci:

- Makalenin içeriği ve yazım formatı incelenir ve iThenticate Programı ile benzerlik taraması yapılır.
- Makalenin İngilizce özetinin, Türkçe öz ile uygunluğu ve yazım dili kontrol edilir.
- Benzerlik oranı %40'ın üzerinde olan makale reddedilir. Benzerlik oranı %20 ile %40 arasında olan (tek bir kaynakla benzerlik %5'ten fazla olmamalıdır), yazım formatına uymayan ya da İngilizce ve Türkçe özetinde düzeltme gereken makale yazara bildirilir ve "iki hafta" içerisinde makalenin düzeltilmesi istenir. Aksi takdirde makale geri çekilmiş kabul edilir.

Dergimiz, makale değerlendirme sürecinde **çift-kör** hakemlik sistemini kullanmaktadır. Buna göre değerlendirme sürecinde hakem ve yazarlar birbirlerinin bilgilerini görememektedir. Bu nedenle, yüklenen ön yükleme formatında yazar(lar)ın isim, adres ve bağlı olduğu kuruluş(lar) yer almamaktadır. Makale değerlendirme sürecindeki adımlar ise aşağıdaki gibidir;

- Baş editör tarafından makaleye Editör atanır.
- Editörler makale için hakemleri atar.
- Hakem değerlendirmesi sonucunda makale reddedilebilir, kabul edilebilir veya makalenin düzeltilmesi istenebilir.
- Hakem görüşlerinin çoğunluğu doğrultusunda makale reddedilmiş ise süreç sonlandırılır ve makale reddedilir.
- Makale için majör / minör düzeltme istenirse hakem görüşleri doğrultusunda yazarın gerekli düzeltmeleri en geç "üç hafta" içerisinde yapması istenir.
- Revize edilmiş makale kabul alırsa düzenleme aşamasına geçilir.

Değerlendirme sürecine ilişkin Akış Şemasına, derginin web sayfasından erişilebilir.

DBMD'ye yayımlanmak üzere gönderilen makaleler; makale gönderim, işlem ve yayın ücretinden muaftır.

Kabul edilen makaleler, **ücretsiz** olarak basılı şekilde ve dergi web sayfasından çevrimiçi (online) olarak yayınlanmaktadır.

JOURNAL OF NAVAL SCIENCES AND ENGINEERING (JNSE)
WRITING RULES

General: Manuscripts must be prepared in MS Word, single-spaced with justify. Font: Times New Roman, 12 points. Margins: left 4,5 cm- right 3,5 cm, top 5 cm- bottom 7 cm, header 3,25 cm- footer 6 cm, gutter 0. Paper type: A4. Page numbers should be on the middle of bottom of page with -1-, -2-, -3- etc. format. Using footnotes is not allowed.

Ethics Committee Approval and/or Legal/Special Permission: The articles must state whether an ethical committee approval and/or legal/special permission is required or not. If these approvals are required, then it should be clearly presented from which institution, on what date and with which decision or number these approvals are obtained.

Body of Text: Follow this order when typing manuscripts: Title, Authors, Abstract, Keywords, Title (Turkish), Abstract (Turkish), Keywords (Turkish), Main Text, Appendix (if any), References.

Title: Title should reflect objectives of the paper clearly, be easily understandable and not exceed 15 words.

Abstracts: Each paper should have an abstract with 100-200 words and have a structured form, i.e. standard structure of an article (background, purpose, material and methods used, results, conclusion).

Paper Length: The manuscript should be minimum 2000 words or 5 pages, maximum 7000 words or 25 pages including references.

Keywords: Author must provide some keywords (between 3 and 5) that will be used to classify the paper.

Unit: International System of Unit (Système Internationale d'Unités; SI) (https://www.britannica.com/science/International-System-of-Units) should be used for all scientific and laboratory data.

References: References should be given according to the APA standard as effective from November, 2020 issue.

Abbreviations and Acronyms: Standard abbreviations and acronyms should be used for each related discipline. Acronyms should be identified at the first occurrence in the text. Abbreviations and acronyms may also be attached to main text as an appendix.

Equations and Formulas: Equations and formulas should be numbered consecutively. These numbers must be shown within parentheses being aligned to the right. In the text, equations and formulas should be referred with their numbers given in parentheses. Comprehensive formulas, not appropriate to be written in the texts, should be prepared in figures.

Figures and Tables: Figures and tables should be numbered consecutively. In the text referring to figures and tables should be made by typing "Figure 1." or "Table 1." etc. A suitable title should be assigned to each of them.

DENİZ BİLİMLERİ VE MÜHENDİSLİĞİ DERGİSİ (DBMD)
YAZIM KURALLARI

Genel Bilgiler: Yazılar; Microsoft Word'de tek satır aralığı ve iki yana yaslanarak hazırlanmalıdır. Yazı tipi: Times New Roman, 12 punto. Kenar boşlukları: sol 4,5 cm- sağ 3,5 cm- üst 5 cm- alt 7 cm- üst bilgi 3,25 cm- alt bilgi 6 cm, oluk 0. Kâğıt ölçüsü: A4. Sayfa numaraları sayfanın alt ortasında -1-, -2-, -3- vb. şeklinde yer almalıdır. Dipnot kullanılmamalıdır.

Etik Kurul İzni ve/veya Yasal/Özel İzin: Makalelerde etik kurul izni ve/veya yasal/özel izin alınmasının gerekip gerekmediği belirtilmiş olmalıdır. Eğer bu izinlerin alınması gerekli ise, izinlerin hangi kurumdan, hangi tarihte ve hangi karar veya sayı numarası ile alındığı açıkça sunulmalıdır.

Yazı Yapısı: Yazı şu sırada hazırlanmalıdır: Başlık, Yazarlar, Özet, Anahtar Kelimeler, Başlık (Türkçe), Özet (Türkçe), Anahtar Kelimeler (Türkçe), Ana Metin, Ek (varsa), Referanslar.

Başlık: Başlık; açık, net, anlaşılır olmalı ve 15 kelimeyi geçmemelidir.

Öz (Abstract): Yazı, 100-200 kelimelik, arka plan, amaç, yöntem, bulgular ve sonuçtan oluşan yapılandırılmış bir özeti içermelidir.

Sayfa Sayısı: Dergiye gönderilecek yazıların boyutu, kaynakça dâhil asgari 2000 kelime veya 5 sayfa, azami 7000 kelime veya 25 sayfa arasında olmalıdır.

Anahtar Kelimeler: Yazıyı sınıflandırmaya yarayacak, anahtar görevi yapan 3-5 kelime yer almalıdır.

Birimler: Yazının uluslararası alanlarda da kolay izlenebilir ve anlaşılabilir olması için Uluslararası Birim Sistemine (https://www.britannica.com/science/International-System-of-Units) uygun olarak hazırlanması gerekir.

Referans: Referanslar Kasım, 2020 sayısından itibaren geçerli olmak üzere APA standardına göre verilmelidir.

Notasyon ve Kısaltmalar: İlgili bilim alanının standart notasyon ve kısaltmaları kullanılmalı, yeni notasyonlar ise metin içinde ilk geçtiği yerde tanımlanmalıdır. Gerekli durumlarda, notasyon ve kısaltmalar ek olarak konulabilir.

Denklem ve Formüller: Denklem ve formüller ardışık olarak numaralandırılmalı ve bu numaralar sağa dayalı parantez içinde yazılmalıdır. Metin içinde denklem ve formüllere parantez içinde yazılan numaraları ile atıfta bulunulmalıdır. Metin arasında verilmesi uygun olmayan kapsamlı formüller şekil olarak hazırlanmalıdır.

Şekiller ve Tablolar: Şekiller ve tablolar, ardışık olarak numaralandırılmalıdır. Bunlara metin içinde "Şekil 1." veya "Tablo 1." şeklinde atıfta bulunulmalıdır. Her bir şekil ve tablo için uygun bir başlık kullanılmalıdır.

Ethical Principles and Publication Policy

Journal of Naval Sciences and Engineering (hereafter JNSE) is a peer reviewed, international, inter-disciplinary journal in science and technology, which is published semi-annually in November and April since 2003. JNSE it is committed to provide a platform where highest standards of publication ethics are the key aspect of the editorial and peer-review processes.

The editorial process for a manuscript to the JNSE consists of a double-blind review, which means that both the reviewer and author identities are concealed from the reviewers, and vice versa, throughout the review process. If the manuscrit is accepted in the review stage of the Editorial Process then, the submission goes through the editing stage, which consists of the processes of copyediting, language control, reference control, layout and proofreading. Reviewed articles are treated confidentially in JNSE.

Papers submitted to JNSE are screened for plagiarism with the iThenticate plagiarism detection tool. In case that the editors become aware of alleged or proven scientific misconduct, they can take the necessary steps. The editors have the right to retract an article whether submitted to JNSE or published in JNSE.

Following the completion of the editing stage, the manuscript is then scheduled for publication in an issue of the JNSE. The articles which are submitted to JNSE to be published are free of article submission, processing and publication charges. The accepted articles are published free-of-charge as online from the journal website and printed. The articles that are accepted to appear in the journal are made freely available to the public via the journal's website. The journal is also being printed by National Defence University Turkish Naval Academy Press on demand. The printed version can be accessed free of charge from the libraries of the Turkish Universities.

JNSE has editors and an editorial board which consists of academic members from at least five different universities. JNSE has an open access policy which means that all contents are freely available without charge to the user or his/her institution. Users are allowed to read, download, copy, distribute, print, search, or link to the full texts of the articles, or use them for any other lawful research purposes.

Publication ethics of the JNSE are mainly based on the guidelines and recommendations which are published by the Committee on Publication Ethics (COPE), World Federation of Engineering Organizations (WFEO), Council of Science Editors (CSE) and Elsevier's Publishing Ethics for Editors statements.

The duties and responsibilities of all parties in the publishing process including editors, authors and others are defined below.

The Responsibilities of the Authors:

-Authors are responsible for the scientific, contextual, and linguistic aspects of the articles which are published in the journal. The views expressed or implied in this publication, unless otherwise noted, should not be interpreted as official positions of the Institution.

-Authors should follow the "Author Guidelines" in JNSE's web page on DergiPark.

-Authors should conduct their researches in an ethical and responsible manner and follow all relevant legislation.

-Authors should take collective responsibility for their work and for the content of their publications.

-Authors should check their publications carefully at all stages to ensure that methods and findings are reported accurately.

-Authors must represent the work of others accurately in citations, quotations and references.

-Authors should carefully check calculations, data presentations, typescripts/submissions and proofs.

-Authors should present their conclusions and results honestly and without fabrication, falsification or inappropriate data manipulation. Research images should not be modified in a misleading way.

-Authors should describe their methods to present their findings clearly and unambiguously.

-Authors accept that the publisher of JNSE holds and retains the copyright of the published articles.

-Authors are responsible to obtain permission to include images, figures, etc. to appear in the article.

-In multi-authored publications -unless otherwise stated- author rankings are made according to their contributions.

-Authors should alert the editor promptly if they discover an error in any submitted.

-Authors should follow the publication requirements regarding that the submitted work is original and has not been published elsewhere in any language.

-Authors should work with the editor or publisher to correct their work promptly if errors are discovered after publication.

-If the work involves chemicals, procedures or equipment that have any unusual hazards inherent in their use, the authors must clearly identify these in the manuscript.

-If the work involves the use of animals or human participants, the authors should ensure that all procedures were performed in compliance with relevant laws and institutional guidelines and that the appropriate institutional committee(s) has approved them; the manuscript should contain a statement to this effect.

-Authors should also include a statement in the manuscript that informed consent was obtained for experimentation with human participants. Because the privacy rights of human participants must always be preserved. It is important that authors have an explicit statement explaining that informed consent has been obtained from human participants and the participants' rights have been observed.

-Authors have the responsibility of responding to the reviewers' comments promptly and cooperatively, in a point-by-point manner.

The Responsibilities of the Reviewers:

-Peer review process has two fundamental purposes as follow: The first purpose is to decide whether the relevant article can be published in JNSE or not and the second purpose is to contribute to the improvement of the weaknesses of the related article before the publication.

-The peer review process for an article to the JNSE consists of a double-blind review, which means that both the reviewer and author identities are concealed from the reviewers, and vice versa, throughout the review process. Reviewed articles are treated confidentially in JNSE.

-Reviewers must respect the confidentiality of peer review process.

-Reviewers must refrain from using the knowledge that they have obtained during the peer review process for their own or others' interests.

-Reviewers should definitely be in contact with the JNSE if they suspect about the identity of the author(s) during the review process and if they think that this knowledge may raise potential competition or conflict of interest.

-Reviewers should notify the JNSE in case of any suspicion regarding the potential competition or conflict of interest during the review process.

-Reviewers should accept to review the studies in which they have the required expertise to conduct an appropriate appraisal, they can comply with the confidentiality of the double-blind review system and that they can keep the details about the peer review process in confidential.

-Reviewers should be in contact with the JNSE in order to demand some missing documents, following the examination of the article, supplementary files and ancillary materials.

-Reviewers should act with the awareness that they are the most basic determinants of the academic quality of the articles to be published in the journal and they should review the article with the responsibility to increase academic quality.

-Reviewers should be in contact with the JNSE editors if they detect any irregularities with respect to the Ethical Principles and Publication Policy.

-Reviewers should review the articles within the time that has been allowed. If they can not review the article within a reasonable time-frame, then they should notify the journal as soon as possible.

-Reviewers should report their opinions and suggestions in terms of acceptance / revision / rejection for the manuscript in the peer review process through the Referee Review Form which is provided by JNSE.

-In case of rejection, reviewers should demonstrate the deficient and defective issues about the manuscript in a clear and concrete manner in the provided Referee Review Form.

-Review reports should be prepared and submitted in accordance with the format and content of the Referee Review Form which is provided by JNSE.

-Review reports should be fair, objective, original and prudent manner.

-Review reports should contain constructive criticism and suggestions about the relevant article.

The Responsibilities of the Editors:

-Editors are responsible of enhancing the quality of the journal and supporting the authors in their effort to produce high quality research. Under no conditions do they allow plagiarism or scientific misconduct.

-Editors ensure that all submissions go through a double-blind review and other editorial procedures. All submissions are subject to a double-blind peer-review process and an editorial decision based on objective judgment.

-Each submission is assessed by the editor for suitability in the JNSE and then, sent to the at least two expert reviewers.

-Editors are responsible for seeking reviewers who do not have conflict of interest with the authors. A double-blind review assists the editor in making editorial decisions.

-Editors ensure that all the submitted studies have passed initial screening, plagiarism check, review and editing. In case the editors become aware of alleged or proven scientific misconduct, they can take the necessary steps. The editors have the right to retract an article. The editors are willing to publish errata, retractions or apologies when needed.

Etik İlkeler ve Yayın Politikası

Deniz Bilimleri ve Mühendisliği Dergisi (Bundan sonra DBMD olarak anılacaktır.); uluslararası düzeyde, hakemli, çok disiplinli, Nisan ve Kasım aylarında olmak üzere 2003 yılından bu yana yılda iki kez yayınlanan, bilim ve teknoloji dergisidir. DBMD yayın etiğinde en yüksek standartların, editoryal ve hakemlik süreçlerinin kilit unsuru olarak değerlendirildiği bir platform sunmayı taahhüt etmektedir.

DBMD'ne gönderilen her bir makale için değerlendirme sürecinde çift-kör hakemlik sistemi uygulanmaktadır. Buna göre, değerlendirme süreci boyunca hakem ve yazarlar birbirlerinin bilgilerini görememektedir. Dergiye gönderilen çalışmaların yazar-hakem ve hakem-yazar açısından süreçlerinde gizlilik esastır. DBMD'ne gönderilen makalelerin değerlendirme sürecindeki inceleme aşamasında kabul edilmeleri halinde, ilgili makaleler için düzenleme aşamasına geçilmektedir. Düzenleme aşamasında, ilgili makaleler yazım formatı ve dilbilgisel yönlerden incelenir. Makalelerin sayfalar üzerindeki biçimi ve yerleşimleri kontrol edilip düzenlenir. Ayrıca referans kontrolü yapılır. DBMD'nde kontrol edilen ve düzenlenen makaleler gizli tutulmaktadır.

DBMD'ne gönderilen makaleler, iThenticate intihal tespit programı aracılığıyla bilimsel çalıntı konusunda kontrol edilir. Editörler, iddia edilen veya kanıtlanmış bir bilimsel kötü kullanımdan ya da usulsüzlükten haberdar olurlarsa bu konuda gerekli adımları atabilirler. Bu anlamda, Editörler gerekli durumlarda DBMD'ne gönderilen ya da DBMD'nde yayınlanmış makaleleri geri çekme hakkına sahiptir.

Düzenleme aşamasının başarılı olarak sonuçlanmasını takiben, ilgili makaleler DBMD'nin bir sayısında yayınlanmak üzere saklı tutulur ve kayıt altına alınır. DBMD'ne yayınlanmak üzere gönderilen makaleler; yazılı materyal gönderme, işleme ve yayınlama süreçlerindeki tüm ücretlerden muaf tutulmaktadır. DBMD'nde yayınlanmak üzere kabul edilen makaleler, derginin internet sitesinden çevrimiçi olarak ücretsiz bir şekilde yayınlanır ve basılır. Dergide yayınlanması kabul edilen çalışmalar, derginin web sitesinden açık erişim ile erişilebilir kılınmıştır. Dergi ayrıca, Milli Savunma Üniversitesi, Deniz Harp Okulu Basımevi tarafından basılmaktadır. Derginin basılı haline Üniversite kütüphanelerinden erişilebilmektedir.

DBMD; editörü ve en az beş değişik üniversitenin öğretim üyelerinden oluşmuş danışman grubu ile açık erişim politikasını benimsemektedir. Buna göre, tüm içerikler ücretsiz olarak kullanıcılar veya kurumlar için ulaşılabilirdir. Kullanıcıların DBMD bünyesindeki makalelerin tam metinlerini okuma, indirme, kopyalama, dağıtma, yazdırma, arama veya bunlara bağlantı verme ve diğer yasal araştırma amaçları için kullanma hakları saklı tutulmaktadır.

DBMD'nin yayın etiği, temel olarak Yayın Etiği Komitesi (COPE), Dünya Mühendislik Kuruluşları Federasyonu (WFEO), Bilim Kurulu Editörleri (CSE) ve Elsevier'in Editörler için Yayın Etiği açıklamaları kapsamında yayınlanmış yönergelere ve önerilere dayanmaktadır.

Editörler, yazarlar ve diğer taraflar da dâhil edilebilecek şekilde yayın sürecindeki görev ve sorumluluklar aşağıdaki gibi tanımlanmıştır.

Yazarların Sorumlulukları:

-Yazarlar, dergide yayınlanan makalelerinin bilimsel, bağlamsal ve dilsel yönlerinden sorumlu tutulmaktadır. Dergide ifade edilen veya ima edilen görüşler, aksi belirtilmediği sürece, Enstitünün resmi görüşü olarak yorumlanamaz ve yansıtılamaz.

-Yazarlar çalışmalarında, DBMD'nin DergiPark internet sayfasında yer alan "Yazım Kuralları"nı dikkate almalıdır.

-Yazarlar araştırmalarını etik ve sorumlu bir şekilde yürütmeli ve ilgili tüm mevzuatları takip etmelidir.

-Yazarlar çalışmaları ve yayınlarının içeriği için ortak sorumluluk almalıdır.

-Yazarlar, yöntemlerin ve bulguların doğru bir şekilde raporlandığından emin olmak için yayınlarını her aşamada dikkatlice kontrol etmelidir.

-Yazarlar, başkalarına ait çalışmaları dolaylı alıntı, doğrudan alıntı ve referanslar ile doğru bir şekilde göstermelidir. Yazarlar, makalelerindeki fikirlerin şekillendirilmesinde etkili ya da bilgilendirici olmuş her türlü kaynağa referans vermelidir.

-Yazarlar çalışmalarındaki hesaplamaları, ispatları, veri sunumlarını ve yazı tiplerini dikkatlice kontrol etmelidir.

-Yazarlar çalışmalarının sonuçlarını dürüstçe; uydurma, çarpıtma, tahrifat veya uygunsuz manipülasyona yer vermeden sunmalıdır. Çalışmalardaki görsel kaynaklar yanıltıcı bir şekilde değiştirilmemelidir.

-Yazarlar, çalışmalarındaki bulguları açık ve net bir şekilde sunmak için araştırma yöntemlerini tanımlamalı ve paylaşmalıdır.

-Yazarlar, yayınlanmış makalelerinin telif haklarını DBMD yayıncısına devrettiklerini kabul etmektedir.

-Yazarlar çalışmalarına çeşitli görsel kaynakları, figürleri, şekilleri vb. dahil etmek için gerekli izinleri almakla yükümlüdür. İlgili çalışmada yer alması gereken resim, şekil vb. anlatımı destekleyici materyaller için gerekli kişilerden ya da kurumlardan izin alınması yazarın sorumluluğundadır.

-Çok yazarlı yayınlarda -aksi belirtilmedikçe- yazar sıralamaları sunulan katkılara göre yapılmalıdır.

-Yazarlar gönderdikleri çalışmada herhangi bir hata tespit ederlerse bu konuda derhal editörü uyarmalıdır.

-Yazarlar dergiye gönderdikleri makalelerin başka bir yerde yayımlanmamış ya da yayımlanmak üzere gönderilmemiş olmaları ile ilgili DBMD'nin DergiPark internet sayfasında yer alan "Yayın Kuralları"nı dikkate almalıdır.

-Yazarlar, ilgili çalışmaları DBMD'nde yayınlandıktan sonra hata tespit ederlerse bu konuda gerekli düzeltmelerin yapılabilmesi amacıyla derhal editör veya yayıncı ile iletişime geçip onlar ile birlikte çalışmalıdır.

-İlgili çalışmada, doğası gereği kullanımlarında olağandışı tehlikeler barındıran çeşitli kimyasallar veya ekipmanlardan yararlanılmış ise yazarların tüm bunları çalışmasında açıkça belirtmesi ve tanımlaması gerekmektedir.

-İnsanlar ve hayvanların katılımını gerektiren çalışmalar için, yazarlar tüm sürecin ilgili yasalara ve kurumsal yönergelere uygun olarak gerçekleştirildiğinden emin olmalıdır ve ilgili komitelerden etik onay alındığını çalışmalarında açık bir şekilde ifade edip belgelendirmelidir.

-İnsanların katılımını gerektiren çalışmalar için, yazarlar kurumsal etik kurul onayı almakla yükümlüdürler. Yazarlar, katılımcıların süreç ile ilgili olarak bilgilendirildiklerini ve bu anlamda, katılımcılardan gerekli izinlerin alındığını bildirmek ve belgelemek zorundadır. Yazarlar, katılımcıların haklarının gözetildiğini açıklayan açık bir bildirim sunmalıdır. Ayrıca bu süreçte, katılımcıların gizlilik hakları her zaman korunmalıdır.

-Yazarlar, hakemlerin değerlendirmelerini, yorumlarını ve eleştirilerini zamanında ve işbirliği içerisinde dikkate almalıdır ve bu konuda, gerekli güncellemeleri yapmalıdır.

Hakemlerin Sorumlulukları:

-Hakem değerlendirme sürecinin iki temel amacı vardır: İlk amaç, ilgili makalenin DBMD'nde yayınlanıp yayınlanamayacağına karar vermektir ve ikinci amaç, yayından önce ilgili makalenin eksik yönlerinin geliştirilmesine katkıda bulunmaktır.

-DBMD'ne gönderilen her bir makale için değerlendirme sürecinde çift-kör hakemlik sistemi uygulanmaktadır. Buna göre, değerlendirme süreci boyunca hakem ve yazarlar birbirlerinin bilgilerini görememektedir. Dergiye gönderilen çalışmaların yazar-hakem ve hakem-yazar açısından süreçlerinde gizlilik esastır.

-Hakemler, değerlendirme sürecinin gizliliğine saygı göstermelidir.

-Hakemler, değerlendirme sürecinde elde ettikleri bilgileri kendilerinin veya başkalarının çıkarları için kullanmaktan kaçınmalıdır.

-Hakemler, değerlendirme sürecinde yazar(lar)ın kimliğinden şüphe etmeleri ve bu bilginin herhangi bir potansiyel rekabet veya çıkar çatışması yaratacağını düşünmeleri halinde mutlaka DBMD ile iletişime geçmelidir.

-Hakemler, değerlendirme sürecinde şüphe ettikleri potansiyel rekabet veya çıkar çatışması durumlarını DBMD'ne bildirmelidir.

-Hakemler, uygun bir değerlendirme yapabilmek için gereken uzmanlığa sahip oldukları, çift-kör hakemlik sisteminin gizliliğine riayet edebilecekleri ve değerlendirme süreci ile ilgili detayları gizli tutabilecekleri çalışmaların hakemliğini kabul etmelidir.

-Hakemler makaleyi, ek dosyaları ve yardımcı materyalleri incelemelerini takiben bazı eksik belgelere ihtiyaç duymaları halinde bunları talep etmek üzere DBMD ile iletişime geçmelidir.

-Hakemler dergide yayınlanacak makalelerin akademik kalitesinin en temel tespit edicisi olduklarının bilinciyle davranmalı ve akademik kaliteyi arttırma sorumluluğuyla inceleme yapmalıdır.

-Hakemler, Etik İlkeler ve Yayın Politikası ile ilgili herhangi bir usulsüzlük tespit etmeleri halinde DBMD editörleri ile irtibata geçmelidir.

-Hakemler, kendilerine tanınan süre içerisinde makaleleri değerlendirmelidir. Şayet uygun bir zaman içerisinde değerlendirme yapamayacaklarsa, bu durumu en kısa zamanda DBMD'ne bildirmelidirler.

-Hakemler, değerlendirme sürecindeki çalışma için kabul etme / yeniden gözden geçirme / reddetme şeklindeki önerilerini DBMD tarafından sağlanan Hakem Değerlendirme Formu aracılığıyla bildirmelidir.

-Sonucu reddetme şeklinde olan değerlendirmeler için hakemler, ilgili çalışmaya dair eksik ve kusurlu hususları Hakem Değerlendirme Formu'nda açık ve somut bir şekilde ortaya koymalıdır.

-Hakem değerlendirme raporlarının, DBMD tarafından sağlanan Hakem Değerlendirme Formu'na uygun biçimde ve içerikte hazırlanması ve gönderilmesi gerekmektedir.

-Hakem değerlendirme raporları adil, objektif, özgün ve ölçülü olmalıdır.

-Hakem değerlendirme raporları, ilgili makale ile ilgili yapıcı eleştiriler ve tavsiyeler içermelidir.

Editörlerin Sorumlulukları:

-Editörler, derginin bilimsel kalitesini arttırmak ve yazarları bilimsel kalitesi yüksek araştırmalar üretmek için desteklemek ile sorumludur. Hiçbir koşulda, intihal ya da bilimsel kötüye kullanıma izin verilmemektedir.

-Editörler, dergiye gönderilen her çalışmanın çift-kör hakemlik sürecine ve diğer editoryal süreçlere tabi olmasını sağlamaktadır. DBMD'ne gönderilen her çalışma, çift-kör hakemlik sürecine ve nesnel değerlendirmeye dayalı editör kararına bağlı tutulmaktadır.

-DBMD'ne gönderilen her bir çalışma, uygunlukları açısından editör tarafından değerlendirilir ve daha sonrasında, incelenmesi ve değerlendirilmesi amacıyla en az iki uzman hakeme gönderilir.

-Editörler, yazarlar ile çıkar çatışması olmayan hakemleri, çalışmayı değerlendirmek üzere atamakla sorumludur. Çift-kör hakemlik süreci, editör için değerlendirme ve düzenleme aşamalarında katkı sağlamaktadır.

-Editörler, DBMD'ne gönderilen tüm çalışmaların ön kontrol, tarama, intihal kontrolü, değerlendirme ve düzenleme aşamalarından geçmesini sağlar. Editörler iddia edilen veya kanıtlanmış bilimsel kötü kullanımdan haberdar olurlarsa makaleyi geri çekebilirler. Editörler, gerekli durumlarda gönderilen çalışmayı düzeltme, geri çekme veya çalışma hakkında özür yayınlama hakkına sahiptir.

NATIONAL DEFENCE UNIVERSITY
BARBAROS NAVAL SCIENCES AND ENGINEERING INSTITUTE
JOURNAL OF NAVAL SCIENCES AND ENGINEERING

VOLUME: 17 **NUMBER: 2** **NOVEMBER 2021** **ISSN: 1304-2025**

CONTENTS / İÇİNDEKİLER

MİLLİ SAVUNMA ÜNİVERSİTESİ
BARBAROS DENİZ BİLİMLERİ VE MÜHENDİSLİĞİ ENSTİTÜSÜ
DENİZ BİLİMLERİ VE MÜHENDİSLİĞİ DERGİSİ

CİLT: 17 **SAYI: 2** **KASIM 2021** **ISSN: 1304-2025**

NATIONAL DEFENCE UNIVERSITY
BARBAROS NAVAL SCIENCES AND ENGINEERING INSTITUTE
JOURNAL OF NAVAL SCIENCES AND ENGINEERING

VOLUME: 17 **NUMBER: 2** **NOVEMBER 2021** **ISSN: 1304-2025**

CONTENTS / İÇİNDEKİLER

MİLLİ SAVUNMA ÜNİVERSİTESİ
BARBAROS DENİZ BİLİMLERİ VE MÜHENDİSLİĞİ ENSTİTÜSÜ
DENİZ BİLİMLERİ VE MÜHENDİSLİĞİ DERGİSİ

CİLT: 17 **SAYI: 2** **NOVEMBER 2021** **ISSN: 1304-2025**